Comprehensive analysis of transitions in ribosomal DNA chromatin states in *S. cerevisiae* during different growth phases

DISSERTATION ZUR ERLANGUNG DES DOKTORGRADES DER NATURWISSENSCHAFTEN (DR. RER. NAT.) DER FAKULTÄT FÜR BIOLOGIE UND VORKLINISCHE MEDIZIN DER UNIVERSITÄT REGENSBURG

vorgelegt von

Virginia-Lorena Babl

aus

Roding

im Jahr

2016

I was just guessing at numbers and figures
pulling the puzzles apart
questions of science, science and progress
do not speak as loud as my heart

Coldplay, The Scientist

Das Promotionsgesuch wurde eingereicht am:

21.10.2016

Die Arbeit wurde angeleitet von:

PD Dr. Joachim Griesenbeck

Unterschrift:

Table of contents

Table of contents

Table of contents

Table of contents

Summary

In the nucleus of eukaryotes DNA is assembled into a large nucleoprotein complex, called chromatin. Histones form the basic chromatin component, the nucleosome. Nucleosomes impair the access of proteins to DNA and may interfere with DNA-dependent processes such as transcription, replication and DNA repair. To make DNA accessible, chromatin has to be a highly dynamic structure. How genomic loci adopt different functional states is still poorly understood. Thus, defined model loci are used to characterize chromatin transitions on the molecular level. One of these model loci is the ribosomal DNA locus in *Saccharomyces cerevisiae* (hereafter called yeast).

Transcription at the ribosomal DNA (rDNA) multicopy gene locus by RNA polymerase I (Pol I) and III (Pol III) accounts for more than 50% of the total RNA production in exponentially growing yeast cells. Although the Pol I transcribed 35S rDNA locus is one of the most actively transcribed loci in the whole genome, around half of the 35S ribosomal RNA (rRNA) genes adopt a nucleosomal, transcriptionally inactive, “closed” state, whereas the other half is in an actively transcribed and nucleosome depleted, “open” state. These states are not stable but change dynamically e.g. during the cell cycle, DNA repair, or growth phase transitions. The exact mechanisms driving these changes in 35S rDNA chromatin are still largely unknown.

When yeast cells transit to stationary phase Pol I transcription is downregulated and rRNA gene chromatin adopts a closed state. Whereas downregulation of RNA polymerase I transcription depends largely on the Tor pathway, the rDNA chromatin transition is dependent on the presence of the deacetylase Rpd3. This thesis showed that the maintenance of the open chromatin state in stationary phase in *rpd3*Δ cells is dependent on Pol I transcription. I provided evidence that Rpd3 might negatively influence Pol I initiation with transition to stationary phase at the level of the specific initiation factor CF (core factor) or via the Pol I stimulating factor Net1. Additionally, this thesis shows that the Pol I subunit Rpa49 is important for the fast and effective loading of Pol I and for the reopening of rDNA copies upon the transition from stationary phase to exponential growth.

From the results, I could propose a model for the chromatin state transitions upon entry and exit from stationary phase. I suggest, that upon exit from exponential phase, Pol I transcription is largely downregulated via the Tor kinase pathway, but a sufficient amount of transcription is still ongoing during the diauxic shift and at post-diauxic growth phase

leading to the persistence of open copies. With transition to stationary phase, the deacetylase Rpd3 mediates the complete shutdown of Pol I transcription and thus closing of the copies. This process is potentially mediated via CF or Net1. Upon exit from stationary phase, Pol I transcription is re-established and this is accompanied by the transition of closed copies to the open chromatin state. The chromatin state transition is established even with low Pol I loading rates, but to achieve high Pol I transcription rates and fast chromatin state transitions, the subunit Rpa49 is required.

Zusammenfassung

Im Zellkern von Eukaryoten liegt die DNA in einem Nukleoproteinkomplex, dem Chromatin vor. Die Hauptkomponenten des Chromatins sind Nukleosomen, die aus Histonproteinen und DNA gebildet werden. Die Assemblierung der DNA in Nukleosomen behindert den Zugang von Proteinen zur DNA und konkurriert mit DNA-abhängigen Prozessen wie Transkription, Replikation und DNA Reparatur. Um diese essentiellen Prozesse dennoch zu gewährleisten, muss sich die Chromatinstruktur dynamisch ändern. Wie genomische Loci verschiedene funktionelle Chromatinzustände annehmen, ist gegenwärtig nur teilweise verstanden. Daher werden verschiedene Modelloci genutzt, um Chromatinübergänge auf dem molekularen Level zu charakterisieren. Einer dieser Loci ist der ribosomale DNA (rDNA) Locus in *Saccharomyces cerevisiae* (nachfolgend Hefe genannt).

Die Transkription am ribosomalen DNA Multikopien-Locus durch RNA Polymerase I (Pol I) und RNA Polymerase III (Pol III) stellt über 50% der Gesamtproduktion an RNA in exponentiell wachsenden Hefezellen dar. Obwohl der Pol I transkribierte 35S rDNA Locus einer der aktivsten des gesamten Genoms ist, nehmen etwa die Hälfte der 35S ribosomalen RNA (rRNA) Gene einen transkriptionell inaktiven, mit Nukleosomen besetzten, sogenannten „geschlossenen“ Zustand ein, während sich die andere Hälfte in einem aktiv transkribierten, Nukleosomen-abgereicherten, offenen Chromatinzustand befindet. Diese Zustände gehen in speziellen Situationen (z.B. im Zellzyklus, bei DNA-Reparatur oder bei Wachstumsphasenübergängen) dynamisch ineinander über. Die molekularen Mechanismen, die diese Veränderungen des 35S rDNA Chromatins hervorrufen, sind weitgehend noch unbekannt.

Wenn Hefezellen in die stationäre Phase wachsen, wird die Pol I Transkription herabreguliert und die rRNA Gene nehmen den geschlossenen Chromatinzustand ein. Während das Herunterregulieren der RNA Polymerase I Transkription größtenteils vom Tor-Signaltransduktionsweg abhängt, wird für den Chromatinübergang der rDNA die Deacetylase Rpd3 benötigt. In dieser Arbeit konnte ich zeigen, dass die Erhaltung des offenen Chromatinzustandes in der stationären Phase in *rpd3*Δ Zellen von Transkription durch Pol I abhängig ist. Es konnten Hinweise erhalten werden, dass Rpd3 die Pol I Initiation während des Übergangs zur stationären Phase über den spezifischen Initiationsfaktor CF (Core Faktor) oder über den Pol I stimulierenden Faktor Net1 negativ beeinflussen könnte. Desweiteren konnte ich zeigen, dass die Pol I Untereinheit Rpa49

wichtig ist, um eine schnelle und effiziente Pol I Beladung und Öffnung der rDNA Kopien zu erreichen, wenn stationäre Hefezellen wieder in das exponentielle Wachstum übergehen.

Die in dieser Doktorarbeit erhaltenen Ergebnisse bilden die Grundlage für ein Modell der Etablierung von rDNA Chromatinzuständen, wenn Hefezellen in die stationäre Phase wechseln und danach wieder exponentiell zu wachsen beginnen. Ich schlage vor, dass mit dem Austritt aus der exponentiellen Wachstumsphase Pol I Transkription nach Inaktivierung des Tor-Kinase-Signaltransduktionsweges stark herabreguliert wird. Mit Voranschreiten zur stationären Phase vermittelt die Deacetylase Rpd3 - möglicherweise durch direkte Regulation der Faktoren CF oder Net1 - das komplette Abschalten der Pol I Transkription, was letztlich zum Schließen der noch offenen 35S rRNA Gen-Kopien führt. Der erneute Übergang in die exponentielle Wachstumsphase ist durch Rpa49-abhängige, hohe Pol I Beladungsraten der 35S rRNA Gene gekennzeichnet, die mit schnellen Übergängen in den offenen Chromatinzustand korrelieren.

I Introduction

I.1 Chromatin

In all organisms from prokaryotes and archaea to eukaryotes DNA is compacted and organized in special (pseudo-)compartments, built of the DNA itself, RNA and specialized proteins. Even if prokaryotic and archaeal DNA is not secluded within a membrane - as it is in eukaryotes within the nucleus - it is organized in the nucleoid (Thanbichler et al., 2005). The organized form of DNA was called chromatin (Alberts et al., 2002; Widom, 1998). The main function of chromatin was thought to be the compaction of DNA to fit it in the limited space of the nucleus (or the cell itself respectively for prokaryotes). For instance, in *Saccharomyces cerevisiae* (hereafter called yeast) 12 Mbp of DNA distributed on 16 chromosomes with a total length of around 0.5cm have to fit in a nucleus with approximately 1.5µm in diameter. However, chromatin might have additional functions other than only fitting DNA in the small space of the nucleus. Some studies indicate that chromatin could be protective to DNA (Lavelle and Foray, 2014; Takata et al., 2013; Yoshikawa et al., 2008). Findings in eukaryotes that main chromatin components called nucleosomes impede transcription *in vitro* (Knezetic and Luse, 1986; Lorch et al., 1987) and that the inhibition of nucleosome formation leads to transcriptional activation (Han and Grunstein, 1988), suggested additional regulatory functions of chromatin. To fulfill these regulatory functions, chromatin has to be a highly dynamic structure, enabling DNA dependent processes like replication, transcription, and repair (Clapier and Cairns, 2009; Ehrenhofer-Murray, 2004; Kornberg and Lorch, 1995; Li et al., 2007; Morales et al., 2001).

I.1.1 The nucleosome is the basic unit of eukaryotic chromatin

Bacterial DNA is mostly arranged in loops (Thanbichler et al., 2005) and histone-like proteins are associated with the DNA (Dame, 2005). Crenarchaea also have nucleoid-organizing proteins like for example Alba and Sul7d, while for Euryarchaea histone proteins were identified as the major chromatin components besides DNA (Reeve, 2003). Finally, in eukaryotes, the nucleosome was identified as the basic repeating unit of chromatin (Kornberg, 1974). The nucleosome is defined as the nucleosome core (Figure 1), the linker histone and the linker DNA region connecting one nucleosome to

the next and consists of approximately 200bp DNA and five different histones: H1, H2A, H2B, H3, and H4 (Kornberg, 1974; Phillips and Johns, 1965).

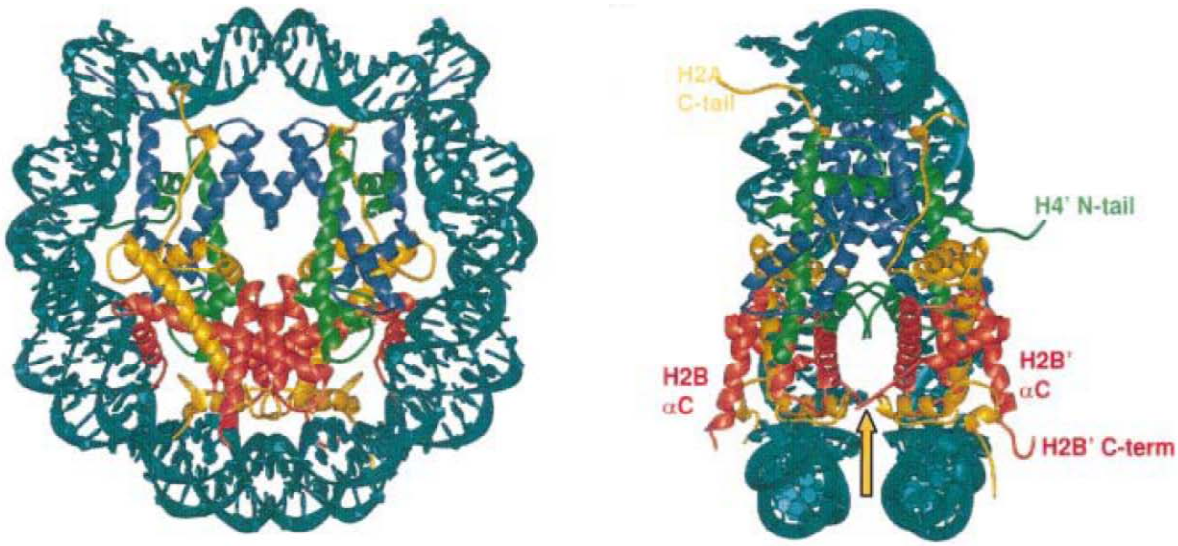

Figure 1: Crystal structure of the yeast nucleosome core particle

Left side: The nucleosome core particle viewed down the superhelical axis. Right side: View from the side, obtained by rotation of 90°around the axis (parts of the DNA are removed for clarity). DNA is shown in turquoise, and the histone chains in yellow (H2A), red (H2B), blue (H3), and green (H4). (from White et al., 2001)

I.1.1.1 Assembly of the nucleosome core particle

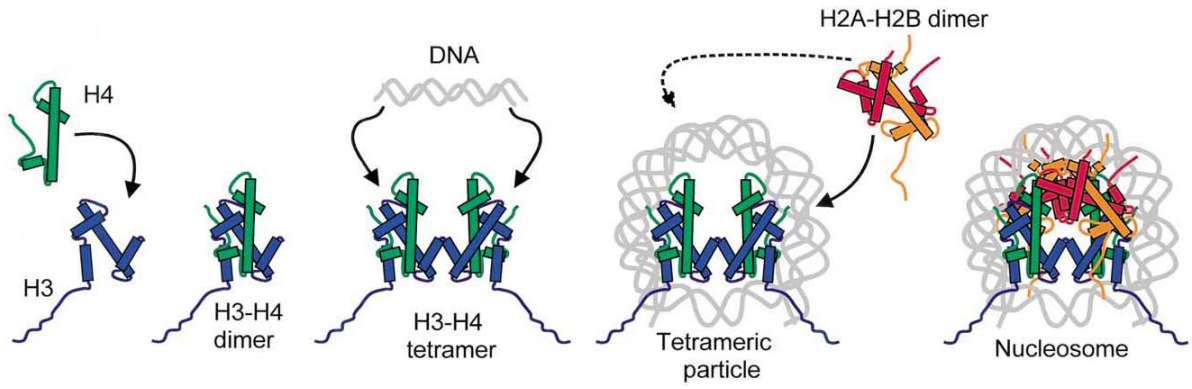

Figure 2: Structure and assembly of the nucleosome core particle

DNA is depicted in grey, H3 is shown in blue, H4 in green, H2A in yellow, and H2B in red.(from Morales et al., 2001)

The nucleosome core particle consists of 146-147bp wrapped approximately 1.7 times around a histone octamer (Davey et al., 2002; Luger et al., 1997; Noll, 1974; White et al., 2001). For the assembly of the nucleosome core particle (Figure 2) the four core histones (H2A, H2B, H3, and H4) interact with each other. First, histone H3 and H4 form a dimer. Afterwards two H3-H4 dimers associate to build a tetramer. The tetrameric particle is formed when DNA wraps around the $(H3\text{-}H4)_2$ tetramer. One heterodimer of H2A and H2B assembles on each side of the tetrameric particle and thus the

nucleosome core particle is formed (Arents and Moudrianakis, 1993; Luger et al., 1997; Morales et al., 2001; Richmond and Davey, 2003).

I.1.1.2 Core histones are the protein scaffold of chromatin

The core histones are among the most conserved proteins in eukaryotes (Baxevanis and Landsman, 1998; DeLange et al., 1969; Sullivan et al., 2002; Thatcher and Gorovsky, 1994). According to the high abundance of these proteins in the cell, several copies of the respective genes are present in the genome. However, there are high discrepancies between different organisms. While in yeast only two gene copies encode for the core histones (Hereford et al., 1979; Smith and Andrésson, 1983), in Drosophila more than 100 (Lifton et al., 1978), and in mice and human more than 50 copies (Marzluff et al., 2002) of the core histone genes are present. Even if the sequence homology level among the four core histones is low, they all share the existence of two functional domains: a common tertiary structure motif named the histone fold (Arents and Moudrianakis, 1995) and the C- and N-terminal tail regions which are rich in lysine and arginine (Figure 3).

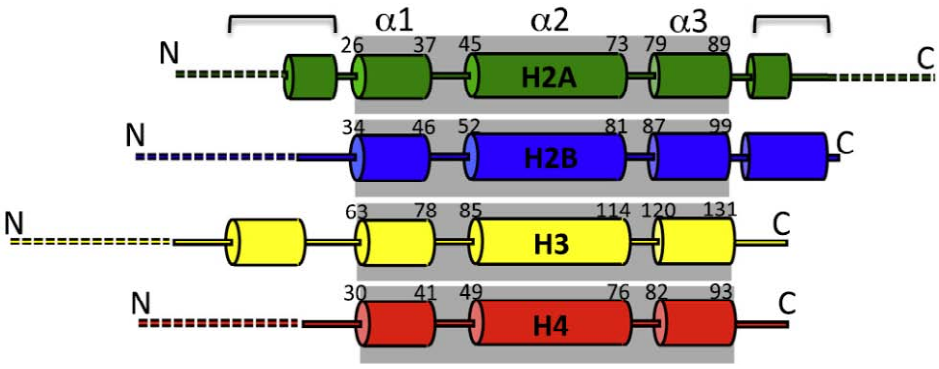

Figure 3: Functional domains of the four core histones

The different histones are colored: green for H2A, blue for H2B, yellow for H3, and red for H4. The α-helices are depicted as columns. Dashed lines represent the histone tails. Grey boxes represent the histone-fold motif. Numbers indicate the first and last amino acid number of the three histone-fold domain helices. (from Cutter and Hayes, 2015)

The histone fold motif is responsible for both histone-histone and histone-DNA interactions (Arents and Moudrianakis, 1993; Arents et al., 1991) and interestingly also found in archaeal histone-like proteins (Pereira and Reeve, 1998; Sandman et al., 2001). All core histones have an N-terminal tail extending from the nucleosome, while H2A has an additional C-terminal tail. Thus, ten tails are present at each nucleosome (Pepenella et al., 2014). The histone tails are targets for posttranslational modifications (PTMs), suggested to result in a "histone-code" which is implicated in chromatin regulation

(Jenuwein and Allis, 2001). PTMs lead to different interactions between histones, DNA and effector proteins and thus influence chromatin structure and function (Choi and Howe, 2009; Strahl and Allis, 2000). PTMs include amongst others acetylation, methylation, phosphorylation, ubiquitylation, and sumoylation (Kouzarides, 2007; Nightingale et al., 2006; Peterson and Laniel, 2004). Variants of some canonical histones exist, that are implicated in association to specific loci, chromatin states, or cell cycle stages (Ahmad and Henikoff, 2002; Kamakaka and Biggins, 2005; Probst et al., 2009). In most cases these replacement histones are deposited by specific chaperones and interact with different modifiers (Elsaesser and Allis, 2010; Foltz et al., 2009; Luk et al., 2010; Tagami et al., 2004). While in higher eukaryotes many variants exist, in yeast so far only two variants were identified: the centromere specific Cse4 (Boeckmann et al., 2013; Meluh et al., 1998; Stoler et al., 1995) and Htz1 which was found to have many different and even contrary functions from transcription activation to repression (Zlatanova and Thakar, 2008).

I.1.1.3 Linker histones

With an average stoichiometry of one per nucleosome histone H1 binds to linker DNA in cells of higher eukaryotes, but differences in the stoichiometry exist between organisms and cell types (Bates and Thomas, 1981; Fan et al., 2003, 2005; Hayes and Wolffe, 1993; van Holde, 1989; Oudet et al., 1975). So far, it is not completely understood what the specific functions of linker histones are. However, studies indicate that histone H1 functions in the stabilization of the DNA wrapping around the nucleosome, in the formation of higher order chromatin structures (Allan et al., 1986; Hansen, 2002; Robinson and Rhodes, 2006; Thoma et al., 1979) and in the proper folding of the mitotic chromosome (Maresca and Heald, 2006). Additionally, H1 was shown to influence nucleosome spacing (Blank and Becker, 1995; Fan et al., 2003), the regulation of gene expression (Fan et al., 2005; Shen and Gorovsky, 1996), and the formation of heterochromatin (Lu et al., 2013). Recent research suggested, that H1 recognizes and binds a trio of juxtaposed DNA surfaces that are formed by the two entering/exiting linker DNA strands and influences the formation of the 30nm fiber *in vitro* (Figure 4) (Song et al., 2014; Syed et al., 2010).

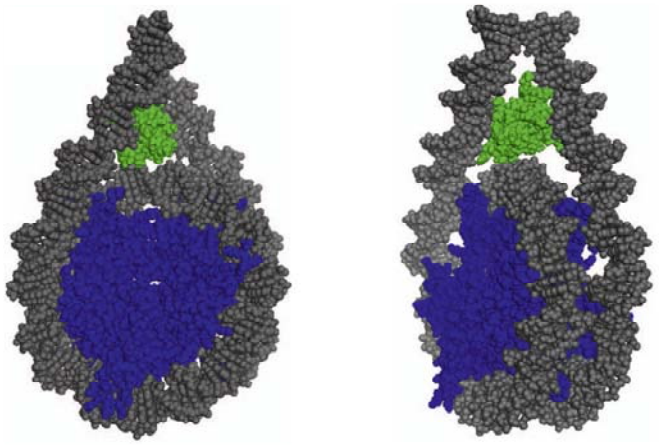

Figure 4: Three-contact model of linker histone binding to a nucleosome
Core histones are shown in blue, DNA is shown in grey, the linker histone globular domain is shown in green. (from Cutter and Hayes, 2015)

Linker histones are less conserved among organisms than core histones, and thus the putative linker histone in yeast (Hho1) shares little sequence homologies with its mammalian counterparts (Landsman, 1996; Ushinsky et al., 1997). Other than some linker histones in higher eukaryotes, Hho1 is not essential in yeast and deletion of the gene neither leads to a specific phenotype, nor does it affect nucleosome spacing or positioning (Patterton et al., 1998; Puig et al., 1999). Additionally, Hho1 is far underrepresented compared to nucleosomes in genome wide chromatin in exponentially growing cells (Freidkin and Katcoff, 2001). However, Hho1 was shown to be recruited to DNA in stationary cells and during gametogenesis, helping chromatin compaction (Bryant et al., 2012; Schäfer et al., 2008). Earlier findings showed preferential Hho1 association with the ribosomal DNA (rDNA) (Freidkin and Katcoff, 2001), where it potentially influences RNA polymerase I (Pol I) processivity and chromatin compaction (Levy et al., 2008).

I.1.2 Higher order chromatin structures

The primary chromatin structure is defined as the regular arrangement of nucleosomes on DNA (nucleosome array) (Woodcock and Dimitrov, 2001), which can be observed under specific conditions in electron microscopy and atomic force microscopy as "beads on a string" (Figure 5 upper part) (Daban, 2011; Olins and Olins, 1974). The 30nm fiber is considered as the chromatin secondary structure (Figure 5 bottom left), even if its existence *in vivo* has been questioned (Fussner et al., 2011; Hansen, 2002; Maeshima et al., 2010; Nishino et al., 2012). However, different models were proposed how the nucleosome array is arranged in a potential 30nm fiber from *in vitro* data (Tremethick, 2007). First, there was the so called one-start helix/solenoid model predicted (Finch and

Klug, 1976; Kruithof et al., 2009): consecutive nucleosomes interact with each other to form a helical structure. The twisting is achieved by bending of linker DNA. Second, the two-start helix/zigzag model was predicted: in this model the interaction takes not directly place between consecutive nucleosomes, but between one nucleosome and the after next, thus leading to a stacking of nucleosomes (Dorigo et al., 2004; Song et al., 2014; Williams et al., 1986). Latest *in vitro* studies suggested that both models are valid. Predominant two start zigzag fibers were interspersed with regions of solenoid-typical bent linker DNA, thus leading to a "heteromorphic" fiber (Grigoryev et al., 2009). Higher order structures of chromatin beyond the 30nm fiber (Figure 5 bottom right) definitely exist *in vivo* as the existence of the metaphase chromosome shows. They have long been thought to be a regular arrangement of loops and intercalations of the previous compaction stage chromatin (Alberts et al., 2002). However, since even the *in vivo* existence of secondary structure chromatin has been recently questioned, the idea of a less ordered tertiary (and higher) structure chromatin came up (Fussner et al., 2011). Nevertheless, most current ideas and knowledge of higher order chromatin structure have been derived from the metaphase chromosome and extrapolated to interphase (Gasser and Laemmli, 1987; Münkel et al., 1999; Paul and Ferl, 1999) and thus it is not certain if they are representative for interphase chromatin.

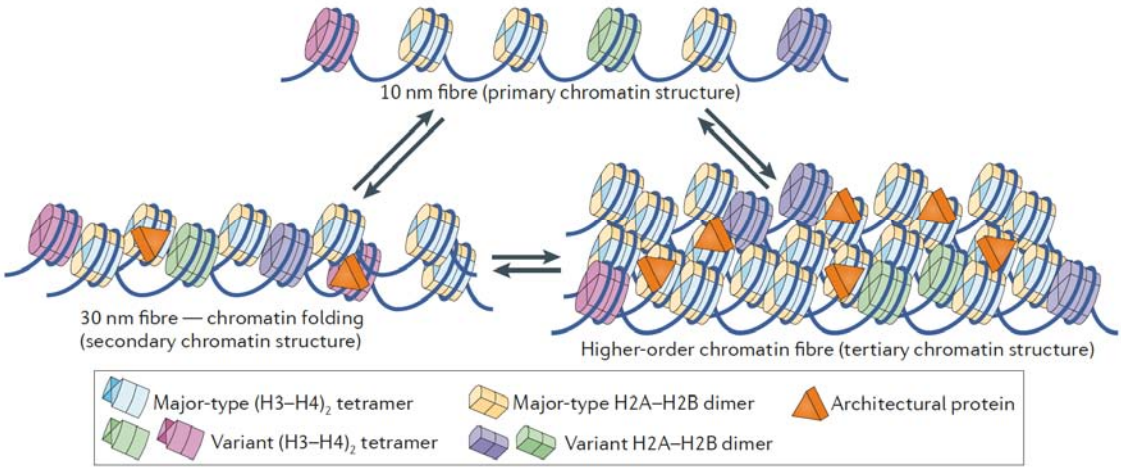

Figure 5: Chromatin higher order structures

The chromatin structures are shown with respect to histone variants and architectural proteins as depicted in the legend at the bottom. Top: The primary chromatin structure is the 10nm fiber, consisting of a nucleosomal array. Bottom left: The secondary structure of chromatin is the 30nm fiber, here depicted as the zigzag model. Tertiary and higher order chromatin structures can be assembled from nucleosomal arrays and secondary structure chromatin by long-range nucleosome interactions. All chromatin structures may be influenced by PTMs, histone variants, chromatin remodeling factors, and architectural proteins. (from Luger et al., 2012)

Even if the exact structure of higher order chromatin is not yet understood, great effort has been made on what contributes to its formation. As mentioned already in the

previous section, the presence of linker histones influences the higher order chromatin structure (Zlatanova et al., 2000). The introduction of PTMs to the histone tails and the replacement of canonical histones with variants seem to be also important for the stability and assembly of higher order chromatin structures (Bönisch and Hake, 2012; Dorigo et al., 2003; Horn and Peterson, 2002; Kan et al., 2007; Pepenella et al., 2014; Shogren-Knaak et al., 2006). Additionally, non-histone factors have impact on higher order chromatin such as high mobility group box proteins that reduce chromatin fiber compaction (Rochman et al., 2010) and Sir proteins that positively regulate heterochromatin formation (Strahl-Bolsinger et al., 1997).

Besides the arrangement of higher order chromatin structures, chromatin is localized to specific regions within the nucleus according to its transcription state. Heterochromatin (inactive chromatin) is located at the nuclear periphery, while euchromatin is predominantly found in the center of the nucleus (Bolzer et al., 2005; Tanabe et al., 2002). First hints for a specific localization of chromatin within the nucleus were already found by electron microscopy (Davies, 1967). The development of modern methods like chromosome conformation capture (3C) and its derivatives (4C, Hi-C) led to the suggestion that nuclear substructures, called topologically associating domains (TADs) may establish a defined nuclear architecture (Dekker et al., 2002; Fraser et al., 2015). While these hypotheses are the basis of a large field of research, the discussion about the biological relevance of these findings is still ongoing.

I.1.3 Chromatin has to be a dynamic structure: assembly, remodeling, and modifications

Chromatin is the native template for all biological processes, that need access to the genetic information. The findings that nucleosomes negatively influence transcription *in vitro* (Knezetic and Luse, 1986; Lorch et al., 1987) and that histone (tail) deletions affect the expression of specific genes (Han and Grunstein, 1988; Kayne et al., 1988) already showed that chromatin has to be a dynamic, but well controlled structure.

I.1.3.1 Chromatin assembly

During replication not only DNA but also the histone content of the cell is duplicated. The assembly of chromatin on newly synthesized DNA relies on two processes: one recycling old histones (see section I.1.3.4) and one which introduces newly synthesized histones. The latter is described subsequently. A very important factor for chromatin assembly is CAF-1 (chromatin assembly factor 1). This evolutionary conserved complex is needed for the deposition of newly synthesized histones H3-H4 on nucleosome free DNA after

replication (Smith and Stillman, 1989). It is recruited to DNA via PCNA (proliferating cell nuclear antigen) (Shibahara and Stillman, 1999) and is supported by a histone chaperone named Asf1 (anti silencing function 1) (Mello et al., 2002; Tyler et al., 1999). Histones H2A-H2B are assembled to complete the nucleosomes via the NAP1 (nucleosome assembly protein 1) chaperone which is possibly supported by FACT (facilitates chromatin transcription) (Krogan et al., 2006; Zlatanova et al., 2007). However, the incorporation of H2A-H2B to the nucleosome could also happen outside of S-phase (Kimura and Cook, 2001). Interestingly, a highly conserved histone tail PTM was shown to be involved in nucleosome assembly (Sobel et al., 1995). Massive acetylation of histones takes place during S-phase and newly synthesized histones are acetylated in the cytoplasm before transport to the nucleus (Jackson et al., 1976; Osley, 1991; Ruiz-Carrillo et al., 1975; Sobel et al., 1995). The acetylation of histones before assembly of the nucleosome may have different functions. First, it could function in neutralization of the positive charge of histones and thus the prevention of non-specific and non-positioned histone-DNA interactions leading to a better targeting of newly synthesized histones to replication forks (Adams and Kamakaka, 1999; Roth and Allis, 1996) and second, since the chaperone CAF-1 preferentially uses acetylated histones (Kaufman et al., 1995; Verreault et al., 1996) this modification could be a direct link between histone synthesis and histone deposition upon replication.

I.1.3.2 Chromatin remodeling

Nucleosomes impair the access to DNA, and thus have to be removed to enable certain nuclear processes. Nucleosome removal can be achieved by complete disassembly of the nucleosome, partial eviction of histone subunits, or sliding of nucleosomes to different sites and is called chromatin remodeling. Specialized enzymes (chromatin remodelers) use the energy from ATP hydrolysis to catalyze these processes (Figure 6) (Clapier and Cairns, 2009). There are five properties shared among all chromatin remodelers: First, they show a high affinity to nucleosomes, second, they are able to recognize PTMs, third, they have a DNA-dependent ATPase domain, fourth, they have subunits regulating the ATPase domain, and fifth, they are enabled to interact with other chromatin modifiers or transcription factors (Clapier and Cairns, 2009). Even if some properties are shared among the chromatin remodelers, there are other properties that lead to a categorization into four superfamilies. The SWI/SNF family has many different functions in sliding and eviction of nucleosomes, but is not involved in chromatin assembly (Mohrmann and Verrijzer, 2005). ISWI family remodelers establish nucleosome spacing during chromatin assembly, and randomize nucleosome positioning

during transcription. Members of the CHD family are mainly involved in the sliding or eviction of nucleosomes to facilitate transcription, but were also shown to have repressive functions (Marfella and Imbalzano, 2007). The INO80 family members are involved in transcription activation and DNA repair and the INO80 related SWR1 leads to incorporation of the H2A.Z histone variant into nucleosomes (Bao and Shen, 2007).

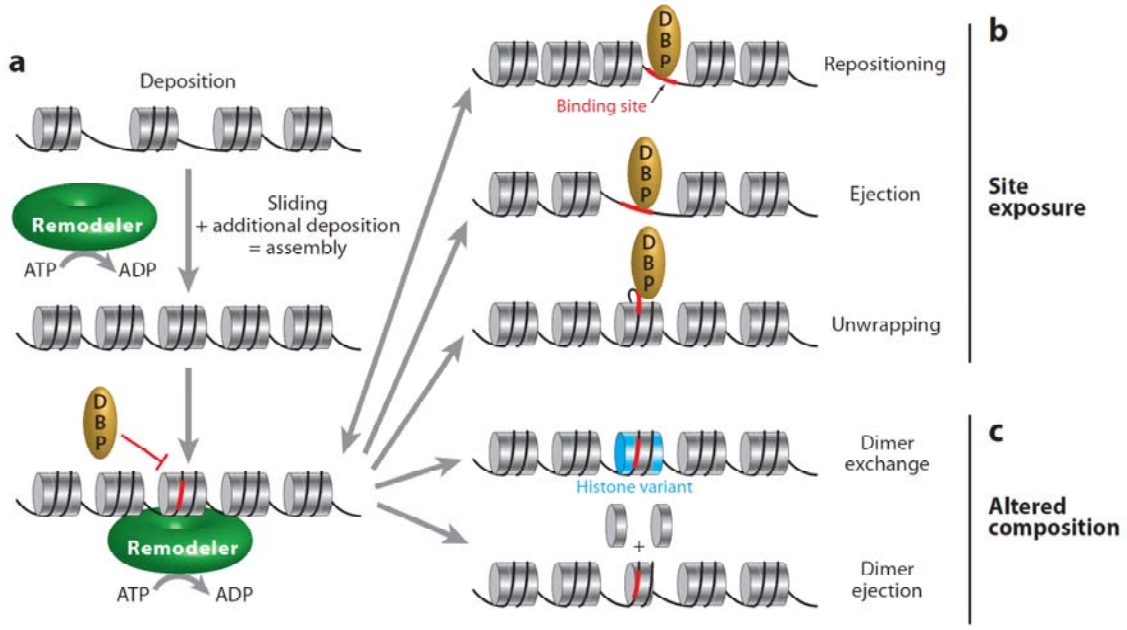

Figure 6: Chromatin remodeler functions

Chromatin remodeling complexes are depicted in green, DNA binding proteins (DBP) in yellow with their binding sites in red, and histone variants are shown in blue. Canonical histones are shown in grey and DNA in black. Remodelers can assist in nucleosome assembly (a), can lead to site exposure to other DNA binding proteins (b), or act on the alteration of nucleosome composition (c).(from Clapier and Cairns, 2009)

Chromatin remodelers are involved in DNA-dependent processes like chromatin assembly, chromosomal dosage compensation, formation of larger chromosomal domains and insulations, DNA replication, DNA repair, chromosome segregation, repression of genes, as well as initiation and elongation of transcription (Clapier and Cairns, 2009). The recruitment of remodelers to specific nucleosomes is achieved by different domains of the remodelers that recognize histone PTMs, such as bromodomains recognizing acetylated and CHD domains recognizing methylated lysines (Clapier and Cairns, 2009).

I.1.3.3 Chromatin modifications

There are two main ways of modifying nucleosomes - the introduction of posttranslational modifications to histones, and the replacement of the canonical histones with variants.

Most PTMs have in common, that they are dynamic signals of chromatin, established by a writer (enzyme complex that sets the modification), possibly used by a reader (enzyme

complex that recognizes the modification and leads to downstream effects), and removed by an eraser (enzyme complex antagonizing the writer) (Marmorstein and Zhou, 2014). The mode of action of chromatin posttranslational modifications is twofold: on the one hand, they can directly lead to a reduction or increase of chromatin stability by decreasing or increasing histone-histone or histone-DNA contacts, on the other hand they can lead to recruitment of nonhistone proteins with enzymatic activity (Kouzarides, 2007). As the table in Figure 7 shows many different histone PTMs have been found that are involved in DNA-dependent process regulation, but acetylation is the best studied (Grunstein, 1997).

Chromatin Modifications	Residues Modified	Functions Regulated
Acetylation	**K**-ac	Transcription, Repair, Replication, Condensation
Methylation (lysines)	**K**-me1 **K**-me2 **K**-me3	Transcription, Repair
Methylation (arginines)	**R**-me1 **R**-me2a **R**-me2s	Transcription
Phosphorylation	**S**-ph **T**-ph	Transcription, Repair, Condensation
Ubiquitylation	**K**-ub	Transcription, Repair
Sumoylation	**K**-su	Transcription
ADP ribosylation	**E**-ar	Transcription
Deimination	**R > Cit**	Transcription
Proline Isomerization	**P-cis > P-trans**	Transcription

Figure 7: Posttranslational modifications of histones and processes they are involved
(from Kouzarides, 2007)

The first acetylation and methylation of histones were already reported in 1964 (Allfrey et al., 1964). Many enzymes catalyzing the transfer of these groups to the lysine/arginine-rich histones have been classified as histone acetyl-, or methyltransferases, even if other proteins have subsequently been identified as alternative targets. Thus it was proposed to rename these enzymes to a more general definition (Allis et al., 2007; Glozak et al., 2005). Today, acetylation is thought to be the most important PTM besides phosphorylation and has been shown to regulate many different cellular processes (Choudhary et al., 2009). Acetylation on lysine residues is written by HATs or KATs (histone or lysine acetyl transferases) and removed by HDACs or KDACs (histone or lysine deacetylases). HATs transfer an acetyl group to the ε-amino group of lysine residues using acetyl-CoA as cofactor (Bannister and Kouzarides, 2011). They can be grouped in three major classes: GNAT (Gcn5-related N-acetyltransferase) (Neuwald and Landsman, 1997), MYST, and p300/CBP families (Drazic et al., 2016). The GNAT family contains amongst others the yeast Gcn5 homologs of higher eukaryotes, PCAF, Hat1, and Elp3. In the MYST family are MOZ, Sas3, Sas2, and Tip60 (yeast NuA4). Grouped to the p300/CBP family are only p300 and CREB binding protein (CBP) (Drazic et al., 2016; Ehrenhofer-Murray, 2004). The effects of acetylation on chromatin vary from a

direct reduction of DNA-histone interaction by neutralizing the positive load of the lysine chain and thus reducing the interaction with the phosphodiester groups of DNA (Dion et al., 2005; Wang and Hayes, 2008) to the recruitment of other enzymes such as the chromatin remodeling complexes SWI/SNF (Hassan et al., 2001, 2002). In general, histone acetylation is linked to transcriptional activity (Li et al., 2007). The erasers of acetyl lysine marks are the histone or lysine deacetylases (HDACs or KDACs). HDACs are grouped into four classes: Class I-III have been classified based on their similarity to the yeast enzymes, Rpd3 (class I), Hda1 (class II), or Sir2 (class III), whereas the human HDAC11 is the only member of class IV (Drazic et al., 2016; Ehrenhofer-Murray, 2004; de Ruijter et al., 2003; Seto and Yoshida, 2014). All enzyme classes except class III are Zn^{2+} dependent, while enzymes belonging to class III need NAD^{+} as cofactor (Buck et al., 2004; Drazic et al., 2016).

Another posttranslational modification of histone tails that plays important roles in chromatin regulation is lysine methylation. HKMTs (histone lysine methyltransferases) contain all a so called SET domain and use SAM (S-Adenosylmethionine) to transfer a methyl group to the ε-amino group of a lysine residue. First, the existence of demethylases has been doubted, but in the recent years identification of different demethylation pathways showed that also methylation is a dynamic chromatin mark (Bannister and Kouzarides, 2011; Ehrenhofer-Murray, 2004; Kouzarides, 2007). Methylation has different influences on transcriptional activity: some methyl-marks lead to repression, while others lead to activation (Li et al., 2007).

The chromatin landscape can further be modified by the incorporation of histone variants in nucleosomes. Other than the canonical histones (Marzluff et al., 2002), most histone variant genes are not selectively expressed during S-phase. Instead, these variants may be incorporated into nucleosomes at specific cell cycle phases or during replication, repair, or transcription processes and their assembly often involves specialized histone chaperones (Bönisch and Hake, 2012; Groth et al., 2007a; Henikoff and Ahmad, 2005; Kamakaka and Biggins, 2005; MacAlpine and Almouzni, 2013).

I.1.3.4 Chromatin dynamics during transcription and replication

I.1.3.4.1 Chromatin dynamics during transcription

Transcription by all RNA polymerases, including the eukaryote specific RNA polymerase II (Pol II), can be divided in three major steps. First, the polymerase finds and binds specific promoter sequences of the gene: the initiation phase (Sainsbury et al., 2015). Second, it starts to transcribe the gene: the elongation phase (Jonkers and Lis, 2015).

And third, the polymerase has to be released from the gene and has to release the transcript: the termination phase (Porrua and Libri, 2015).

Especially in the first two phases chromatin structure can operate in a regulative manner. Early studies on chromatin and transcription showed that nucleosomes prevent transcription initiation (Han and Grunstein, 1988; Knezetic and Luse, 1986; Lorch et al., 1987) and promoters and enhancers of active genes are hypersensitive to DNase I digest (Wu et al., 1979). Thus, it was suggested that promoters of actively transcribed genes have to be nucleosome free. However, this view had been challenged by the idea that special forms of the nucleosome exist, which are established by chromatin remodeling enzymes and allow transcription initiation (Paranjape et al., 1994). The modern view, of transcription initiation in the chromatin context is a complex interplay between the presence of AT rich sequences and thus reduced nucleosome stability at the promoter regions of many genes (Drew and Travers, 1985; Segal et al., 2006), histone posttranslational modifications like acetylation or methylation (Pokholok et al., 2005; Workman and Kingston, 1998), incorporation of histone variants (Ranjan et al., 2013; Zhang et al., 2005), and the maintenance of an initiation competent promoter chromatin conformation by chromatin remodeling enzymes (Ganguli et al., 2014; Hartley and Madhani, 2009). It was shown that the eviction of one H2A-H2B dimer from the nucleosome is sufficient to allow Pol II transcription elongation through chromatin and FACT is the complex which renders this process (Belotserkovskaya et al., 2003; Hsieh et al., 2013; Kireeva et al., 2002; Kulaeva et al., 2009). Additionally, Asf1 was shown to promote histone eviction during transcription (Mousson et al., 2007).

However, also PTMs play a role in transcription elongation. Figure 8 gives an overview about histone modifications that are implicated in transcriptional activation or repression suggesting a role of PTMs in the fine tuning of gene expression.

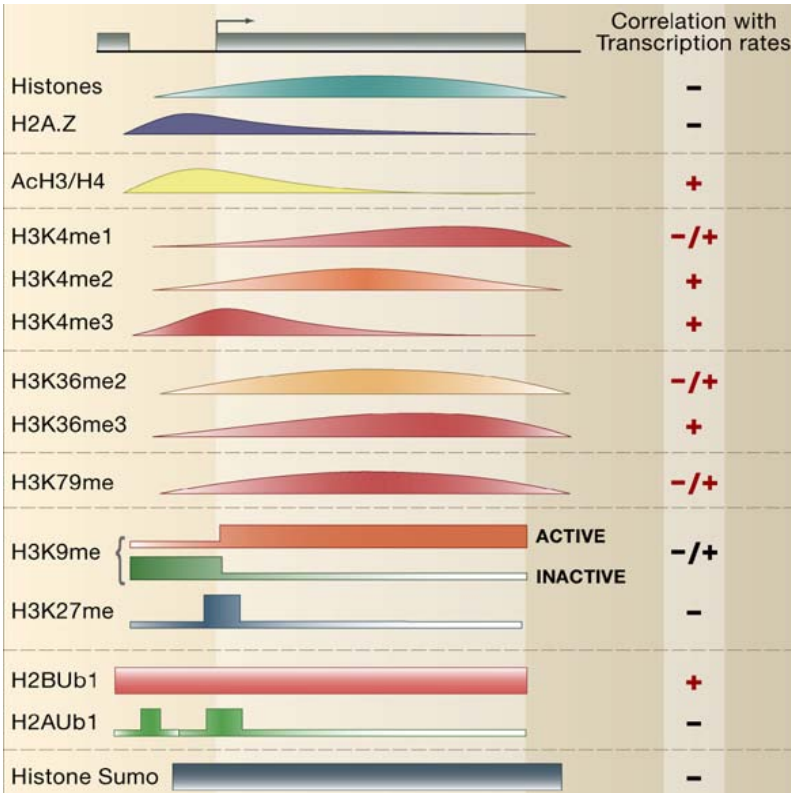

Figure 8: Genome-wide histone PTMs that function in transcriptional activation or repression

The curves represent the relative genome-wide frequency of histone molecules or PTMs throughout an arbitrary gene. In the right panel it is indicated if the respective histone molecule or PTM is correlated with gene repression (-) or activation (+). (from Li et al., 2007)

I.1.3.4.2 Chromatin dynamics during replication

Another DNA dependent process involving drastic dynamic transitions in chromatin structure is DNA replication. After replication initiation, nucleosomes are disassembled into $(H3\text{-}H4)_2$ tetramers or H3-H4 dimers and H2A-H2B dimers ahead of the replication fork, while in the wake of the fork, a mix of old and newly synthesized histones is used to deposit new nucleosomes onto the daughter strands (Annunziato, 2005; Gruss et al., 1993; Jackson, 1988; Sogo et al., 1986). Eukaryotic replisomes contain different histone chaperones (Alabert and Groth, 2012) such as Asf1 and FACT (Abe et al., 2011; Groth et al., 2007b; Tyler et al., 1999; Wittmeyer and Formosa, 1997; Wittmeyer et al., 1999) that accept the $(H3\text{-}H4)_2$ tetramers (or dimers respectively) or the H2A-H2B dimers and pass them on to CAF-1 (Shibahara and Stillman, 1999; Smith and Stillman, 1989). Since parental histones are deposited within approximately 400bp on the nascent DNA, the inheritance of epigenetic marks might be ensured (Perry et al., 1993; Radman-Livaja et al., 2011). However, the exact mechanisms of inheritance of chromosomal marks is still under discussion. At least two possible modes are discussed in the following (Whitehouse and Smith, 2013). One is dependent on the parental histones and predicts that some of the old histones associated with a certain genomic locus carrying the

corresponding PTM are transmitted to the daughter strands in the wake of the replication fork. These modified histones are then recognized by specialized enzymes that establish this PTM onto nearby nucleosomes, leading to local maintenance of chromatin marks. An example for this mechanism is H3K9me3 (Canzio et al., 2011). The second possible mode is that PTMs on histones are removed before or during replication and the nucleosomes on the nascent DNA strands gain their modifications via nonhistone proteins that recognize specific elements within the DNA. For information about the assembly of newly synthesized histones into chromatin see section I.1.3.1.

I.1.3.4.3 Model loci for the investigation of chromatin dynamics

From this overview it is obvious that chromatin research has to deal with a vast amount of factors that influence chromatin establishment, maintenance and dynamics. Importantly, the factors and machineries acting on chromatin can be reciprocally influenced by the local chromatin state. Chromatin dynamics can be investigated either on a genome wide level using high throughput methods, or at the level of single genes or loci. In yeast, several model loci have served as a paradigm for defined chromatin transitions such as the *PHO5* locus as a single gene locus (Korber and Barbaric, 2014), or the ribosomal DNA (rDNA) locus as a multicopy gene locus (Conconi, 2005; Conconi et al., 1989; Dammann et al., 1993).

I.2 The ribosomal RNA gene locus

In a growing cell approximately 50% (in yeast up to 80%) of the total RNA production is dedicated to ribosomal RNA (rRNA) to cover the cells demand for millions of ribosomes. Due to the large costs a cell invests in the production of ribosomes, ribosome biosynthesis has to be a well controlled and regulated process that can rapidly adapt to growth, environmental, or developmental changes. Besides the control of ribosomal protein synthesis, regulation on the level of rRNA production is one of the cellular switches to meet this need (Grummt, 2003; Moss, 2004; Moss and Stefanovsky, 2002; Warner, 1999).

I.2.1 The nucleolus as the site of ribosome biogenesis

Other than protein coding genes, the rRNA genes are not transcribed by Pol II, but specialized RNA polymerases: RNA polymerase III (Pol III) and RNA polymerase I (Pol I). The latter primarily dedicated to transcribe the large rRNA precursor (47S in mammals, 35S in yeast) (Nogi et al., 1991a). Additionally, transcription of rRNA takes

place in a specialized nuclear compartment, the nucleolus. The nucleolus is the site where rRNA, dedicated ribosomal biogenesis factors and some of the ribosomal proteins meet to assemble into the first precursors of the large and small ribosome subunits (Mélèse and Xue, 1995). However, since the nucleolus harbors many proteins not involved in ribosome biogenesis, nucleoli may have other functions beyond the production of ribosomes (Andersen et al., 2005; Pederson, 1998; Politz et al., 2002; Visintin and Amon, 2000).

Depending on different factors such as cell cycle state, growth conditions, cellular age, or organism each cell contains at least one nucleolus that is in mammals structured in three subcompartments as defined by electron microscopy: the fibrillar centers (FC), the dense fibrillar compartment (DFC), and the granular compartment (GC). Pol I transcription takes place at the transition from FC to DFC, transcripts are enriched in the DFC and are then passed on to the GC where assembly of pre-ribosomes takes place (Fatica and Tollervey, 2002; Hernandez-Verdun, 2006; Raska et al., 2006; Raška et al., 1995, 2006; Scheer and Hock, 1999). In yeast there is consistently only one nucleolus found that has potentially only a bipartite structure (fibrillar and granular compartments) and is in close vicinity to the nuclear envelope (Thiry and Lafontaine, 2005). It covers up to one third of the nucleus and is crescent-shaped (Léger-Silvestre et al., 1999; Yang et al., 1989). Additionally, it was found that the nucleolar morphology changes in specific Pol I mutant strains indicating that Pol I - apart of its function in rRNA synthesis - could have a structural role in the formation of the nucleolus (Oakes et al., 1993).

I.2.2 Structure of the rDNA locus in yeast

In haploid yeast cells only one nucleolus is formed, which contains the rDNA, located in one cluster of many transcription units on the right arm of chromosome twelve. In this cluster 150 to 200 rRNA gene copies are arranged head to tail towards the centromere (Hamperl et al., 2013; Petes, 1979; Petes and Botstein, 1977; Philippsen et al., 1978). Each copy contains several important genetic (*cis*-) elements within a size of 9.1kb (Figure 9). Thus, the rDNA accounts for approximately 10% of the yeast genome (Warner, 1989). In addition to the chromosomal rDNA repeats small extrachromosomal rDNA circles (ERCs) containing one or more rRNA gene copies have been identified (Meyerink et al., 1979) and were suggested to play a role in cellular aging (Kaeberlein, 2010; Sinclair and Guarente, 1997). ERCs most likely originate due to the genomic instability of the rDNA locus and may be involved in a process which guarantees a

constant rDNA copy number despite ongoing recombination events (Kobayashi, 2006, 2011).

Each rDNA copy of the array except the telomere-proximal consists of 6.6kb coding for the large rRNA precursor and an intergenic spacer (IGS; sometimes referred to as non transcribed spacer: NTS) which is divided in two parts (IGS1 and IGS2) by the 5S rRNA gene which is transcribed by Pol III (Srivastava and Schlessinger, 1991; Venema and Tollervey, 1999; Warner, 1989). The telomere-proximal copy is only 3.6kb in size and contains the 5S rRNA gene in a modified form (McMahon et al., 1984). 35S as well as 5S rRNA genes are contained within one rDNA repeat unit, but are transcribed in different directions. Such a configuration is only found in a few organisms, but might have been the initial arrangement before – as found in higher eukaryotes - 5S and large rRNA precursor genes were separated to different loci (Haeusler and Engelke, 2006; Srivastava and Schlessinger, 1991).

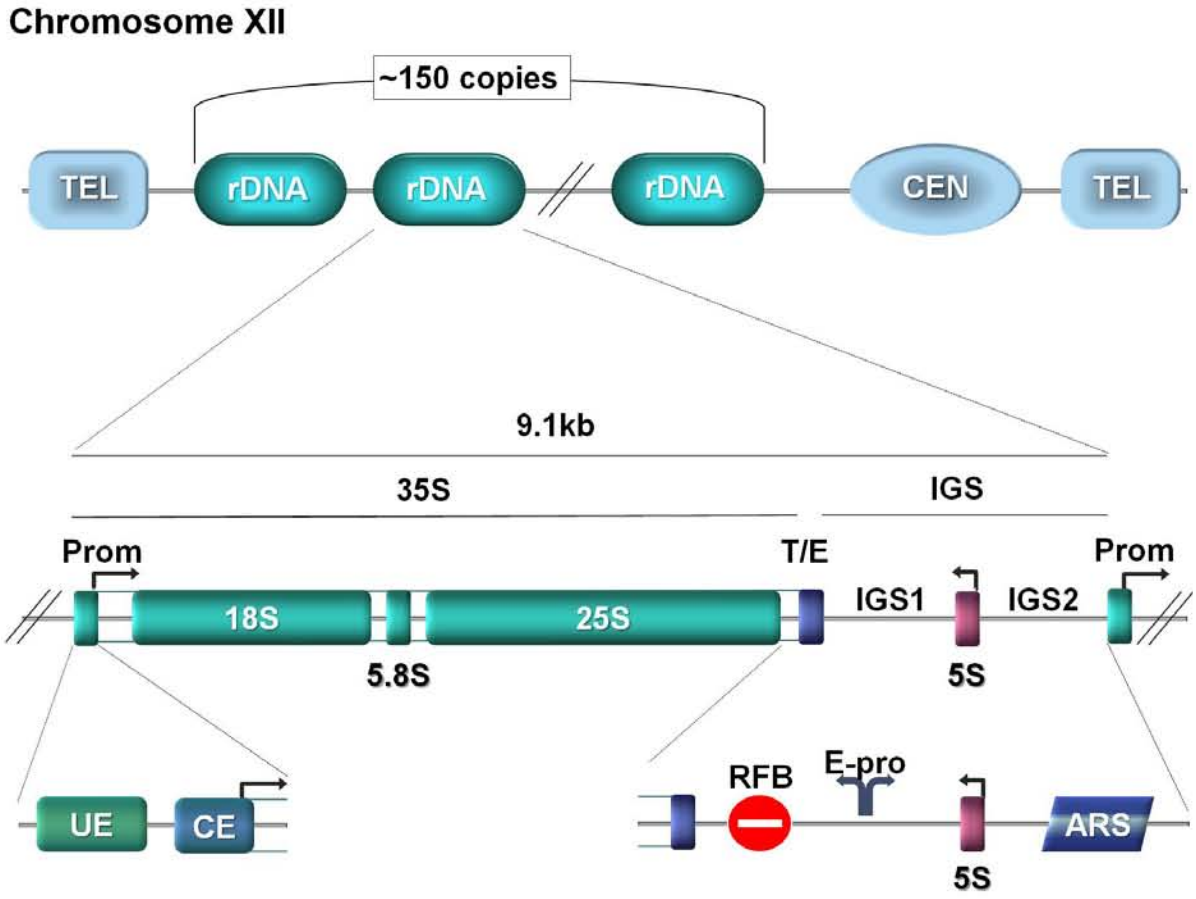

Figure 9: The rDNA locus of *Saccharomyces cerevisiae*

Scheme of the yeast rDNA locus on chromosome XII. Telomere (TEL) and centromere (CEN) location are indicated as grey squares or ovals. rDNA copies are indicated as petrol colored ovals. In the middle part one copy is depicted in more detail: It is 9.1kb in size and consists of the Pol I transcribed 35S rRNA (which is later processed to the 18S, the 5.8S, and the 25S rRNA) gene locus and the intergenic spacer (IGS) which is separated in two parts (IGS1 and 2) by the Pol III transcribed 5S rRNA gene (transcription start sites and

directions of the polymerases are indicated by black arrows). The terminator (T) is located at the 3' end of the 35S rRNA gene and overlaps with the enhancer region (E). At the bottom the 35S rRNA gene promoter (Prom) and the IGS region are shown in detail: The promoter consists of the upstream element (UE) and the core element (CE). Within IGS1 the replication fork barrier (RFB) and the bidirectional Pol II promoter (E-pro) are shown. The autonomously replicating sequence (ARS) is depicted in IGS2. (modified from Babl, 2012; Goetze et al., 2010; Wittner, 2012)

One of the elements contained in the IGS is an autonomously replicating sequence (Figure 9, ARS). It is located a few hundred base pairs upstream to the Pol I initiation site and replication proceeds bidirectionally. However, it was shown that only approximately one out of three ARSs fires during one S phase and a positive correlation between replication start and transcriptional activity of the downstream 35S rRNA gene was suggested (Fangman and Brewer, 1991; Muller et al., 2000). Replication commences while rRNA gene transcription is still ongoing (Saffer and Miller, 1986). Whereas the replication fork moving towards the 35S rDNA promoter is unidirectional with Pol I transcription, the replication fork moving towards the 3' end of the 35S rRNA moves in the opposite direction of Pol I transcription. This fork is blocked at the replication fork barrier (Figure 9, RFB), which is located in IGS1 near the 3' end of the 35S rRNA gene presumably to avoid collision of both machineries (Brewer and Fangman, 1988; Brewer et al., 1992; Kobayashi et al., 1992). Fob1 (fork blocking protein 1) was shown to be required for efficient stalling of the replication machinery (Kobayashi, 2003; Kobayashi and Horiuchi, 1996) and plays also a role in recombination events at the rDNA that influence copy number and ERC formation (Kobayashi et al., 1998). A third *cis*-element contained also in the IGS1 is a bidirectional Pol II promoter called expansion promoter (Figure 9, E-pro). Transcription from this promoter is normally repressed by Sir2 (component of the RENT complex, see section I.2.4). If this repression is incomplete, upregulated Pol II transcription probably interferes with sister-chromatid cohesion and leads to rDNA instability and potentially cellular senescence (Ganley et al., 2005; Kobayashi, 2006; Saka et al., 2013; Santangelo et al., 1988).

Transcription of Pol I yields the large rRNA precursor (35S pre-rRNA) which is processed to the mature 18S, 5.8S, and 25S rRNAs upon later steps of ribosome biosynthesis. The 35S pre-rRNA contains a 5' external transcribed spacer (ETS1), one internal transcribed spacer (ITS1) between the 18S and the 5.8S sequence, one ITS between the 5.8S and the 25S sequence (ITS2), as well as a 3' ETS (ETS2) (Fromont-Racine et al., 2003; Srivastava and Schlessinger, 1991; Venema and Tollervey, 1999). The transcription of the 35S rRNA is under the control of different regulatory elements. The Pol I promoter is located between -146 and +8 bp from the transcription start site and is divided in three domains, which is a difference to the two domain promoter in higher eukaryotes: the core

promoter region or core element (Figure 9, CE) (bp -28 to +8) and the upstream element (Figure 9, UE) which is itself bipartite (one domain from -146 to -91 and the second domain from -76 to -51) (Kempers-Veenstra et al., 1985; Keys et al., 1996; Kulkens et al., 1991; Musters et al., 1989; Planta, 1997) (see section I.2.4.1 for detailed information about the Pol I pre-initiation complex and transcription initiation). At the 3' end of the 35S coding region is the terminator region, which partly overlaps with an enhancer region. 90% of transcription stops at the main termination site (93bp downstream of the 25S 3' end) which consists of a T-rich element and a Reb1 binding site, but a second fail-safe termination site (T-rich 2) is another 250bp downstream at the beginning of the RFB (Lang et al., 1994; Reeder and Lang, 1997; Reeder et al., 1999; van der Sande et al., 1989). More recent studies suggested that not Reb1 binds to the Reb1 binding site *in vivo,* but the Reb1 homolog Nsi1, and that this protein is important for efficient Pol I transcription termination *in vitro* and *in vivo* (Merkl et al., 2014; Reiter et al., 2012). However, efficient termination seems to be dispensable for rRNA processing and ribosome synthesis as revealed by a study where the deletion of termination sites did not affect cell growth (Wai et al., 2001). The enhancer region partly overlaps with the terminator region and was originally found to increase Pol I transcription 15 to 30 fold (Elion and Warner, 1984, 1986). The so called "ribomotor" model was suggested in which the terminator/enhancer region is important for efficient recycling of Pol I and/or transcription factors due to a looping of rDNA copies or by keeping the spatial organization of copies in an optimal way (Kempers-Veenstra et al., 1985; Kulkens et al., 1992). Even if it was first thought that Reb1 might act as a factor in the "ribomotor" since it has one binding site within the enhancer region and one in proximity to the promoter region it was later shown that this is not the case (Kulkens et al., 1989). Nevertheless, the Pol I transcription enhancing function of this region was later questioned at all (Wai et al., 2001).

I.2.3 Chromatin states of the large rRNA precursor genes

While the IGS region of the rDNA appears to be uniformly assembled into nucleosomes, at least two different chromatin states exist for the 35S rRNA gene copies: an actively transcribed, nucleosome depleted state and a transcriptionally inactive, nucleosomal state (Hamperl et al., 2013; Lucchini and Sogo, 1998).

Among the first methods to analyze rDNA chromatin were electron micrographs of actively transcribed large rRNA precursor genes. In these chromatin Miller spreads (named after the investigator who developed this technique) (Miller and Beatty, 1969)

actively transcribed rDNA genes from a large variety of different organisms share an almost identical “Christmas tree”-like appearance (Figure 10 top) (Borkhardt and Nielsen, 1981; Foe et al., 1976; Scheer and Benavente, 1990; Scheer et al., 1977; Trendelenburg et al., 1973): In these electron micrographs, the rDNA and the tightly packed Pol I molecules represent the "stem" of the tree, the nascent rRNAs represent the "branches" of the tree, and even "Christmas baubles" at the end of the branches are formed by co-transcriptionally assembling ribosomal proteins and ribosome biogenesis factors.

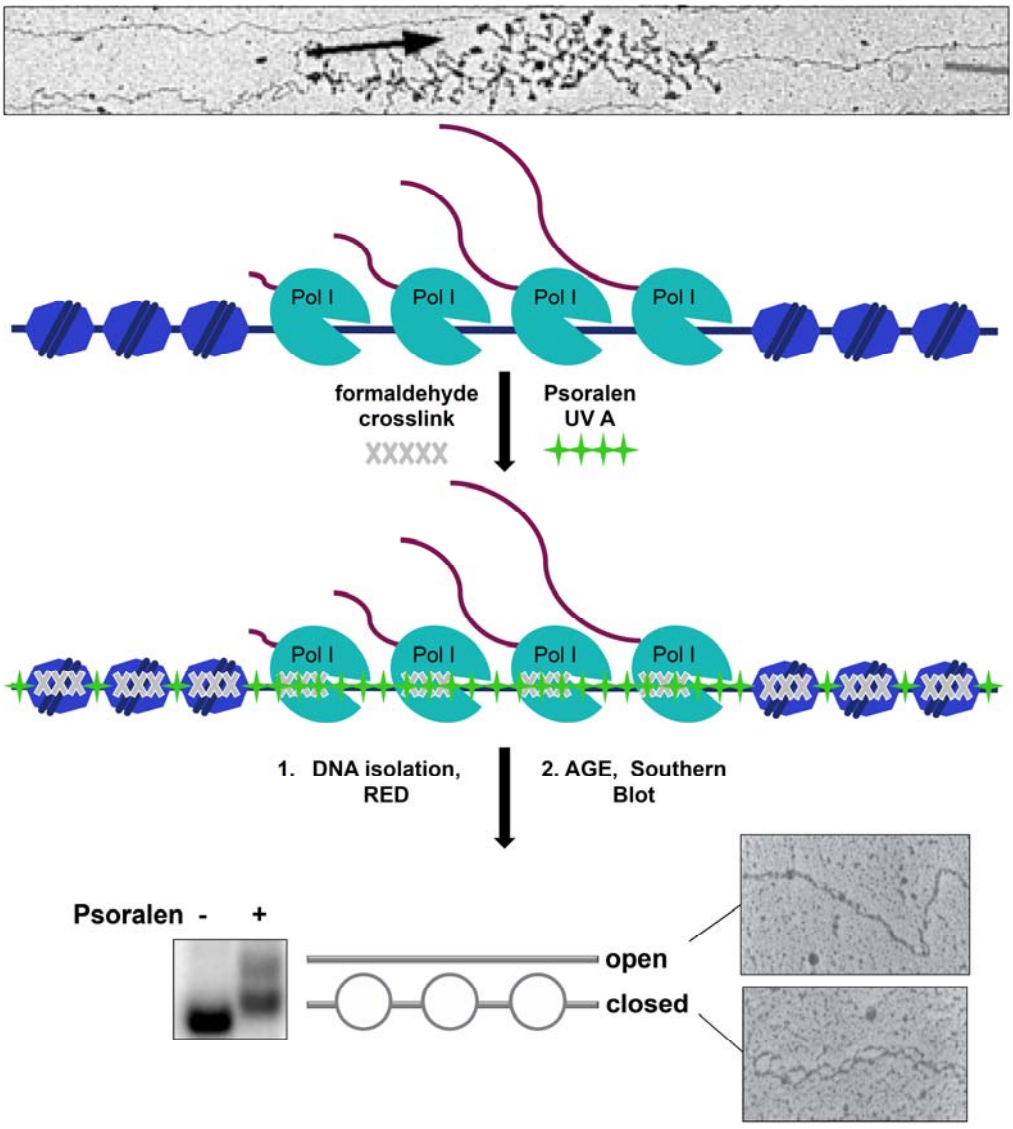

Figure 10: Chromatin states at the yeast rDNA locus as revealed by psoralen photocrosslinking

At the top a chromatin Miller spread is shown (from French et al., 2003) where the arrow indicates transcription start and direction of one actively transcribed rDNA copy. DNA is shown as a dark blue line. Copies are either nucleosomal (blue octamers) or actively transcribed (turquoise Pol I) and rRNA is transcribed (purple lines). For simplicity the nucleosomal IGS is not indicated. After formaldehyde crosslink of proteins to DNA (grey crosses) the nuclei are irradiated with UV light in the presence of psoralen (green crosses). Psoralen preferentially crosslinks nucleosome free DNA. After DNA isolation and restriction enzyme digest (RED) agarose gel electrophoresis (AGE) separates one slow (open) and one faster (closed) migrating band -if psoralen was added-

as detected in a Southern blot with a probe against the 35S rRNA genes. In the right panel another method of detection is shown: here the purified fragments are detected by electron microscopy under denaturing conditions. The closed copies appear as consecutive single stranded DNA bubbles (due to psoralen crosslink takes only place in the linker DNA between nucleosomes) and the open copies appear as a rod like structure (due to a full psoralen crosslink).(modified from Babl, 2012; Dammann et al., 1993)

Another possibility to investigate chromatin structure uses the fact that the nucleosome protects the assembled DNA against nuclease digestion (Hewish and Burgoyne, 1973). Even if the analysis of the rDNA locus with this method yielded no apparent difference to other genomic loci in some studies (Culotta and Sollner-Webb, 1988; Jones et al., 2007; Lohr, 1983), other studies already hinted towards a somewhat more specific and alternative chromatin structure at the rDNA in dependence of the transcriptional state (Conconi, 1987; Davis et al., 1983; Johnson et al., 1978, 1979; Muscarella et al., 1987; Prior et al., 1983).

With the use of psoralen photocrosslinking analysis (Figure 10) clear evidence for at least two different chromatin states at the large rRNA precursor genes was obtained (Conconi et al., 1989; Dammann et al., 1993; Toussaint et al., 2005).

Psoralen is a DNA intercalating drug which mainly intercalates in nucleosome-free DNA as it is present at promoters, replication origins, enhancers, or linker DNA between nucleosomes (Hanson et al., 1976; Sogo et al., 1984, 1986). Upon irradiation with UV-A light psoralen induces covalent bonds between the two single DNA strands. Additionally, psoralen incorporation leads to a changed electrophoretic mobility in native agarose gel electrophoresis (AGE). The more psoralen is bound between DNA, the slower the fragment migrates in AGE. For the large rRNA precursor gene copies two populations of crosslinked DNA can be observed in exponentially growing cells. One slow migrating fraction, which was described as mainly nucleosome depleted, but associated with Pol I and the Pol I related high mobility group box protein Hmo1, and one faster migrating fraction that is associated with histones (see next section for detailed information) (Conconi et al., 1989; Lucchini and Sogo, 1992; Merz et al., 2008; Wittner et al., 2011). Additionally, psoralen crosslinked 35S rRNA genes have been investigated with electron microscopic analysis under denaturing conditions after agarose gel electrophoresis (Figure 10 bottom right) which further supported that two chromatin states with different psoralen accessibility are existing and the faster migrating band was to a lesser extent crosslinked by psoralen than the slow migrating band (Dammann et al., 1993). The nucleosome depleted state was called the "open" and the nucleosomal state was called the "closed" chromatin state.

I.2.4 Composition and dynamics of yeast rDNA chromatin

Interestingly, the chromatin states of the 35S rRNA genes are dynamic and can be converted into each other under different conditions leading to major changes in their protein composition.

I.2.4.1 Composition of 35S rDNA chromatin

The state-of-the-art technique to analyze chromatin composition is chromatin immunoprecipitation (ChIP) (see Figure 27 and associated section for details) (Collas, 2010). ChIP allows to draw quantitative conclusions about the association of a protein of interest with the rDNA, but with this technique one is not able to distinguish between the chromatin states and thus, the chromatin composition of the individual chromatin states remains unclear. A well suited method for the analysis of association of a protein with rDNA copies in a specific chromatin state is the combination of chromatin endogenous cleavage (ChEC) and psoralen photocrosslinking (ChEC-psoralen) (see Figure 23 and associated section for details) (Goetze et al., 2010; Griesenbeck et al., 2012; Merz et al., 2008; Wittner et al., 2011). Many protein factors associating with the 35S rRNA gene copies have been identified genetically or by a more recent comprehensive proteomic analysis (Hamperl et al., 2014) (see Figure 11 for an overview about some of the proteins at the 35S rRNA gene promoter region). Some of these are described in more detail in the next sections.

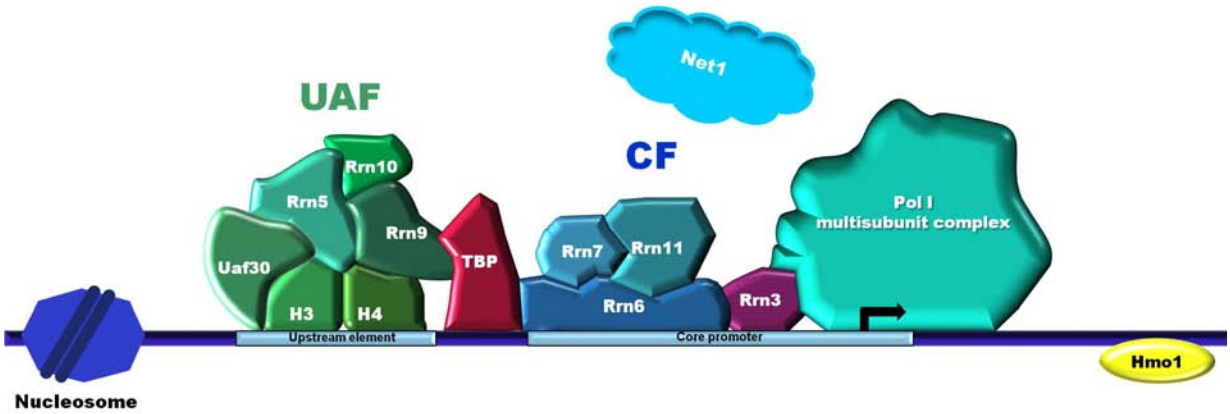

Figure 11: Components of the rDNA promoter region

DNA is depicted as a dark blue line, special DNA sequences are colored in light blue and their name is indicated. Upstream to the promoter region a nucleosome is indicated (blue octamer with DNA around it). The transcription initiation factors are colored and the names of the subunits are indicated: Upstream activating factor (UAF) subunits green, TBP red, core factor (CF) subunits blue, Rrn3 purple. The Pol I multisubunit complex is shown in turquoise. Two additional factors, implicated in Pol I transcription are indicated: Hmo1 in yellow and Net1 in light blue. See text for detailed information about the single components. (modified from Babl, 2012; Moss, 2004; Schneider, 2012)

I.2.4.1.1 RNA polymerase I

Pol I is a multisubunit complex consisting of 14 proteins. Some of these proteins are shared among polymerases I, II, and III but some are specific for Pol I (Figure 12) (Cramer et al., 2008; Vannini and Cramer, 2012). It is likely that it is due to these specific subunits that Pol I specifically transcribes the 35S rRNA gene (Viktorovskaya and Schneider, 2015).

Subunit name	Mass (kDa)	Pol I	Pol II	Pol III
A190	186.4	*RPA190*	*RPB1*	*RPC160*
A135	135.7	*RPA135*	*RPB2*	*RPC128*
A43	36.2	*RPA43*	*RPB7*	*RPC25*
A14	14.6	*RPA14*	*RPB4*	*RPC17*
A12	13.7	*RPA12*	*RPB9*	*RPC11*
AC40	37.7	*RPC40*	*RPB3*	*RPC40*
AC19	16.1	*RPC19*	*RPB11*	*RPC19*
ABC27	25.1	*RPB5*	*RPB5*	*RPB5*
ABC23	17.9	*RPB6*	*RPB6*	*RPB6*
ABC14.5	16.5	*RPB8*	*RPB8*	*RPB8*
ABC10α	7.7	*RPB10*	*RPB10*	*RPB10*
ABC10β	8.3	*RPB12*	*RPB12*	*RPB12*
A49	46.6	*RPA49*		*RPC34*
A34.5	26.9	*RPA34*		*RPC31*
				RPC37
				RPC53
				RPC82

Figure 12: Shared and specific subunits of Pol I, II, and III

Shared subunits are shaded in grey: Subunits shared among all polymerases in light grey, subunits shared among Pol I and Pol III in dark grey. (from Schneider, 2012)

The catalytic activity relies as also for Pol II and Pol III on the ten subunit core (A190, A135, AC40, AC19, ABC27, ABC23, ABC14.5, ABC10a, ABC10b, and A12) (Merkl, 2013; Vannini and Cramer, 2012). A12 is important for the intrinsic RNA cleavage activity of Pol I (Kuhn et al., 2007; Ruan et al., 2011). The specific subunits of Pol I fulfill different functions: A43 and A14 form a heterodimer acting as an interaction platform between the polymerase and the initiation factor Rrn3 (see below for detailed information) (Blattner et al., 2011; Engel et al., 2016; Milkereit and Tschochner, 1998; Peyroche et al., 2000; Pilsl et al., 2016). Interestingly, mammalian homologs exist for all subunits except A14 (Shematorova and Shpakovskiĭ, 2002; Yamamoto et al., 2004). A49 and A34 also are found as a heterodimer in structural analyses and are related to the Pol II transcription factors TFIIF and TFIIE (Engel et al., 2013; Fernández-Tornero et al., 2013; Kuhn et al., 2007; Vannini and Cramer, 2012). These subunits were shown to play a role in the recruitment of Rrn3, as well as in its dissociation from Pol I after promoter escape, in the achievement of high Pol I loading rates, in promoter dependent transcription, and for general Pol I activity (Albert et al., 2011; Beckouet et al., 2008; Geiger et al., 2010;

Hanada et al., 1996; Liljelund et al., 1992). Additionally, Rpa49 is potentially involved in overcoming of obstacles such as nucleosomes during transcription elongation (Geiger et al., 2010; Merkl, 2013).

Accordingly, to date Pol I transcription is the only process which is required for the conversion of the closed to the open rDNA chromatin state (Dammann et al., 1995; Goetze et al., 2010; Hontz et al., 2008; Merz et al., 2008; Wittner et al., 2011).

In principle Pol I transcription might be regulated at the level of the amount of open rDNA copies or the number of polymerases per actively transcribed gene (Aprikian et al., 2001; Reeder, 1989; Schultz et al., 1992). However, more recent studies hint towards the latter way of regulation. A strong increase in the number of polymerases per gene was found for yeast strains with a reduced rDNA copy number suggesting that the high demand for rRNA can be satisfied by a higher number of polymerases per gene (French et al., 2003). In support to a regulation at the level of Pol I loading, it was found that a strong reduction in Pol I transcription with transition to stationary phase was not correlating with the weaker reduction in the fraction of open copies (Fahy et al., 2005). Additionally, in the absence of the deacetylase Rpd3 Pol I transcription might be strongly downregulated in stationary phase, despite the fact that a major fraction of rDNA copies resides in the open chromatin state (Sandmeier et al., 2002), thus indicating that open copies do not inevitable correspond to high transcriptional activity. Inhibition of the target of rapamycin (Tor) pathway which occurs naturally at the transition to stationary phase downregulating Pol I transcription (Heitman et al., 1991; Zaragoza et al., 1998), also does not lead to a reduction in actively transcribed copies (Claypool et al., 2004). Additional evidence for an uncoupling of Pol I transcription and open rDNA copy number came from the finding that the open rDNA copy number does not change even if Pol I transcription was completely shut off, as long as replication is prevented and the high mobility group box protein Hmo1 is present (Wittner et al., 2011).

I.2.4.1.2 The high mobility group box protein Hmo1

Hmo1 binds to the entire 35S rRNA gene region, but is only associated with open copies (Berger et al., 2007; Hall et al., 2006; Kasahara et al., 2007; Merz et al., 2008).

With some shared characteristics Hmo1 is a *bona fide* homolog of the mammalian upstream binding factor (UBF) (Albert et al., 2012). Pol I transcription is needed to recruit Hmo1 to the rDNA, but even after shutdown of Pol I transcription Hmo1 stays associated with the rDNA (Goetze et al., 2010; Merz et al., 2008; Wittner et al., 2011). It was found to be a genetic suppressor of the growth defect of a Pol I subunit (Rpa49) mutant (Gadal

et al., 2002), but unlike UBF Hmo1 is not necessary for the recruitment of Pol I to the 35S rRNA genes (Mais et al., 2005; Merz et al., 2008; Wittner et al., 2011). Accordingly, these studies showed that the fraction of open copies is not significantly reduced, when *HMO1* is deleted. Hmo1 was found to bind especially nucleosome depleted regions like promoters of highly transcribed genes such as ribosomal protein genes, its association was suggested to play a role in the coordination of the Tor dependent regulation of rRNA transcription and ribosomal protein gene expression, and its association with DNA of specific topology and co-localization with topoisomerase II indicates a role in genome stability (Berger et al., 2007; Bermejo et al., 2009; Hall et al., 2006; Kasahara et al., 2011). It was suggested, that the presence of Hmo1 impairs replication independent nucleosome deposition (Wittner et al., 2011). However, it still has to be declared if Hmo1 is recruited to the rRNA specifically, or if it rather randomly binds nucleosome free DNA and then protects these regions from nucleosome deposition.

I.2.4.1.3 Histones

Histone proteins are the components of nucleosomes, which are the basic repeating units of (rDNA) chromatin (see section I.2.3). However, there has been some controversy in the literature about the nature of open 35S rDNA chromatin. Using ChIP, significant levels of histones were found in unphased nucleosomes even at open 35S rRNA genes (Jones et al., 2007), whereas with the method of ChEC-psoralen histones were found to be largely depleted from the open 35S rDNA fraction, while closed 35S rRNA genes were fully assembled into nucleosomes (Merz et al., 2008; Wittner et al., 2011). It has been speculated that the fraction of nucleosomal 35S rRNA gene copies might play a role in genome stability and protection of DNA (Ide et al., 2010; Kobayashi, 2011).

Additionally, histones H3 and H4 are part of the upstream activating factor (UAF) (Keener et al., 1997) (see next section for detailed information).

Interestingly, in yeast, nucleosomes and thus histones are deposited onto newly synthesized rDNA upon each round of replication even if the replicated rDNA gene copy was formerly actively transcribed and nucleosome depleted (Lucchini and Sogo, 1995; Lucchini et al., 2001).

Despite the core histones, also the putative linker histone Hho1 is associated with the rDNA (Babl, 2012; Freidkin and Katcoff, 2001). Hho1 was suggested to play a role in Pol I processivity on the one hand (Levy et al., 2008) and more generally in chromatin compaction and thus potentially also in rDNA chromatin compaction on the other hand (Bryant et al., 2012; Georgieva et al., 2012; Schäfer et al., 2008).

I.2.4.1.4 The Pol I pre-initiation complex

At least 25 different proteins are involved in proper initiation and transcription of the 35S rRNA genes. The 14 subunits of Pol I (see above), the six subunit complex of the upstream activating factor (UAF), the TATA box binding protein (TBP; in yeast Spt15), the three subunits of core factor (CF), and Rrn3 (Figure 11) (Nogi et al., 1991b; Schneider, 2012). Besides Rrn3 only CF is essential for basal transcription *in vitro*, while UAF and TBP are needed for elevated transcription levels (Keener et al., 1998; Musters et al., 1989; Steffan et al., 1998).

UAF consists of six subunits: Rrn5, Rrn9, Rrn10, Uaf30, and the histones H3 and H4 and is associated with the upstream element (UE) of the promoter (Keener et al., 1997; Keys et al., 1996; Siddiqi et al., 2001). TBP associates probably as bridge between UAF (Rrn9) and CF (Rrn6) (Steffan et al., 1998). CF consists of Rrn6, Rrn7, and Rrn11 and binds to the core element (CE) of the promoter (Keys et al., 1994; Lalo et al., 1996; Lin et al., 1996). Rrn3 interacts with the A43 subunit of Pol I, but was recently shown to have also a DNA binding domain (Blattner et al., 2011; Engel et al., 2016; Milkereit and Tschochner, 1998; Peyroche et al., 2000; Pilsl et al., 2016; Stepanchick et al., 2013).

The recruitment of UAF to the UE is probably possible due to the high DNA binding affinity of the histones, but sequence specificity is mediated by Uaf30 (Goetze et al., 2010; Hontz et al., 2008; Keener et al., 1997; Keys et al., 1996). Interestingly, neither Pol I activity nor CF association is needed for the recruitment of UAF to its binding site (Bordi et al., 2001; Goetze et al., 2010). Rrn5, Rrn9, and Rrn10 are *in vivo* essential for polymerase specificity, since the deletion of these subunits leads to transcription of the 35S rRNA genes by Pol II. Deletion of *UAF30* still allows Pol I transcription besides transcription by Pol II even if the overall promoter structure is drastically changed (Goetze et al., 2010; Hontz et al., 2008; Vu et al., 1999).

TBP alone is not able to stimulate Pol I transcription, but it leads to increased transcription rates in the presence of CF (Bedwell et al., 2012). Interestingly, overexpression of TBP can induce CF dependent transcription at a level close to WT even if UAF is absent (Aprikian et al., 2000).

There are different models for the promoter recruitment of CF. On the one hand it was found that CF stably associates with its binding site once recruited by UAF even in the absence of Pol I transcription (Goetze et al., 2010; Steffan et al., 1996), on the other hand it was suggested that CF binds at and dissociates from the promoter together with Pol I at each transcription cycle (Aprikian et al., 2001; Bordi et al., 2001).

Rrn3 directly interacts with the Pol I subunit A43 and with the CF subunit Rrn6 (Engel et al., 2016; Peyroche et al., 2000; Pilsl et al., 2016; Yamamoto et al., 1996). Interestingly, less than 55% of the total cellular amount of Rrn3 and less than 5% of Pol I are involved in the formation of the initiation competent complex of Rrn3-Pol I (Bier et al., 2004; Milkereit and Tschochner, 1998; Milkereit et al., 1997).

From all of these studies the current model for the Pol I transcription initiation process can be drawn. UAF stably binds to the upstream element. TBP functions as a bridge and leads to the UAF dependent recruitment of CF. After the recruitment of CF, the initiation competent complex of Pol I and Rrn3 is recruited and transcription starts. After transcription started Rrn3 dissociates from Pol I. However, it still remains unclear, if CF and TBP stay associated with the promoter or if they also dissociate and re-initiate for further rounds of transcription (Aprikian et al., 2001; Bordi et al., 2001; Steffan et al., 1996).

I.2.4.1.5 Net1 and the RENT complex

The regulator of nucleolar silencing and telophase exit (RENT) complex consists of three subunits (Net1, Sir2, and Cdc14) and associates at two sites within the rDNA locus: at a region within the IGS1 and at a region at the 35S rRNA gene promoter (Goetze et al., 2010; Huang and Moazed, 2003; Straight et al., 1999). Sir2 was identified as an NAD^+ dependent deacetylase involved in the transcriptional silencing of Pol II at the rDNA (Bryk et al., 1997; Smith and Boeke, 1997). Recruitment of the RENT complex to the rDNA is strictly dependent on Net1, but additionally Fob1 is needed for efficient recruitment to the IGS1 and Pol I is possibly needed for efficient recruitment to the promoter region (Huang and Moazed, 2003; Shou et al., 2001; Straight et al., 1999). Additionally, a role for Uaf30 in the recruitment of the RENT complex to the 35S rRNA promoter was suggested (Goetze et al., 2010). Net1 interaction with the 35S rDNA promoter in turn appears to be required for efficient Pol I transcription, in agreement with the observation that Net1 associates preferentially with the promoter regions of open rRNA genes (Goetze et al., 2010; Shou et al., 2001).

1.2.4.2 Chromatin dynamics at the 35S rRNA gene locus

Dynamic changes in 35S rRNA gene chromatin states have been correlated to processes such as transcription, replication, or repair. In the past years, the question of how the rDNA chromatin states are established and maintained and which environmental influences lead to changes in chromatin state and composition was in the focus of many studies in different organisms (Figure 13) (Hamperl et al., 2013).

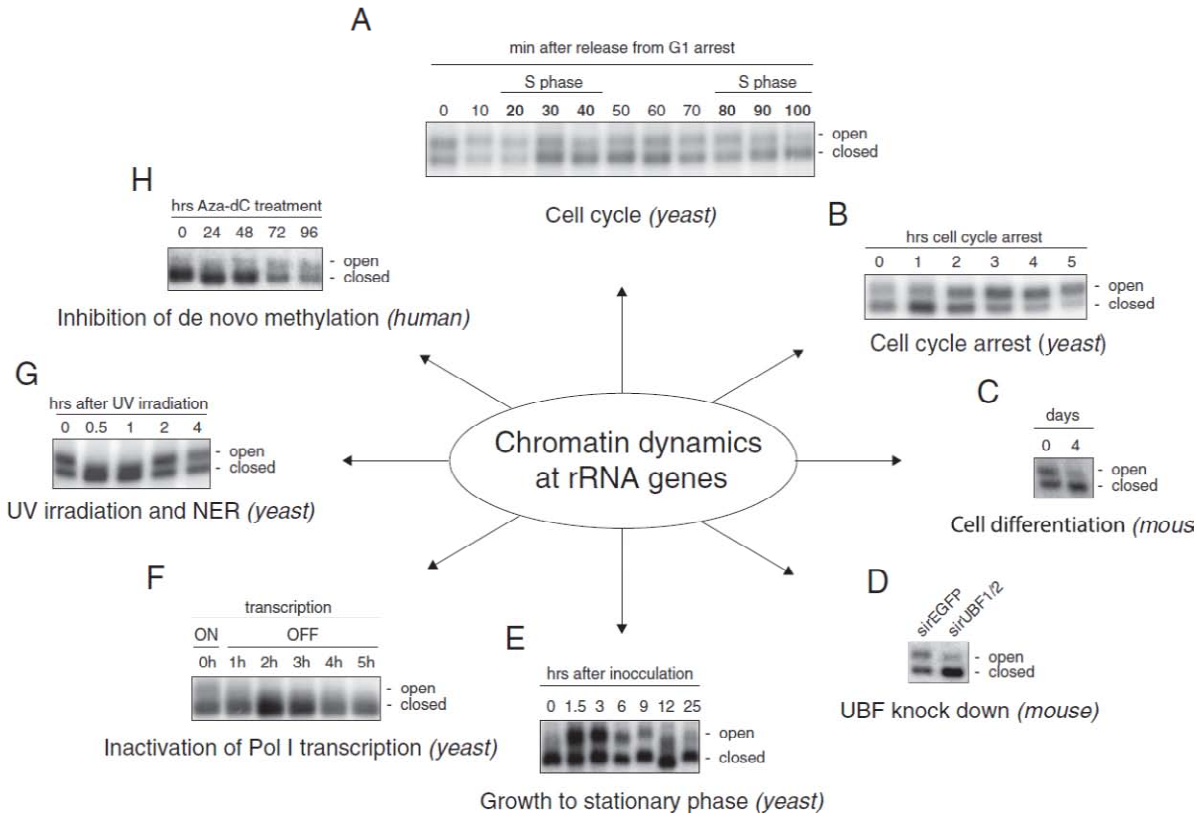

Figure 13: rRNA gene chromatin dynamics in different organisms

Southern blots visualizing DNA-fragments derived from large rRNA precursor genes after psoralen photocrosslinking are shown. (A) Cell cycle dependent chromatin dynamics in yeast. (B) Opening of copies upon arrest in G1 phase in yeast. (C) Closing of copies upon differentiation of mouse granulocytes. (D) Closing of copies upon UBF knock down in mouse. (E) Closing of copies upon transition to stationary phase in yeast. (F) Closing of copies upon inactivation of Pol I transcription in yeast. (G) Chromatin dynamics during nucleotide excision repair (NER) in yeast. (H) opening of copies upon inhibition of de novo methylation in human. (from Hamperl et al., 2013 and references therein)

In yeast it was suggested early after the definition of the two chromatin states at the 35S rRNA gene locus, that these states are not stable and inherited. Thus, the fraction of approximately 50% open copies observed in exponentially growing cells can vary according to growth conditions and each of the individual rDNA copies can adopt either the open or the closed chromatin state (Dammann et al., 1995; Lucchini and Sogo, 1995). Accordingly, analysis of the 35S rRNA gene chromatin state during the cell cycle showed that the amount of open copies decreases during S phase (Figure 13 A) and that the closed chromatin state is established during replication independently of the transcriptional activity of the individual copies before replication (Lucchini et al., 2001; Wittner et al., 2011). The open state is then re-established during the G1 phase of the cell cycle and in the absence of replication almost all copies adopt the open chromatin state (Figure 13 B), thus confirming that replication is the dominant process converting rRNA genes to the closed chromatin state (Wittner et al., 2011).

From some studies using Pol I (initiation factor) mutants it was supposed that the presence of the open state is linked to Pol I transcription (Goetze et al., 2010; Hontz et al., 2008; Merz et al., 2008). Recently, this model has been confirmed (Figure 13 F), since the shutdown of Pol I transcription leads to an almost complete closing of copies (Wittner et al., 2011). Interestingly, the same study could show that the complete opening of copies during G1 arrest is not linked to a high polymerase load on the individual genes, but Pol I association seems to be rather diluted to many copies. This could be another confirmation of the model that transcriptional activity is not necessarily regulated at the level of the amount of open copies as discussed in section I.2.4.1.1. Another factor which is involved in the maintenance of the open chromatin state is Hmo1. Thus, in the absence of replication, Hmo1 is required to keep 35S rRNA genes in the open chromatin state, when Pol I transcription is shut off (Wittner et al., 2011). The finding that replication of chromosome twelve (which contains the rDNA locus) is impaired in a strain, where all copies are heavily loaded with Pol I and actively transcribed (Ide et al., 2010), may substantiate the idea that transcription antagonizes replication in the establishment of 35S rDNA chromatin states.

Another DNA dependent process which leads to dynamic changes of the chromatin state of 35S rRNA genes is repair upon DNA damage (Figure 13 G) (Conconi, 2005; Conconi et al., 2002; Tremblay et al., 2014). Upon UV light induced DNA damage, copies adopt the closed chromatin state and re-opening is in good correlation with resumption of transcription. The inhibition of DNA repair does not prevent closing of copies, but re-opening does not occur. In those experiments replication has been prevented by the addition of hydroxyurea, indicating that there are replication-independent processes in the cell leading to closing of copies. This is in full accordance to the finding that even upon cell-cycle arrest in G1 nucleosomes can be deposited on the rDNA, if Pol I and Hmo1 are absent (Wittner et al., 2011).

When yeast cells transit to stationary phase, rDNA copies get closed (Figure 13 E) (Babl, 2012; Claypool et al., 2004; Dammann et al., 1993; Fahy et al., 2005; Johnson et al., 2013; Sandmeier et al., 2002). Since replication as well as transcription are thought to be largely absent in stationary phase, the 35S rRNA gene chromatin changes observed in adaptation to environmental conditions are a particular case that will be described in detail in the next chapter.

I.3 Chromatin dynamics at the 35S rRNA gene locus and the stationary phase

I.3.1 The stationary phase in yeast

Prokaryotic and also eukaryotic microorganisms such as yeast are able to switch to a resting state when they are starving for nutrients like carbon, nitrogen, phosphate, or sulfur. Specific characteristics that are established during the transition to this state enable the cells to survive prolonged periods of starvation and to re-start proliferation upon re-feeding with the limiting nutrients (Choder, 1993; Kolter et al., 1993; Lillie and Pringle, 1980; Werner-Washburne et al., 1993). This resting state is referred to as G_0, quiescence, or stationary phase and can last for months or even years (Fuge et al., 1994; Granot and Snyder, 1993; Lillie and Pringle, 1980). Under certain conditions, such as in bottled beer in a shipwreck, yeast cultures can even survive for up to 200 years (Neuhaus, 2010; Prokesch, 1991).

Most probably there is a basic program for the entry into stationary phase independent of which nutrient becomes limiting, but nutrient-specific additional programs exist as adaptation to their exhaustions (Carroll and O'Shea, 2002; Gasch et al., 2000). However, most of the current knowledge about stationary phase comes from cultures that were grown in rich medium containing glucose as carbon source (Figure 14) and it was suggested that this is the only way that cells enter a real stationary phase (Granot and Snyder, 1991; Werner-Washburne et al., 1996). Here, cells pass through different phases and gain the ability to withstand environmental stresses, but are at the same time able to profit the most from high nutrient conditions (Herman, 2002; Werner-Washburne et al., 1993; Winderickx et al., 2003; Zaman et al., 2008).

When yeast cells are inoculated in rich medium (YPD), there is a lag phase during which the cells adapt to the new growth conditions. During the following exponential growth phase glucose fermentation is used for fast proliferation. At the point when glucose becomes limiting, the cells shortly arrest their growth and switch their metabolism to respiration. This is called the diauxic shift. Subsequently ethanol which was produced during fermentative growth is oxidized in the post-diauxic shift growth phase and the cultures exhibit a much slower growth. After four to seven days past inoculation, when even the ethanol becomes exhausted, cells cease proliferation and enter the stationary phase (Gray et al., 2004; Smets et al., 2010; Werner-Washburne et al., 1993, 1996).

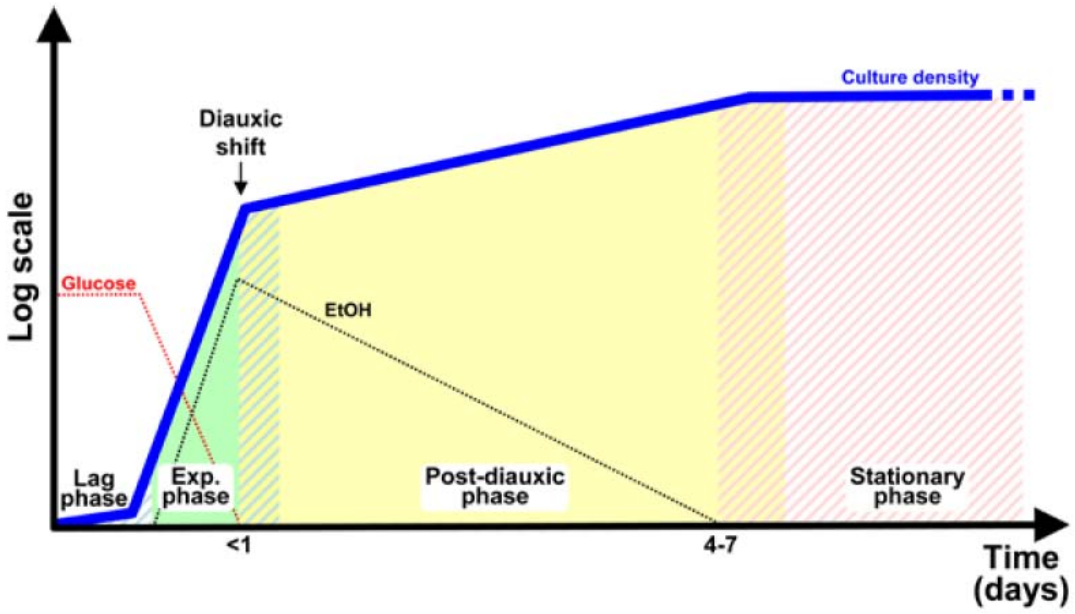

Figure 14: Growth phases of yeast in glucose containing rich medium

A blue line represents the growth curve. After inoculation cells adapt to the fresh medium (lag phase). This is followed by exponential growth where glucose is used in fermentation and ethanol is produced (exp. phase). Within less than one day after inoculation the point where glucose is exhausted is reached and a short cell cycle arrest takes place where the cells metabolism switches from fermentation to respiration (diauxic shift). In the following slow growth phase ethanol is consumed as carbon source (post-diauxic phase). At the point when also ethanol is consumed (4-7 days after inoculation), the cells enter the stationary phase, where no growth takes place. (from Busti et al., 2010)

Saccharomyces cerevisiae preferentially uses glucose over other mono- and disaccharides as carbon source. But it is particular in its carbon metabolism (Figure 15), since it does not consume glucose by respiration and oxidative phosphorylation as it is the case in higher eukaryotes, but uses fermentation of glucose to produce ethanol and acetate even if oxygen is available and respiration would be energetically more favorable (Smets et al., 2010). Thereby yeast cells show good correlation between glucose uptake and ethanol secretion (Huberts et al., 2012). Underlying this phenomenon is the repression of respiratory pathways through the presence of glucose. This is called the Crabtree effect and is also found in tumors and malignant tissues (Crabtree, 1929; Wojtczak, 1996). The evolutionary sense of this effect in yeast is diversely discussed (Pfeiffer and Morley, 2014). On the one hand it is thought that aerobic fermentation is a trade-off of traits, meaning that ATP, as well as other molecules needed for rapid cell proliferation can either be produced rapidly (high rate) or in the highest possible amount (high yield) (Pfeiffer et al., 2001; Vander Heiden et al., 2009). On the other hand aerobic fermentation is thought to correspond to the make-accumulate-consume strategy (Piskur et al., 2006; Rozpędowska et al., 2011). Here, the repression of an energetically more efficient metabolism (respiration) leads to ethanol production to prevent growth of other

microorganisms which may compete for nutrients with the yeast cell (Thomson et al., 2005). Additionally, ethanol has the advantage to serve as carbon source, when the primary carbon source is exhausted as it is the case upon transition to stationary phase.

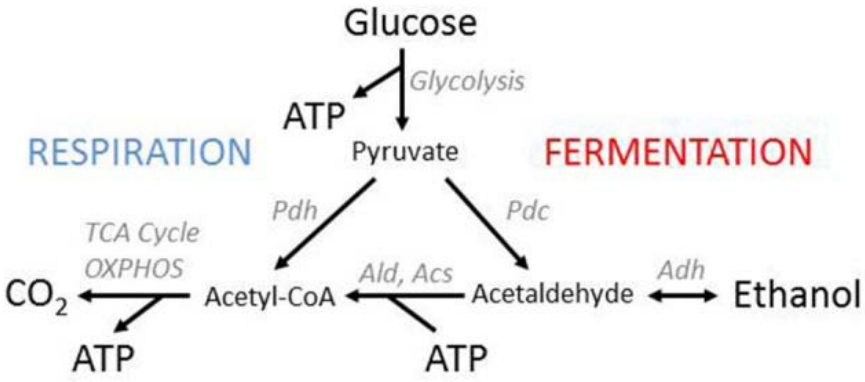

Figure 15: Energy metabolism pathways in yeast

Two pathways for energy (ATP) production from glucose are present in yeast: respiration and fermentation. Both start with glycolysis and thus production of pyruvate and ATP. In fermentation pyruvate is converted to ethanol, thereby recycling NAD^+ from glycolysis. In respiration pyruvate is completely oxidized to CO_2 during the tricarboxylic acid (TCA) cycle and oxidative phosphorylation (OXPHOS), yielding additional ATP but requiring oxygen. In yeast ethanol produced during fermentation and accumulating in the environment can be used for respiration when glucose becomes depleted. (from Pfeiffer and Morley, 2014)

During transition to stationary phase not only the carbon metabolism changes and cells cease to proliferate, but also other physiological and morphological changes take place (De Virgilio, 2012; Gray et al., 2004; Herman, 2002; Werner-Washburne et al., 1996). Even before glucose is exhausted, glycogen accumulation starts and peaks at the diauxic shift to serve as an energy depot for prolonged times of starvation. Additionally, trehalose is produced during diauxic shift and post-diauxic shift phase to increase stress tolerance of the cell by its protective biophysical properties. Both, glycogen and trehalose, are then consumed after long periods of starvation, the latter only when glycogen is exhausted (François and Parrou, 2001; Lillie and Pringle, 1980). Additionally, the cell walls change and thicken. They have less pores and a high amount of mannoproteins associated, which leads to a different appearance in phase-contrast microscopy (De Nobel et al., 1990; Lesage and Bussey, 2006; de Nobel et al., 1990; Zlotnik et al., 1984). Phosphate accumulates in the vacuole (Kornberg et al., 1999; Thomas and O'Shea, 2005). During the diauxic shift additional triglycerides and steryl esters are produced as a long time metabolic energy depot and stored in lipid droplets, which are then rapidly degraded after re-feeding (Hiltunen et al., 2003; Kurat et al., 2006, 2009). Resistances against various stresses such as thermal and oxidative stress, and decreased sensitivity against toxic agents, as well as condensation of chromosomes are additionally part of the stationary phase entry program (Cyrne et al., 2003; de Nobel et

al., 2000; Piñon, 1978; Plesset et al., 1987). Especially during starvation for nitrogen, but to a lesser extent also upon starvation for other nutrients like carbon, macroautophagy takes place to recycle bulk proteins and damaged or unused organelles and thereby enhancing stationary phase survival (Gresham et al., 2011; He and Klionsky, 2009; Takeshige et al., 1992; Tsukada and Ohsumi, 1993; Yang et al., 2006). In good correlation with enhanced respiration more mitochondria are present (Stevens, 1981).

In general, transcription rates are decreased in stationary phase (Choder, 1991). At least one fourth of the yeast genome is transcriptionally reprogrammed during diauxic shift, post-diauxic growth phase, and stationary phase and this is mediated by influencing transcription factors, by the recruitment of repressors to the promoter of specific genes, or by influencing the chromatin structure (DeRisi et al., 1997; Gasch et al., 2000; Lempiäinen and Shore, 2009; Radonjic et al., 2005; Schäfer et al., 2008).

Translation is massively (approximately 300fold) downregulated during the transition to stationary phase, mainly due to a repression of ribosomal protein and translation factor gene transcription and the inhibition of ribosome production (Boucherie, 1985; DeRisi et al., 1997; Fuge et al., 1994; Ju and Warner, 1994).

The stationary phase is usually reached after at least seven days of growth after inoculation. Whereas stationary cells were often considered to be a homogenous population, recent studies identified different cell populations in stationary phase cultures (Allen et al., 2006; Aragon et al., 2008; Davidson et al., 2011; McKnight et al., 2015). These cell populations are on the one hand daughter cells and young mothers which are long-lived and have been termed quiescent cells and on the other hand cells which are non-quiescent and lose their reproductive capacity, exhibit genomic instability, and become senescent and apoptotic.

Stationary phase cultures have recently got in the focus of aging research. Therefore two different yeast aging processes have been defined. The first is the so called replicative aging and is a measurement of the total number of cell divisions a single cell can undergo, and the second is the so called chronological aging which is the total lifetime of a cell including the replicative life and the quiescent state. Indeed in some of these studies proteins and other factors were identified that influence longevity in yeast, metazoans and also mammalian cells (Kaeberlein, 2010).

Upon transfer of stationary phase cells to fresh medium containing all nutrients, the cells' metabolism is again reprogrammed and exit from stationary phase is initiated. Thus, the cells lose thermotolerance and their thick and resistant cell walls, carbohydrate stores

(trehalose and glycogen) are mobilized, transcription and translation rates increase, and finally the cells start to proliferate again (Werner-Washburne et al., 1993). Most of the transcriptional changes appear already within five to ten minutes after re-feeding and approximately one third of all protein coding genes is affected by these changes among them the ribosomal protein genes (Gray et al., 2004; Martinez et al., 2004).

I.3.2 Signaling pathways regulating entry and exit from stationary phase

Three main signal transduction pathways are involved in the regulation of growth phase transitions to stationary phase. The Tor pathway, the PKA pathway, and the Snf1 pathway. Tor and PKA pathways are negative regulators of the entry to stationary phase, while Snf1 positively regulates the transition to stationary phase. Additional pathways that are involved in stationary phase regulation are the cell wall integrity (or PKC) and the Pho85 pathway (De Virgilio, 2012; Galdieri et al., 2010; Gray et al., 2004; Smets et al., 2010).

I.3.2.1 The Tor kinase pathway

The serine/threonine kinase Tor (target of rapamycin) pathway is a conserved signaling network that regulates cell growth (Figure 16) (Heitman et al., 1991). It consists of two complexes -TORC1 and TORC2- with only the first being sensitive to the antibiotic rapamycin and much better characterized. TORC1 is thought to be involved in temporal aspects of cell growth in dependence of nutrients such as nitrogen or to a lesser extent glucose, while TORC2 presumably is involved in spatial regulation of cell growth like actin polarization (De Virgilio and Loewith, 2006a, 2006b; Rohde et al., 2008). One of the major activators of TORC1 is the presence of glutamine (Crespo et al., 2002). A key node of the TORC1 pathway is the Tap42-associated phosphatase, which is released into the cytosol upon rapamycin treatment or nitrogen starvation and leads ultimately to expression of genes that are involved in the growth on poor nitrogen sources (Shamji et al., 2000; Yan et al., 2006). Additionally, TORC1 negatively regulates the transcription activators Gcn4 and Rtg1 and 2 which are involved in gene expression for amino acid biosynthesis (Liu et al., 2003; Natarajan et al., 2001). It negatively regulates the expression of stress response genes (Santhanam et al., 2004) and inhibits autophagy (Chang et al., 2009).

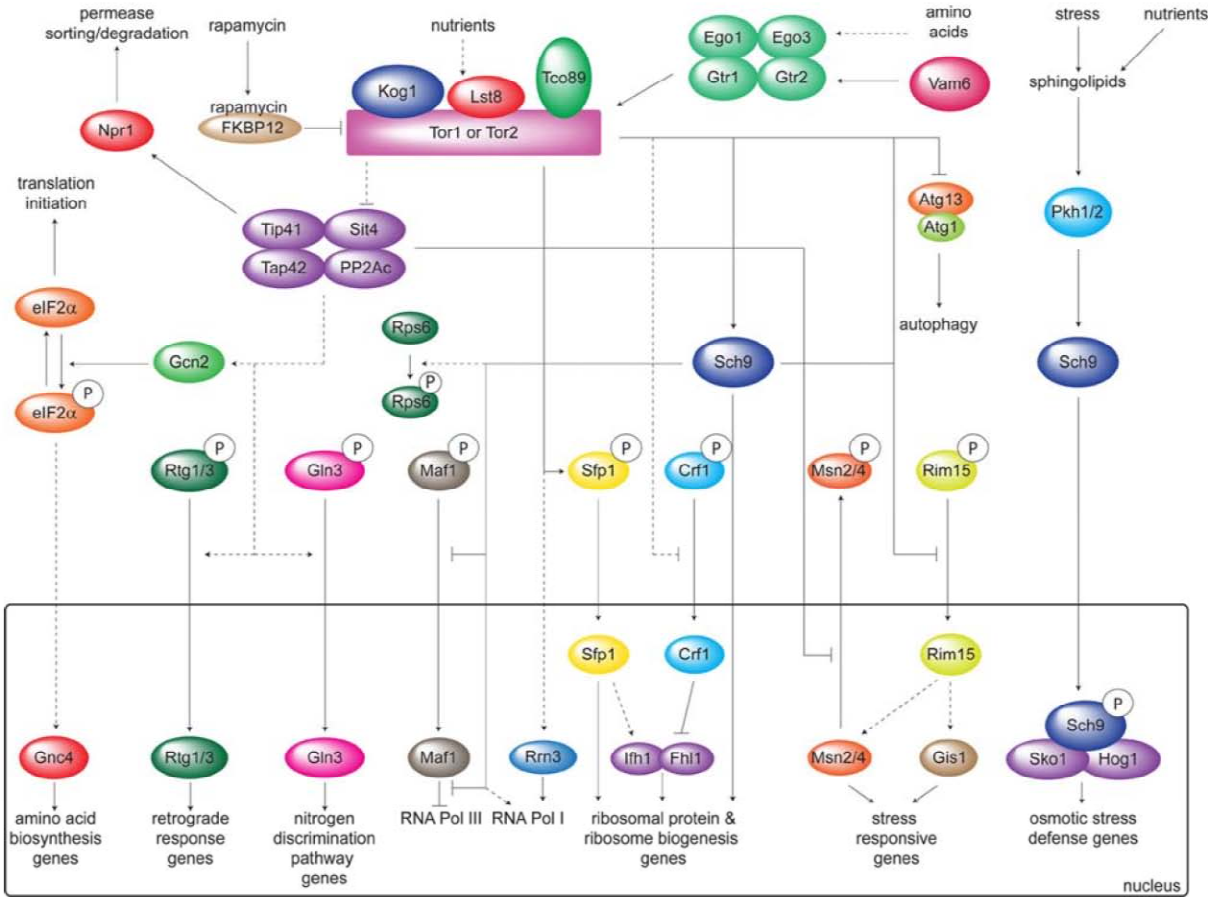

Figure 16: The Tor pathway in yeast

The presence of nutrients leads to activation of TORC1, thus resulting in protein synthesis and inhibition of stress response, autophagy, and pathways that positively regulate growth on poor nitrogen media. Arrows or bars indicate activation or repression, respectively. Dashed lines indicate indirect or putative interactions. For interaction details see the main text of the reference. (from Smets et al., 2010)

Further, TORC1 is involved in the regulation of protein synthesis at the level of ribosome biogenesis. It regulates ribosomal protein, rRNA, and ribosome biogenesis (Ribi) regulon gene expression (Jorgensen et al., 2004). Under rich nutrient conditions Tor1 binds to the rDNA and stimulates Pol I and Pol III transcription (Li et al., 2006). Pol III is regulated by inhibition of its repressor Maf1 by Tor1 or the Tor-pathway associated Sch9 (Huber et al., 2009; Wei et al., 2009). Tor positively stimulates Pol I transcription either by the modulation of Pol I-Rrn3 interaction (Claypool et al., 2004; Philippi et al., 2010; Reiter et al., 2011), and/or by direct recruitment of Pol I to the 35S rRNA promoter via the Sch9 signaling pathway (Huber et al., 2009). TORC1 potentially integrates the regulation of ribosomal protein (RP) gene expression and rDNA transcription via Hmo1, since it was shown that Hmo1 association with RP promoters and the rDNA is dependent on TORC1 (Berger et al., 2007).

I.3.2.2 The protein kinase A (PKA) pathway

The cAMP dependent protein kinase A (cAMP-PKA) pathway is involved in metabolism, stress response, and proliferation regulation in dependence of the presence of a carbon source and is thus a negative regulator of transition to stationary phase (De Virgilio, 2012; Gray et al., 2004; Smets et al., 2010). It stimulates glycolysis, cell growth, cell cycle progression, and the mobilization of glycogen and trehalose, but downregulates gluconeogenesis and stress resistance (Figure 17) (Gancedo, 2008; Santangelo, 2006; Tamaki, 2007; Thevelein et al., 2000). The PKA hetero-tetramer complex consists of two catalytic subunits (composed of Tpk1-3) and two regulatory subunits (Bcy1) and its activity is dependent on the presence of cAMP (Kuret et al., 1988; Toda et al., 1987a, 1987b). Interestingly, deletion of *BCY1* leads to the prevention of cell cycle arrest upon transition to stationary phase, inability to grow on non-glucose media, and heat-shock sensitivity (Toda et al., 1987a). The PKA pathway is dependent on an intracellular glucose signal and an extracellular glucose signal. For the intracellular signal, the presence of phosphorylated glucose is essential (Beullens et al., 1988; Thevelein et al., 2000). The Ras proteins transmit this signal by stimulating the activity of adenylate cyclase, thus resulting in the synthesis of cAMP from ATP (Casperson et al., 1983, 1985; Field et al., 1988; Matsumoto et al., 1984). Extracellular glucose detection is mediated by G-protein coupled receptors, which then activate the cAMP-PKA pathway probably also via adenylate cyclase (Peeters et al., 2006). PKA is a very important regulator especially at the exit from glucose-starvation. It was shown, that 90% of all transcriptional changes appearing in this situation are regulated by the PKA pathway (Wang et al., 2004). PKA has a dual role in the regulation of gene expression. On the one hand it directly negatively regulates the kinases Rim15 and Yak1, which are involved in stimulation of stress response, thermotolerance, synthesis of glycogen and trehalose, G1-arrest upon starvation, and respiratory growth. On the other hand the PKA pathway directly influences the effectors of the Rim15 and Yak1 pathways: the transcription factors Msn2, Msn4, and Gis1 (Cameroni et al., 2004; Roosen et al., 2005; Zhang et al., 2009). PKA is involved in the activation of ribosomal protein gene expression via stimulation of the transcription activator Sfp1 and inhibits the repressive function of Crf1 (Marion et al., 2004; Martin et al., 2004). Additionally, the PKA pathway stimulates 5S rRNA transcription by inhibition of the Pol III repressor Maf1 (Moir et al., 2006).

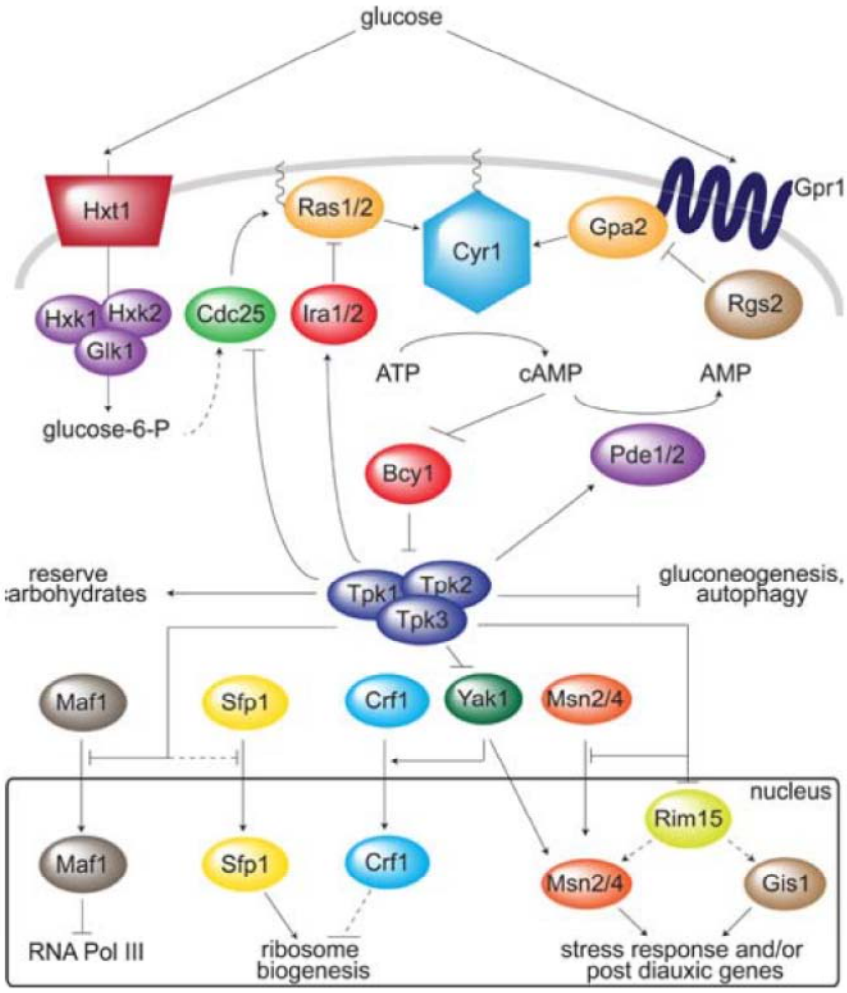

Figure 17: The PKA pathway in yeast

Glucose addition to glucose-starved cultures leads to activation of the pathway. This leads to a rapid switch from respiratory growth to fermentative growth. Arrows or bars indicate activation or repression, respectively. Dashed lines indicate indirect or putative interactions. For detailed information see the main text of the reference. (from Smets et al., 2010)

I.3.2.3 The Snf1 kinase pathway

The Snf1 pathway becomes active upon glucose exhaustion and leads to activation of genes that are needed during respirative growth, for gluconeogenesis, the TCA cycle, and uptake and metabolism of carbon sources other than glucose (Gancedo, 1998; Hedbacker and Carlson, 2008; Ronne, 1995).

The Snf1-complex is a member of the highly conserved Snf1/AMP activated protein kinases (AMPK) family (Hardie, 2007) and consists of the catalytic subunit (Snf1), one of three possible scaffold subunits (Gal83, Sip1, or Sip2) and a regulatory subunit (Snf4) (Jiang and Carlson, 1997; McCartney et al., 2005). Its activation is mainly dependent on the upstream kinases Elm1, Sak1, and Tos3, which phosphorylate a conserved threonine residue (Sutherland et al., 2003). Inactivation of Snf1 in the presence of high glucose levels is predominantly achieved by the phosphatase complex Glc7-Reg1

(McCartney and Schmidt, 2001; Rubenstein et al., 2008). The effectors of the Snf1 pathway are the transcriptional repressor Mig1, which is inhibited upon phosphorylation and the transcriptional activators Cat8 and Sip4 which are activated upon Snf1-dependent phosphorylation. (Lesage et al., 1996; Papamichos-Chronakis et al., 2004; Randez-Gil et al., 1997; Treitel and Carlson, 1995). Additionally, Snf1 was shown to affect transcription on the level of chromatin, since it is also a histone kinase and phosphorylation of histone tails recruits the co-activator and acetyltransferase Gcn5 (van Oevelen et al., 2006). Snf1 plays a role in the recombination regulation at the rDNA (Lin et al., 2003) and its regulatory subunit Sip2 was shown to be target of the NuA4 acetyltransferase and the Rpd3 deacetylase, thereby regulating the cells replicative life span (Lu et al., 2011). Interestingly, for higher eukaryotes a direct link between AMPK and Pol I transcription has recently been found. It suggests, that upon glucose starvation TIF-1A (the mammalian homolog to Rrn3) is phosphorylated by AMPK and this leads to downregulation of transcription (Hoppe et al., 2009). However, no such effect has been described for Snf1 in yeast.

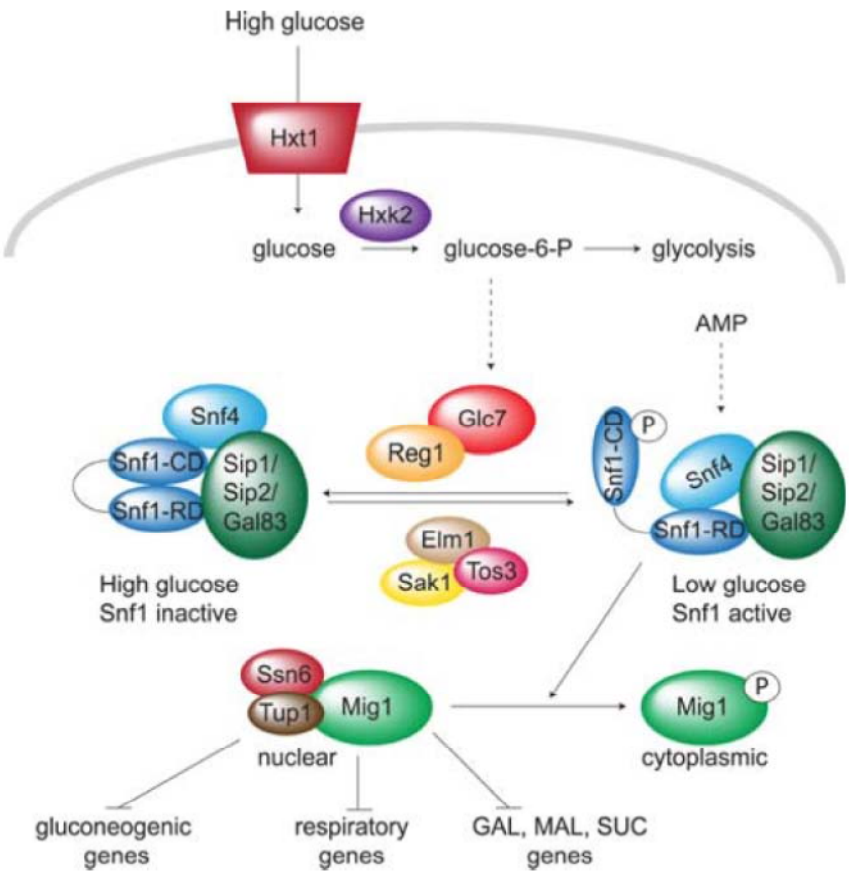

Figure 18: The Snf1 pathway in yeast

Presence of high glucose levels keeps the Snf1 pathway inactive. Upon glucose exhaustion the upstream kinases Elm1, Sak1, and Tos3 phosphorylate Snf1 which leads to activation of the Snf1 pathway. Arrows or bars indicate

activation or repression, respectively. Dashed lines indicate indirect or putative interactions. For detailed information see the main text of the reference. (from Smets et al., 2010)

I.3.3 Chromatin dynamics at the 35S rDNA locus upon growth to stationary phase

The demand for ribosomes is high in exponentially growing and rapidly proliferating cells (approximately 200.000 ribosomes are synthesized per cell division) (Warner, 1999). In contrast slowly proliferating or non-proliferating cells such as after the diauxic shift or in stationary phase only have a very low rate of ribosome synthesis and only less than one fourth of the ribosomes of an exponentially growing cell (Ju and Warner, 1994). Accordingly, the production of all ribosomal components such as ribosomal proteins and rRNA decreases drastically and increases again upon re-feeding in response to the PKA and Tor kinase pathways (Claypool et al., 2004; Fahy et al., 2005; Klein and Struhl, 1994; Neuman-Silberberg et al., 1995; Powers and Walter, 1999; Sandmeier et al., 2002; Waldron, 1977; Zaragoza et al., 1998).

The drastic decrease in Pol I transcription (Babl, 2012; Claypool et al., 2004; Fahy et al., 2005; Sandmeier et al., 2002) is accompanied by a change in the chromatin state of the 35S rRNA gene copies. The approximately 50% open rDNA copies in exponentially growing cells are closed when the cells approach stationary phase (Figure 13 E; Figure 19 WT) (Babl, 2012; Dammann et al., 1993; Fahy et al., 2005; Johnson et al., 2013; Sandmeier et al., 2002). However, as already discussed in section I.2.4.1.1 it is unlikely that the reduction in the number of open repeats fully accounts for the down-regulation of 35S rRNA transcription. Instead, the closing of copies with transition to stationary phase might be a consequence of reduced transcription.

In fact, there is evidence that Pol I transcription is regulated at the level of transcription initiation. Thus, the transcription limiting formation of the Rrn3-Pol I complex was shown to be strongly affected by the transition to stationary phase or inhibition of the Tor pathway by rapamycin (Claypool et al., 2004; Milkereit and Tschochner, 1998; Peyroche et al., 2000; Philippi et al., 2010; Zaragoza et al., 1998). Accordingly, upon Tor activation, TORC1 is targeted to the nucleus, and might directly act at the 35S rRNA gene promoter to enhance transcription (Li et al., 2006). However, Pol I PIC formation is only partially affected upon growth to stationary phase since the Pol I transcription factor UAF remains associated with the rDNA under these conditions (Claypool et al., 2004).

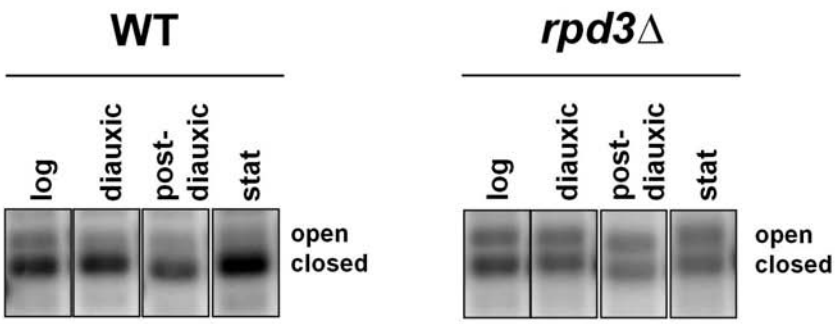

Figure 19: Chromatin dynamics at the 35S rRNA gene locus upon transition to stationary phase in WT and *rpd3*Δ cells

The figure shows typical 35S rRNA gene chromatin dynamics of *RPD3* and *rpd3*Δ cultures grown to stationary phase as already described (Babl, 2012; Sandmeier et al., 2002). Samples were collected in exponential phase (log), approximately at the diauxic shift (diauxic), in the post-diauxic shift phase (post-diauxic) and in stationary phase (stat). The respective chromatin state from which the bands are derived is indicated on the right (open and closed).

Nevertheless, it is not known how exactly the closing of copies is correlated with the reduction in Pol I transcription. Interestingly, it was shown that open copies can persist even in stationary phase and under strongly decreased Pol I transcription conditions, if the deacetylase Rpd3 is absent (Figure 19 *rpd3*Δ) (Babl, 2012; Johnson et al., 2013; Sandmeier et al., 2002). Thus, Rpd3 was suggested to play a major role in the closing process of 35S rDNA copies potentially by acting as a histone chaperone (Johnson et al., 2013).

Rpd3 was identified as the catalytic subunit of three different histone deacetylase complexes (Rpd3L, Rpd3S, and Rpd3µ) (Baker et al., 2013; Carrozza et al., 2005; McDaniel and Strahl, 2013; Rundlett et al., 1996; Yang and Seto, 2008). Rpd3L was suggested to play a role in ribosome biogenesis and heat shock response and in the nucleosome deposition on the rDNA genes (Huber et al., 2011; Johnson et al., 2013; Ruiz-Roig et al., 2010), Rpd3S is thought to maintain chromatin integrity and acts as a repressor of cryptic transcription (Wagner and Carpenter, 2012), while Rpd3µ is involved in the oxidative stress response (Baker et al., 2013). In general, Rpd3L is recruited to its target promoters via Ume6 and leads to transcriptional repression (Kadosh and Struhl, 1997).

It was suggested that the mentioned downregulation of Pol I transcription by the inactivation of the Tor pathway is mediated via Rpd3 dependent chromatin changes (Tsang et al., 2003), but this hypothesis was later challenged by a further study (Oakes et al., 2006). From this study it was suggested, that the Tor signaling inhibition affects Pol I transcription without involvement of Rpd3 and that the observed change in

chromatin state upon transition to stationary phase is Rpd3 dependent, but independent of Tor signaling inhibition.

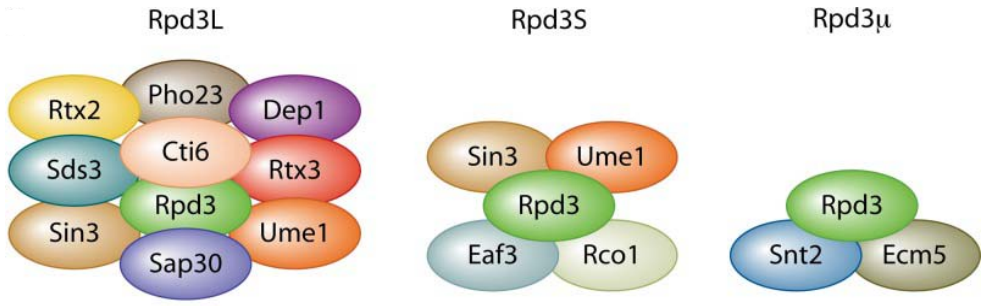

Figure 20: The three different Rpd3 complexes

The Rpd3L complex consists of nine further subunits plus Rpd3, Rpd3S contains four further subunits, and Rpd3µ only two further subunits. Rpd3µ shares no subunits except Rpd3 with Rpd3L or Rpd3S, while Rpd3S shares beside Rpd3 the subunits Ume1 and Sin3 with the Rpd3L complex. Rco1 and Eaf3 are specific for Rpd3S, while Rxt2, Sds3, Sap30, Rxt3, Pho23, Cti6, and Dep1 are specific for Rpd3L. (from McDaniel and Strahl, 2013)

I.4 Objectives

This PhD thesis aimed to shed further light on mechanisms involved in chromatin dynamics at the 35S rRNA genes in yeast cells upon transition to and exit from stationary phase.

So far various studies have investigated the changes in rDNA chromatin upon the transition to stationary phase (Claypool et al., 2004; Dammann et al., 1993; Fahy et al., 2005, Sandmeier 2003, Johnson 2013). From these studies there was good evidence that 35S rRNA transcription is downregulated at the level of Pol I PIC formation targeting the Rrn3-Pol I complex, and that this downregulation correlates in part with the transition of open 35S rDNA copies to the closed chromatin state. As mentioned above, deletion of the gene coding for the deacetylase Rpd3 leads to the maintenance of open 35S rDNA copies in stationary cells, despite a strong down-regulation of Pol I transcription in this condition (Babl, 2012; Sandmeier et al., 2002; Johnson 2012). This uncoupling of Pol I transcription and the maintenance of the open 35S rDNA chromatin state is reminiscent to the persistence of open 35S rRNA gene chromatin in G1 arrested cells upon shutdown of Pol I transcription (Wittner et al., 2011). In the latter study Hmo1 was identified as a key factor for the Pol I transcription independent maintenance of open 35S rDNA chromatin. This led to the hypothesis that Hmo1 acetylation might stabilize its association with the 35S rDNA and that deacetylation by Rpd3 upon growth to stationary phase would result in its dissociation and thus to closing of 35S rRNA genes. Surprisingly, a detailed study revealed that Hmo1 is not necessary to maintain the open chromatin state

in stationary phase in the absence of Rpd3 (Babl, 2012). In the latter study, the molecular mechanism responsible for the Rpd3-dependent closing of 35S rDNA chromatin upon growth to stationary could not be identified, which in turn defined the primary goal of this work.

A second aim of this thesis was the initial analysis of 35S rRNA gene chromatin transition to the open state upon exit from stationary phase. Until now, only the process of Pol I transcription was shown to be absolutely required to open 35S rRNA gene chromatin (Wittner et al., 2011), but it is so far unknown if Pol I needs additional factors to accomplish the transition to the open state. Interestingly, data from *in vitro* transcription experiments suggested that Pol I itself, but not Pol I depleted of the Rpa49/Rpa34 heterodimer, can transcribe through a nucleosomal template (Merkl, 2013). Therefore, it was speculated that the Rpa49/Rpa34 dimer might be involved in chromatin opening by the Pol I complex. Thus, in this thesis it was tested if the *in vitro* data could be substantiated by *in vivo* experiments.

II Results

During this PhD thesis chromatin structure and dynamics at the ribosomal DNA locus were investigated. Special focus laid on chromatin changes accompanying the transition to stationary phase.

The results section is arranged in four parts: First -to facilitate interpretation of the results- an overview about culture conditions and the main methods employed for rDNA chromatin analysis is given. Second, a comprehensive analysis of rDNA chromatin composition was conducted to determine the molecular events leading to dynamic changes in rDNA chromatin structure when cells grow to stationary phase (see section II.2). Third, the deletion of *RPD3* was used to potentially identify the mechanisms leading to these changes (see section II.3). And fourth, the influence of the Pol I subunit Rpa49 on rDNA chromatin dynamics upon exit from stationary phase was investigated (see section II.4).

II.1 Experimental setup

II.1.1 Overview about cell culture conditions and sample collection

Since many different yeast strains were investigated during this thesis, consistent sampling was important to reach high comparability between the single analyses. Therefore the different cell cultures were conducted under the same conditions and in the same manner for the analyzed strains.

To investigate changes in rDNA chromatin composition in yeast cells upon growth to stationary phase cell samples of a continuous culture were treated with formaldehyde at specific time points to crosslink proteins to their respective DNA-binding sites. Afterwards ChEC, ChEC-psoralen, or ChIP experiments were carried out with these samples.

The experimental setup used for experiments in sections II.2 and II.3 is shown in Figure 21.

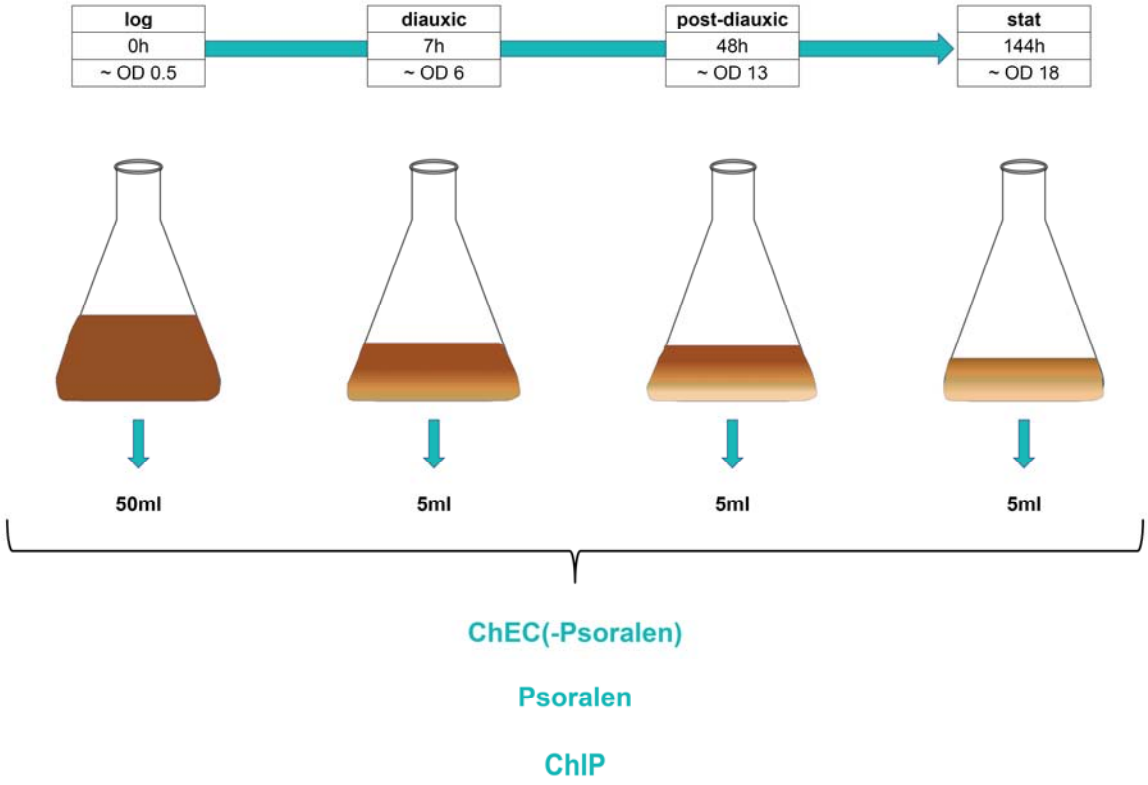

Figure 21: Experimental setup to investigate changes in rDNA chromatin upon growth to stationary phase
From a 5ml pre-culture of the respective yeast strain fresh medium was inoculated in the evening and grown over night to reach exponential phase ("log", OD~0.5). 50ml of the log culture were subjected to formaldehyde crosslinking. Cells were collected and frozen in liquid nitrogen. After sample collection of the log sample the culture was further incubated for 7h to 9h to reach the diauxic shift ("diauxic", OD between 5 and 7), 48h ("post-diauxic", OD between 12 and 14) and 144h ("stat", OD between 16 and 20), and 5ml samples were processed as described for the log sample. All samples of such a time-course experiment were collectively subjected to either ChEC(-psoralen), psoralen, or ChIP analyses.

Investigation of the influence of the conserved Pol I subunit Rpa49 on rDNA chromatin changes during the exit from stationary phase (see section II.4) was conducted with samples collected according to Figure 22. Cells of the respective yeast strains (*RPA49* under the control of the endogenous promoter or under the control of a galactose inducible promoter) were grown to post-diauxic growth phase and afterwards fresh pre-warmed medium was inoculated with these cells. Time-course sampling and formaldehyde crosslink took place. Afterwards the cell samples were used for psoralen and ChIP analyses.

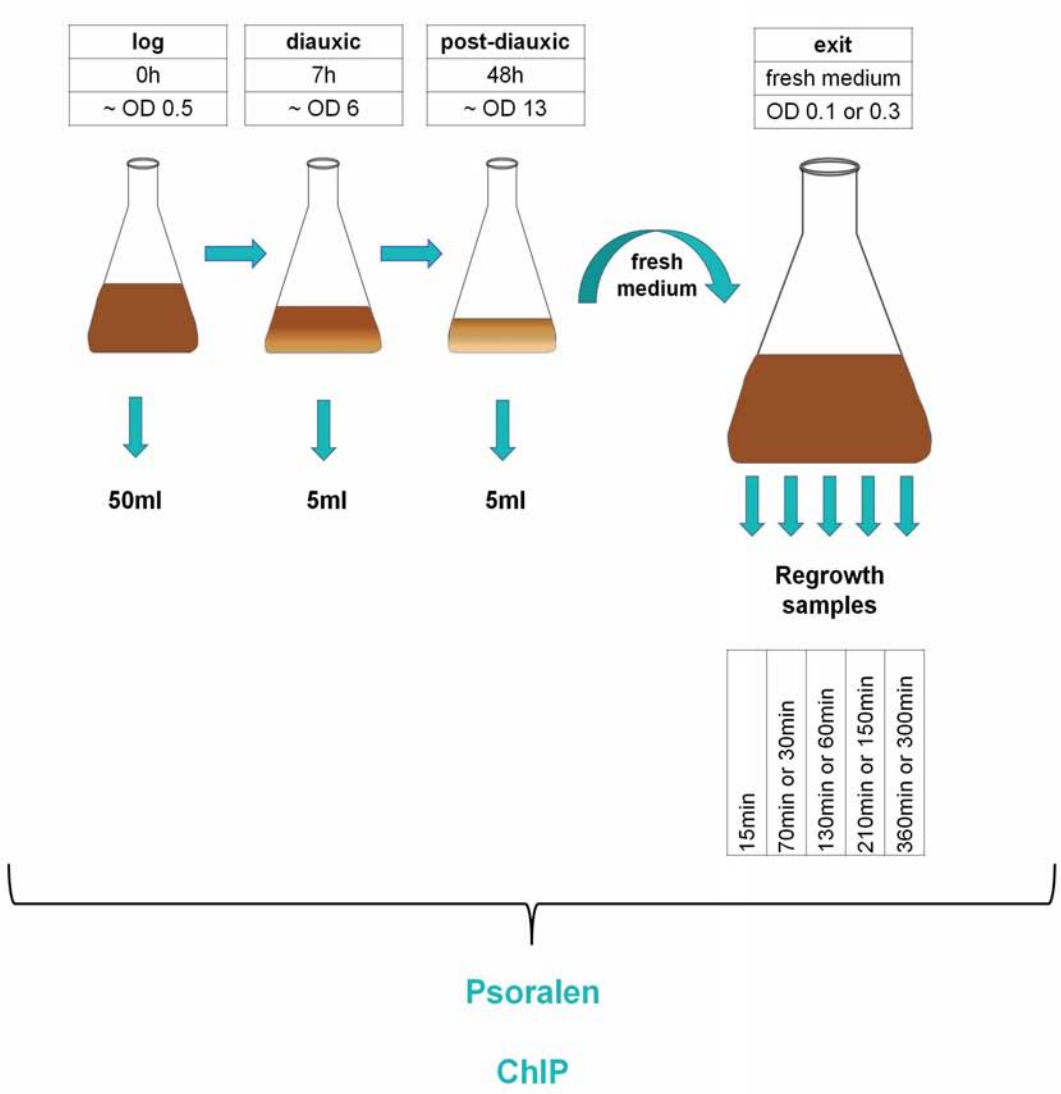

Figure 22: Experimental setup to investigate changes in rDNA chromatin upon exit from stationary phase
From a 5ml pre-culture of the respective yeast strain fresh medium was inoculated in the evening and grown over night to reach exponential phase ("log", OD~0.5). 50ml of the log culture were subjected to formaldehyde crosslinking. Cells were collected and frozen in liquid nitrogen. After sampling of the log sample the culture was further incubated for 7h to 9h to reach the diauxic shift ("diauxic", OD between 5 and 7) and 48h ("post-diauxic", OD between 12 and 14) and 5ml samples were processed as described for the log sample. From the post-diauxic culture fresh pre-warmed medium was inoculated to an OD of approximately 0.1 (section II.4.1) or 0.3 (sections II.4.2 and II.4.3). For investigation of rDNA chromatin changes upon exit from stationary phase 15min after inoculation the first "Regrowth" sample was collected and subjected to formaldehyde crosslink. Additional "Regrowth" sampling took place 70min or 30min, 130min or 60min, 210min or 150min and 360min or 300min (all second time-points refer to sections II.4.2 and II.4.3). Most samples of such a time-course experiment were collectively subjected to either psoralen, or ChIP analyses.

II.1.2 ChEC, ChEC-psoralen and ChIP experiments and their quantification

Many of the analyses within this thesis were carried out using Chromatin Endogenous Cleavage (ChEC) (Schmid et al., 2004) (Figure 23: A). Optionally, ChEC was performed

in combination with psoralen photocrosslinking (ChEC-psoralen) (Griesenbeck et al., 2012; Merz et al., 2008) (Figure 23 B).

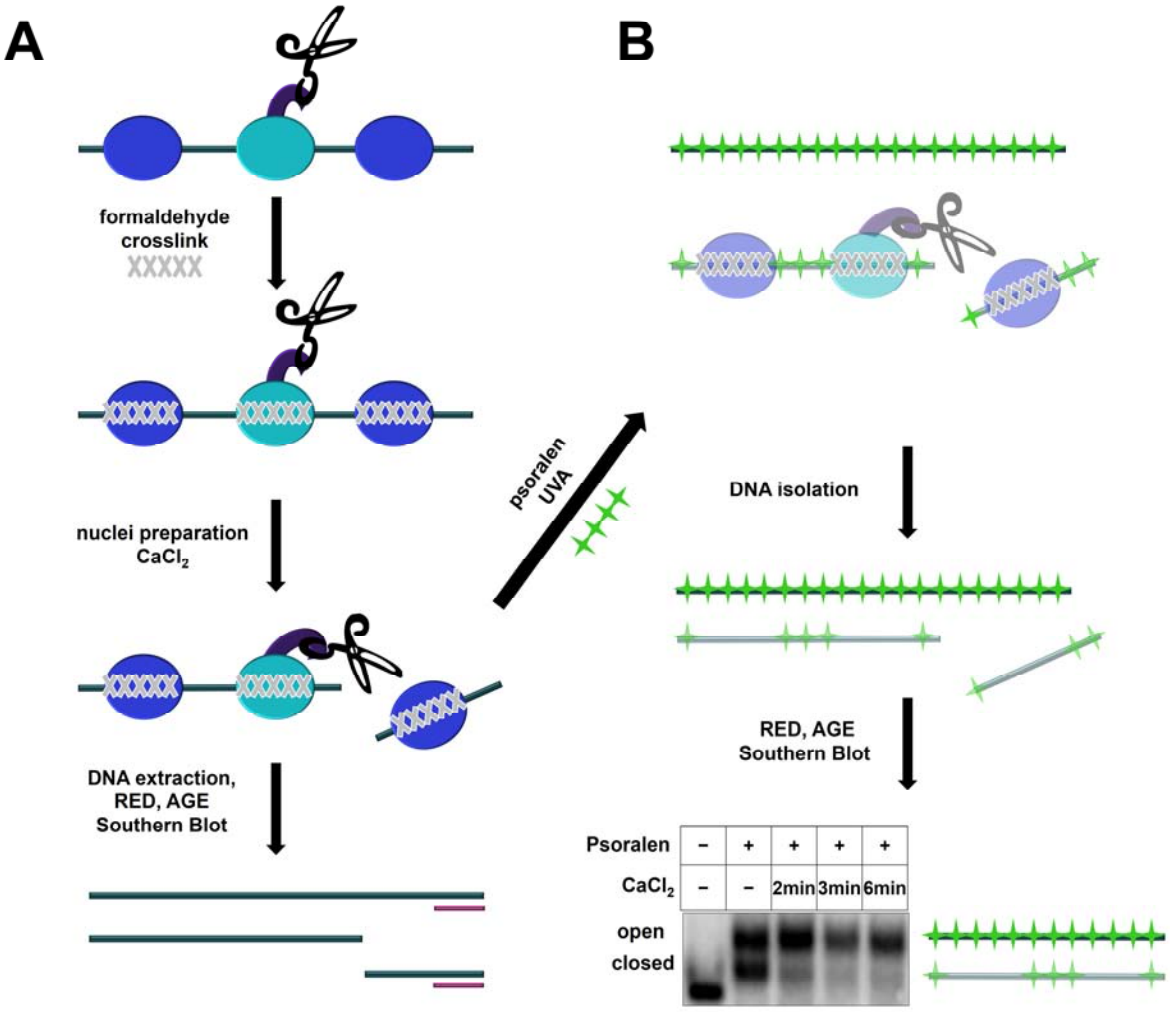

Figure 23: Scheme for ChEC (A) and ChEC-psoralen (B) analysis

(A) ChEC: Yeast cells are generated in which the protein of interest is expressed from the endogenous locus as an MNase fusion protein (depicted as an oval with scissors). After formaldehyde crosslinking (depicted as grey crosses) of proteins (blue and turquoise ovals) to DNA (depicted as dark blue line) and nuclei preparation MNase is activated by addition of $CaCl_2$. Samples are collected before and after different times of $CaCl_2$ addition. After DNA extraction, restriction enzyme digest (RED), agarose gel electrophoresis (AGE), and Southern blot the cleaved and uncleaved fragments can be detected by indirect end-labeling (probes are indicated as purple lines; see Figure 24 for localization of restriction sites and probes used in this work). **(B)** ChEC-psoralen: To determine the preferential association of a protein of interest with one of the two rDNA chromatin states ChEC was combined with psoralen analysis. Psoralen photocrosslinking (depicted as green crosses) was performed after ChEC analysis (see Figure 10 for details of psoralen photocrosslinking analysis). After DNA isolation, restriction enzyme digest, agarose gel electrophoresis, and Southern blot, the psoralen crosslinked DNA fragments derived from the respective chromatin states can be detected using radioactively labeled probes (see Figure 24 for detailed information). For ChEC-psoralen experiments the chromatin state where the protein of interest is preferentially binding is degraded upon activation of MNase and in correlation with association frequency (displayed as fading). In this figure ChEC-psoralen analysis is exemplary shown for a strain expressing a histone-MNase fusion protein. The Southern blot was hybridized with a probe detecting both fragments of the 35S rRNA gene locus after digestion with EcoRI (3.5kb probe, see Figure 24). Here, only the 18S fragment signal is shown.

In the first lane an ethanol control (no psoralen was added) is shown. The other lanes show the open and closed copy signals without (-), 2min, 3min and 6min of ChEC ($CaCl_2$). The histone-MNase degrades closed (nucleosomal) 35S rRNA gene copies.

In ChEC and ChEC-psoralen experiments the protein of interest is fused to MNase. Under normal conditions MNase is not active in yeast cells but can be activated in the experiment by the addition of Ca^{2+} ions. This leads then to cutting events nearby the binding site of the fusion protein. After DNA isolation, restriction enzyme digest, agarose gel electrophoresis and Southern blot with specific radioactively labeled probes, changes in cleavage sites and frequency can be monitored at any genomic locus of interest. In this study only one rDNA specific probe was used for ChEC and two different probes were used for ChEC-psoralen (see Figure 24 for an overview about all relevant restriction sites and the localization of radioactively labeled probes).

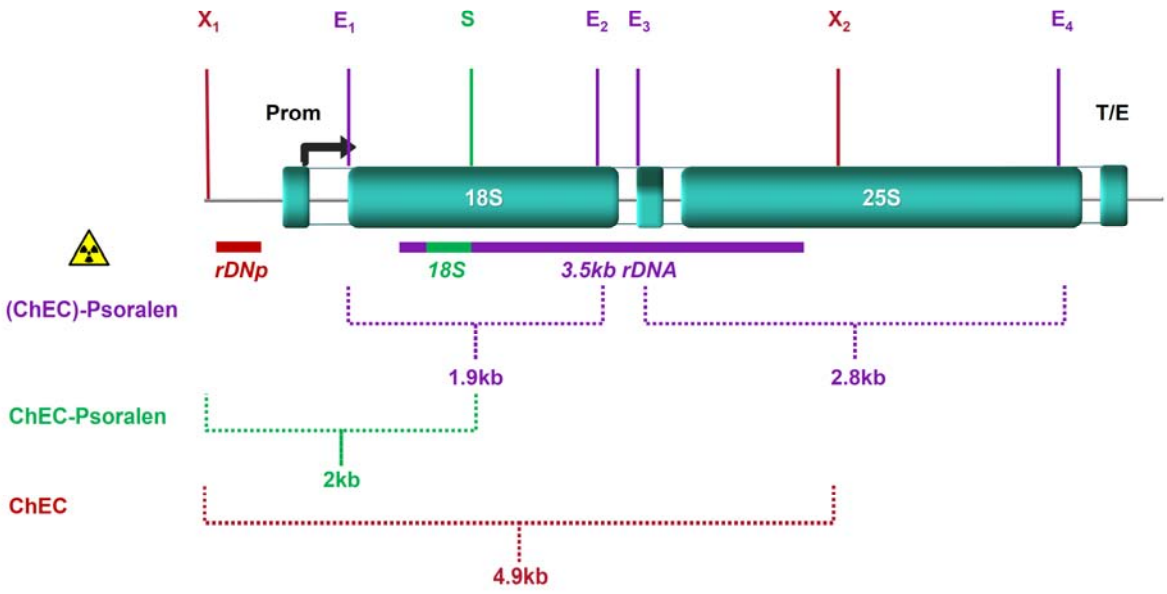

Figure 24: Relevant restriction sites and location of Southern blot probes within the rDNA locus

Only the restriction sites that are relevant for the analysis are indicated: XcmI sites are indicated as red X (1 and 2), EcoRI sites are indicated as violet E (1,2,3,4), the relevant SacII site is indicated as green S. The location of the respective probes is indicated under the rDNA locus scheme (rDNp = rDNA promoter probe used for detection of the XcmI produced promoter fragment; 18S = rDNA promoter probe used to detect the XcmI/SacII produced promoter fragment; 3.5kb rDNA = 35S rRNA gene probe used to detect EcoRI produced fragments. As indicated in the bottom half of the figure the 3.5kb rDNA probe is used for analysis of ChEC-psoralen or only psoralen experiments and detects 1.9kb (18S) and 2.8kb (25S) EcoRI-fragments. The 18S probe is used for ChEC-psoralen analysis of fusion proteins that cleave within the promoter region of the 35S rRNA gene and detects a 2kb XcmI/SacII fragment. For the analysis of ChEC experiments the rDNA promoter probe (rDNp) detects a 4.9kb rDNA fragment.

While ChIP is the predominant method to quantify DNA-protein interactions (see Figure 27 for a cartoon describing ChIP), ChEC experiments may also provide quantitative information (Babl et al., 2015). In this thesis quantification of ChEC results was made in

two different ways: First, for MNase fusion proteins that bind to many sites throughout the rDNA, the signal of the undigested fragment after each time point of ChEC was quantified. After normalization of these signals to a reference locus with no cleavage sites for the respective MNase fusion protein, the percentage of the non-degraded rDNA fragment in each lane of the blot was calculated. Second, for MNase fusion proteins that have only a single binding site at the rDNA the signal obtained for the cleaved fragment was divided by the sum of the signals obtained for cleaved and non-degraded fragment. Thus, the cleavage efficiency, could be calculated. For a detailed overview of ChEC quantification in this thesis see Figure 25.

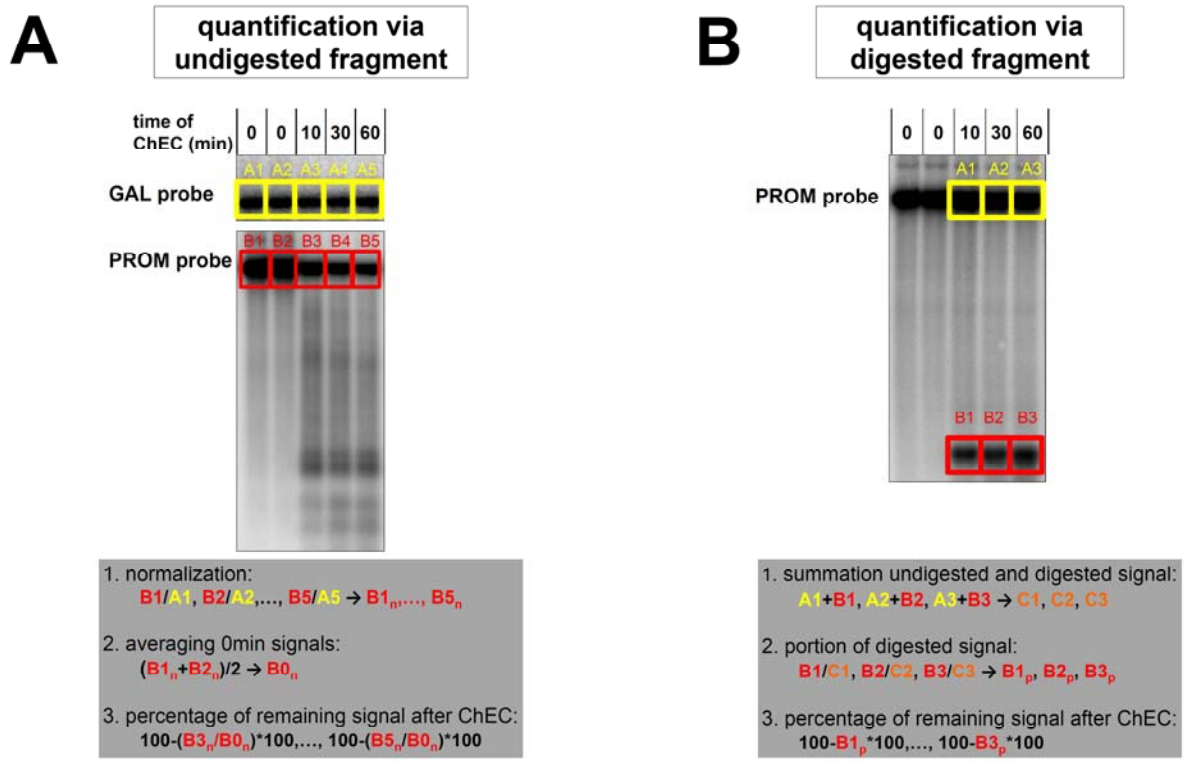

Figure 25: Quantification methods for ChEC samples

(A) Quantification of ChEC of fusion proteins which cleave multiple times in the analyzed rDNA-fragment (in this case Hmo1-MNase). ChEC was performed as described in the introduction. DNA was isolated from different samples taken before and after activation of the MNase with $CaCl_2$ (time of ChEC [min]). The samples were subjected to Southern blot analysis with probes detecting either the GAL1-10 reference locus (GAL probe), at which no Hmo1 association is observed, or the rDNA locus (PROM probe). First, the signal intensity of the non-degraded rDNA fragment after hybridization with the PROM probe (red rectangles, B1-5) was divided by the signal intensity of the respective fragment after hybridization with the GAL probe (yellow rectangles, A1-5) to derive the normalized rDNA signal intensity ($B1_n$-5_n). Second, the mean of the normalized rDNA signal intensities of the samples without MNase activation (0min) was calculated ($B0_n$). Third, the degradation efficiency was calculated as the ratio between $B3_n$-5_n, and $B0_n$ which was subtracted from 1 and multiplied by 100, yielding the percentage of non-degraded signal at the respective time point of ChEC. **(B)** Quantification of ChEC of fusion proteins with distinct cleavage sites within the analyzed rDNA-fragment (in this case Rrn9-MNase). The signal intensity of the degraded fragment obtained after hybridization with the PROM probe (red rectangles, B1-3) was divided by the sum of the signal intensities of the non-degraded fragment (yellow rectangles, A1-A3) and of the

degraded fragment (B1-B3). The obtained value was subtracted from 1 and multiplied by 100 to yield the percentage of non-degraded signal at the respective time point of ChEC.

Even if ChEC quantification provides information in good compliance with ChIP results (see section II.3.2) there are some limitations for ChEC-(psoralen): 1) ChEC analyses carried out with fusion proteins that bind to many genomic sites and are very abundant like histone-MNase do not allow normalization of DNA load using a reference locus. Additionally, these proteins can release themselves from their respective binding sites in genomic DNA during ChEC and can then act in the same manner as free MNase which leads to nonspecific degradation events; 2) due to the formaldehyde fixation it is also possible that MNase is compromised in its activity, thus leading to lesser degradation than actual association of the fusion protein with the respective locus (Babl et al., 2015).

To interpret ChEC data correctly it is also noteworthy to mention that an increase in cleavage events in close proximity to the hybridization site of the respective probe only allows to draw conclusions about this specific cleavage site but gives no suitable information about cleavage events and association of the fusion protein further downstream of this site (no detection of longer fragments once the smaller fragment has been produced). The use of additional probes for Southern blot hybridization may circumvent this problem.

ChEC-psoralen (Figure 23 B) analysis allows to monitor changes in protein association and chromatin state the protein of interest is preferentially associated with. Since a control sample with no activation of MNase is included in the analysis it also reveals some information about changes in chromatin state upon growth phase transitions. The quantification methods described in Figure 26 were used for both, ChEC-psoralen, and psoralen analyses. For the profile analysis the signal intensity profile is plotted against the migration in the gel. For the calculation of the percentage the peak area for the signals for open and closed copies was calculated. The respective percentage was derived from the portion of the single peak areas of the sum of both peak areas.

To interpret especially the percentage calculations correctly one has to keep in mind that the calculation is derived from fitted graphs. If the software which was used for the calculation was not able to identify two peaks, the opportunity to force it to find a second peak (usually for the open signal) was used. Thus values lower than approximately 10% should be treated as background or calculation artifact. The opportunity to add a second peak was only used to make sure no signals are missed due to a software threshold.

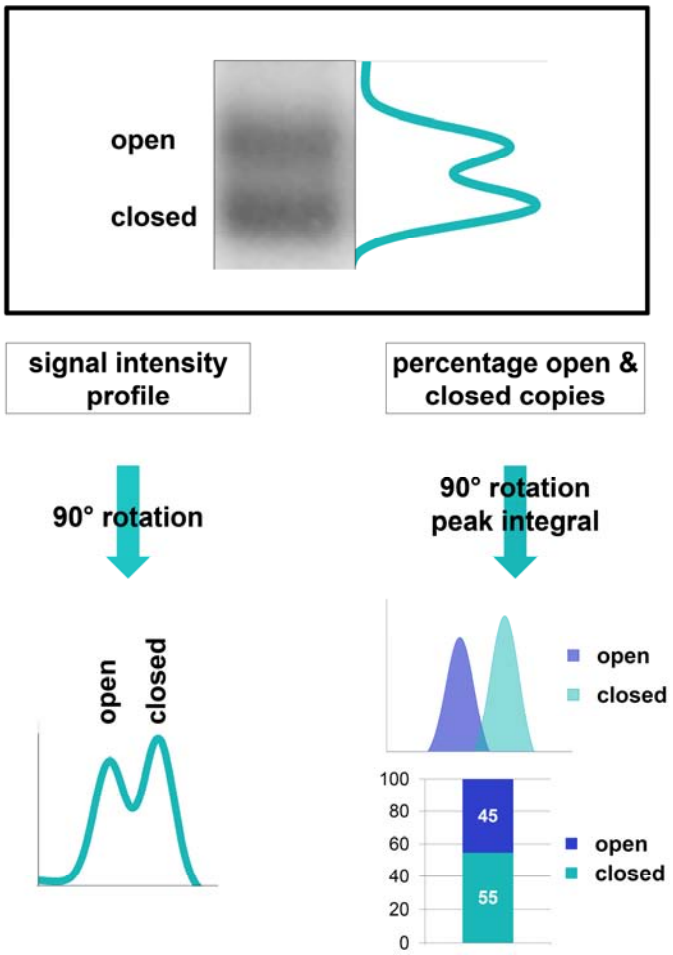

Figure 26: Profile analysis and quantification for psoralen samples

For profile analysis the signal intensities within one lane were first recorded using a FLA3000 system and then processed using the Peakfit software. Left side: The profile of signal intensities of fragments derived from open and closed 35S rRNA gene copies is plotted against the distance of migration in the gel. The first peak reflects the signal from open copies and the second peak the signal from closed copies. Right side: For calculation of the percentage of open and closed copies the profile was resolved in two single Gaussian distributions. The peak area was determined by integration. The percentage of open and closed copies was calculated by dividing the peak area for either open, or closed copies by the sum of the peak areas from open and closed copies. For Southern blot hybridization with the 3.5kb rDNA probe, the 18S fragment signal was used for profile analysis and percentage calculation throughout the whole thesis.

As already mentioned ChIP (Gilmour and Lis, 1985; Jackson, 1978; Orlando, 2000) (Figure 27) is the predominant method for quantitative protein-DNA interaction analyses. For comparison of ChEC and ChIP results some of the already ChEC analyzed proteins were additionally analyzed in ChIP in section II.3.2.

After ChIP the immunoprecipitated DNA can be analyzed using different methods such as sequencing, microarray, PCR, or qPCR. In this study ChIP was followed by qPCR analysis. The relevant amplicons are shown in Figure 28.

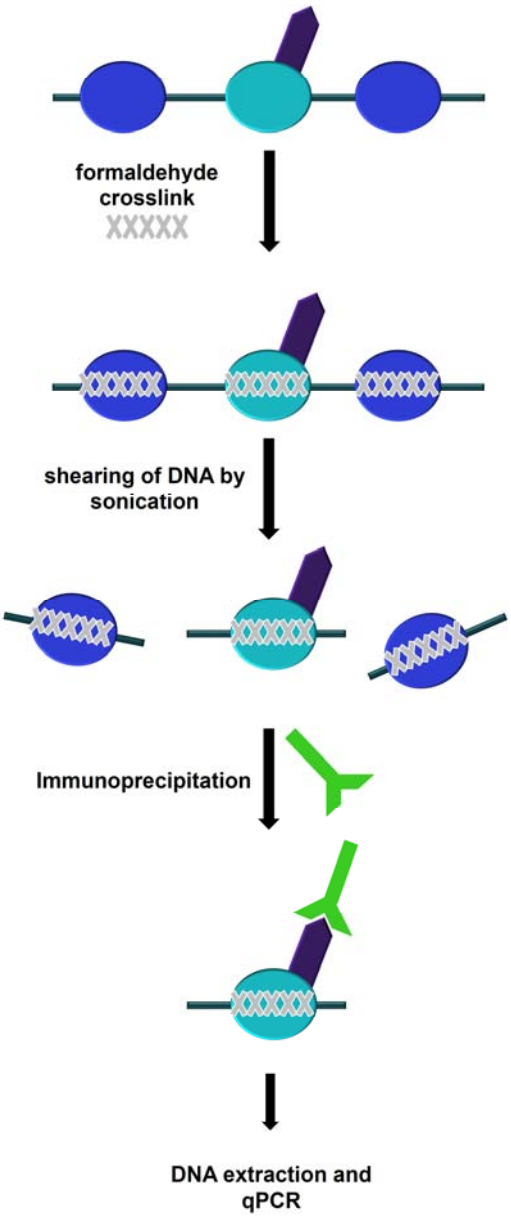

Figure 27: Cartoon of ChIP

The protein of interest (depicted as a turquoise oval) is expressed from the endogenous locus with an epitope tag (in this study either the TAP-tag or a protein A-tag) (depicted as a purple wedge). After formaldehyde crosslink (depicted as grey crosses) of proteins (blue and turquoise ovals) to DNA (aquamarine line) sonication is used for shearing of DNA. Hereafter a first sample is collected as input control. Afterwards an antibody (in this study IgG-sepharose) (depicted as a green Y) binding to the epitope tag is used for immunoprecipitation. Due to the formaldehyde crosslink not only the protein of interest but also the DNA loci where this protein is associated with are precipitated. After immunoprecipitation DNA is extracted and analyzed by qPCR. The comparison of DNA content in the input sample and in the immunoprecipitated sample allows to calculate the percentage of co-precipitated DNA for any genomic locus of interest.

Figure 28: qPCR amplicons of the rDNA locus used in this study

The cartoon of the rDNA locus (see Figure 9 for details) shows the DNA regions analyzed by qPCR in this study (depicted as purple lines): The UE amplicon is used for proteins that bind to the upstream element of the promoter, the Prom amplicon is used for proteins that bind to the core element of the promoter, the 18S and 25S amplicons are used for proteins that bind to the 18S or respectively to the 25S region of the 35S rRNA gene, and the 5S amplicon is either used for proteins that bind to the 5S rRNA gene or as a background control.

II.2 Comprehensive analysis of chromatin composition with transition to stationary phase

To investigate changes in rDNA chromatin composition in yeast cells upon growth to stationary phase, cell samples of a continuous culture were treated with formaldehyde at specific time points to crosslink proteins to their respective DNA-binding sites. The experimental setup used for the experiments in this section is shown in Figure 21.

II.2.1 Association of Pol I and Hmo1 decreased when yeast cells exit exponential growth phase

RNA Polymerase I is associated with open chromatin and it was shown that it might be the most important factor for the establishment of open 35S rRNA copies (Wittner et al., 2011). Additionally, it was shown with different methods that Pol I transcription and association decrease when cells exit exponential growth phase (Babl, 2012; Babl et al., 2015; Claypool et al., 2004; Fahy et al., 2005; Sandmeier et al., 2002). Therefore, as a first step in the present comprehensive analysis, the loss of Pol I association with the rDNA was correlated with the observed closing of 35S rRNA gene copies (Figure 19).

Hmo1 is a member of the HMG box proteins and was shown to be associated with open 35S rRNA gene chromatin. It prevents replication independent nucleosome deposition at the rDNA (Merz et al., 2008; Wittner et al., 2011). Consistently, Hmo1 was shown to partially leave the 35S rRNA genes when cells exit stationary phase (Babl, 2012; Johnson et al., 2013). Again, these findings were reproduced at the beginning of this work.

II.2.1.1 Pol I rDNA association drastically decreased upon growth to stationary phase

For the analysis of Pol I association with transition to stationary phase ChEC and ChEC-psoralen experiments with a strain expressing the largest Pol I subunit (Rpa190) as a fusion protein with MNase were carried out. To gain a detailed view on the dynamics of Pol I association, cells from four different time points of the growth experiment, exponential phase (log), diauxic shift (diauxic), post-diauxic shift phase (post-diauxic), and stationary phase (stat), were analyzed in the ChEC analysis (Figure 29 A and B).

In samples taken during exponential growth phase the Rpa190-MNase fusion protein led to cutting events throughout the whole 35S rRNA gene region within the analyzed XcmI fragment (Figure 29 A "log"), while with exit from exponential growth phase these cutting events drastically decreased and were almost completely missing at the stationary phase time-point (Figure 29 A "diauxic", "post-diauxic", "stat"). A cutting event appeared in samples taken after exit from exponential growth phase in the upper half of the autoradiograph (Figure 29 A, rhomb on the right). However this cutting event was probably not MNase mediated, since it was also visible in the lanes where no MNase activation took place. In good agreement with the disappearance of Pol I-MNase fusion protein mediated cleavage events, the degradation of the full-length XcmI fragment was strongly diminished in samples from cells which left exponential phase (Figure 29 B): While in exponential phase samples around 50% MNase-mediated degradation was observed after 30min of ChEC, only 10% of the full-length fragment were degraded in samples taken during the diauxic shift and within the post-diauxic growth phase. Finally, in stationary phase samples no significant degradation was measured. For the ChEC-psoralen analysis only cells from the "log" and "stat" culture were analyzed (Figure 29 C-E). In the samples collected at exponential phase the DNA fragments derived from the open and the closed chromatin state were clearly visible for the 18S and 25S rDNA regions before MNase activation (Figure 29 C, lane “log 0”). In samples collected at stationary phase, the signal for the fragment derived from the open chromatin state decreased significantly and collapsed to a smear migrating right above the fragment derived from the closed chromatin state (Figure 29 C, lane “stat 0”). Activation of MNase led to a complete degradation of the fragments derived from open copies in exponential phase samples, while in stationary phase samples MNase activation did not significantly alter the relative amounts of fragments derived from open and closed 35S rRNA genes (Figure 29 C and D, “60min ChEC”). While the calculation of the relative amount of open to closed copies resulted in 32% open without MNase activation and 9% open after

60min of MNase activation for the log phase sample, the portion of open copies stayed at 17% for both ChEC time points in stationary phase.

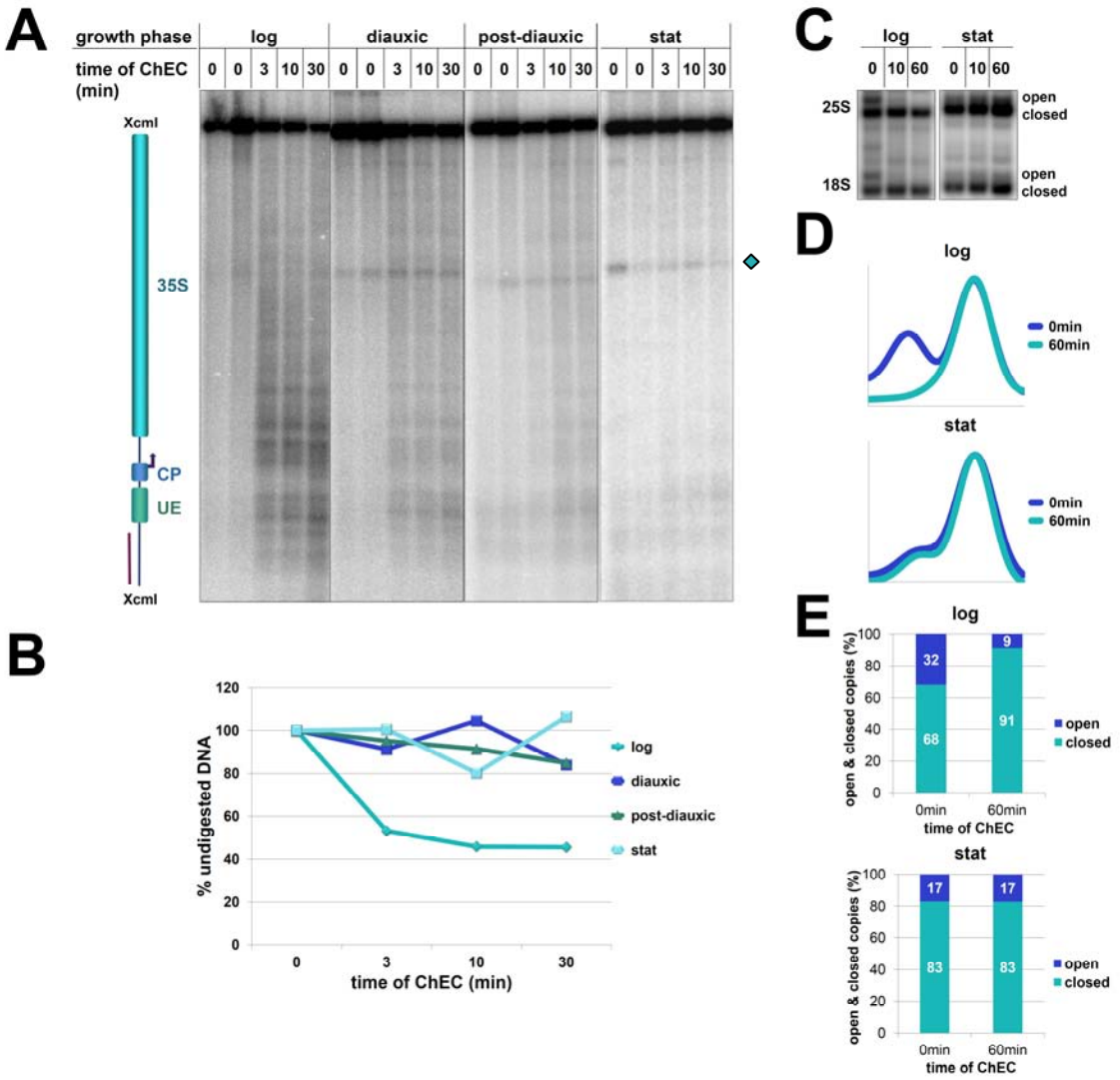

Figure 29:Rpa190-MNase mediated cleavage and psoralen accessibility at the rDNA upon transition to stationary phase

Strain y1717 (Rpa190 with C-terminal MNase expressed from the endogenous locus) was cultivated, and samples were collected from cells during exponential growth (log), during the diauxic shift (diauxic), during post-diauxic growth (post-diauxic) and at stationary phase (stat) according to Figure 21 (see OD Figure 1 in the appendix for the respective ODs). ChEC and ChEC-psoralen analyses were conducted as described in Material and Methods (see also Figure 23) **(A)** Analysis of ChEC samples: An autoradiograph of a Southern blot after hybridization with rDNp probe is shown. The origin of the sample and the time of ChEC after the addition of calcium in minutes is indicated at the top. The cartoon on the left shows the analyzed XcmI fragment of the rDNA locus, a purple bar indicates the position of the radioactively labeled probe. A rhomb on the right side of the autoradiograph marks an unspecific fragment. **(B)** Quantification of Rpa190-MNase mediated degradation shown in (A): The analysis was conducted according to Figure 25A. The percentage of undigested fragment is plotted against the time of ChEC for the different samples, labeled as shown in the legend of the graph. **(C)** ChEC-psoralen analysis of log and stat samples. An autoradiograph after hybridization with the 3.5kb rDNA probe is shown. The origin of the sample and the time of ChEC after the addition of calcium in minutes is indicated at the top. On the left it is indicated from which EcoRI rDNA fragment the signal is derived. On the right the positions of fragments derived from either the open or the closed chromatin state are labeled. **(D)** Profile analysis of the

ChEC-psoralen signals shown in (C) without MNase activation and 60min after addition of $CaCl_2$ according to Figure 26. **(E)** Ratio of open and closed rDNA copies in log and stat samples. The calculation was made according to Figure 26. The exact percent value is indicated as white numbers in the bars.

These results are in good agreement with earlier observations (Babl, 2012), and indicate that Pol I transcription and association with the rDNA locus strongly decrease in good correlation with the closing of rDNA chromatin. The fact that not all of the open rDNA copies are degraded in ChEC-psoralen analyses further suggests that a small fraction of the open rRNA genes are not associated with Pol I.

II.2.1.2 Hmo1 association with the rDNA was altered upon growth to stationary phase

Analysis of Hmo1 association with the rDNA upon transition to stationary phase was conducted in a strain expressing Hmo1 as a fusion protein with MNase. The results of ChEC and ChEC-psoralen experiments with exponential and stationary phase samples are shown in Figure 30.

The Hmo1-MNase fusion protein led to cleavage events throughout the whole 35S rRNA gene region within the analyzed XcmI fragment in samples from exponentially growing cells (Figure 30 A "log"). In contrast to the results obtained for Rpa190-MNase expressing cells, significant Hmo1-MNase mediated cleavage was still detectable in stationary phase samples (Figure 30 A "stat"). However, the cleavage pattern was shifted towards more prominent cutting events nearby the promoter region of the gene. Quantification of degradation revealed that the Hmo1-MNase mediated cleavage of the full-length XcmI fragment was decreased but still substantial in samples collected in stationary phase (Figure 30 B). ChEC-psoralen analysis showed that the open fraction was reduced in stationary phase, but still detectable as a distinct band clearly separated from the fragment derived from closed copies (Figure 30 C and D, compare "log 0" and "stat 0") as opposed to the smear observed in "stat" samples of the Rpa190-MNase expressing strain (Figure 29 C and D). Another difference to Rpa190-MNase was that the stationary phase persisting open copies were still degraded by Hmo1-MNase (Figure 30 C-E "stat 60min"). This indicates that Hmo1 was still preferentially associated with open copies in stationary phase. The efficiency of degradation was high for exponential phase samples (Figure 30 E "log"; from 29% open copies to a background level of 8% open copies) as well as for stationary phase samples (Figure 30 E "stat"; from 17% open copies to background level of 8%).

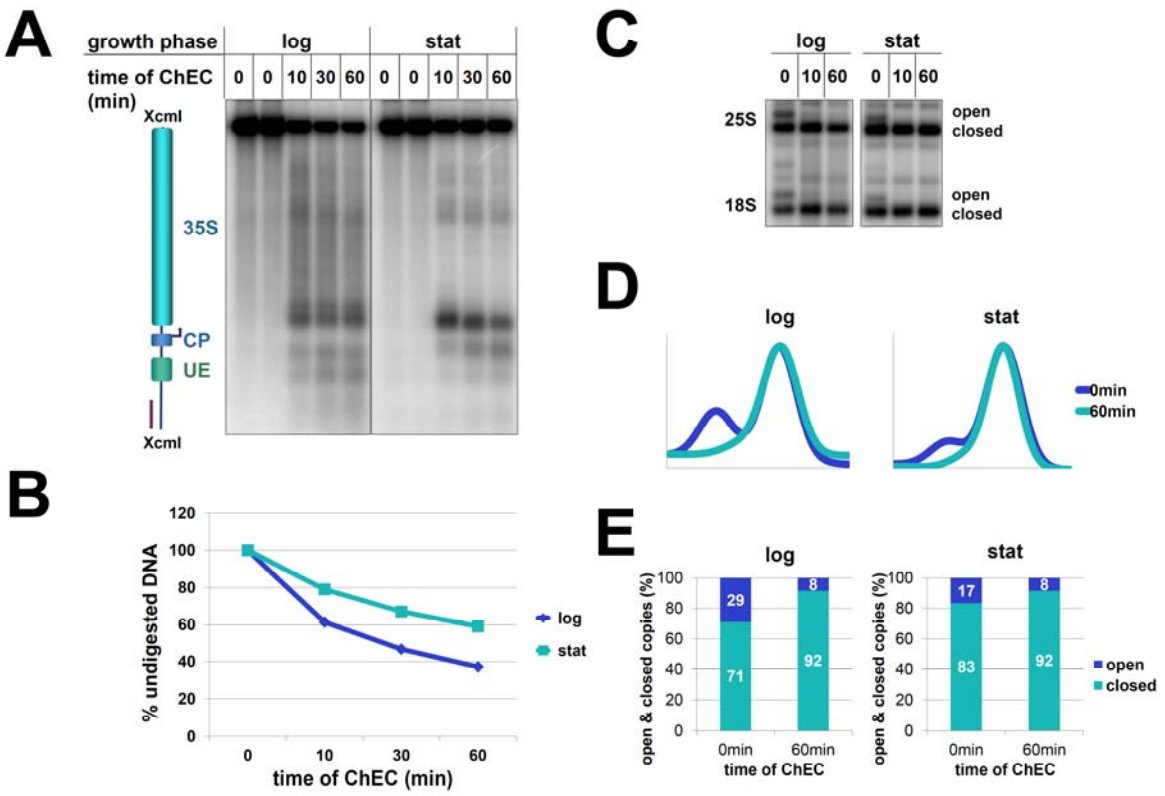

Figure 30: Hmo1-MNase mediated cleavage and psoralen accessibility at the rDNA upon transition to stationary phase

Strain y1761 (Hmo1 with C-terminal MNase expressed from the endogenous locus) was cultivated and samples were collected and analyzed in ChEC and ChEC-psoralen experiments as described in the legend to Figure 29 (see OD Figure 2 in the appendix for the respective ODs). **(A)** Analysis of ChEC samples: An autoradiograph of a Southern blot after hybridization with the rDNp probe is shown. **(B)** Quantification of Hmo1-MNase mediated degradation shown in (A): The analysis was conducted according to Figure 25A. **(C)** ChEC-psoralen analysis of EcoRI digested samples. An autoradiograph after hybridization with the 3.5kb rDNA probe is shown. **(D)** Profile analysis of the ChEC-psoralen signals shown in (C). **(E)** Ratio of open and closed rDNA copies in log and stat samples.

In summary, Hmo1-MNase association with open 35S rRNA gene copies was slightly decreased in stationary phase in good correlation with the overall reduction of open 35S rRNA gene copies. Other than Rpa190-MNase there was still degradation of the remaining open fraction by Hmo1-MNase. These results confirm earlier findings that Hmo1-MNase was still robustly associated with open 35S rRNA gene copies upon exit from exponential growth phase (Babl, 2012).

II.2.2 Association of histones indicated nucleosome assembly

While open 35S rRNA gene copies are nucleosome depleted, closed copies are packed into nucleosomes (Dammann et al., 1993; Merz et al., 2008; Wittner et al., 2011). Since 35S rRNA gene copies adopt the closed, presumably nucleosomal chromatin state with

transition to stationary phase (Figure 19) (Babl, 2012; Johnson et al., 2013; Sandmeier et al., 2002) histones were included in the comprehensive analysis. As a member of the core histones histone H3 (Hht1) was included in the analysis. Additionally, the putative linker histone Hho1 (Landsman, 1996; Ushinsky et al., 1997) was part of this study, since it was shown to be involved in higher order compaction of chromatin (Georgieva et al., 2012; Schäfer et al., 2008).

II.2.2.1 Hht1 associated preferentially with closed rDNA copies

ChEC-psoralen analysis of rDNA chromatin was conducted with a strain expressing one of the two H3 copies (Hht1) as a fusion protein with MNase. Samples from exponential and stationary phase were analyzed (Figure 31).

Hht1-MNase meditated degradation of the XcmI rDNA fragment was high in samples taken during exponential growth as well as at stationary phase (Figure 31 A and B). Especially in stationary phase samples, the cleavage pattern was more distinct when compared to the cleavage pattern of Rpa190-MNase (Figure 29 A) or of Hmo1-MNase (Figure 30 A). Degradation analysis showed almost complete degradation of the XcmI rDNA fragment in samples from exponentially growing cells and stationary phase cells (Figure 31 B). This is in accordance with the fact that the rDNA XcmI fragment includes a part of the rDNA IGS which is assembled into nucleosomes (Dammann et al., 1993; Merz et al., 2008). Furthermore, in addition to its incorporation into nucleosomes, H3 is a component of the Pol I initiation factor UAF (Keener et al., 1997), and thus expected to be associated with both, open and closed 35S rRNA genes.

However, this quantification should be taken with care, since for abundant chromatin components like histone proteins, normalization of DNA load to a reference locus is not possible and might obscure potential differences (Babl et al., 2015; Griesenbeck et al., 2012). Furthermore, a release of Hht1-MNase from its DNA binding site upon ChEC, could result in substantial concentrations of free MNase fusion protein due to the high cellular abundance of Hht1. This could in turn lead to strong degradation of the rDNA fragment, even if Hht1-MNase had not been crosslinked to this DNA.

The amount of open copies was reduced upon growth to stationary phase from 35% open copies to 19% open copies (Figure 31 C to E "log 0" compared to "stat 0"). In samples from cells in exponential phase the fraction of rDNA copies derived from closed copies was almost completely degraded upon activation of MNase but in stationary phase a significant amount of fragments derived from closed copies resisted MNase cleavage (Figure 31 E). Since only one of the two H3 gene copies (*HHT1* and not *HHT2*)

has been manipulated to express an MNase fusion protein, it is possible that differential incorporation of the tagged and untagged H3 proteins into nucleosomes during exponential growth or in stationary phase might impact the degree of degradation determined in the ChEC-psoralen experiment.

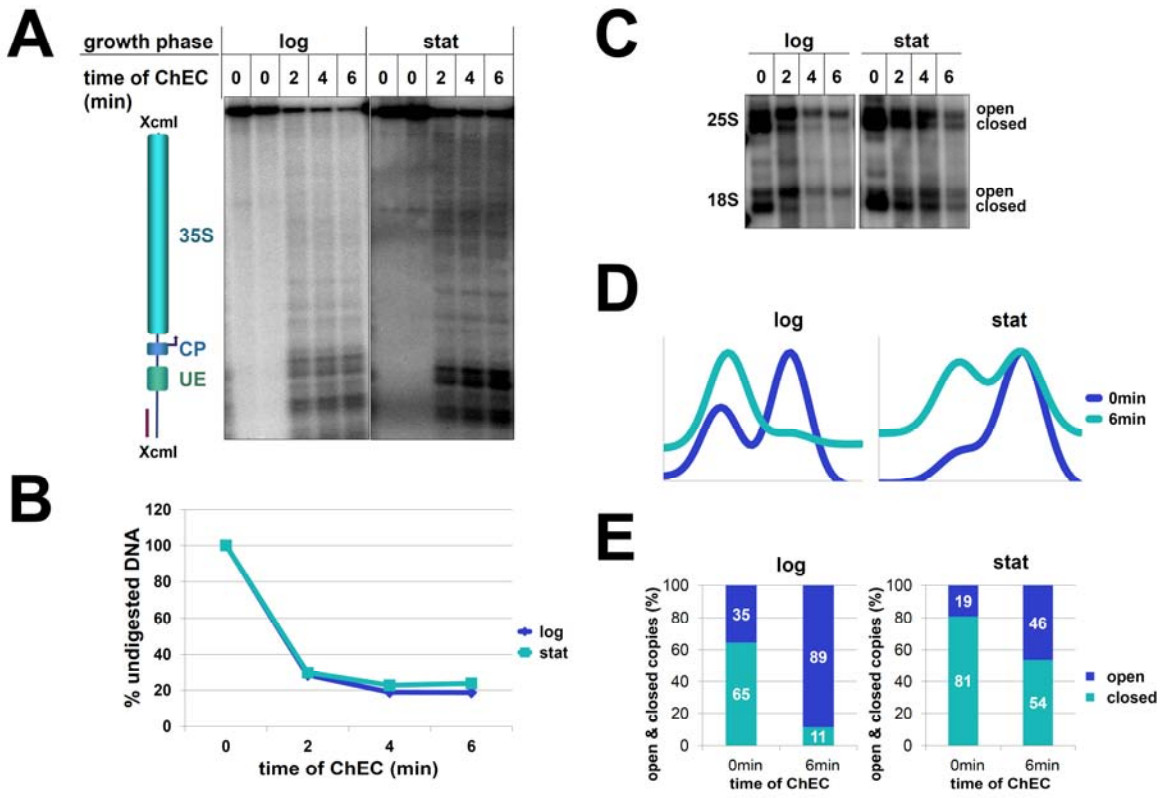

Figure 31: Hht1-MNase mediated cleavage and psoralen accessibility at the rDNA upon transition to stationary phase

Strain y1995 (Hht1 with C-terminal MNase expressed from the endogenous locus) was cultivated and samples were collected and analyzed in ChEC and ChEC-psoralen experiments as described in the legend to Figure 29 (see OD Figure 3 in the appendix for the respective ODs). **(A)** Analysis of ChEC samples: An autoradiograph of a Southern blot after hybridization with the rDNp probe is shown. **(B)** Quantification of Hht1-MNase mediated degradation shown in (A): The analysis was conducted according to Figure 25 A without normalization to a reference locus. **(C)** ChEC-psoralen analysis of EcoRI digested samples. An autoradiograph after hybridization with the 3.5kb rDNA probe is shown. **(D)** Profile analysis of the ChEC-psoralen signals shown in (C). **(E)** Ratio of open and closed rDNA copies in log and stat samples.

In summary, Hht1-MNase showed preferential degradation of closed rDNA copies in samples taken both, during exponential growth and in stationary phase.

II.2.2.2 Hho1 association with closed rDNA copies increased

Exponential and stationary phase samples from a strain expressing the putative yeast linker histone Hho1 as a fusion protein with MNase were analyzed in ChEC and ChEC-psoralen experiments (Figure 32).

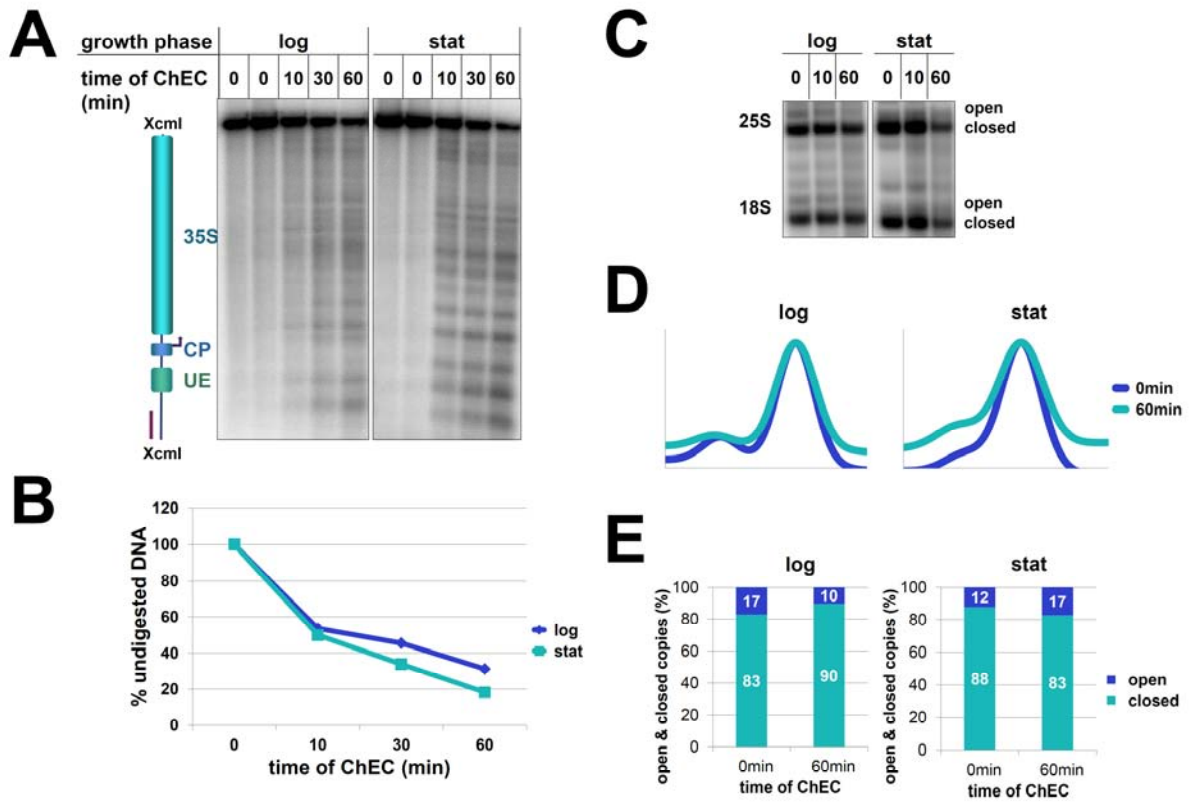

Figure 32: Hho1-MNase mediated cleavage and psoralen accessibility at the rDNA upon transition to stationary phase

Strain y1145 (Hho1 with C-terminal MNase expressed from the endogenous locus) was cultivated and samples were collected and analyzed in ChEC and ChEC-psoralen experiments as described in the legend to Figure 29 (see OD Figure 4 in the appendix for the respective ODs). **(A)** Analysis of ChEC samples: An autoradiograph of a Southern blot after hybridization with the rDNp probe is shown. **(B)** Quantification of Hho1-MNase mediated degradation shown in (A): The analysis was conducted according to Figure 25 A without normalization to a reference locus. **(C)** ChEC-psoralen analysis of EcoRI digested samples. An autoradiograph after hybridization with the 3.5kb rDNA probe is shown. **(D)** Profile analysis of the ChEC-psoralen signals shown in (C). **(E)** Ratio of open and closed rDNA copies in log and stat samples.

The activation of MNase led to cleavage events in samples collected in exponential and in stationary phase. In samples from exponential phase no clear cleavage pattern was observed but the cutting events were spread along the whole 35S rRNA gene region contained in the XcmI fragment (Figure 32 A, “log” samples). In stationary phase a regular cleavage pattern indicative for a positioned nucleosomal array was observed upon activation of MNase (Figure 32 A, “stat” samples). As shown in Figure 32 B, the degradation efficiency was only slightly increased in stationary phase. Again, as for Hht1-MNase, no normalization of DNA load to a reference locus was possible for Hho1-MNase, which could impact the quantification. This becomes more probable, when data from a previous study are taken into account, where the degradation efficiency increased more clearly than in the present dataset (Babl, 2012). Interestingly, only a small portion of copies was in the open chromatin state in exponential phase but the amount was

further reduced in stationary phase (Figure 32 C-E "log 0" and "stat 0"). Activation of MNase led to a slight degradation of open copies in exponential phase (reduction from 17% open to 10% open), while in stationary phase preferentially the closed copies were degraded (reduction from 88% closed copies to 83% closed copies) (Figure 32 E).

Taken together these results indicate, that the association of Hho1-MNase with the rDNA was increased in stationary phase. Additionally, Hho1-MNase was preferentially degrading rDNA fragments derived from open copies in exponential phase and from closed copies in stationary phase. These results are in good correlation to previous findings (Babl, 2012).

II.2.3 Pol I PIC formation was partly affected by transition to stationary phase

Since the previous results (Figure 29) strongly supported earlier reports suggesting that the association of Pol I with the rDNA decreases drastically upon transition to stationary phase (Claypool et al., 2004; Fahy et al., 2005; Sandmeier et al., 2002), it was interesting to investigate at which point this regulation takes place. In previous studies it was already shown that the amount of the initiation competent form of Pol I is decreased upon exit from exponential phase, correlating with impaired TOR signaling under those conditions (Milkereit and Tschochner, 1998). Additionally, it was shown that in contrast to Pol I, the Pol I initiation factor UAF remained associated with the rDNA promoter region in stationary phase (Claypool et al., 2004). However, there were no data available dealing with other factors involved in Pol I pre-initiation complex formation including Spt15, and CF (Figure 11). Therefore ChEC and ChEC-psoralen analyses were performed with strains expressing the UAF subunit Rrn9, the yeast TBP Spt15, and the CF subunit Rrn7 as MNase fusion proteins. Additionally, Net1-MNase was included in the analysis since Net1 stimulates Pol I transcription (Shou et al., 2001) and associates with the promoter region of open 35S rRNA genes (Goetze et al., 2010; Huang and Moazed, 2003).

II.2.3.1 The UAF component Rrn9 was associated with open rDNA chromatin in exponential phase and with closed rDNA chromatin in stationary phase

Together with Rrn10, Rrn5, Uaf30, H4, and H3 Rrn9 is a member of UAF. To investigate changes in the association of this complex with the rDNA upon transition to stationary phase ChEC and ChEC-psoralen experiments with a strain expressing Rrn9 as a fusion protein with MNase were carried out (Figure 33).

The activation of Rrn9-MNase led to a single cleavage at the upstream element. This cleavage was present in exponential and stationary phase (Figure 33 A). Quantification of the relative intensity of the cleaved fragment signal compared to the full-length fragment signal indicated that Rrn9-MNase stayed associated with the rDNA in stationary phase at the same level as in exponential phase. However, the degradation efficiency was not very high (approximately 20% degradation) (Figure 33 B). The amount of open copies was strongly reduced in stationary phase with only a smear of rDNA fragments (derived from partially open rRNA genes) migrating right above the band derived from closed copies (Figure 33 C "log 0" compared to "stat 0"). While in samples from cells at exponential growth phase preferentially the open copies were degraded, Rrn9-MNase was associated with closed or partially closed copies in samples collected from stationary cells (Figure 33 C-E). This was well reflected by the electrophoretic mobility of the fragments which were cleaved by Rrn9-MNase (Figure 33 C intensified autoradiograph at the bottom).

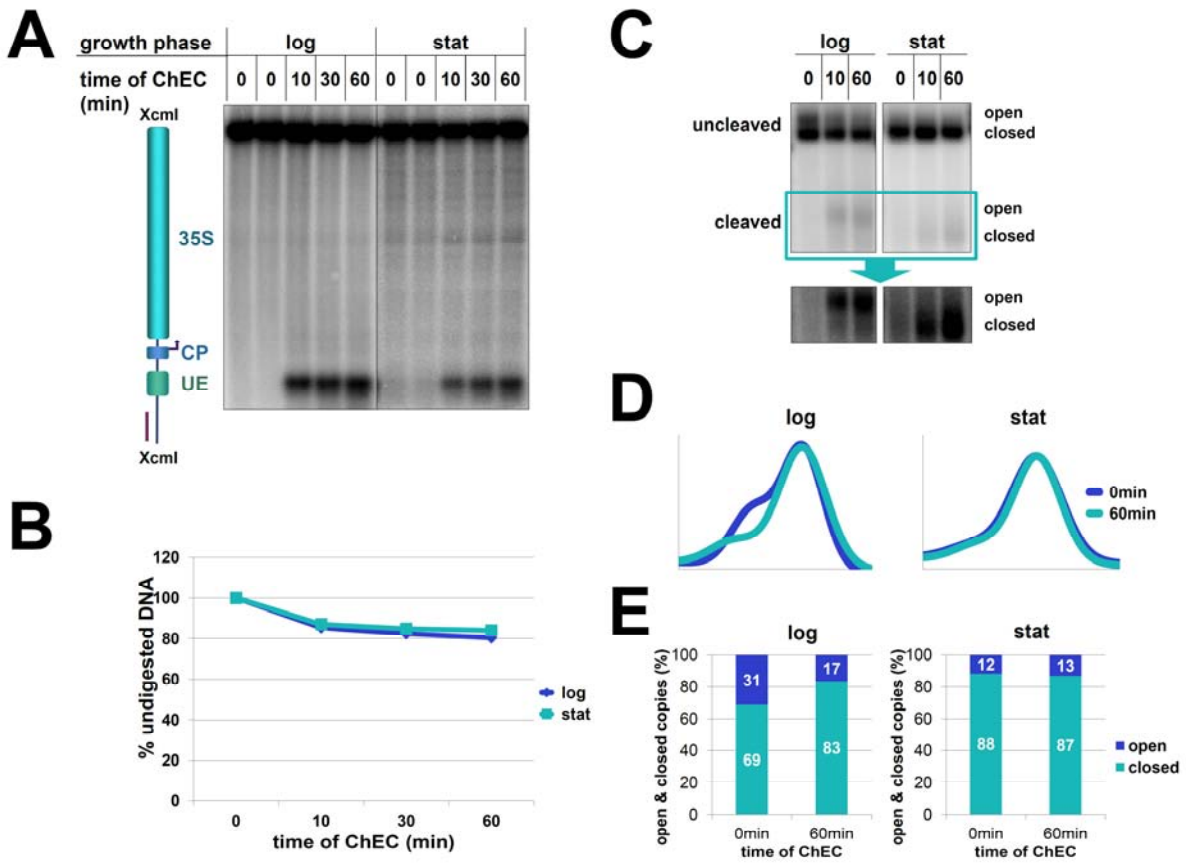

Figure 33: Rrn9-MNase mediated cleavage and psoralen accessibility at the rDNA upon transition to stationary phase

Strain y1151 (Rrn9 with C-terminal MNase expressed from the endogenous locus) was cultivated and samples were collected and analyzed in ChEC and ChEC-psoralen experiments as described in the legend to Figure 29 (see OD Figure 5 in the appendix for the respective ODs). **(A)** Analysis of ChEC samples: An autoradiograph of a Southern blot after hybridization with the rDNp probe is shown. **(B)** Quantification of Rrn9-MNase mediated

degradation shown in (A): The analysis was conducted according to Figure 25 B. **(C)** ChEC-psoralen analysis of XcmI/SacII digested samples. An autoradiograph after hybridization with the 18S probe is shown. Positions of the uncleaved and the cleaved fragment are given on the left. A longer exposure of the framed blot region visualizing the cleaved fragments is shown at the bottom. **(D)** Profile analysis of the signals of the uncleaved fragments of the ChEC-psoralen experiment shown in (C). **(E)** Ratio of open and closed rDNA copies in log and stat samples.

In summary, Rrn9-MNase stayed associated with the upstream element of at least 20% of 35S rRNA gene copies in exponential and stationary phase samples. Whereas Rrn9-MNase bound rRNA genes were predominantly in the open chromatin state in exponential phase, Rrn9-MNase cleaved rRNA genes were in the closed chromatin state in stationary phase samples.

II.2.3.2 Spt15 stayed associated with the promoter region when cells transit to stationary phase

The yeast homolog of TBP is Spt15 (Eisenmann et al., 1989). Since it is also part of the Pol I PIC a strain expressing an MNase fusion protein of Spt15 was analyzed in ChEC and ChEC-psoralen experiments (Figure 34).

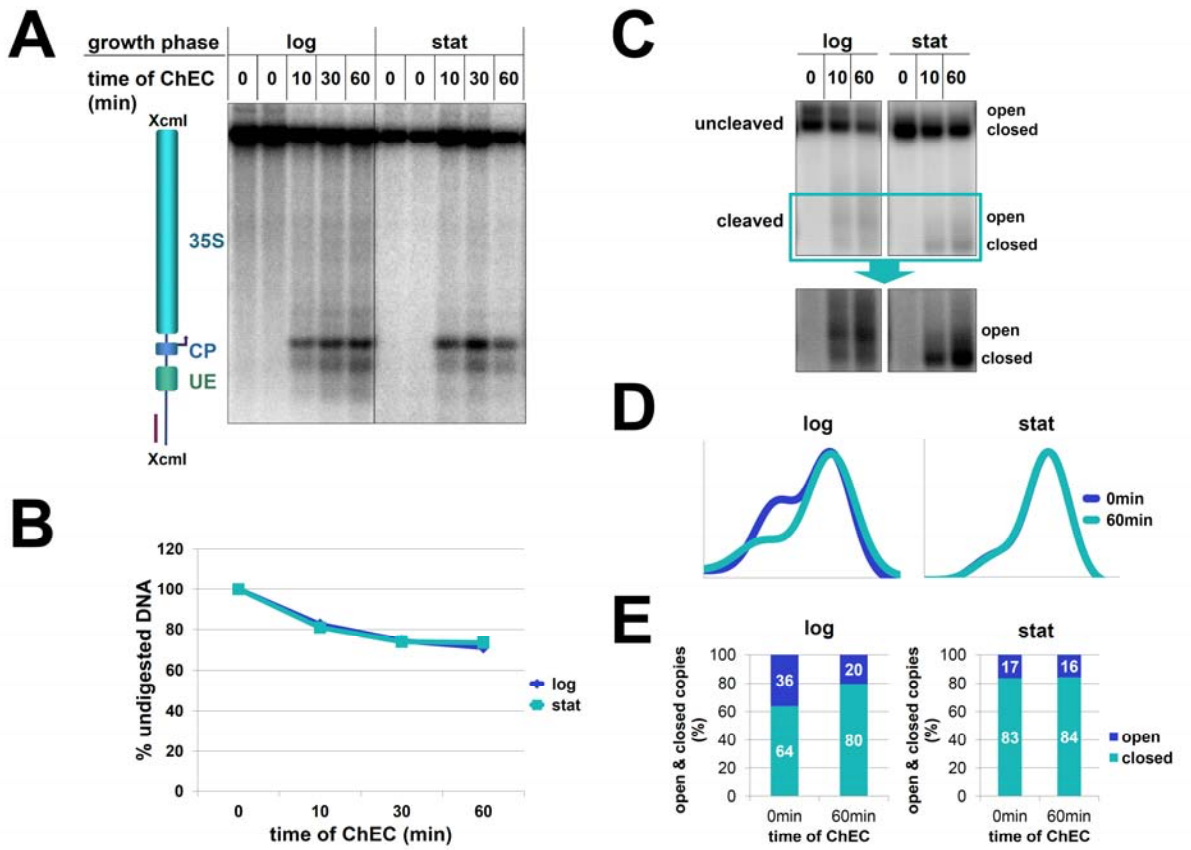

Figure 34: Spt15-MNase mediated cleavage and psoralen accessibility at the rDNA upon transition to stationary phase

Strain y1185 (Spt15 with C-terminal MNase expressed from the endogenous locus) was cultivated and samples were collected and analyzed in ChEC and ChEC-psoralen experiments as described in the legend to Figure 29 (see OD Figure 6 in the appendix for the respective ODs). **(A)** Analysis of ChEC samples. An autoradiograph of a

Southern blot after hybridization with the rDNp probe is shown. **(B)** Quantification of Spt15-MNase mediated degradation shown in (A). The analysis was conducted according to Figure 25 B. **(C)** ChEC-psoralen analysis of XcmI/SacII digested samples. An autoradiograph after hybridization with the 18S probe is shown. Positions of the uncleaved and the cleaved fragment are given on the left. A longer exposure of the framed blot region visualizing the cleaved fragments is shown at the bottom. **(D)** Profile analysis of the signals of the uncleaved fragments of the ChEC-psoralen experiment shown in (C). **(E)** Ratio of open and closed rDNA copies in log and stat samples.

As observed earlier (Merz et al., 2008) the major cleavage event occurred at a distinct site within the CP and a series of weaker cuts over a region covering the UE of the rDNA promoter region. The CE cut was dominant. However, there was no change in the extent of cleavage in samples derived from stationary phase cells. Thus, the degradation efficiency was approximately 20% in exponential and stationary phase samples (Figure 34 B). Thus, Spt15-MNase stayed associated with its binding site even in stationary phase. ChEC-psoralen analysis revealed that most of the copies adopted the closed chromatin state in stationary phase. However, a minor fraction of fragments derived from the remaining open or partially open copies migrated right above the band derived from closed copies as a smear (Figure 34 C "log 0" compared to "stat 0"). While in samples from cells at exponential growth phase preferentially the open copies were degraded, Spt15-MNase was associated with closed or partially closed copies in samples collected from stationary cells (Figure 34 C-E). This was well reflected by the electrophoretic mobility of the fragments which were cleaved by Spt15-MNase (Figure 34 C intensified autoradiograph at the bottom).

Thus, similarly to Rrn9-MNase, Spt15-MNase appeared to stay associated with the rDNA even in stationary phase samples. As also seen for Rrn9-MNase, Spt15-MNase cleaved preferentially within the rDNA promoter region of open 35S rRNA gene copies samples from exponentially growing cells, whereas it cut preferentially the promoter region of closed 35S rRNA genes in stationary phase samples.

II.2.3.3 Association of the CF component Rrn7 with the rDNA promoter was decreased in stationary phase

Together with Rrn6 and Rrn11 Rrn7 is one of three subunits of CF. To investigate whether CF association with the rDNA promoter changes in samples withdrawn from exponentially growing and stationary phase cells, a strain expressing an Rrn7-MNase fusion protein was subjected to ChEC and ChEC-psoralen experiments (Figure 35).

Activation of Rrn7-MNase led to two cutting events of approximately same intensity in exponential phase samples (Figure 35 A). The first cleavage event was located at the core promoter (CP) and the other located in close proximity of the 5’ end of the upstream element. It had been speculated that this cleavage pattern is the result of a specific

promoter architecture (Merz et al., 2008). In stationary phase the signal of the cleaved fragments strongly decreased especially for the cut near the upstream element (cut2, Figure 35 A). The degradation efficiency decreased from approximately 20% in exponential phase to less than 5% in stationary phase (Figure 35 B). ChEC-psoralen analysis showed that the copies were closed in stationary phase (51% open in exponential phase and only a background level of 11% open in stationary phase) (Figure 35 C-E "log 0" compared to "stat 0"). Rrn7-MNase associated preferentially with the open chromatin state. Nevertheless, not all open copies were degraded during the ChEC time course. Interestingly, while in ChEC (Figure 35 A) both cleaved fragments appeared to have a similar intensity, in ChEC-psoralen the cleaved promoter fragment (cut1) had a higher intensity (Figure 35 C compare "open (cut1)" and "open (cut2)"). This indicates that there were possibly different promoter conformations: One that only led to cleavage at the upstream element site (probably a lower fraction due to the reduced signal of "open (cut2)" in ChEC-psoralen), one that only allowed cleavage at the CP site (due to the clearly detectable signal of "cut1" in ChEC), and one that led to cleavage at both sites (due to the different signal intensity relations in ChEC and ChEC-psoralen).

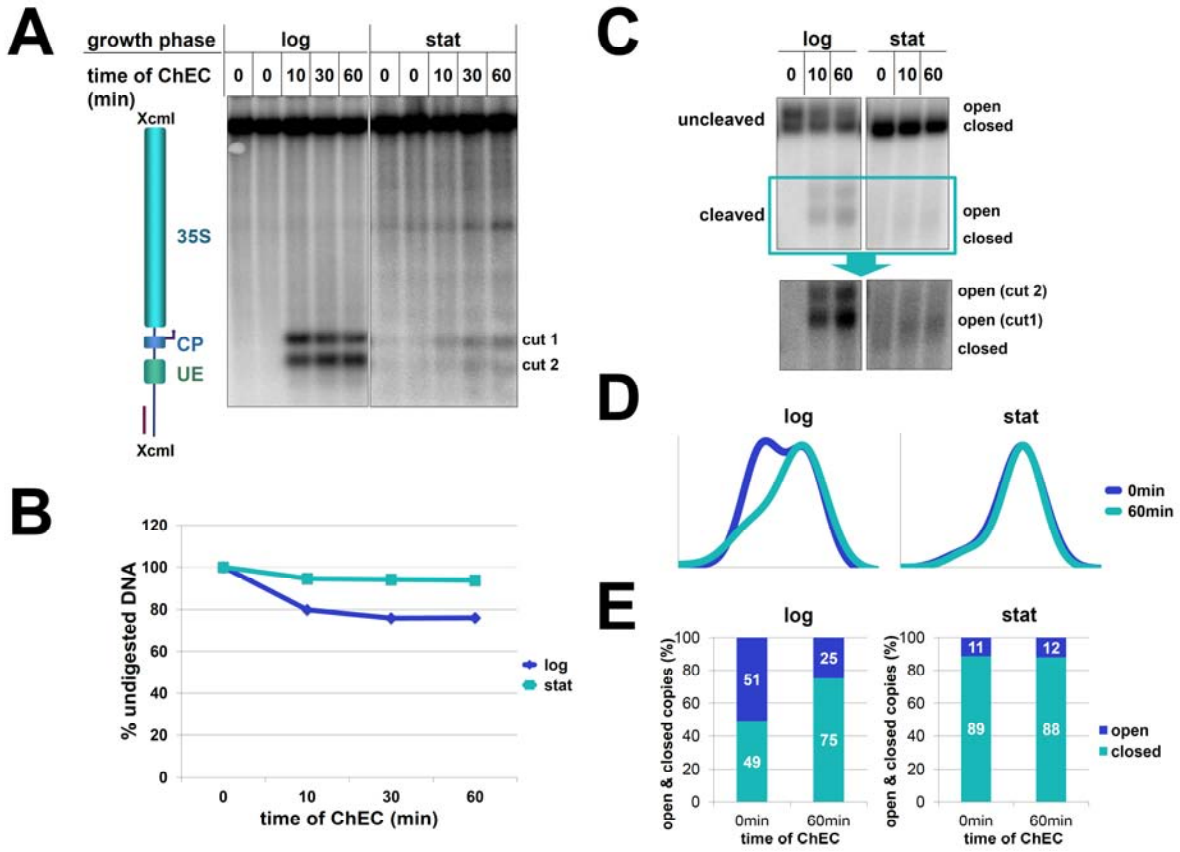

Figure 35: Rrn7-MNase mediated cleavage and psoralen accessibility at the rDNA upon transition to stationary phase

Strain y881 (Rrn7 with C-terminal MNase expressed from the endogenous locus) was cultivated and samples were collected and analyzed in ChEC and ChEC-psoralen experiments as described in the legend to Figure 29

(see OD Figure 7 in the appendix for the respective ODs). **(A)** Analysis of ChEC samples. An autoradiograph of a Southern blot after hybridization with the rDNp probe is shown. The position of two fragments originating from distinct cleavage events is shown on the right (cut1 and cut2) **(B)** Quantification of Rrn7-MNase mediated degradation shown in (A): The analysis was conducted according to Figure 25 B. **(C)** ChEC-psoralen analysis of XcmI/SacII digested samples. An autoradiograph after hybridization with the 18S probe is shown. Positions of the uncleaved and the cleaved fragment are given on the left. A longer exposure of the framed blot region visualizing the cleaved fragments is shown at the bottom. The position of two fragments originating from distinct cleavage events is shown on the right (cut1 and cut2) **(D)** Profile analysis of the signals of the uncleaved fragments of the ChEC-psoralen experiment shown in (C). **(E)** Ratio of open and closed rDNA copies in log and stat samples.

In summary, Rrn7-MNase was preferentially associated with open 35S rDNA copies in exponential phase, but Rrn7-MNase mediated rDNA degradation was drastically decreased in stationary phase.

II.2.3.4 Net1 association with the promoter region decreased upon transition to stationary phase

Net1 stimulates Pol I rDNA transcription (Shou et al., 2001) and interacts with the rDNA promoter (Goetze et al., 2010; Huang and Moazed, 2003). To correlate Net1-rDNA interaction with the decrease in Pol I transcription upon transition to stationary phase (Figure 29) a yeast strain expressing Net1-MNase was analyzed in the comprehensive analysis in ChEC and ChEC-psoralen experiments (Figure 36).

Net1-MNase led to cleavage events at the promoter region and at the beginning of the 35S rDNA gene during ChEC time-course. In stationary phase samples the cutting events at the 18S part of the 35S rDNA gene disappeared and cleavage at the promoter site decreased (Figure 36 A). Overall degradation of the full-length XcmI fragment was decreased in stationary phase samples (Figure 36 B). ChEC-psoralen analysis revealed that the overall amount of open 35S rRNA gene copies decreased in stationary phase (Figure 36 C - E "log 0" compared to "stat 0"). In exponential phase samples the complete fraction of open copies was degraded by Net1-MNase (Figure 36 C - E "log"). Upon growth to stationary phase the fraction of open copies decreased substantially with fragments derived from partially open copies migrating as a smear right above the fragments derived from the closed copies (Figure 36 C and D "stat 0"). However, these remaining open copies were still degraded by Net1-MNase after activation of the MNase (Figure 36 C - E).

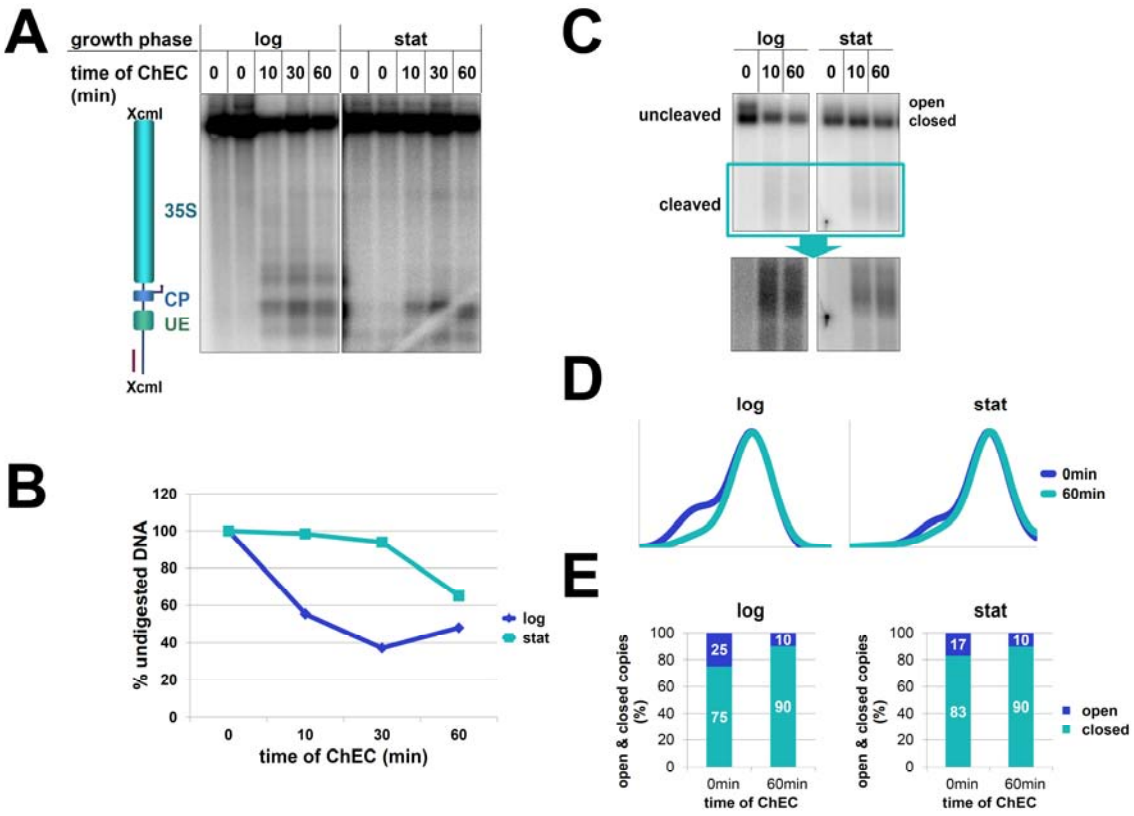

Figure 36: Net1-MNase mediated cleavage and psoralen accessibility at the rDNA upon transition to stationary phase

Strain y1453 (Net1 with C-terminal MNase expressed from the endogenous locus) was cultivated and samples were collected and analyzed in ChEC and ChEC-psoralen experiments as described in the legend to Figure 29 (see OD Figure 8 in the appendix for the respective ODs). **(A)** Analysis of ChEC samples. An autoradiograph of a Southern blot after hybridization with the rDNp probe is shown. **(B)** Quantification of Net1-MNase mediated degradation shown in (A): The analysis was conducted according to Figure 25 A. **(C)** ChEC-psoralen analysis of XcmI/SacII digested samples. An autoradiograph after hybridization with the 18S probe is shown. Positions of the uncleaved and the cleaved fragments are given on the left. A longer exposure of the framed blot region visualizing the cleaved fragments is shown at the bottom. **(D)** Profile analysis of the signals of the uncleaved fragments of the ChEC-psoralen experiment shown in (C). **(E)** Ratio of open and closed rDNA copies in log and stat samples.

This indicates, that Net1-MNase was preferentially associated with open 35S rDNA chromatin in exponential phase as well as in stationary phase. The overall association of Net1-MNase with the rDNA promoter dropped in correlation with the decrease in open rDNA copies. These findings resembled the results obtained in the strain expressing Rpa190-MNase (Figure 29).

In conclusion the comprehensive analysis of protein-rDNA interactions upon growth to stationary phase confirmed that Pol I association is affected by the transition to stationary phase in good correlation with a transition of rRNA genes to the closed chromatin state. The data indicated that the chromatin transition is accompanied by the formation of more regularly spaced nucleosomal arrays and -consistent with previous observations- the association of the yeast linker histone Hho1 (Babl, 2012; Schäfer et al., 2008). In

agreement with the study by Claypool et al. (2004) UAF association with the rDNA promoter was not affected upon growth to stationary phase, as it was also the case for yeast TBP, Spt15. The present work further revealed that Pol I PIC formation might be specifically affected at the level of CF- and Net1-rDNA interaction under these conditions.

II.3 The influence of *RPD3* deletion on stationary phase rDNA chromatin

Pol I association and transcription are drastically decreased after exit from stationary phase (Babl, 2012; Claypool et al., 2004; Fahy et al., 2005; French et al., 2003; Sandmeier et al., 2002) (Figure 29). This observation has been mainly attributed to the target of rapamycin (Tor) pathway, which affects the formation of the initiation competent Rrn3-Pol I complex (Claypool et al., 2004; Milkereit and Tschochner, 1998; Peyroche et al., 2000). In wildtype yeast cells the impaired Pol I transcription generally coincides with the transition of rRNA genes to the closed chromatin state (see Figure 19 and section II.2) (Babl, 2012; Sandmeier et al., 2002). Interestingly, Sandmeier et al. (2002) reported that a deletion of the *RPD3* gene, coding for a major histone deacetylase, interferes with the closing of rRNA genes in stationary phase, despite the fact that Pol I transcription was largely impaired under these conditions. In the following sections this phenomenon is called the "*rpd3*Δ phenotype".

In exponentially growing cells Pol I transcription is responsible to establish and maintain open 35S rRNA gene chromatin, whereas 35S rRNA genes adopt the closed chromatin state upon replication (Wittner et al., 2011). In the absence of replication, however, open 35S rRNA gene chromatin can be maintained even in the absence of Pol I transcription by the HMG-box protein Hmo1 (Wittner et al., 2011). Since in stationary *rpd3*Δ cells Pol I transcription was suggested to be downregulated as a consequence of Tor pathway inactivation (Claypool et al., 2004; Oakes et al., 2006), it was tempting to speculate that Hmo1 was implicated in the maintenance of the open rRNA gene chromatin state under these conditions. However, a double deletion mutant (*rpd3*Δ*hmo1*Δ*)* did not confirm this hypothesis, indicating that Hmo1 is not absolutely required to maintain the open 35S rRNA gene chromatin state in stationary phase (Babl, 2012). Recently, a study suggested that the *rpd3*Δ phenotype is due to impaired nucleosome deposition and thus a defect in closing of copies (Johnson et al., 2013). However, a preceding analysis showed not only a prevented closing of rDNA copies, but that the fraction of open copies

even increased with transition to stationary phase, thus suggesting a potential role of an "opening factor" (Babl, 2012).

At the beginning of this study, it was therefore first tested if Pol I transcription –despite being impaired due to Tor pathway inactivation- is involved in the establishment of the *rpd3*Δ phenotype. Second, the comprehensive ChEC(-psoralen) analysis conducted in *RPD3* strains (see previous section) was extended to *rpd3*Δ strains and validated by ChIP experiments to identify factors that are involved in the establishment of the *rpd3*Δ phenotype.

II.3.1 Pol I transcription established the *rpd3*Δ phenotype and was supported by Hmo1

To study the effects of Pol I initiation and transcription on 35S rRNA gene chromatin state in stationary phase, we used strains carrying a temperature sensitive (ts) allele of *RRN3* (*rrn3-ts*) in which Pol I initiation can be shut down by temperature shift (Claypool et al., 2004). We subjected *rrn3-ts* strains carrying different combinations of either wildtype *RPD3, HMO1,* or mutant *Δrpd3, Δhmo1* alleles to growth experiments (see Figure 37 for the experimental setup).

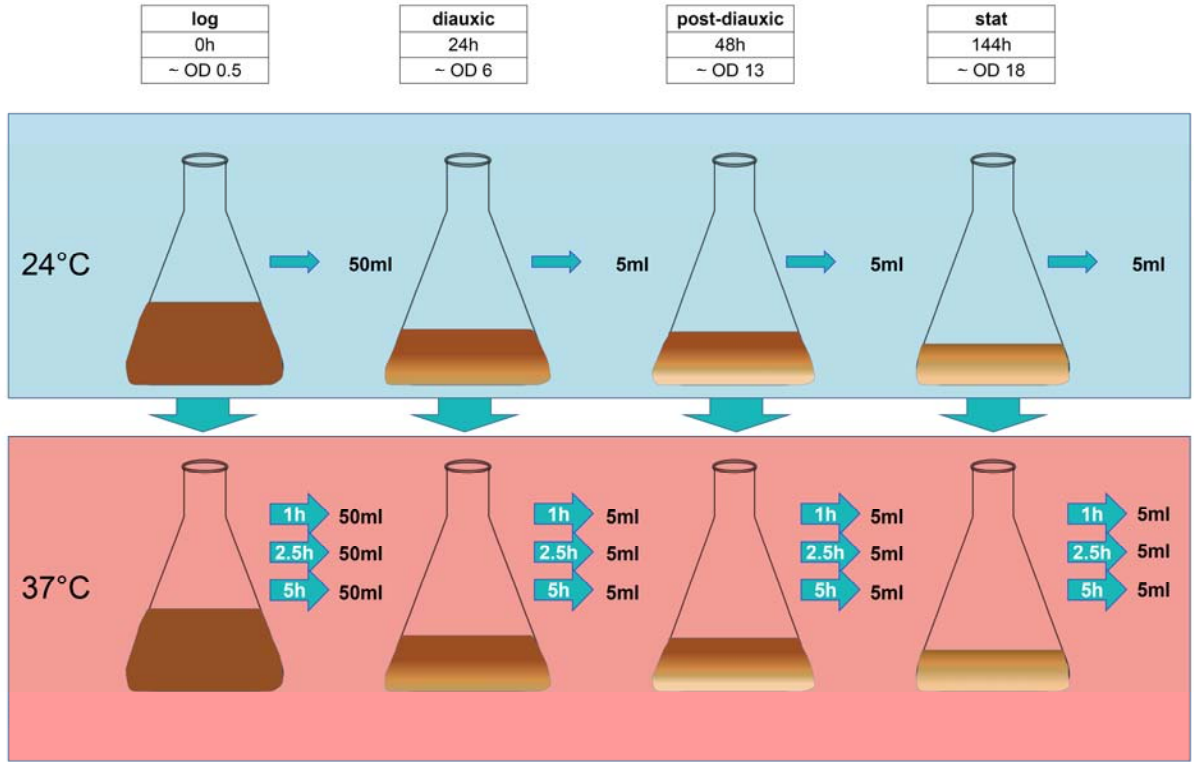

Figure 37: Experimental setup for conditional shut-down of Pol I transcription in yeast strains upon growth to stationary phase.

Yeast strains carrying a temperature sensitive allele of *RRN3* (*rrn3S213P, rrn3-ts*) (Claypool et al., 2004) were inoculated in four different flasks and grown in parallel: One that was grown to exponential phase (log), one that

was grown to the diauxic shift (diauxic), one that was grown to post-diauxic phase (post-diauxic), and one that was grown to stationary phase (stat) at the permissive temperature (24°C, indicated by a blue background). The respective culture times until sample collection from the "log" culture were 24h for the diauxic shift culture, 48h for the post-diauxic shift culture and 144h for the stationary phase culture. At the indicated culture phase a sample was collected (50ml for the log sample, 5ml for the diauxic, the post-diauxic, and the stationary phase sample) and treated as described in the legend of Figure 21. Afterwards the cultures were further incubated at the restrictive temperature for 5h (37°C, indicated by a red background). 1h, 2.5h, and 5h after the temperature shift further samples were collected (50ml for the log sample, 5ml for the diauxic, the post-diauxic, and the stationary phase sample) and treated as the samples before. All samples were then subjected to psoralen analysis.

The main culture was divided in four subcultures, which were either cultivated to exponential phase, diauxic shift, post-diauxic phase, or stationary phase at the permissive temperature (24°C). After sample collection the rest of the culture was incubated at the restrictive temperature of 37°C, inactivating Pol I transcription. Samples were collected at different times after temperature shift to analyze the chromatin state of the rDNA by psoralen photocrosslinking.

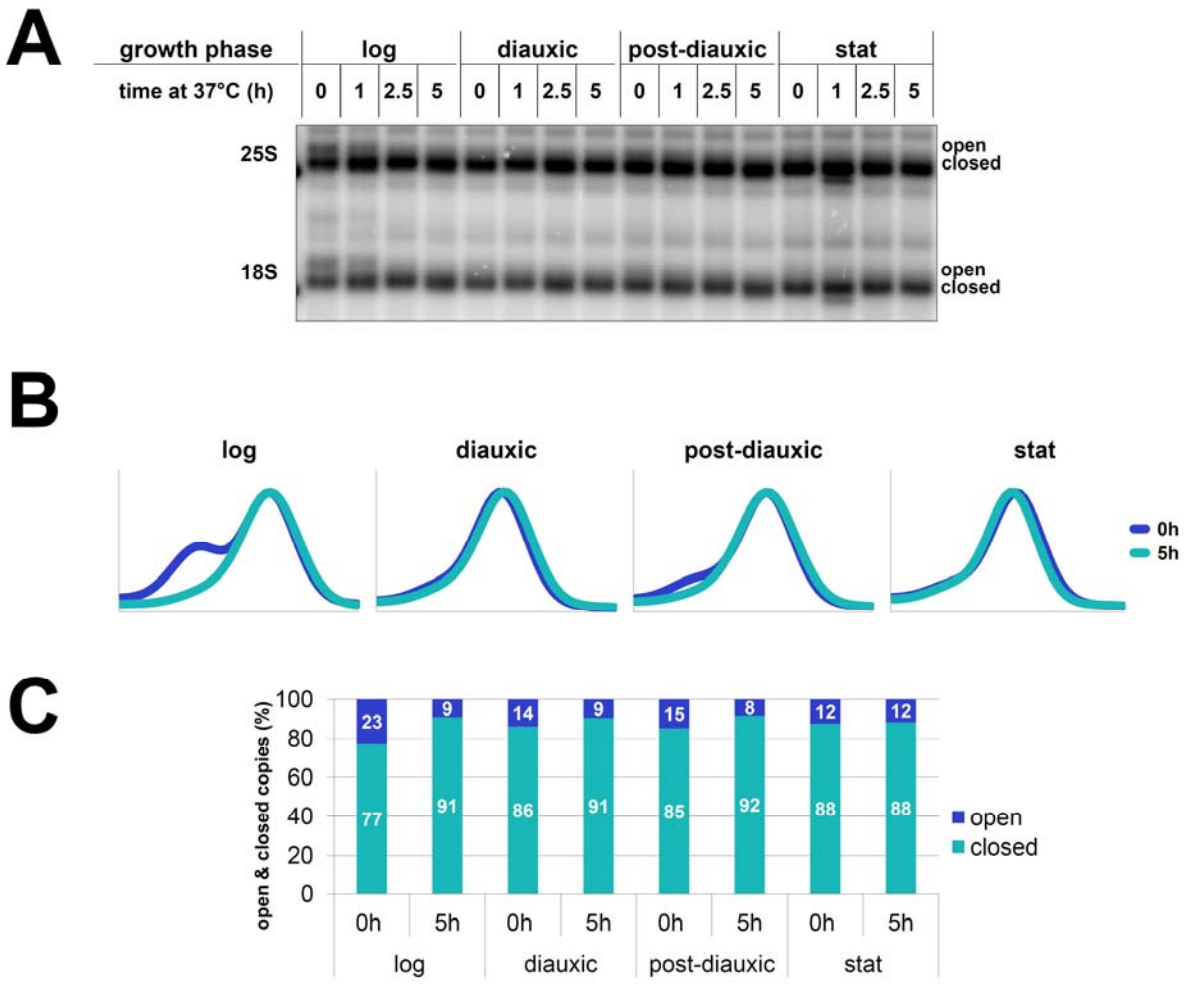

Figure 38: Chromatin dynamics at the rDNA upon conditional shutdown of Pol I transcription initiation in an *rrn3ts RPD3 HMO1* strain at different growth phases

Strain y354 (*rrn3ts RPD3 HMO1*) was cultured according to Figure 37 (see OD Figure 9 in the appendix for the ODs of the respective cultures). **(A)** Psoralen analysis. An autoradiograph after hybridization with the 3.5kb rDNA

probe is shown. The origin of the sample is indicated at the top. On the left it is indicated from which EcoRI rDNA fragment the signal is derived. On the right the positions of fragments derived from either the open or the closed chromatin state are labeled. **(B)** Profile analysis of the psoralen samples shown in (A) according to Figure 26. **(C)** Ratio of open and closed rDNA copies. The calculation was made according to Figure 26. The exact percent values are indicated as white numbers in the bars.

As expected, in an *rrn3ts RPD3 HMO1* strain 35S rRNA gene copies adopted the closed state with exit from exponential phase during growth at the permissive temperature (Figure 38 A - C "log" - "stat" "0h"). While in exponential phase 23% of the copies were in the open chromatin state in stationary phase only a background level of 12% remained open. The fragment derived from the open 35S rRNA gene copies migrated as a smear right above the fragments derived from the closed copies in all phases except the exponential phase. While inactivation of Pol I initiation by a temperature shift did not affect psoralen accessibility of the already closed 35S rRNA genes in post exponential phase cultures, it led to almost complete closing of open 35S rDNA copies in exponentially growing cells (Figure 38 A - C "log" - "stat" "5h"). This result is in good correlation with earlier studies (Babl, 2012; Wittner et al., 2011).

An *rrn3ts rpd3*Δ *HMO1* strain had a substantial amount of open copies after the exit from exponential phase (Figure 39 A - C, "0h"). However, the *rpd3*Δ phenotype was less pronounced than in an *RRN3* strain with prolonged growth and the fragment derived from the open 35S rRNA gene copies was migrating only as smear above the fragments derived from the closed copies in later growth phases (Figure 19). This could be due to a reduced protein stability or an increased proteolysis of the mutant Rrn3ts protein under nutritional stress conditions (see Hilt and Wolf (1992) for a review about proteolysis and stress in yeast). Nonetheless, an increase in temperature to the restrictive temperature led to a reduction of the amount of open copies in all growth phases (Figure 39 A - C "0h" compared to "5h"). In all growth phases, even 5h after the temperature shift a significant fraction of 35S rRNA genes still adopted an open chromatin state (compare Figure 39 "5h" to Figure 38 "5h").

Taken together, these data suggested, that the shutdown of Pol I initiation leads to a closing of 35S rRNA gene copies even in the absence of Rpd3. However, not all copies adopted the closed chromatin state. For the exponential phase the results are in good correlation with an earlier study (Babl, 2012).

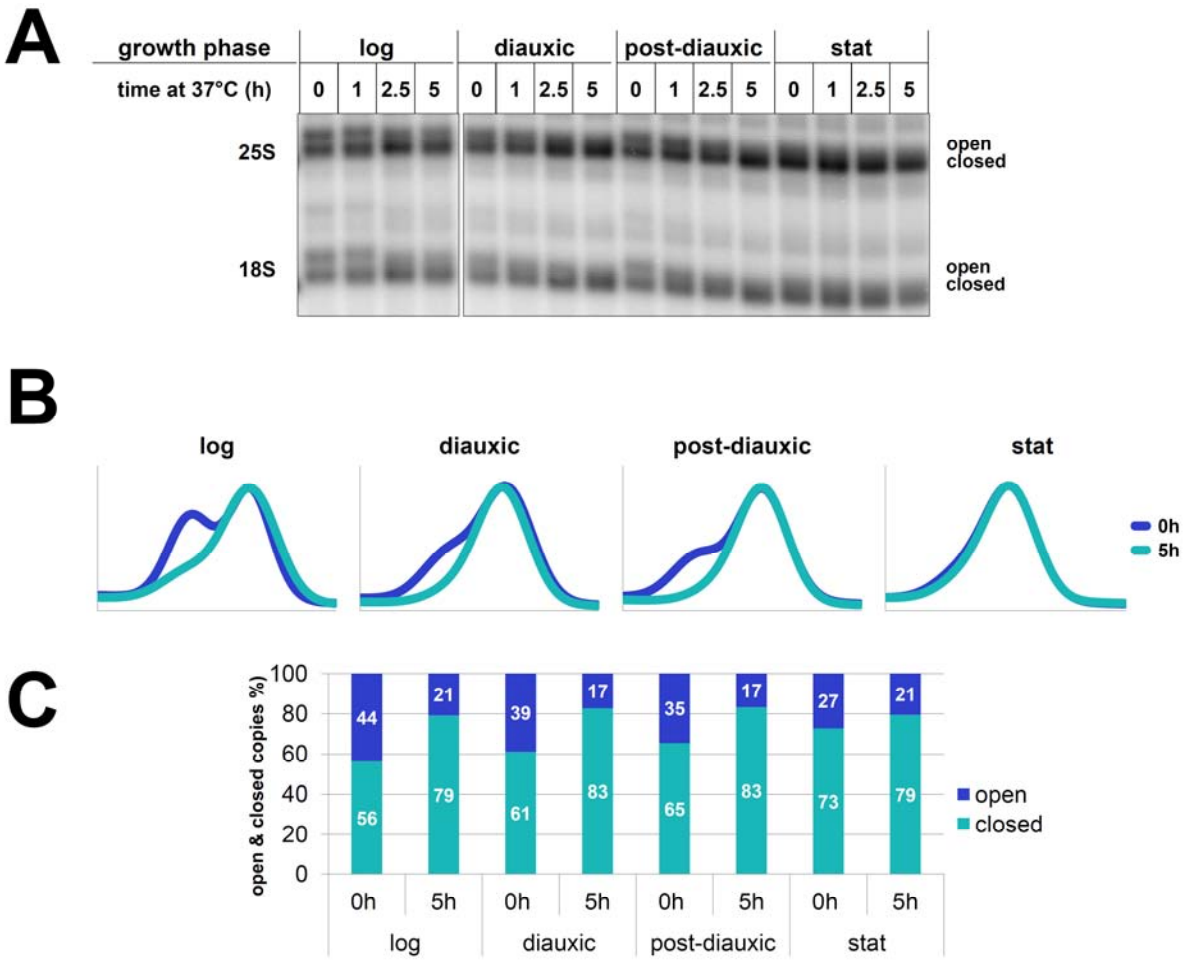

Figure 39: Chromatin dynamics at the rDNA upon conditional shutdown of Pol I transcription initiation in an *rrn3ts rpd3*Δ *HMO1* strain at different growth phases

Strain y2921 (*rrn3ts rpd3*Δ *HMO1*) was cultured according to Figure 37 (see OD Figure 9 in the appendix for the ODs of the respective cultures). **(A)** Psoralen analysis. An autoradiograph after hybridization with the 3.5kb rDNA probe is shown. The origin of the sample is indicated at the top. On the left it is indicated from which EcoRI rDNA fragment the signal is derived. On the right the positions of fragments derived from either the open or the closed chromatin state are labeled. **(B)** Profile analysis of the psoralen samples shown in (A) according to Figure 26. **(C)** Ratio of open and closed rDNA copies. The calculation was made according to Figure 26. The exact percent values are indicated as white numbers in the bars.

An *rrn3ts RPD3 hmo1*Δ strain showed complete closing of 35S rRNA gene copies with transition to stationary phase (Figure 40 A - C "0h"). In diauxic shift samples still a significant amount of open copies compared to the corresponding WT strain was observed (Figure 40 A - C "diauxic" "0h" compared to Figure 38 A - C "diauxic" "0h").This could be due to the slow growth of the *hmo1*Δ mutant (see OD Figure 9 in the appendix for ODs of the respective cultures). Thus the *hmo1*Δ strain was probably still in exponential phase or at the very beginning of the diauxic shift at the time when the "diauxic" sample was collected. Upon temperature shift to the restrictive temperature open 35S rDNA copies adopted the closed chromatin state in exponential phase and

diauxic shift cultures (Figure 40 A - C "5h") similar to the corresponding WT strain (Figure 38 A - C "5h").

In summary, deletion of *HMO1* in an *rrn3ts* strain led to similar 35S rRNA gene chromatin dynamics as already observed for the corresponding WT strain.

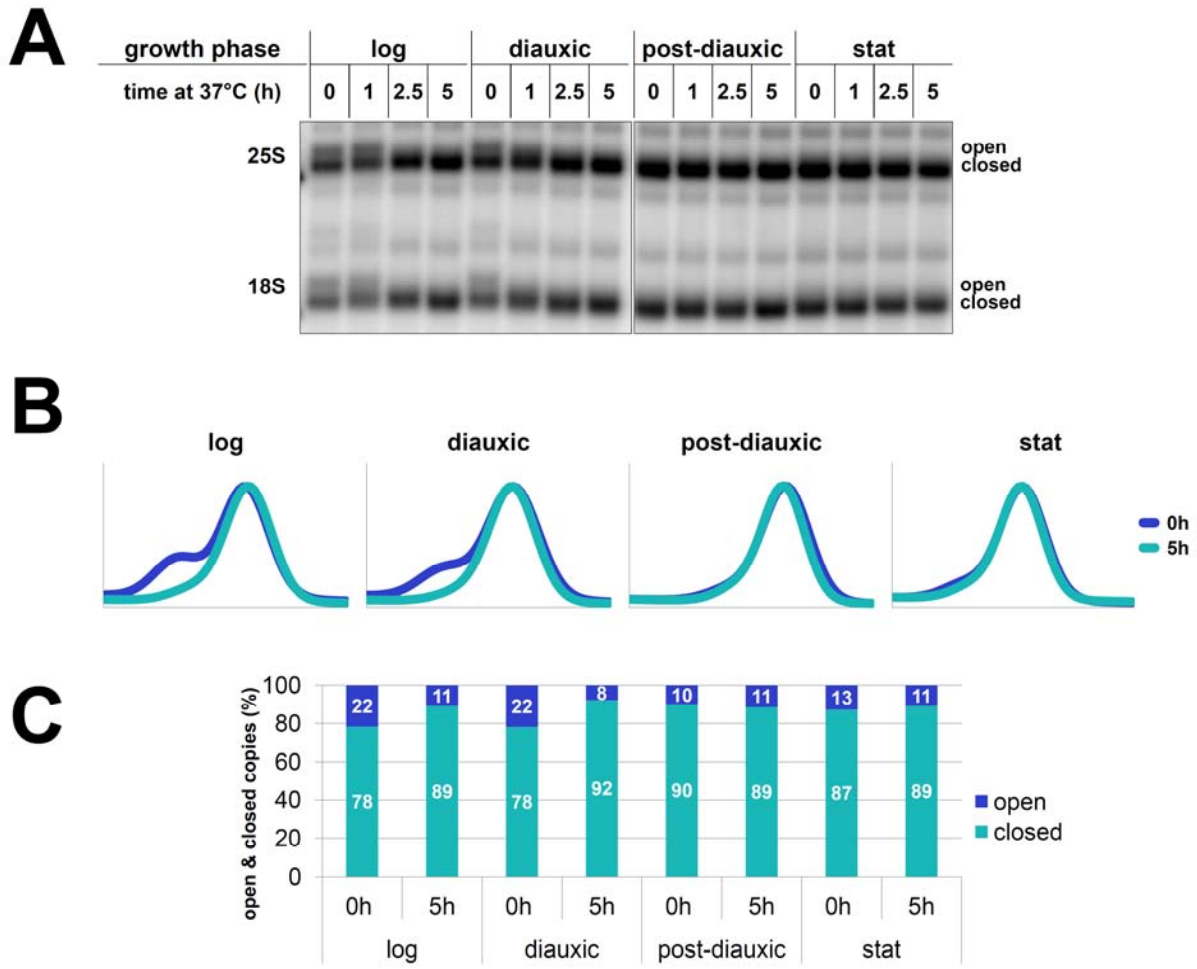

Figure 40: Chromatin dynamics at the rDNA upon conditional shut-down of Pol I transcription initiation in an *rrn3ts RPD3 hmo1*∆ strain at different growth phases

Strain y2945 (*rrn3ts RPD3 hmo1*∆) was cultured according to Figure 37 (see OD Figure 9 in the appendix for the ODs of the respective cultures). **(A)** Psoralen analysis. An autoradiograph after hybridization with the 3.5kb rDNA probe is shown. The origin of the sample is indicated at the top. On the left it is indicated from which EcoRI rDNA fragment the signal is derived. On the right the positions of fragments derived from either the open or the closed chromatin state are labeled. **(B)** Profile analysis of the psoralen samples shown in (A) according to Figure 26. **(C)** Ratio of open and closed rDNA copies. The calculation was made according to Figure 26. The exact percent values are indicated as white numbers in the bars.

Analysis of an *rrn3ts rpd3*∆ *hmo1*∆ strain revealed a significant number of open 35S rRNA genes in all samples collected upon growth to stationary phase (Figure 41 A - C "0h"). This is in good agreement with a previous study (Babl, 2012) and confirmed that the *rpd3*∆ phenotype can be established in the absence of Hmo1. As observed, for the *rrn3ts rpd3∆ HMO1* strain (Figure 39, and discussion in main text) the fraction of open

35S rRNA genes seemed to be less than in *rpd3*Δ *HMO1 RRN3* strains (Figure 19 "*rpd3*Δ"). To exclude an effect of growth temperature itself on the chromatin dynamics, additional *RRN3 rpd3*Δ cultures were incubated according to Figure 37 (data not shown). Here, the establishment of the *rpd3*Δ phenotype was unaffected. Thus, the reduced number of open 35S rRNA gene copies appeared to be a phenotype of the *rrn3ts* genetic background. When compared to the *rrn3ts rpd3Δ HMO1* strain, the shutdown of Pol I transcription initiation in the *rrn3ts rpd3*Δ *hmo1*Δ strain led to a more efficient closing of 35S rRNA gene copies in all growth phases (Figure 41 A - C "5h").

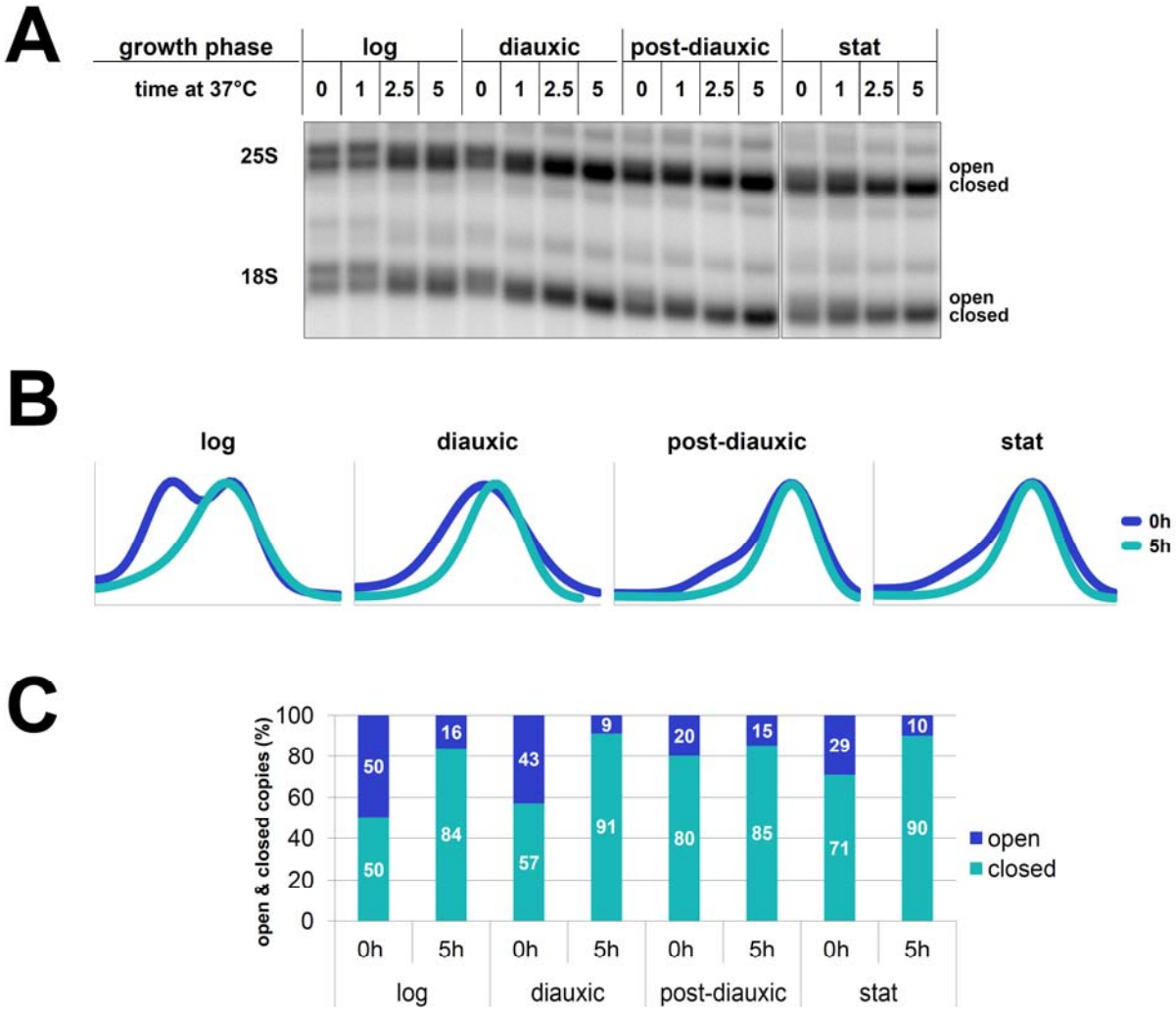

Figure 41: Chromatin dynamics at the rDNA upon conditional shut-down of Pol I transcription initiation in an *rrn3ts rpd3*Δ *hmo1*Δ strain at different growth phases

Strain y2947 (*rrn3ts rpd3*Δ *hmo1*Δ) was cultured according to Figure 37 (see OD Figure 9 in the appendix for the ODs of the respective cultures). **(A)** Psoralen analysis. An autoradiograph after hybridization with the 3.5kb rDNA probe is shown. The origin of the sample is indicated at the top. On the left it is indicated from which EcoRI rDNA fragment the signal is derived. On the right the positions of fragments derived from either the open or the closed chromatin state are labeled. **(B)** Profile analysis of the psoralen samples shown in (A) according to Figure 26. **(C)** Ratio of open and closed rDNA copies. The calculation was made according to Figure 26. The exact percent values are indicated as white numbers in the bars.

Taken together, the shutdown of Pol I transcription initiation led to closing of 35S rRNA gene copies in all strains analyzed. This finding was surprising for *rpd3Δ* strains in stationary phase, since it indicated, that the *rpd3*Δ phenotype is rather due to a dysregulation of Pol I transcription maintaining the open chromatin state than a consequence of defective nucleosome assembly/stabilization, as previously suggested (Johnson et al., 2013). Additionally, the observed closing of 35S rDNA copies was more efficient, when *HMO1* was additionally deleted. This suggests a potential role of Hmo1 in stabilization of open copies in the absence of Pol I transcription, consistent with a previous study (Wittner et al., 2011).

II.3.2 ChEC and ChIP analyses revealed differences in PIC factor association between *RPD3* and *rpd3*Δ strains

The findings described in section II.3.1 suggested that the *rpd3*Δ phenotype is rather established by a dysregulation in Pol I association than by a defect in closing of open 35S rRNA gene copies. However, it was not clear at which point Rpd3 might regulate Pol I association with the rDNA and which other factors might be affected by a deletion of *RPD3*. For this reason the comprehensive analysis in *RPD3* strains described in section II.2 was extended to *rpd3*Δ strains.

II.3.2.1 Pol I association with the rDNA decreased, while Hmo1 association persisted in *rpd3*Δ cells upon growth to stationary phase

Sandmeier et al. (2002) found a slight but not significant increase in Pol I transcription in stationary phase in an *rpd3*Δ strain compared to an *RPD3* strain. Additionally, a previous analysis suggested that Pol I might still partially be associated with open 35S rRNA gene copies in an *rpd3*Δ background in the post-diauxic growth phase (Babl, 2012).

In previous studies it was suggested that Hmo1 is still at least partially associated with the rDNA in an *rpd3*Δ background in stationary phase (Babl, 2012; Johnson et al., 2013). However, these studies were contradicting since Johnson et al. (2013) found no increased association of Hmo1 with the 35S rRNA gene region in an *rpd3*Δ background compared to WT, while in our laboratory the association of Hmo1-MNase with the rDNA in post-diauxic growth phase was significantly higher in an *rpd3*Δ strain (Babl, 2012).

In the first part of this comprehensive analysis in the *rpd3*Δ background the results for Pol I and Hmo1 were extended to stationary phase to confirm earlier findings.

II.3.2.1.1 Pol I association with the rDNA in *rpd3*Δ cells decreased but was still partially maintained upon growth to stationary phase

ChEC and ChEC-psoralen experiments with a strain expressing Rpa190 as a fusion protein with MNase were used for the analysis of Pol I association with transition to stationary phase in an *rpd3*Δ background (Figure 42). For obtaining a detailed view on the Pol I association dynamics, samples from four different time points of the growth experiment were analyzed as described already for the respective *RPD3* strain.

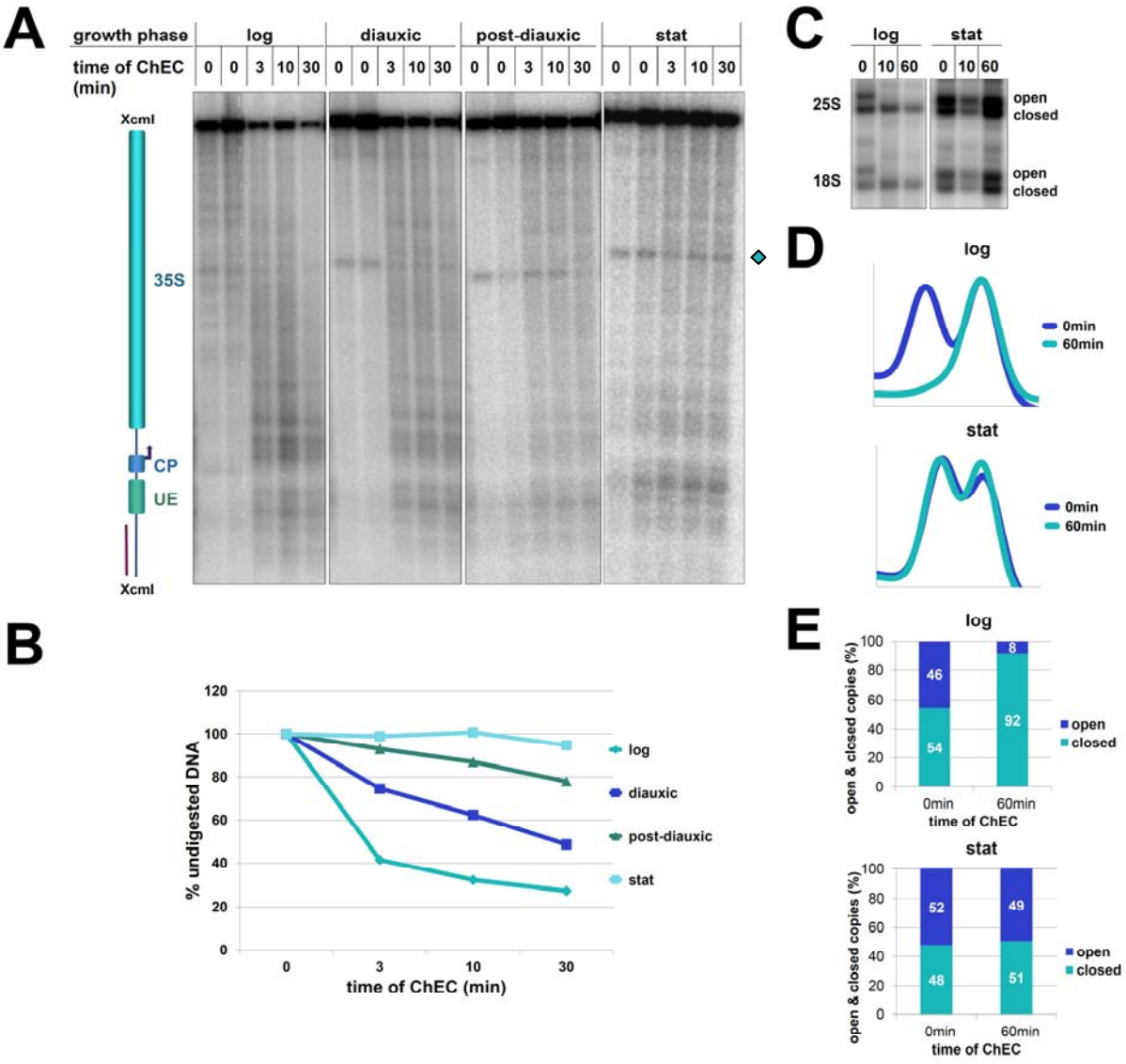

Figure 42: Rpa190-MNase mediated cleavage and psoralen accessibility at the rDNA upon transition to stationary phase in an *rpd3*Δ background

Strain y2256 (Rpa190 with C-terminal MNase expressed from the endogenous locus, *rpd3*Δ*)* was cultivated and samples were collected and analyzed in ChEC and ChEC-psoralen experiments as described in the legend to Figure 29 (see OD Figure 10 in the appendix for the respective ODs). **(A)** Analysis of ChEC samples: An autoradiograph of a Southern blot after hybridization with the rDNp probe is shown. A rhomb on the right side of the autoradiograph marks an unspecific fragment. **(B)** Quantification of Rpa190-MNase mediated degradation shown in (A): The analysis was conducted according to Figure 25 A. **(C)** ChEC-psoralen analysis of log and stat

samples. An autoradiograph after hybridization with the 3.5kb rDNA probe is shown. **(D)** Profile analysis of the ChEC-psoralen signals shown in (C). **(E)** Ratio of open and closed rDNA copies in log and stat samples.

Rpa190-MNase fusion protein mediated cutting events throughout the whole 35S rRNA gene region were observed within the analyzed XcmI fragment in samples taken during exponential phase (Figure 42 A "log"). In samples taken after the exit from exponential phase the cutting events drastically decreased (Figure 42 A "diauxic", "post-diauxic", "stat"). An unspecific cleavage appeared especially in samples taken after exponential phase (Figure 42 A, rhomb on the right) as already described for the corresponding *RPD3* strain (Figure 29 A, rhomb on the right). As Figure 42 B shows, the degradation of the full-length XcmI fragment strongly decreased after exit from exponential phase to only a few percent degradation in stationary phase samples. However, for the stationary phase samples there was already cleavage taking place without activation of MNase (Figure 42 A "stat" "0min"). This could indicate that Rpa190-MNase is prematurely activated *in vivo* or during sample preparation in the *rpd3*Δ background, which might have obscured the result of the degradation analysis leading to an underestimation of the actual degradation.

Only "log" and "stat" samples were included in the ChEC-psoralen analysis (Figure 42 C - E). As expected, the signal derived from the open copies was clearly visible in samples from exponential phase, but also in samples from stationary phase (Figure 42 C "log" and "stat" "0"). The amount of open copies was even increased in samples from stationary phase cells. After activation of MNase the fragments derived from open copies were completely degraded in exponential phase samples, while this fragment largely resisted degradation in stationary phase samples (Figure 42 C and D "60min ChEC"). The activation of MNase resulted in a decrease of the relative amount of open copies from 46% to 8% in exponential phase samples and only from 52% to 49% in stationary phase samples (Figure 42 E). This indicates that the open copies in stationary phase were not heavily loaded with Pol I as it was the case in exponential phase.

ChEC degradation analysis allows at least in part to deduce quantitative information about the association of protein factors with rDNA. To confirm ChEC results performed in strains expressing Rpa190-MNase, ChIP analyses were conducted with samples from *RPD3* and *rpd3*Δ strains expressing Rpa135 C-terminally fused to a TAP tag (Figure 43). In *RPD3* and *rpd3*Δ cells the amount of 35S rDNA fragments co-precipitating with Rpa135-TAP decreased after exit from exponential phase. There was only a minor difference in co-precipitation of a Pol I promoter fragment with Rpa-135-TAP in the *rpd3*Δ strain when compared to the *RPD3* strain at all growth phases analyzed (Figure 43,

graph “Prom”). Co-precipitation of two fragments located in the 18S and 25S rDNA regions in the “post-diauxic” and “stat” samples was however up to 3-fold higher in the *rpd3*Δ strain when compared to the *RPD3* strain (Figure 43, graphs "18S" and “25S”). This indicated that a significant population of the 35S rDNA fragments was still associated with Pol I at stationary phase in an *rpd3*Δ strain. No significant co-precipitation with Rpa135-TAP was found for a fragment including the Pol III transcribed 5S rRNA gene, serving as a background control (Figure 43, graph “5S”).

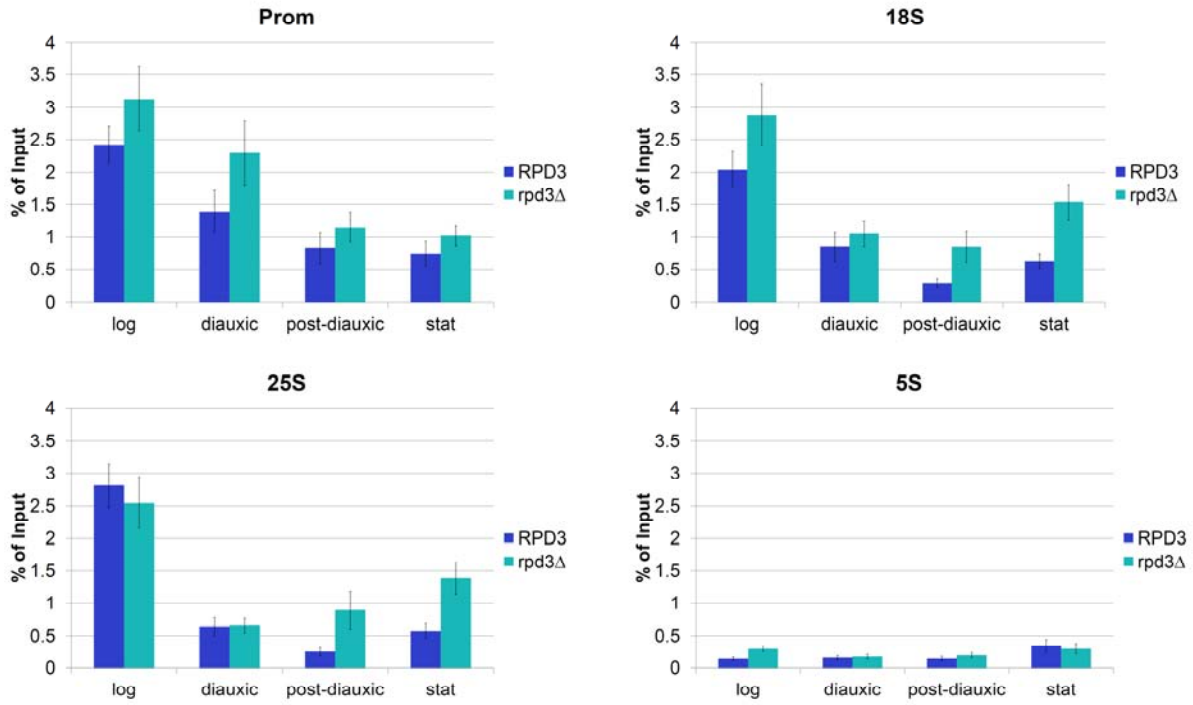

Figure 43: Rpa135-TAP specifically co-precipitated 35S rDNA fragments upon transition to stationary phase in *RPD3* and *rpd3Δ* strains

Yeast strains y3078 (Rpa135 with a C-terminal TAP-tag expressed from the endogenous locus, *RPD3*) and y3136 (Rpa135 with a C-terminal TAP-tag expressed from the endogenous locus, *rpd3*Δ) were cultured and samples were collected according to Figure 21 (see OD Figure 11 in the appendix for the respective ODs). ChIP was performed according to Figure 27 with IgG sepharose. The graphs depict the percentage of the input of the respective DNA fragment (indicated at the top of each diagram) co-precipitating with the TAP-tagged fusion protein at the indicated growth phases. Error bars indicate standard deviation errors derived from three independent ChIP experiments, each analyzed in triplicate qPCRs. The positions of the respective qPCR amplicons within the rDNA locus are depicted in Figure 28. The 5S qPCR amplicon serves as a background control for DNA co-precipitating with Rpa135-TAP.

Consistent with earlier findings (Babl, 2012; Sandmeier et al., 2002), ChEC and ChIP analyses indicate that Rpa190-MNase and Rpa135-TAP association with the rDNA are decreased upon transition to stationary phase in *RPD3* and *rpd3*Δ cells. In support to the idea that residual Pol I transcription is required for the maintenance of the open

chromatin state in *rpd3*Δ cells at stationary phase, Pol I–rDNA association is partially maintained in this condition.

II.3.2.1.2 Hmo1 association with the rDNA in *rpd3Δ* cells was altered and slightly increased upon growth to stationary phase

For the analysis of Hmo1 association with the rDNA samples from exponentially growing and stationary cells of an *rpd3*Δ strain expressing Hmo1 as a fusion protein with MNase were used for ChEC and ChEC-psoralen experiments (Figure 44).

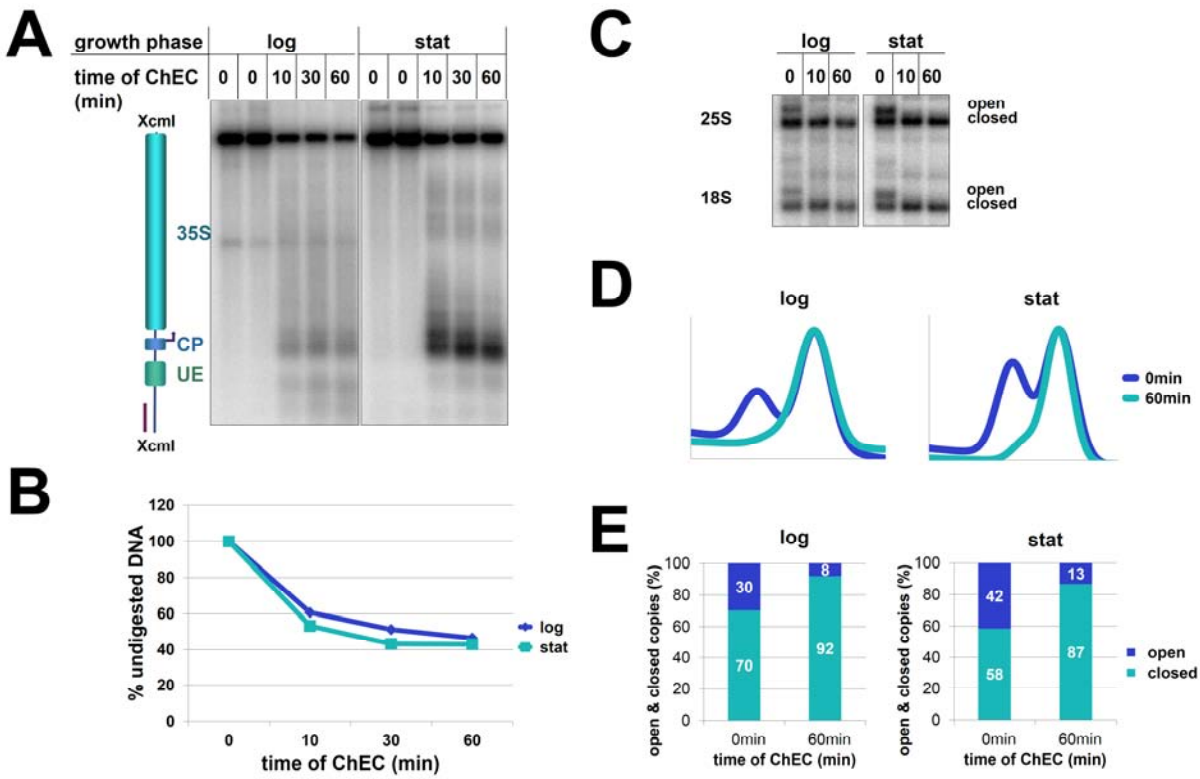

Figure 44: Hmo1-MNase mediated cleavage and psoralen accessibility at the rDNA upon transition to stationary phase in an *rpd3*Δ background

Strain y2257 (Hmo1 with C-terminal MNase expressed from the endogenous locus, *rpd3Δ)* was cultivated and samples were collected and analyzed in ChEC and ChEC-psoralen experiments as described in the legend to Figure 29 (see OD Figure 12 in the appendix for the respective ODs). **(A)** Analysis of log and stat ChEC samples: An autoradiograph of a Southern blot after hybridization with the rDNp probe is shown. **(B)** Quantification of Hmo1-MNase mediated degradation: The analysis was conducted according to Figure 25 A. **(C)** ChEC-psoralen analysis of EcoRI digested samples. An autoradiograph after hybridization with the 3.5kb rDNA probe is shown. **(D)** Profile analysis of the ChEC-psoralen signals shown in (C). **(E)** Ratio of open and closed rDNA copies in log and stat samples.

As observed for Rpa190-MNase expressing *rpd3*Δ cells activation of Hmo1-MNase led to cleavage throughout the whole 35S rRNA gene region within the analyzed XcmI and EcoRI fragments in samples taken during exponential growth (compare “log” in Figure 42 A, C, and Figure 44 A, C). In contrast to Rpa190-MNase, Hmo1-MNase fully degraded the same fragments in samples taken at stationary phase (compare “stat” in Figure 42 A,

C, and Figure 44 A, C). As already observed for Hmo1-MNase mediated cleavage in an *RPD3* strain (Figure 30), the ChEC cleavage pattern of Hmo1-MNase in *rpd3*Δ cells shifted towards more prominent cutting events at the promoter region of the gene in samples from stationary phase (Figure 44 A). In contrast to the results obtained with the *RPD3* strain, the overall degradation of the full-length XcmI fragment was slightly increased (Figure 44 B). This correlated well with an increase in the fraction of open copies in stationary phase samples when compared with exponential phase samples (Figure 44 C "0"). After activation of MNase all open copies were degraded in samples from exponential phase as well as from samples taken at stationary phase (Figure 44 C-E "60min", compare “log” with “stat”). However, in stationary phase samples a weak smear migrating right above the band derived from the closed copies fragment (probably derived from copies that were in the transition between open and closed chromatin state) resisted Hmo1-MNase mediated degradation. This indicates, that Hmo1 was preferentially associated with fully open rDNA copies in exponential as well as in stationary phase in the absence of Rpd3.

Taken together, Hmo1 associated with open 35S rRNA gene copies in exponential and in stationary phase in the *rpd3*Δ background. Thus, Hmo1, but not necessarily Pol I (see II.3.2.1.1), appears to be a general component of open 35S rRNA gene chromatin.

II.3.2.2 Histone association with the rDNA in *rpd3*Δ cells was slightly reduced upon growth to stationary phase

Due to the persistence of open copies in stationary phase *rpd3*Δ strains, it was expected that histone association is reduced under these conditions compared to *RPD3* strains. In a previous study it was also shown that the association of the putative linker histone Hho1 is reduced in an *rpd3*Δ strain after exit from exponential phase (Babl, 2012) and that diauxic shift dependent histone H4 and histone H2B deposition on the rDNA was reduced upon *RPD3* deletion (Johnson et al., 2013).

II.3.2.2.1 H3 association with the rDNA in *rpd3Δ* cells was slightly reduced upon growth to stationary phase

Association dynamics of histone H3 in an *rpd3*Δ strain were investigated conducting ChEC and ChEC-psoralen experiments with a strain expressing Hht1 as a fusion protein with MNase (Figure 45).

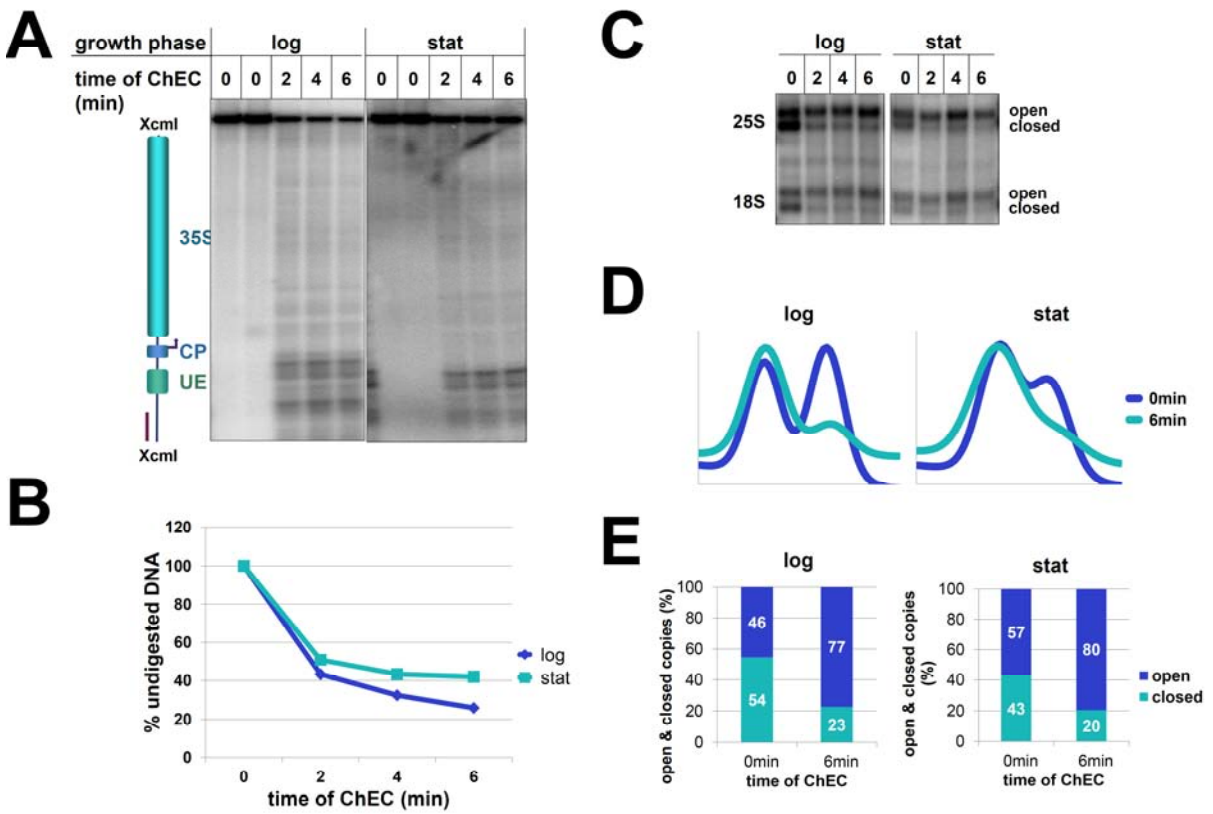

Figure 45: Hht1-MNase mediated cleavage and psoralen accessibility at the rDNA upon transition to stationary phase in an *rpd3*Δ background

Strain y2344 (Hht1 with C-terminal MNase expressed from the endogenous locus, *rpd3*Δ*)* was cultivated and samples were collected and analyzed in ChEC and ChEC-psoralen experiments as described in the legend to Figure 29 (see OD Figure 13 in the appendix for the respective ODs). **(A)** Analysis of log and stat ChEC samples: An autoradiograph of a Southern blot after hybridization with the rDNp probe is shown. **(B)** Quantification of Hht1-MNase mediated degradation: The analysis was conducted according to Figure 25 A without normalization to a reference locus. **(C)** ChEC-psoralen analysis of EcoRI digested samples. An autoradiograph after hybridization with the 3.5kb rDNA probe is shown. **(D)** Profile analysis of the ChEC-psoralen signals shown in (C). **(E)** Ratio of open and closed rDNA copies in log and stat samples.

Activation of MNase led to strong degradation of the XcmI rDNA fragment in samples from exponentially growing cells as well as stationary cells (Figure 45 A). In contrast to experiments with *RPD3* cells (Figure 31 A), there was no clear change in the cleavage pattern observable when exponential phase samples were compared with stationary phase samples. The most prominent cutting events were located at the upstream element. This could be due to the fact that H3 is also a component of UAF. Interestingly, the prominent cleavage site at the 5' region of the upstream element was slightly decreased in stationary phase samples compared to exponential phase samples. This indicates a possible change in the promoter structure in stationary cells. The quantification of degradation analysis showed that the overall Hht1-MNase mediated degradation was slightly decreased in stationary phase compared to exponential phase (Figure 45 B). This is in good correlation with an overall increase of the amount of open,

nucleosome depleted 35S rRNA gene copies (from 46% to 57%) in stationary phase as revealed by ChEC-psoralen analysis (Figure 45 C - E "0min"). Activation of MNase led to a strong degradation of the fragment derived from closed rDNA copies in samples from exponential phase as well as from stationary phase (Figure 45 C - E "6min"). However, some fragments derived from closed copies resisted Hht1-MNase cleavage. This could be due to a preferential incorporation of the untagged histone H3 version as already described for the respective *RPD3* strain.

In summary, Hht1-MNase degraded preferentially closed rDNA copies in exponential and in stationary phase samples, but compared to the *RPD3* strain, overall degradation efficiency was reduced in good correlation with the higher amount of open 35S rRNA gene copies in stationary phase.

II.3.2.2.2 Hho1 association with the rDNA in *rpd3Δ* cells was reduced upon growth to stationary phase

ChEC and ChEC-psoralen experiments with a strain expressing Hho1 as a fusion protein with MNase were used to analyze association dynamics of Hho1 in exponential and stationary phase in the *rpd3*Δ background (Figure 46).

Hho1-MNase activation led to cleavage throughout the whole 35S rRNA gene region of the XcmI fragment in samples collected in both exponential phase and stationary phase (Figure 46 A). In contrast to the experiments using an *RPD3* strain only a moderate change in the cleavage pattern was observed when exponential phase samples were compared with stationary phase samples in *rpd3*Δ cells. The overall degradation efficiency of the full-length fragment decreased in stationary phase (Figure 46 B). However, as already described for the *RPD3* strain no normalization of DNA load to a reference locus was possible. Nevertheless, the quantified degradation amount was in good correlation with an overall increase of open 35S rRNA gene copies (from 23% to 41%) as revealed by ChEC-psoralen analysis (Figure 46 C - E "0min"). Activation of MNase led to almost complete degradation of the band derived from the open copies fragment in samples from exponential phase, while in samples from stationary phase preferentially the band derived from the closed copies fragment was degraded (Figure 46 C - E "60min"). However, a substantial fraction of the fragments derived from the closed 35S rDNA copies resisted Hho1-MNase degradation indicating that not all closed copies are decorated with Hho1 in stationary phase.

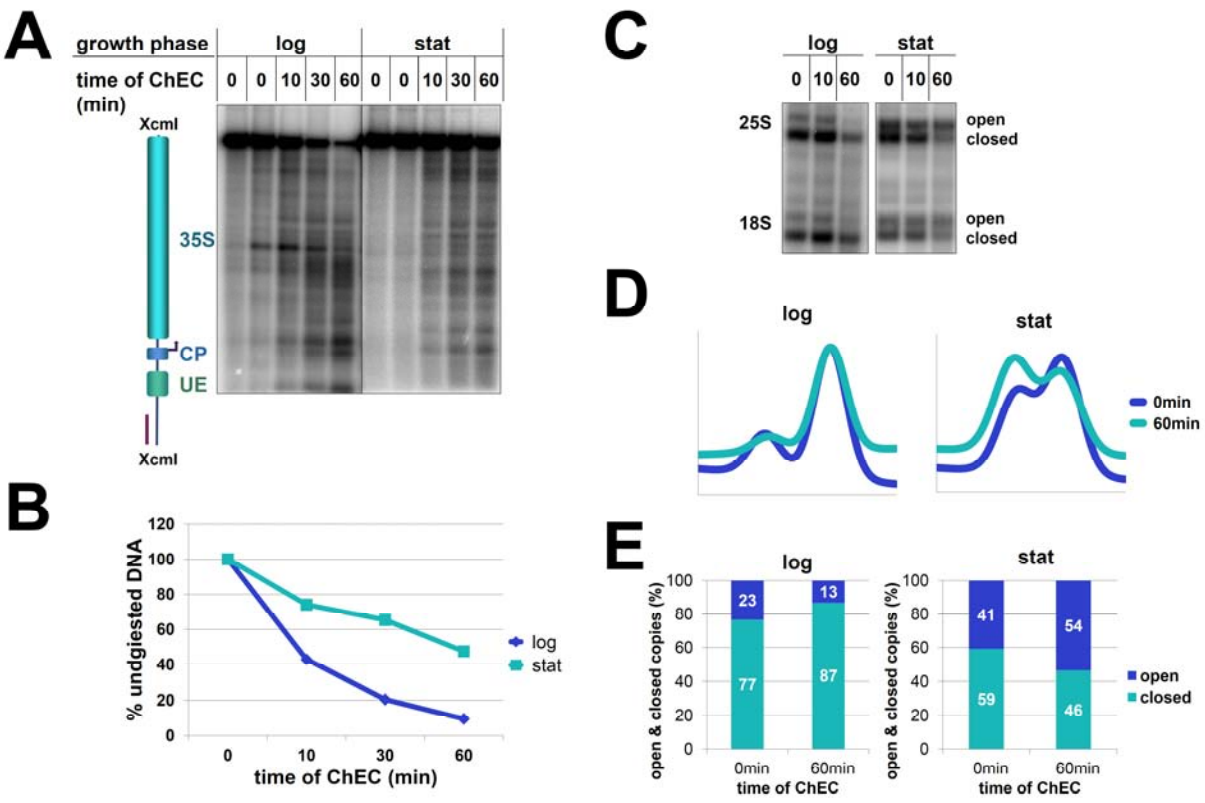

Figure 46: Hho1-MNase mediated cleavage and psoralen accessibility at the rDNA upon transition to stationary phase in an *rpd3*Δ background

Strain y2616 (Hho1 with C-terminal MNase expressed from the endogenous locus, *rpd3*Δ*)* was cultivated and samples were collected and analyzed in ChEC and ChEC-psoralen experiments as described in the legend to Figure 29 (see OD Figure 14 in the appendix for the respective ODs). **(A)** Analysis of log and stat ChEC samples: An autoradiograph of a Southern blot after hybridization with the rDNp probe is shown. **(B)** Quantification of Hho1-MNase mediated degradation: The analysis was conducted according to Figure 25A without normalization to a reference locus. **(C)** ChEC-psoralen analysis of EcoRI digested samples. An autoradiograph after hybridization with the 3.5kb rDNA probe is shown. **(D)** Profile analysis of the ChEC-psoralen signals shown in (C). **(E)** Ratio of open and closed rDNA copies in log and stat samples.

Taken together, association of Hho1-MNase was decreased in stationary phase samples in the *rpd3*Δ background. This is in contrast to the results obtained for the corresponding *RPD3* strain. Similar to the *RPD3* strain, the preferential Hho1-MNase mediated degradation changed from open copies in exponential phase to closed copies in stationary phase.

II.3.2.3 PIC formation in *rpd3*Δ cells was only slightly impaired with transition to stationary phase

Since the association of Pol I was slightly increased in stationary phase in *rpd3*Δ strains when compared to *RPD3* strains, it became interesting to determine the origin of this phenomenon. Thus, it could be that either Pol I transcription initiation is dysregulated either at the level of the Pol I enzyme itself or more upstream at the level of one of the

transcription initiation factors leading to the *rpd3*Δ phenotype. Therefore, the components of the Pol I PIC and additionally Net1 that were already part of the comprehensive analysis conducted in section II.2 were analyzed also in the *rpd3*Δ background.

II.3.2.3.1 Rrn9 stayed associated with open 35S rRNA gene copies in *rpd3*Δ cells upon growth to stationary phase

For the analysis of UAF association with the rDNA in stationary phase in an *rpd3*Δ background ChEC and ChEC-psoralen experiments with a strain expressing the UAF component Rrn9 as a fusion protein with MNase were performed (Figure 47).

Rrn9-MNase activation led to a single cleavage at the upstream element (UE) and this cleavage was of similar intensity in exponential and stationary phase samples (Figure 47 A). As observed for Rpa190-MNase expressing strains (Figure 42 A, “stat", "0min”), a slight cleavage at the binding site of Rrn9-MNase took already place without activation of MNase in samples taken at stationary phase (Figure 47 A, “stat, "0min”). The Rrn9-MNase mediated degradation in *rpd3*Δ cells was at a similar level in samples taken during exponential growth or at stationary phase (Figure 47 B), as already observed for the corresponding *RPD3* strain (Figure 33 B). The amount of open copies was equal in samples from exponentially growing and from stationary cells (Figure 47 C - E "0min"). However, in stationary phase a weak intermediate smear between the fragments derived from the open and the fragments derived from the closed 35S rDNA copies led to a poor separation of both bands. Both, in samples from exponential phase and in samples from stationary phase activation of MNase led to a preferential degradation of open copies (Figure 47 C - E "60min"). This was also well reflected by the electrophoretic migration of the cleaved fragments (Figure 47 C - E "60min", intensified autoradiograph at the bottom). However, in stationary phase also the intermediate copies were degraded to some extent (Figure 47 C "60min", intensified autoradiograph at the bottom).

Thus, Rrn9-MNase stayed associated with the upstream element in exponential and stationary phase samples as already observed for the *RPD3* strain, but in contrast to *RPD3* it was also in stationary phase samples preferentially associated with open 35S rRNA gene copies in the *rpd3*Δ background.

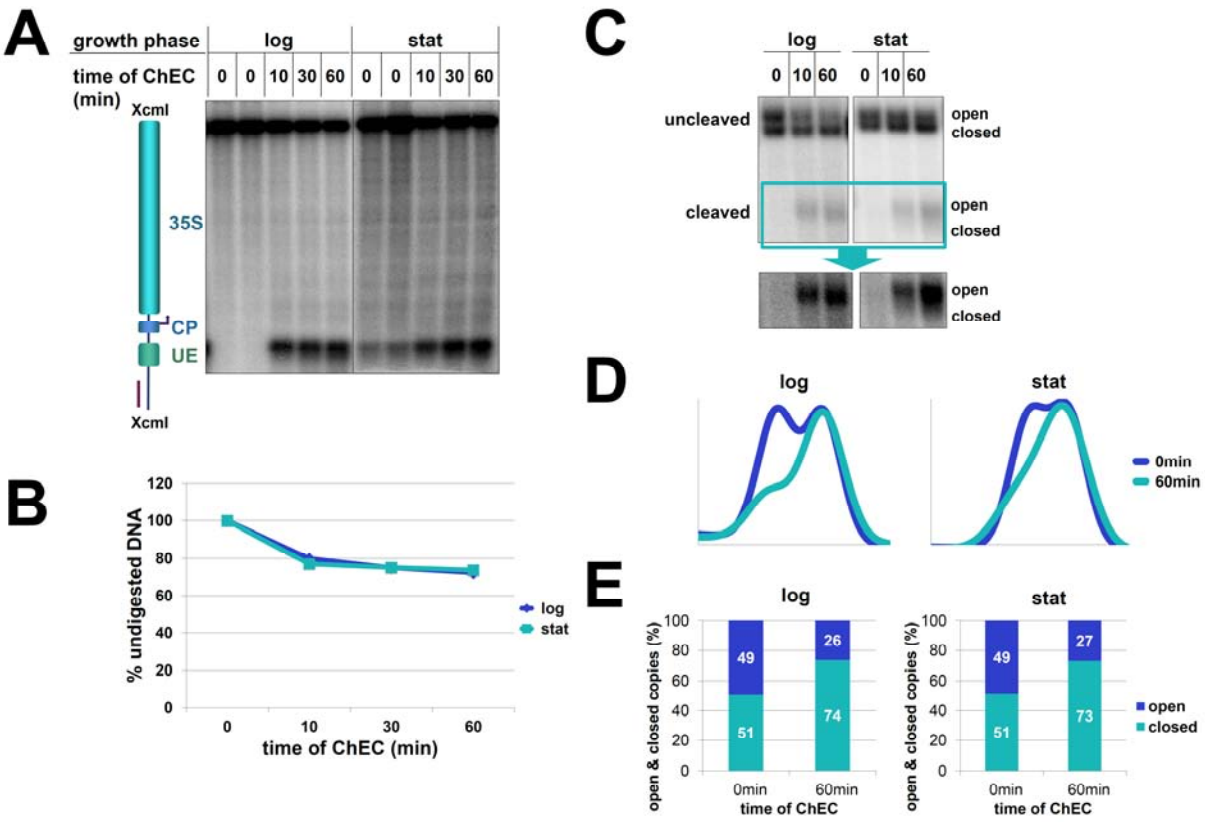

Figure 47: Rrn9-MNase mediated cleavage and psoralen accessibility at the rDNA upon transition to stationary phase in an *rpd3*Δ background

Strain y3028 (Rrn9 with C-terminal MNase expressed from the endogenous locus, *rpd3*Δ) was cultivated and samples were collected and analyzed in ChEC and ChEC-psoralen experiments as described in the legend to Figure 29 (see OD Figure 15 in the appendix for the respective ODs). **(A)** Analysis of ChEC samples: An autoradiograph of a Southern blot after hybridization with the rDNp probe is shown. **(B)** Quantification of Rrn9-MNase mediated degradation shown in (A): The analysis was conducted according to Figure 25B. **(C)** ChEC-psoralen analysis of XcmI/SacII digested samples. An autoradiograph after hybridization with the 18S probe is shown. Positions of the uncleaved and the cleaved fragments are given on the left. A longer exposure of the framed blot region visualizing the cleaved fragments is shown at the bottom. **(D)** Profile analysis of the signals of the uncleaved fragments of the ChEC-psoralen experiment shown in (C). **(E)** Ratio of open and closed rDNA copies in log and stat samples.

ChIP analyses with Rrn9-TAP expressing *RPD3* or *rpd3*Δ cells largely confirmed the ChEC data. No significant differences in the amount of co-precipitated rDNA promoter DNA including the UE bound by UAF were detectable (Figure 48, “UE”). Surprisingly, only a very low percentage of UE DNA was co-precipitated in exponential phase samples, while the amount of co-precipitated UE DNA increased in the post-diauxic growth phase and at stationary phase. The poor co-precipitation of UE DNA with Rrn9-TAP in exponential phase, which was close to background levels (Figure 48, “5S”), correlated with poor growth observed especially for the *rpd3*Δ strain (see OD Figure 16 for details). This could indicate that the C-terminal TAP-tag at the UAF subunit interfered with assembly of the complex at the rDNA. Interestingly, *RPD3* and *rpd3*Δ strains

expressing another subunit of UAF as TAP fusion protein (Rrn5-TAP) had a similar growth defect (data not shown).

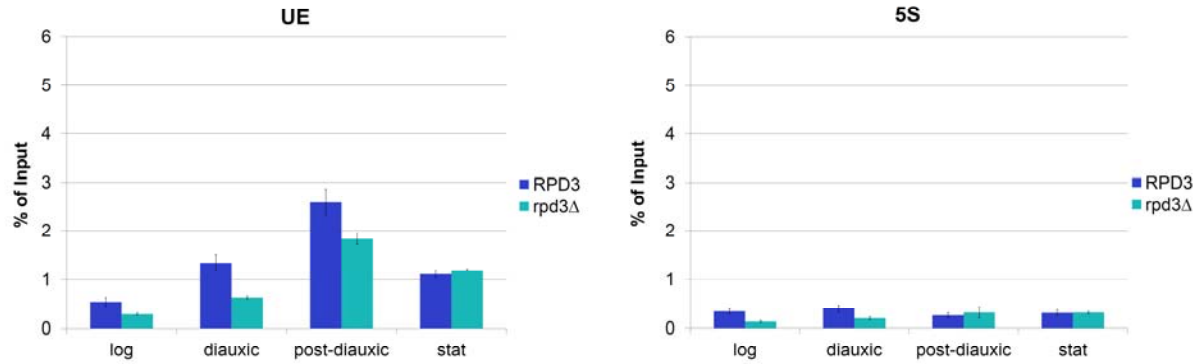

Figure 48: Rrn9-TAP co-precipitated DNA upon transition to stationary phase in *RPD3* and *rpd3Δ* strains
Yeast strains y3118 (Rrn9 with a C-terminal TAP-tag expressed from the endogenous locus, *RPD3*) and y3124 (Rrn9 with a C-terminal TAP-tag expressed from the endogenous locus, *rpd3*Δ) were cultured and samples were collected according to Figure 21 (see OD Figure 16 in the appendix for the respective ODs). ChIP was performed according to Figure 27 with IgG sepharose. The graphs depict the percentage of the input of the respective DNA fragment (indicated at the top of each diagram) co-precipitating with the TAP-tagged fusion protein at the indicated growth phases. Error bars indicate standard deviation errors derived from three independent ChIP experiments, each analyzed in triplicate qPCRs. The respective qPCR amplicons are depicted in Figure 28. The 5S qPCR amplicon serves as a background control for Rrn9-TAP co-precipitated DNA.

Thus, Rrn9-MNase and Rrn9-TAP stayed associated with the upstream element in exponential and stationary phase samples in *RPD3* and *rpd3*Δ cells. In contrast to *RPD3* Rrn9-MNase was also in stationary phase samples preferentially associated with open 35S rRNA gene copies in the *rpd3*Δ background as revealed by ChEC-psoralen analysis.

II.3.2.3.2 Spt15 stayed associated with open 35S rRNA gene copies in *rpd3*Δ cells upon growth to stationary phase

For the analysis of association dynamics of Spt15 with the rDNA in an *rpd3*Δ strain, ChEC and ChEC-psoralen experiments with a strain expressing Spt15 as a fusion protein with MNase were conducted (Figure 49).

Such as observed for the *RPD3* strain, the major cleavage event was at a distinct site within the core promoter (CP). As already observed for Rpa190-MN, and Rrn9-MNase premature cleavage was already present without activation of MNase in stationary phase samples (Figure 49 A). The degradation efficiency stayed approximately at 20% in samples from exponential and from stationary phase (Figure 49 B).

ChEC-psoralen analysis showed that the fraction of open 35S rRNA gene copies slightly increased when cells transit from exponential to stationary phase. However, the separation of the bands derived from open and closed copies was worse in stationary

phase samples (Figure 49 C and D "0min"). MNase activation led to preferential degradation of open copies in both, samples from exponential and from stationary phase (Figure 49 C - E). However, in stationary phase samples also the intermediate smear between open and closed copies was partially degraded by Spt15-MNase (Figure 49 C intensified autoradiograph at the bottom).

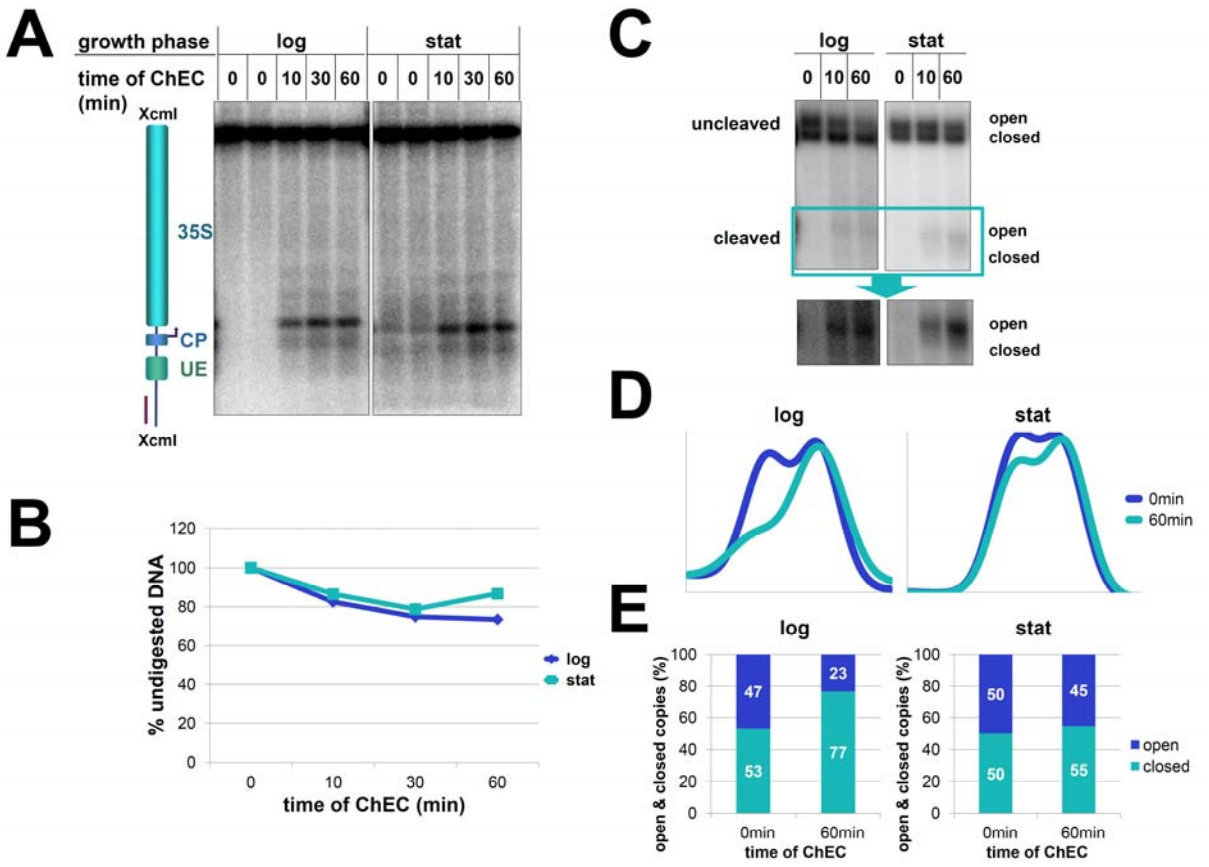

Figure 49: Spt15-MNase mediated cleavage and psoralen accessibility at the rDNA upon transition to stationary phase in an *rpd3*Δ background

Strain y3030 (Spt15 with C-terminal MNase expressed from the endogenous locus, *rpd3*Δ) was cultivated and samples were collected and analyzed in ChEC and ChEC-psoralen experiments as described in the legend to Figure 29 (see OD Figure 17 in the appendix for the respective ODs). **(A)** Analysis of ChEC samples. An autoradiograph of a Southern blot after hybridization with the rDNp probe is shown. **(B)** Quantification of Spt15-MNase mediated degradation shown in (A). The analysis was conducted according to Figure 25B. **(C)** ChEC-psoralen analysis of XcmI/SacII digested samples. An autoradiograph after hybridization with the 18S probe is shown. Positions of the uncleaved and the cleaved fragment are given on the left. A longer exposure of the framed blot region visualizing the cleaved fragments is shown at the bottom. **(D)** Profile analysis of the signals of the uncleaved fragments of the ChEC-psoralen experiment shown in (C). **(E)** Ratio of open and closed rDNA copies in log and stat samples.

ChIP analysis with *RPD3* and *rpd3*Δ strains expressing Spt15-TAP confirmed that the association of Spt15 with the 35S rRNA gene promoter stayed at a similar level in both strains in exponential and in stationary phase (Figure 50 "Prom"). Spt15 –the yeast TBP- is a general and conserved transcription factor, which plays a role in transcription

initiation of the three different nuclear RNA polymerases. In this regard it was interesting, to compare Spt15-TAP association with the Pol I dependent rDNA promoter with Spt15-TAP association with the Pol III dependent 5S rRNA promoter and the Pol II dependent *RPS23A* promoter. In contrast to the results obtained for the Pol I dependent promoter, Spt15-TAP association with the Pol II and Pol III-dependent promoters dropped substantially with the transition to stationary phase in *RPD3* and *rpd3*Δ strains (Figure 50 "5S" and "RPS23A"). Different to the ChIP performed with samples of the *RPD3* strain, the amount of 5S rDNA and *RPS23A* promoter DNA co-precipitating with Spt15-TAP decreased not before the post-diauxic phase in the *rpd3*Δ strain. However, this result is explainable by a lower OD of the *rpd3*Δ diauxic shift sample. Thus, this strain was possibly still in the late exponential phase at the time of sample collection (see OD Figure 18 in the appendix for details). These results suggest a differential regulation of Spt15-TAP interaction with the 35S rRNA promoter and the 5S and RPS23A promoters.

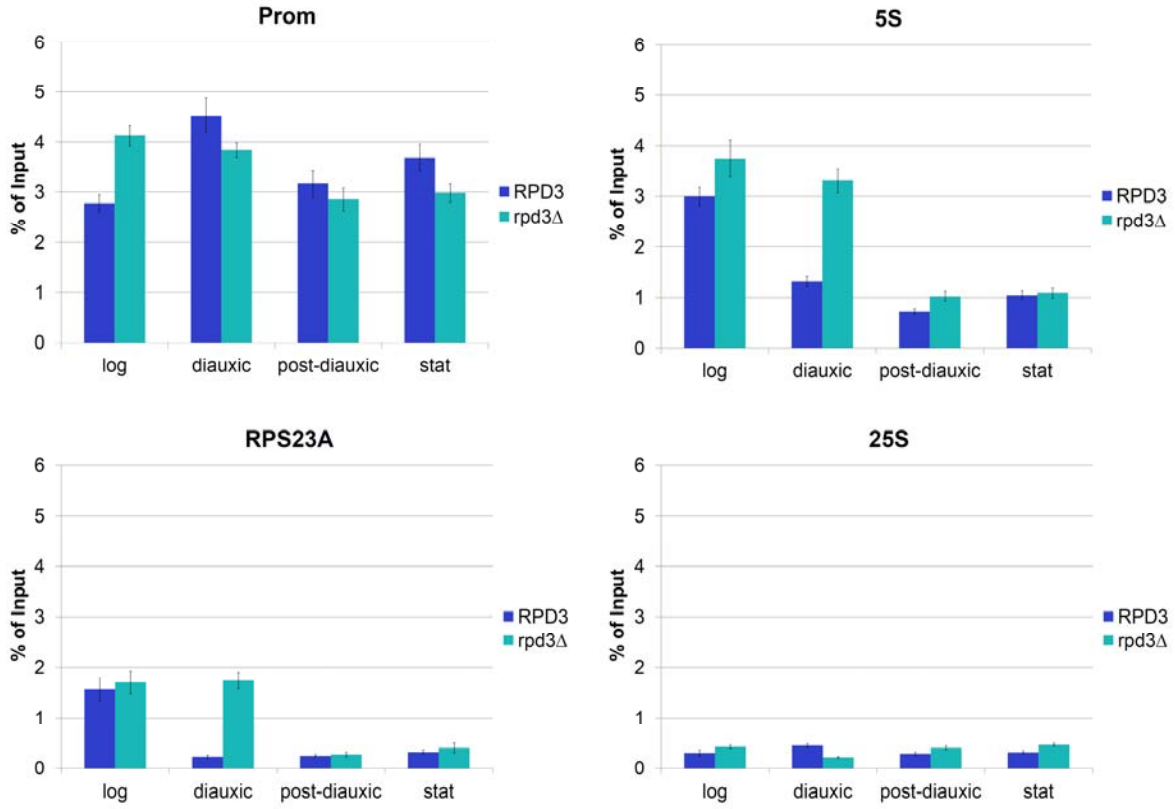

Figure 50: Spt15-TAP co-precipitated DNA upon transition to stationary phase in *RPD3* and *rpd3Δ* strains

Yeast strains y3327 (Spt15 with a C-terminal TAP-tag expressed from the endogenous locus, *RPD3*) and y3329 (Spt15 with a C-terminal TAP-tag expressed from the endogenous locus, *rpd3*Δ) were cultured and samples were collected according to Figure 21 (see OD Figure 18 in the appendix for the respective ODs). ChIP was performed according to Figure 27 with IgG sepharose. The graphs depict the percentage of the input of the respective DNA fragment (indicated at the top of each diagram) co-precipitating with the TAP-tagged fusion protein at the indicated growth phases. Error bars indicate standard deviation errors derived from three independent ChIP experiments, each analyzed in triplicate qPCRs. The respective qPCR amplicons are depicted in Figure 28. The 25S qPCR amplicon serves as a background control for Spt15-TAP co-precipitated DNA.

Taken together, Spt15-MNase and Spt15-TAP stayed associated with their binding site at the 35S rDNA promoter in exponential and stationary phase samples in *rpd3*Δ and *RPD3* cells. In contrast to the results in the *RPD3* strain, Spt15-MNase was also in stationary phase samples preferentially associated with open 35S rRNA gene copies in the *rpd3*Δ background as revealed by ChEC-psoralen analysis.

II.3.2.3.3 Rrn7 is significantly associated with the rDNA promoter in *rpd3*Δ cells but not in *RPD3* cells upon growth to stationary phase

ChEC and ChEC-psoralen experiments with a strain expressing Rrn7 as a fusion protein with MNase were used to analyze association dynamics of CF in exponential and stationary phase in the *rpd3*Δ background (Figure 51).

Rrn7-MNase led to two prominent cutting events in exponential phase and - in contrast to Rrn7-MNase mediated cleavage in the respective *RPD3* strain (Figure 35 A) - also in stationary phase samples (Figure 51 A). However, the relative amounts of the two cleaved fragments changed between exponential phase and stationary phase samples. In exponential phase samples both fragments yielded a signal of approximately same intensity. In contrast, in stationary phase samples the signal obtained from the smaller fragment (produced by cleavage in close proximity of the 5' end of the UE) was much weaker than the signal obtained from the larger fragment (obtained after cleavage at the CP). This could hint towards a specific promoter architecture under high transcription conditions as already discussed for the *RPD3* strain. As already observed and discussed for Rpa190-MNase, Rrn9-MNase and Spt15-MNase, a slight cleavage was already visible without activation of MNase (Figure 51 A). The degradation efficiency stayed in contrast to the respective *RPD3* strain approximately at 20% in exponential and stationary phase samples in the *rpd3*Δ strain (Figure 51 B). ChEC-psoralen analysis revealed that the *rpd3*Δ phenotype was slightly compromised in the Rrn7-MNase strain: While in exponential phase samples 55% of the copies were in the open chromatin state, only 27% were still open in stationary phase samples and the separation of open and closed copies was worse than in exponential phase samples (Figure 51 C -E "0min"). This could hint towards a role of Rrn7 in the establishment of the *rpd3*Δ phenotype after exponential phase, which is affected by the fusion to MNase. Rrn7-MNase was preferentially associated with the open chromatin state, but not all open copies were degraded upon activation of MNase (Figure 51 C - E "60min"). As Figure 51 C (intensified autoradiograph at the bottom) shows, the change in the cleavage intensity of both cuts was well reflected also in ChEC-psoralen analysis. Thus, the promoter

architecture seems to change likely as a consequence of a downregulation of Pol I transcription under these conditions (see II.3.2.1.1).

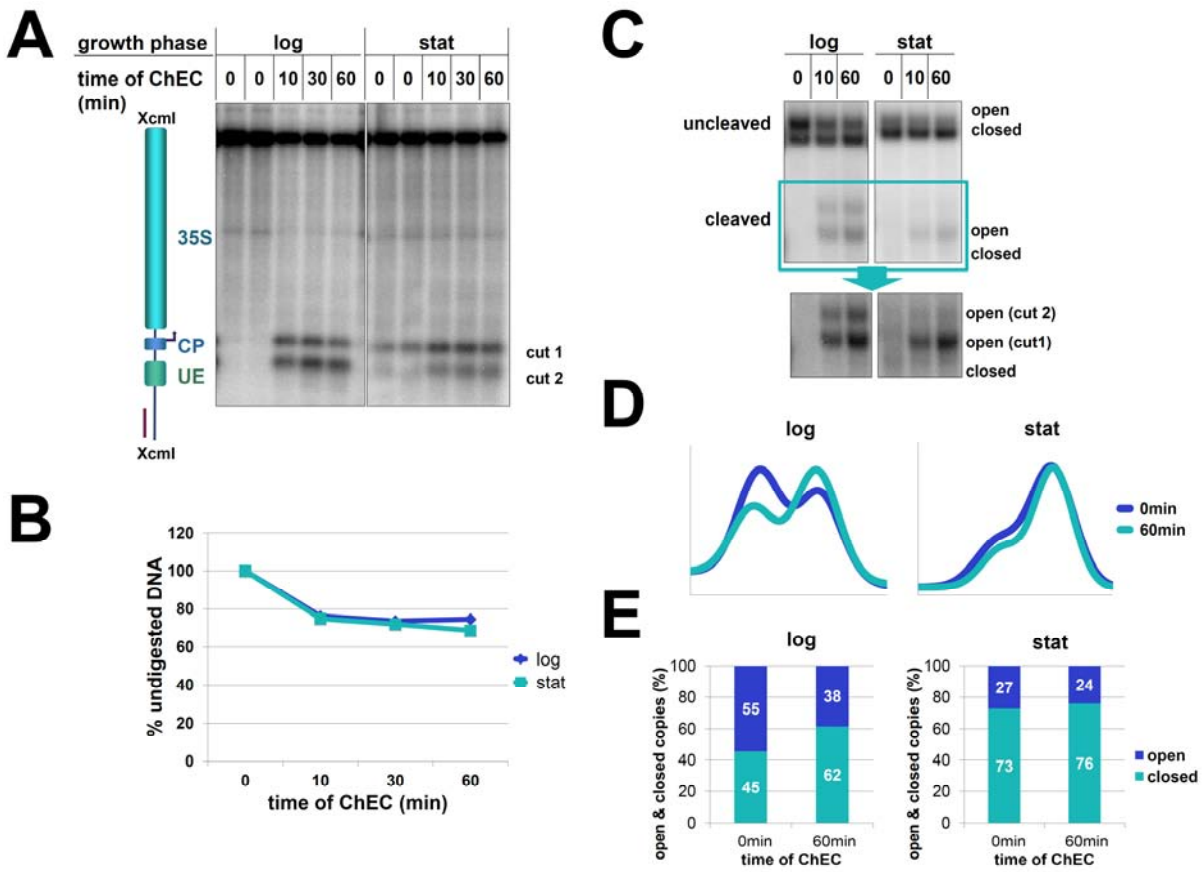

Figure 51: Rrn7-MNase mediated cleavage and psoralen accessibility at the rDNA upon transition to stationary phase in an *rpd3*Δ background

Strain y3024 (Rrn7 with C-terminal MNase expressed from the endogenous locus, *rpd3*Δ) was cultivated and samples were collected and analyzed in ChEC and ChEC-psoralen experiments as described in the legend to Figure 29 (see OD Figure 19 in the appendix for the respective ODs). **(A)** Analysis of ChEC samples. An autoradiograph of a Southern blot after hybridization with rDNp probe is shown. The position of two fragments originating from distinct cleavage events is shown on the right (cut1 and cut2) **(B)** Quantification of Rrn7-MNase mediated degradation shown in (A): The analysis was conducted according to Figure 25B. **(C)** ChEC-psoralen analysis of XcmI/SacII digested samples. An autoradiograph after hybridization with the 18S probe is shown. Positions of the uncleaved and the cleaved fragment are given on the left. A longer exposure of the framed blot region visualizing the cleaved fragments is shown at the bottom. The position of two fragments originating from distinct cleavage events is shown on the right (cut1 and cut2) **(D)** Profile analysis of the signals of the uncleaved fragments of the ChEC-psoralen experiment shown in (C). **(E)** Ratio of open and closed rDNA copies in log and stat samples.

Additional ChIP analysis with *RPD3* and *rpd3*Δ strains expressing Rrn7-TAP (Figure 52) was slightly contradicting to the ChEC results for the *rpd3*Δ strain: While ChEC revealed similar association levels in exponential and stationary phase samples, in ChIP the amount of Rrn7-TAP co-precipitated DNA was reduced after exit from exponential phase. However, the amount of co-precipitated DNA was still significantly higher than in the

corresponding *RPD3* samples. One possible explanation for the differences between ChEC and ChIP might be, that –similar to the observations with Rrn9- and Rrn5-TAP - the TAP tag of Rrn7 could interfere with the proper recruitment of CF to the core promoter and the proper establishment of the *rpd3*Δ phenotype. Along these lines, the establishment of the *rpd3*Δ phenotype was also affected in the *rpd3*Δ strain expressing Rrn7-MNase (see above). Alternatively, the TAP-tag could be partially masked by another protein in samples taken after the exponential phase.

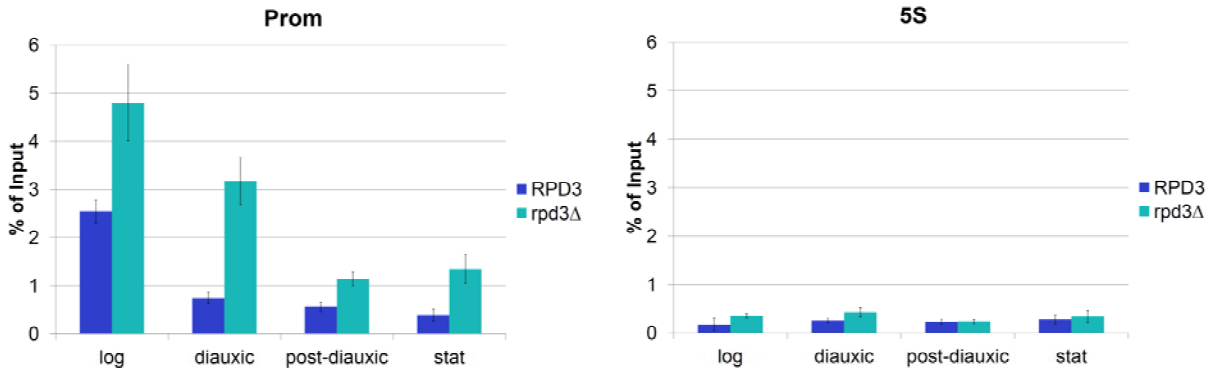

Figure 52: Rrn7-TAP co-precipitated DNA upon transition to stationary phase in *RPD3* and *rpd3Δ* strains

Yeast strains y3116 (Rrn7 with a C-terminal TAP-tag expressed from the endogenous locus, *RPD3*) and y3122 (Rrn7 with a C-terminal TAP-tag expressed from the endogenous locus, *rpd3*Δ) were cultured and samples were collected according to Figure 21 (see OD Figure 20 in the appendix for the respective ODs). ChIP was performed according to Figure 27 with IgG sepharose. The graphs depict the percentage of the input of the respective DNA fragment (indicated at the top of each diagram) co-precipitating with the TAP-tagged fusion protein at the indicated growth phases. Error bars indicate standard deviation errors derived from three independent ChIP experiments, each analyzed in triplicate qPCRs. The respective qPCR amplicons are depicted in Figure 28. The 5S qPCR amplicon serves as a background control for Rrn7-TAP co-precipitated DNA.

Taken together, Rrn7-MNase stayed associated with the core promoter of open 35S rRNA genes even in stationary phase in an *rpd3*Δ background. In ChIP the amount of co-precipitated DNA was reduced in samples taken after exponential phase, but still substantially higher than for the corresponding *RPD3* strain. Thus, Rrn7 could be a molecular switch which is dysregulated when Rpd3 is missing.

II.3.2.3.4 Rrn3 association with the rDNA is partially maintained in *rpd3*Δ cells but not in *RPD3* cells upon growth to stationary phase

Interaction of the initiation competent Rrn3-Pol I complex with the 35S rDNA promoter is likely a downstream event of CF recruitment to CP. Therefore, it was tested if - in addition to the dysregulated Pol I association with the rDNA - Rrn3-rDNA promoter interaction might be altered in *rpd3*Δ strains compared to *RPD3* strains upon growth to stationary phase.

For the analysis of the association of Rrn3 after exit from exponential phase in *RPD3* and *rpd3*Δ strains only data from ChIP experiments in strains expressing Rrn3-TAP are shown (Figure 53). ChEC experiments in Rrn3-MNase expressing strains were also performed but yielded only very weak cleavage events even in exponential phase samples (data no shown). The amount of Rrn3-TAP co-precipitated 35S rDNA promoter DNA decreased in all samples from the diauxic shift to stationary phase, and was close to background levels in post-diauxic and stationary phase samples for the *RPD3* strain (Figure 53, compare "Prom" with "5S"). However, in *rpd3*Δ samples significant amounts of promoter DNA co-precipitated with Rrn3-TAP for all samples from diauxic shift to stationary phase.

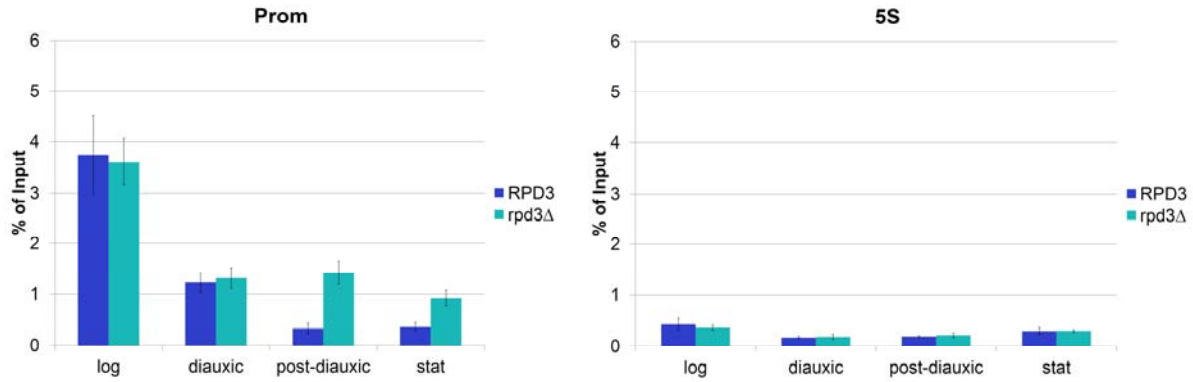

Figure 53: Rrn3-TAP co-precipitated DNA upon transition to stationary phase in *RPD3* and *rpd3Δ* strains

Yeast strains y3120 (Rrn3 with a C-terminal TAP-tag expressed from the endogenous locus, *RPD3*) and y3126 (Rrn3 with a C-terminal TAP-tag expressed from the endogenous locus, *rpd3*Δ) were cultured and samples were collected according to Figure 21 (see OD Figure 21 in the appendix for the respective ODs). ChIP was performed according to Figure 27 with IgG sepharose. The graphs depict the percentage of the input of the respective DNA fragment (indicated at the top of each diagram) co-precipitating with the TAP-tagged fusion protein at the indicated growth phases. Error bars indicate standard deviation errors derived from three independent ChIP experiments, each analyzed in triplicate qPCRs. The respective qPCR amplicons are depicted in Figure 28. The 5S qPCR amplicon serves as a background control for Rrn3-TAP co-precipitated DNA.

Taken together, the amount of Rrn3 that was associated with the rDNA promoter was higher in the *rpd3*Δ strain compared to the respective WT.

II.3.2.3.5 Net1 association with the rDNA upon growth to stationary phase stayed higher in *rpd3*Δ cells compared to *RPD3* cells

For the analysis of association dynamics of Net1 with the rDNA in an *rpd3*Δ strain, ChEC and ChEC-psoralen experiments with a strain expressing Net1 as a fusion protein with MNase were conducted (Figure 54).

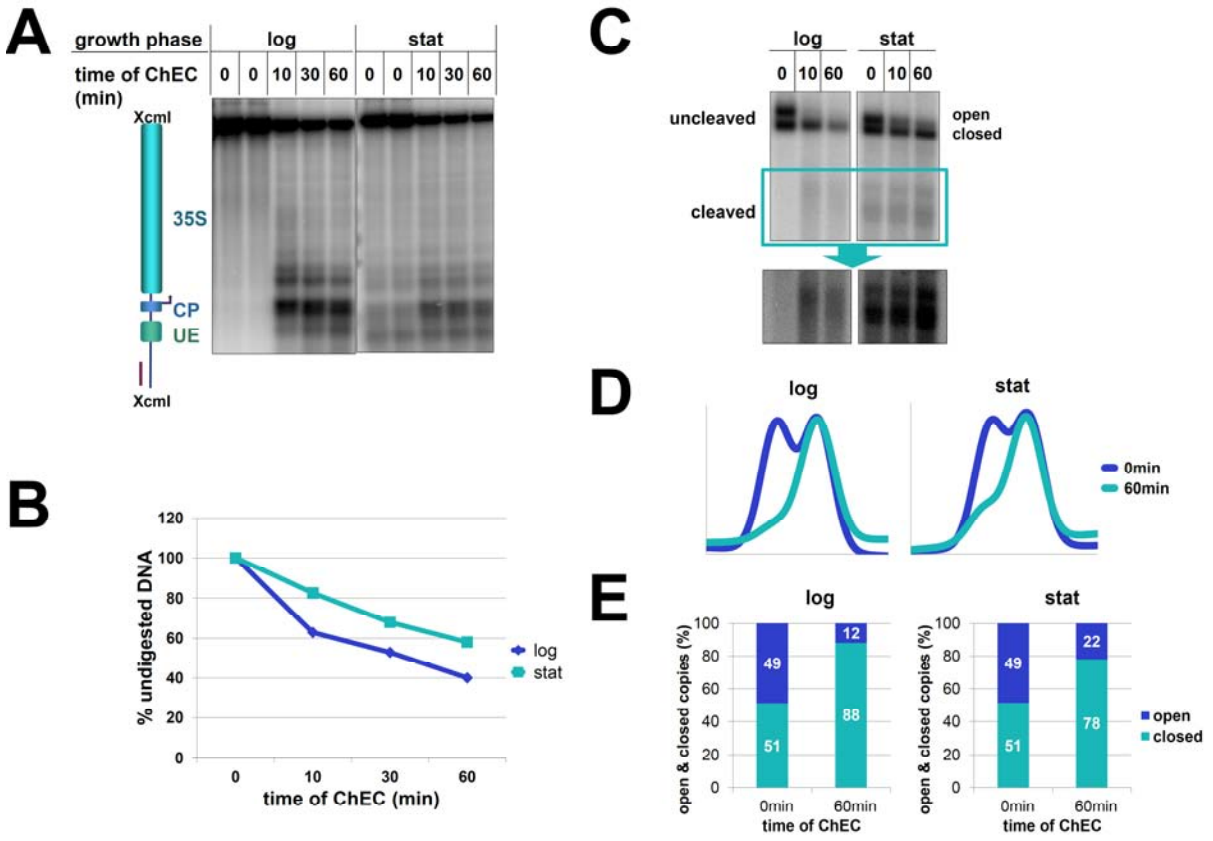

Figure 54: Net1-MNase mediated cleavage and psoralen accessibility at the rDNA upon transition to stationary phase in an *rpd3*Δ background

Strain y3033 (Net1 with C-terminal MNase expressed from the endogenous locus, *rpd3*Δ) was cultivated and samples were collected and analyzed in ChEC and ChEC-psoralen experiments as described in the legend to Figure 29 (see OD Figure 22 in the appendix for the respective ODs). **(A)** Analysis of ChEC samples. An autoradiograph of a Southern blot after hybridization with the rDNp probe is shown. **(B)** Quantification of Net1-MNase mediated degradation shown in (A): The analysis was conducted according to Figure 25A. **(C)** ChEC-psoralen analysis of XcmI/SacII digested samples. An autoradiograph after hybridization with the 18S probe is shown. Positions of the uncleaved and the cleaved fragments are given on the left. A longer exposure of the framed blot region visualizing the cleaved fragments is shown at the bottom. **(D)** Profile analysis of the signals of the uncleaved fragments of the ChEC-psoralen experiment shown in (C). **(E)** Ratio of open and closed rDNA copies in log and stat samples.

Activation of the MNase led to cleavage events at the promoter region and within the external transcribed spacer 1 (ETS1) of the 35S rDNA. As already described for Rpa190-MNase, Rrn9-MNase, Spt15-MNase, and Rrn7-MNase cleavage was already observed without activation of MNase. There was no obvious change in the cleavage pattern in stationary phase as it was observed for the respective *RPD3* strain. However, the decrease in overall cleavage intensity appeared to be weaker in the *rpd3*Δ strain (Figure 54 A). This was well reflected by the quantification of degradation efficiency (Figure 54 B).

ChEC-psoralen analysis showed that the amount of open 35S rRNA gene copies stayed at the same level in stationary phase as in exponential phase in the *rpd3*Δ strain (Figure 54 C - E "0min") in contrast to the *RPD3* strain (Figure 36 C - E "0min"). Net1-MNase preferentially degraded open copies in exponential as well as in stationary phase samples. However, in stationary phase a substantial amount of open copies resisted degradation (Figure 54 C - E "60min").

ChIP analysis with *RPD3* and *rpd3*Δ strains expressing Net1-TAP confirmed that the association of Net1 with the 35S rRNA gene promoter after exit from exponential phase was significantly higher when *RPD3* was deleted (Figure 55). The amount of 35S rRNA gene promoter DNA co-precipitating with Net1-TAP was reduced upon transition to stationary phase in *RPD3* as well as in *rpd3*Δ cells. The reduction was more drastic in WT samples approaching background levels at stationary phase (Figure 55, compare “Prom” with “5S”). In contrast, Net1-TAP co-precipitated still significant amounts of 35S rDNA promoter DNA in *rpd3*Δ samples taken at stationary phase.

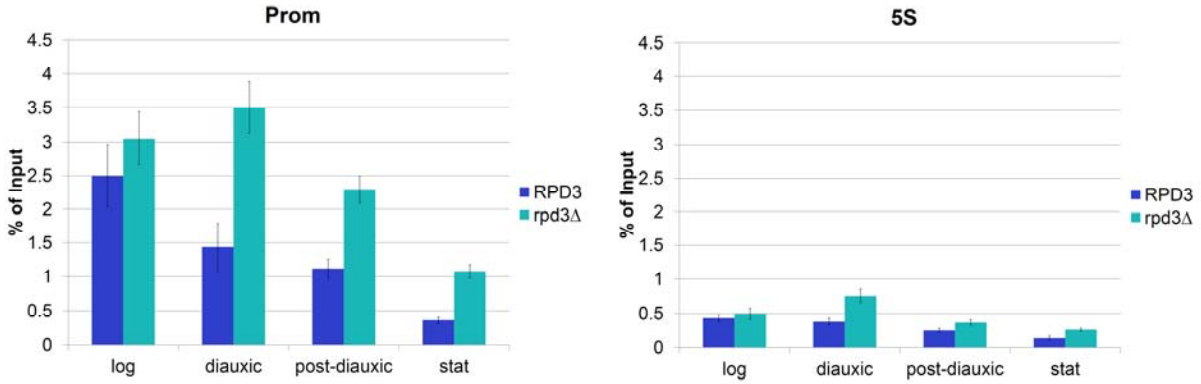

Figure 55: Net1-TAP co-precipitated DNA upon transition to stationary phase in *RPD3* and *rpd3Δ* strains

Yeast strains y2017 (Net1 with a C-terminal TAP-tag expressed from the endogenous locus, *RPD3*) and y3131 (Net1 with a C-terminal TAP-tag expressed from the endogenous locus, *rpd3*Δ) were cultured and samples were collected according to Figure 21 (see OD Figure 23 in the appendix for the respective ODs). ChIP was performed according to Figure 27 with IgG sepharose. The graphs depict the percentage of the input of the respective DNA fragment (indicated at the top of each diagram) co-precipitating with the TAP-tagged fusion protein at the indicated growth phases. Error bars indicate standard deviation errors derived from three independent ChIP experiments, each analyzed in triplicate qPCRs. The respective qPCR amplicons are depicted in Figure 28. The 5S qPCR amplicon serves as a background control for Net1-TAP co-precipitated DNA.

In summary, Net1-MNase and Net1-TAP stayed associated with the 35S rRNA gene copies in stationary phase samples in the *rpd3*Δ strain, whereas its association was drastically decreased in the *RPD3* strain. This observation makes Net1 another potential target for Rpd3-dependent regulation.

In conclusion, the extension of the comprehensive analysis to *rpd3*Δ strains showed similarities and differences in Pol I PIC association between *RPD3* and *rpd3*Δ. Thus, two possible candidates for Rpd3-dependent regulation of Pol I recruitment to the 35S rDNA promoter upon growth to stationary phase could be identified.

Net1 was found as one of these factors. To further investigate whether Net1 plays a role in the establishment of the *rpd3*Δ phenotype we used a strain expressing an allele *net1trunc* in which the region coding for the putative Pol I transcription stimulating domain of Net1 (MDM-domain) is deleted (Hannig, 2015). Cells expressing *net1trunc* are viable but strongly impaired in growth and efficient recruitment of Pol I to the 35S rRNA genes. Therefore, strains carrying all possible combinations of *NET1*, *net1trunc*, *RPD3*, *rpd3*Δ alleles were subjected to psoralen photocrosslinking experiments with different samples taken upon growth from exponential to stationary phase (Figure 56).

As expected most of the 35S rRNA gene copies of the samples collected from the *NET1 RPD3* strain adopted the closed chromatin state with transition to stationary phase (Figure 56 "*NET1RPD3*"). In the *NET1rpd3*Δ strain the fraction of open 35S rDNA increased upon growth to stationary phase, thus well representing the *rpd3*Δ phenotype (Figure 56 "*rpd3*Δ"). Truncation of the Net1 MDM-domain in strain *net1truncRPD3* led to a decrease in the amount of open 35S rRNA gene copies in exponential phase when compared to the corresponding NET1 strain *NET1RPD3*. Upon transition to stationary phase all open copies adopted the closed chromatin state in *net1truncRPD3* cells, even more effective than observed for the respective WT strain (Figure 56, compare "*net1trunc*" with "*NET1RPD3*"). Interestingly, the truncation of the Net1 MDM-domain in combination with a deletion of *RPD3* in strain *net1truncrpd3*Δ partially compromised the establishment of the *rpd3*Δ phenotype (Figure 56 "*net1truncrpd3*Δ"): In exponential phase more copies were in the open chromatin state in the *net1truncrpd3*Δ strain when compared to the *net1truncRPD3* strain, whereas more open copies were observed in the *NET1RPD3* and *NET1rpd3*Δ strains (Figure 56 A and B “log”). Whereas there was an initial opening of 35S rDNA copies in the diauxic shift sample of strain *net1truncrpd3*Δ, copies adopted the closed chromatin state upon growth to stationary phase very similar to the closing observed in the *NET1RPD3* strain (Figure 56 A and B “stat”).

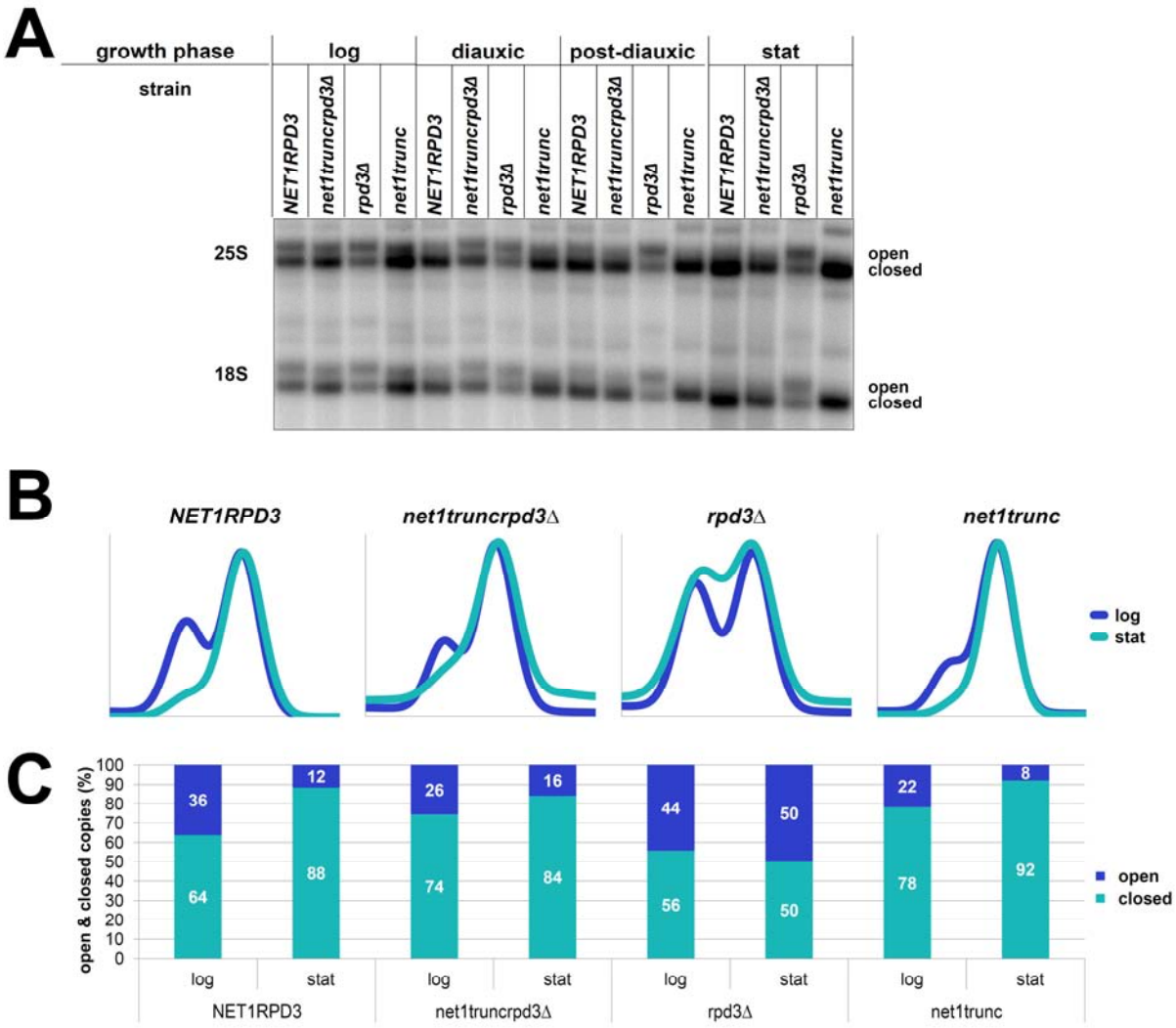

Figure 56: Psoralen accessibility upon growth to stationary phase in dependence of *RPD3* and *NET1* deletions

Yeast strains y3725 (*NET1 RPD3*), y3673 (*net1trunc RPD3*), y3672 (*NET1 rpd3Δ),* y3671 (*net1trunc rpd3Δ)* were cultured according to Figure 21 (see OD Figure 24 in the appendix for culture ODs). **(A)** Psoralen analysis. An autoradiograph after hybridization with the 3.5kb rDNA probe is shown. The origin of the sample is indicated at the top. On the left it is indicated from which EcoRI rDNA fragment the signal is derived. On the right the positions of fragments derived from either the open or the closed chromatin state are labeled. **(B)** Profile analysis of the psoralen samples shown in (A) according to Figure 26. **(C)** Ratio of open and closed rDNA copies. The calculation was made according to Figure 26. The exact percent values are indicated as white numbers in the bars.

Taken together, these results indicate that Net1 might play a role in the Rpd3 dependent regulation that leads to a proper establishment of the closed chromatin state in stationary phase. However, the truncation of the MDM domain of Net1 only partially compromised the *rpd3Δ* phenotype, thus suuggesting that other factors or other domains of Net1 may play a role in the Rpd3 dependent regulation.

II.4 The impact of Rpa49 on the establishment of the open 35S rRNA gene chromatin state

While the previous section aimed at the characterization of the transition to the closed rDNA chromatin state, the last part of this thesis focused on the transition to the open chromatin state. Pol I transcription is so far the only known requirement to establish the open, nucleosome depleted chromatin state, but it is an open question if this is achieved by the action of the Pol I enzyme alone or other unknown factors.

Rpa49 is one of the 14 subunits of RNA polymerase I and important for efficient Pol I loading (Liljelund et al., 1992). Interestingly, a previous study suggested that RNA polymerase I lacking the A49 subunit has a reduced ability to transcribe through nucleosomal templates *in vitro* (Merkl, 2013). Most of the 35S rRNA gene copies adopt the closed, nucleosomal chromatin state past the end of exponential growth phase correlating with the shutdown of Pol I transcription (Fahy et al., 2005; Sandmeier et al., 2002, Babl 2012, this work). Upon exit from stationary phase rapid resumption of Pol I transcription was observed, correlating with re-establishment of open 35S rRNA gene chromatin (Fahy, 2005, Sandmeier, 2002, Johnson 2013). Thus the exit from stationary phase was chosen to investigate, if the absence of Rpa49 compromises the Pol I ability to transcribe through and thus to open nucleosomal 35S rRNA genes *in vivo*. In this section cells were only cultured to post-diauxic shift phase, in which 35S rRNA genes have adopted the closed chromatin state and Pol I transcription had ceased.

II.4.1 Absence of Rpa49 delayed a proper re-establishment of open 35S rRNA gene chromatin upon exit from post diauxic shift phase

It was first tested if the absence of Rpa49 has an effect on the establishment of open 35S rRNA chromatin *in vivo*. To this end a strain was created in which *RPA49* is under the control of a galactose inducible and glucose repressible promoter (p*GAL1:RPA49* subsequently called *rpa49*↓). This strain additionally expressed Rpa135 in fusion with protein A (Rpa135-ProtA) from its endogenous locus, enabling the analysis of Pol I association with rDNA in subsequent ChIP experiments. Strain *rpa49*↓ was cultured in YPD medium to late post-diauxic shift phase to deplete Rpa49. Afterwards the exit from stationary phase was initiated by transfer of the cells to either fresh YPD (further depletion of Rpa49) or fresh YPG (expression of *RPA49*) medium. Depletion and (re)expression of Rpa49 was verified by Western blot analysis (see Supplemental Figure

6 in the appendix). As a control the corresponding WT strain with *RPA49* under its own promoter (*pRPA49:RPA49*, subsequently called *RPA49*), which also expressed Rpa135-ProtA from its endogenous locus, was subjected to the same cultivation protocol. Samples were taken at different times and analyzed by psoralen photo-crosslinking (Figure 57) and ChIP (Figure 58).

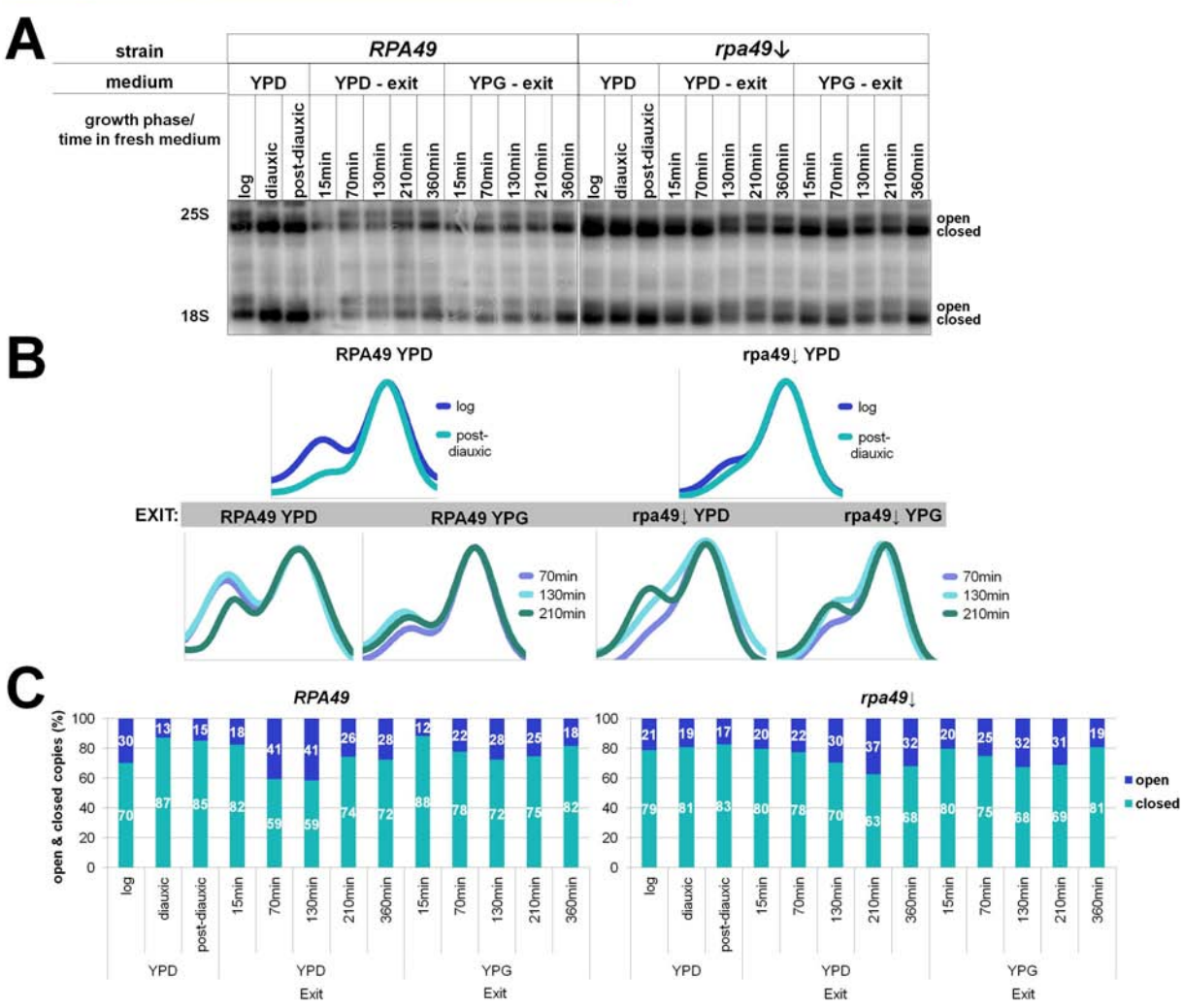

Figure 57: Psoralen accessibility upon growth to and exit from post diauxic shift phase in the presence and after depletion of *Rpa49*

Yeast strains y207 (*RPA49*) and y2670 (*rpa49*↓) were cultured in YPD to post-diauxic shift phase and then re-inoculated in YPD and YPG medium according to Figure 22 (see OD Figure 25 in the appendix for culture ODs). Samples were taken during growth to post-diauxic shift phase and upon re-growth for indicated times. For *rpa49*↓ cells, YPD media represses *RPA49* expression, while *RPA49* expression is induced in YPG. **(A)** Psoralen analysis. An autoradiograph after hybridization with the 3.5kb rDNA probe is shown. The origin of the sample is indicated at the top. On the left it is indicated from which EcoRI rDNA fragment the signal is derived. On the right the positions of fragments derived from either the open or the closed chromatin state are labeled. **(B)** Profile analysis of the psoralen samples shown in (A) according to Figure 26. The upper graphs show profiles upon entry to post-diauxic phase and the lower graphs show profiles upon exit from this phase (EXIT, grey background). **(C)** Ratio of open and closed rDNA copies. The calculation was made according to Figure 26. The exact percent values are indicated as white numbers in the bars.

Psoralen analysis in an *RPA49* strain from samples collected during the transition to stationary phase confirmed previous data that most 35S rRNA gene copies adopted the closed chromatin state in late post diauxic phase (Figure 57: "*RPA49*", "YPD", "log"-"post-diauxic"). Transfer of cells to fresh YPD medium led to a strong increase in open 35S rRNA genes reaching maximum of 41% of open copies within 70min post inoculation (Figure 57: "RPA49", "YPD", "70min"). The same proportion of copies was still in the open conformation after 130min. However, after 210min and 360min the fraction of open copies was again reduced. This closing of copies correlated well with a concomitant increase in the OD of the culture (see OD Figure 25 in the appendix): The first clear increase in the optical density of the culture was observed at 210min and the next at 360min post inoculation in YPD. Thus, the decrease in the fraction of open copies could be correlated to re-proliferation and thus to the process of replication in accordance with previous observations (Wittner et al., 2011). The exit from post-diauxic shift phase in fresh galactose containing medium also led to re-establishment of open chromatin at the rDNA with similar kinetics as observed for glucose containing medium (Figure 57: "*RPA49*", "YPG"). However, the maximum amount of open copies was lower than in glucose containing medium with a maximum of 28% open copies after 130min.

Already in exponential phase psoralen analysis revealed a reduced fraction of open copies in strain *rpa49*↓ when compared to the *RPA49* strain (Figure 57: compare "*rpa49*↓" with "*RPA49*", "log") this fraction was decreased upon cultivation to post diauxic shift phase (Figure 57: compare "*rpa49*↓" "log - post-diauxic"). The separation of the band derived from the open copies and the band derived from the closed copies was worse in the *rpa49*↓ strain when compared to the separation of the bands in the *RPA49* strain. Exit from post diauxic shift phase in glucose containing medium led to re-establishment of open chromatin, but with delayed kinetics when compared to the *RPA49* strain (Figure 57: compare "*rpa49*↓" with "*RPA49*", "YPD", "15min"-"360min"). A significant increase in the fraction of open copies was only visible after 130min and the maximum fraction of open copies reached a value of 37% after 210min, which was slightly lower than 41% of open copies for the corresponding *RPA49* strain after 130min. As described above, separation of the band derived from the open copies fragment and the band derived from the closed copies fragment was not as good in the *rpa49*↓ strain, as in the *RPA49* strain. A reduction in the fraction of open copies in the *rpa49*↓ strain occurred 360min after the transfer to fresh YPD, correlating with the first increase in the optical density of the culture (see OD Figure 25 in the appendix). The exit from stationary phase in fresh galactose containing medium and thus induction of *RPA49* had similar kinetics as the *RPA49* strain subjected to the same cultivation protocol (Figure 57:

compare "*rpa49*↓" with "*RPA49*", "YPG", "15min"-"360min"). However, the separation of the open and closed copies derived bands was worse in *rpa49*↓ cells than in *RPA49* WT cells in samples taken 15min and 70min after transfer to YPG, whereas band separation became similar at later time points. Although Western blot analysis indicated that Rpa49 was increasingly expressed in *rpa49*↓ cells after transfer to YPG (see Supplemental Figure 6 in the appendix) it could be that the Rpa49 levels were initially still too low at these time points to overcome the depletion effect. Nevertheless, the maximum amount of open copies reached in YPG medium was higher in the *rpa49*↓ strain than in the *RPA49* strain. This indicates, that the overexpression of Rpa49 might positively stimulate Pol I association and thus opening of 35S rRNA gene copies.

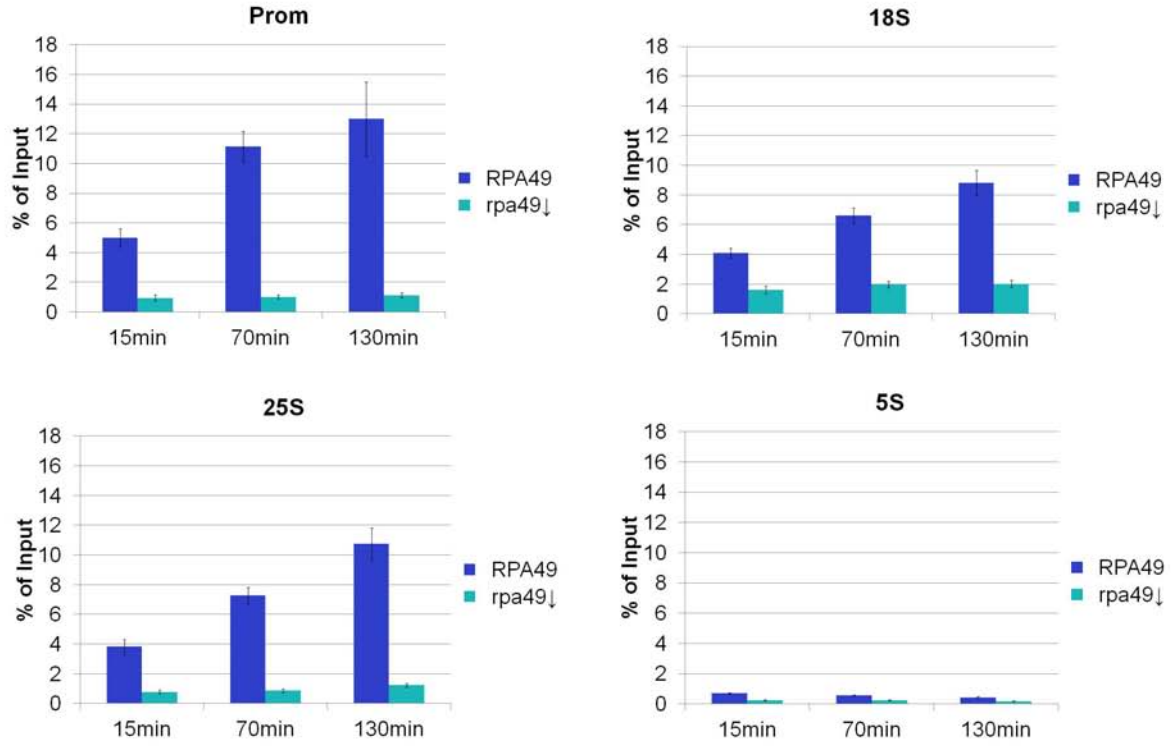

Figure 58: Rpa135-ProtA ChiP experiments upon exit from post diauxic shift phase in the presence and after depletion of *Rpa49*

Yeast strains y2534 (Rpa135 with a C-terminal ProtA-tag expressed from the endogenous locus, *RPA49* under control of the endogenous promoter) and y2670 (Rpa135 with a C-terminal ProtA-tag expressed from the endogenous locus, *RPA49* under control of a *GAL1* promoter at the endogenous locus (here called *rpa49*↓)) were cultured in YPD to post-diauxic phase (depletion of Rpa49 in *rpa49*↓). Cells were then re-inoculated in fresh YPD for the indicated times and samples were collected according to Figure 22 (see OD Figure 26 in the appendix for the culture ODs). ChIP was performed according to Figure 27 with IgG sepharose. The graphs depict the percentage of the input of the respective DNA fragment (indicated at the top of each diagram) co-precipitating with the ProtA-tagged fusion protein at the indicated growth phases. Error bars indicate standard deviation errors derived from three independent ChIP experiments, each analyzed in triplicate qPCRs. The respective qPCR amplicons are depicted in Figure 28. The 5S qPCR amplicon serves as a background control for Rpa135-ProtA co-precipitated DNA.

Additionally, samples from the re-growth experiment in YPD medium (15min, 70min, 130min after inoculation) were analyzed in ChIP experiments with Rpa135-ProtA as bait protein (Figure 58). No difference in the bait protein amount, that cannot be explained by differences in the OD were observed (Supplemental Figure 7). For the *RPA49* samples (Figure 58 "*RPA49*") the amount of co-precipitated DNA drastically increased upon re-growth. The highest amounts of co-precipitated DNA were observed for the promoter amplicon followed by the 25S qPCR amplicon. Under Rpa49 depletion conditions (Figure 58 "*rpa49*↓") the amount of Rpa135-ProtA co-precipitated DNA stayed at a very low level throughout all analyzed time points. In contrast to the *RPA49* strain, the highest co-precipitation with Rpa135-ProtA from *rpa49*↓ samples was observed for the “18S” qPCR amplicon. Neither for *RPA49* nor for *rpa49*↓ samples significant amounts of 5S rDNA were co-precipitated.

Taken together, the depletion of Rpa49 in the *rpa49*↓ strain led to a massive reduction in Pol I association with the 35S rRNA genes compared to the corresponding *RPA49* strain. This is in line with previous observations showing that Rpa49 is implicated in Pol I PIC formation (Beckouet et al., 2008), and a high rate of Pol I loading on 35S rRNA genes (Albert et al., 2011). Whereas Pol I-rDNA interaction is strongly impaired upon Rpa49 depletion, the defect in the formation of open chromatin was relatively mild. Thus, even very low levels of Pol I seem to be sufficient for the re-establishment of open, nucleosome depleted 35S rRNA gene copies upon exit from post-diauxic phase.

II.4.2 Deletion of *RPD3* facilitated open 35S rRNA gene chromatin formation but had only a slight effect on Pol I association with rDNA in the absence of Rpa49

As shown in the previous section, depletion of Rpa49 led to delayed and partly impaired establishment of open 35S rRNA gene copies and a drastically reduced amount of Pol I association with the rDNA upon exit from post diauxic shift phase. One possible explanation for this phenomenon could be that Pol I lacking Rpa49 does not efficiently transcribe nucleosomal templates and might dissociate from rDNA upon collision with nucleosomes. Since deletion of *RPD3* prevents nucleosome assembly on 35S rRNA genes upon transition to stationary phase (Babl, 2012; Johnson et al., 2013; Sandmeier et al., 2002) it was tested if Pol I transcription in the *rpa49*↓ strain could be rescued by an additional deletion of *RPD3*. *rpa49*↓/*rpd3*Δ and *RPA49*/*rpd3*Δ cells were cultured in YPD medium and samples were analyzed in psoralen photocrosslinking (Figure 59) and ChIP (Figure 60) experiments. *RPA49* and *RPD3* have been reported to be synthetically lethal

(Lin et al., 2008). Thus, the analyzed strains might be viable due to a leaky *GAL* promoter, which is not tightly repressed by glucose, and thus leads to residual Rpa49 background expression.

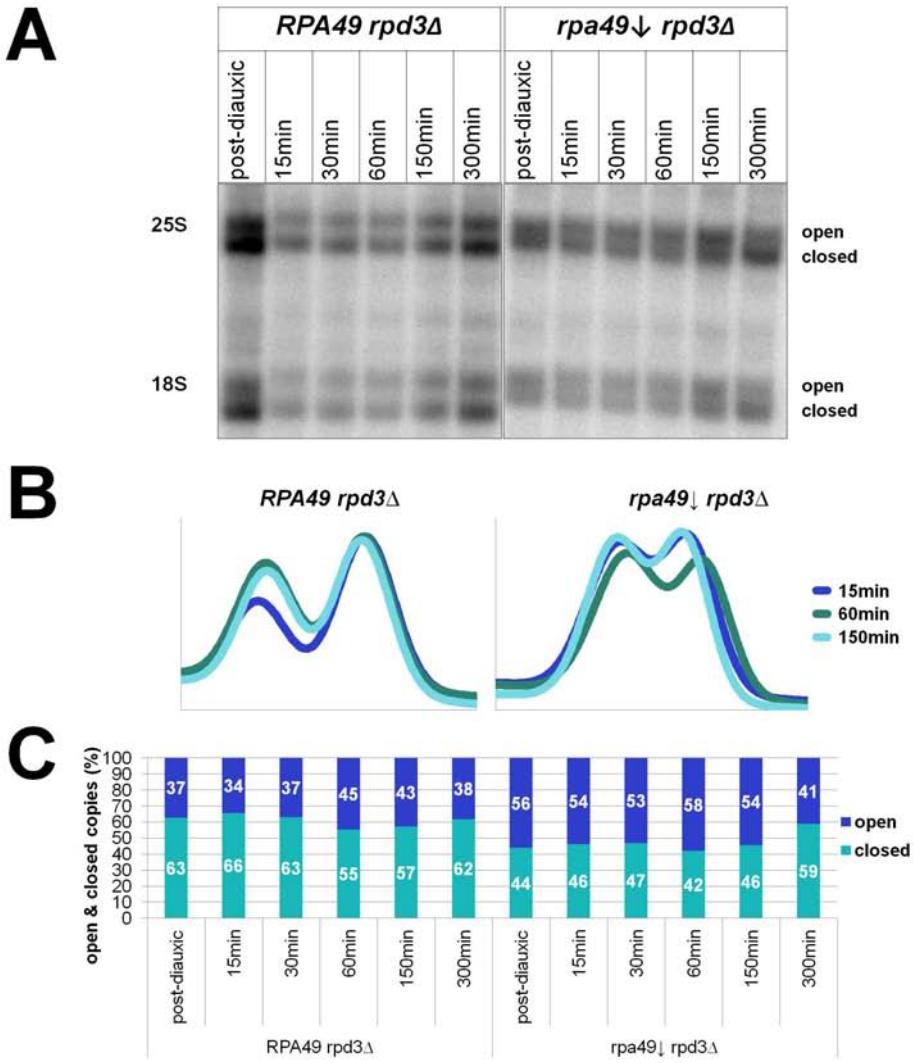

Figure 59: : Psoralen accessibility upon growth to and exit from post diauxic shift phase in *RPD3* deletion strains in the presence and after depletion of Rpa49

Yeast strains y3323 (*RPA49, rpd3Δ*) and y3325 (*rpa49*↓ under control of a GAL1 promoter at the endogenous locus, *rpd3Δ*) were cultured in YPD and then re-inoculated in fresh YPD medium according to Figure 22 and Figure 57 (see OD Figure 27 in the appendix for culture ODs). **(A)** Psoralen analysis. An autoradiograph after hybridization with the 3.5kb rDNA probe is shown. The origin of the sample is indicated at the top. On the left it is indicated from which EcoRI rDNA fragment the signal is derived. On the right the positions of fragments derived from either the open or the closed chromatin state are labeled. **(B)** Profile analysis of the psoralen samples shown in (A) according to Figure 26. **(C)** Ratio of open and closed rDNA copies. The calculation was made according to Figure 26. The exact percent value is indicated as white numbers in the bars.

In the *RPA49*/*rpd3*Δ strain 37% of 35S rRNA gene copies were in the open chromatin state in post diauxic shift phase. However, the exit from post diauxic shift phase led to further increase in the portion of open copies peaking 60min after the transfer to fresh

YPD medium (Figure 59 "*RPA49 rpd3*Δ"). At 150min and 300min after the transfer a reduction of the fraction of open copies was observed, correlating with cell division (see OD Figure 27 in the appendix). Interestingly, in the *rpa49*↓*/rpd3*Δ background, a higher fraction of copies was in the open chromatin conformation already in stationary phase (Figure 59 "*rpa49*↓ *rpd3*Δ"). However, the separation of fragments derived from open copies and fragments derived from closed copies was worse than in the *RPA49/rpd3*Δ strain. Upon exit from post diauxic shift only a very slight increase in the fraction of open copies was observed peaking 60min after the transfer to fresh medium. Nevertheless, separation of the two bands representing open and closed copies was slightly better compared to the post diauxic shift sample, but still worse than in the *RPA49/rpd3*Δ samples. This indicates, that many copies were in an intermediate state between actively transcribed, nucleosome depleted and fully packed into nucleosomes.

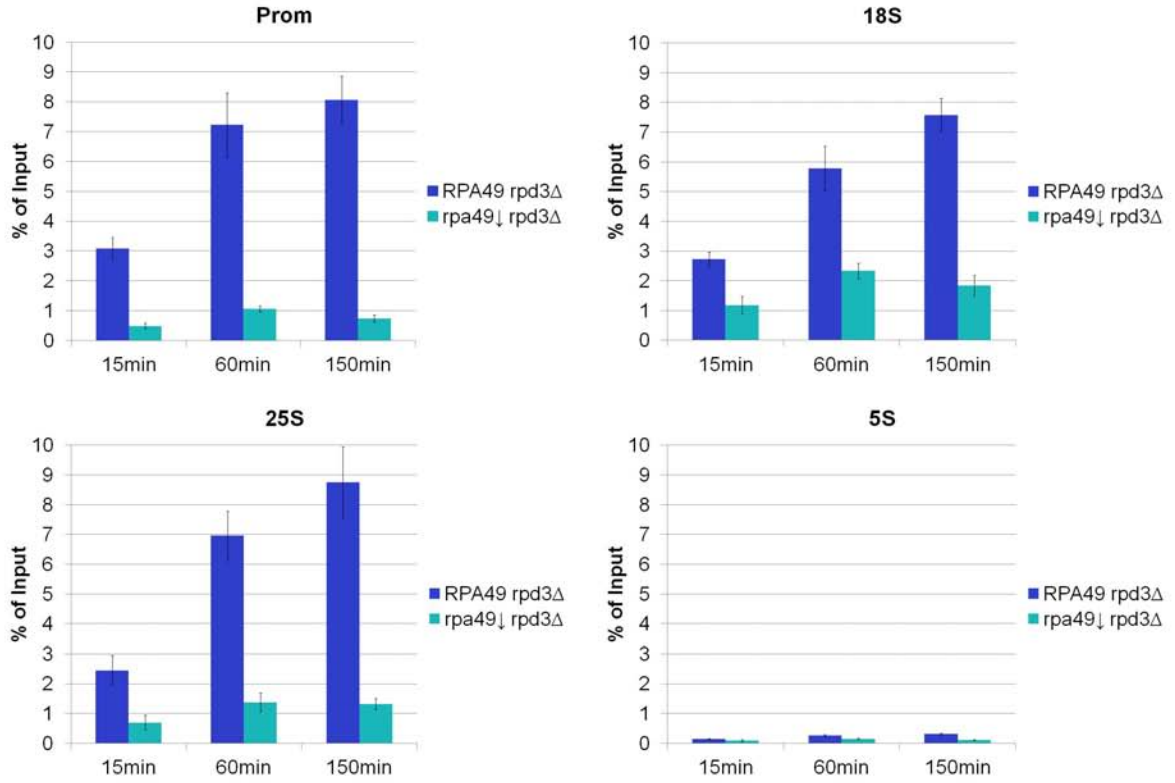

Figure 60: Rpa135-ProtA ChiP experiments upon exit from post diauxic shift phase in rpd3Δ strains in the presence and after depletion of Rpa49

Yeast strains y3323 (Rpa135 with a C-terminal ProtA-tag expressed from the endogenous locus, *RPA49* under control of the endogenous promoter, *rpd3*Δ) and y3325 (Rpa135 with a C-terminal ProtA-tag expressed from the endogenous locus, *rpa49*↓ under control of a GAL1 promoter at the endogenous locus, *rpd3*Δ) were cultured in YPD and samples were collected according to Figure 22 and Figure 58 (see OD Figure 28 in the appendix for the culture ODs). ChIP was performed according to Figure 27 with IgG sepharose. The graphs depict the percentage of the input of the respective DNA fragment (indicated at the top of each diagram) co-precipitating with the ProtA-tagged fusion protein at the indicated growth phases. Error bars indicate standard deviation errors derived from three independent ChIP experiments, each analyzed in triplicate qPCRs. The respective qPCR amplicons are

depicted in Figure 28. The 5S qPCR amplicon serves as a background control for Rpa135-ProtA co-precipitated DNA.

ChIP analysis from samples after exit from post-diauxic shift phase with Rpa135-ProtA as bait protein revealed a drastic increase in the amount of co-precipitated DNA for the *RPA49/rpd3*Δ strain, while in the *rpa49*↓*/rpd3*Δ strain the amount of co-precipitated DNA only slightly increased and was at a very low level compared to the *RPA49* samples at all analyzed time points (Figure 60). Interestingly, the amount of co-precipitated DNA was again highest for the promoter amplicon and the 25S amplicon in the *RPA49* and for the 18S amplicon for the *rpa49*↓ strain, as already observed for the analysis in the *RPD3* background (Figure 58).

In summary, the additional deletion of *RPD3* did not rescue the effect of Rpa49 depletion. Even if many 35S rRNA gene copies were already in the open chromatin state in the *rpd3*Δ background, the amount of Pol I was still drastically reduced when Rpa49 was depleted. These findings suggest that the presence of a nucleosome-depleted template does not increase the recruitment of Pol I lacking the Rpa49 subunit. Furthermore, this confirmed previous observations that the number of open copies is not necessarily an indication for the amount of associated Pol I (see section II.3, and French et al., (2003)).

II.4.3 Expression of the Rpa49 C-terminal domain, but not the N-terminal domain rescued Pol I recruitment to 35S rDNA and the 35S rDNA chromatin transition upon Rpa49 depletion

In previous studies separate functions could be assigned to the N-terminal and the C-terminal domains of Rpa49. Whereas the N-terminal part of Rpa49 is important for the assembly of the Rpa49/Rpa34 dimer and the RNA cleavage activity of Pol I (Geiger et al., 2010) the Rpa49 C-terminus supported Pol I processivity *in vitro* (Geiger et al., 2010), and recruitment of Pol I to 35S rRNA genes (Beckouet et al., 2008). However, it was not clear which of the two Rpa49 domains is important for the Pol I ability to open nucleosomal DNA. Therefore, either the full length Rpa49, or the C-terminal domain of Rpa49, or the N-terminal domain were additionally expressed under control of the *PGK1* promoter in Rpa49 depletion strains (*rpa49*↓), as well as in *RPA49* strains. Psoralen photocrosslinking (Figure 61) and ChIP (Figure 62) experiments were performed with samples taken upon exit from post-diauxic shift phase.

In samples from post-diauxic shift phase psoralen photocrosslinking analysis revealed that most of the 35S rRNA gene copies were in the closed chromatin state independently of Rpa49 being depleted or which Rpa49 construct was additionally expressed (Figure 61 “post-diauxic”). Differences between the strains expressing the different Rpa49 constructs emerged only upon exit from post-diauxic phase (Figure 61, “15min-300min”). The additional expression of full-length Rpa49 led to a proper re-establishment of the open 35S rDNA chromatin state in the *RPA49* and the *rpa49*↓ strain (Figure 61 "RPA49 + *full*" and "*rpa49*↓ + *full*"). Thus indicating that the additional expression of the full-length protein is sufficient to overcome the defect of the Rpa49 depletion mutant. Nevertheless, the maximum amount of open copies reached was slightly reduced in the *rpa49*↓ strain. Also the psoralen analysis of samples taken from *RPA49* and *rpa49*↓ strains with additional expression of the C-terminal part of Rpa49 yielded similar results (Figure 61 "RPA49 + *C-Term*" and "*rpa49*↓ *C-Term*"): Upon transfer to fresh medium both strains were able to re-establish 35S rRNA gene copies in the open chromatin state. Still, the maximum amount of open copies was slightly reduced in the *rpa49*↓ strain (Figure 61 C compare "*RPA49* + *C-Term*" and "*rpa49*↓ *C-Term*"). Additionally, the expression of the C-terminus of Rpa49 in the *rpa49*↓ strain yielded in a slightly reduced amount of open copies compared to the expression of the full-length Rpa49 in the same background (Figure 61, compare "*rpa49*↓+ *C-Term*" and "*rpa49*↓ + *full*"). These results indicate that the expression of the C-terminal domain of Rpa49 alone is sufficient to overcome the Rpa49 depletion defect in terms of 35S rRNA gene chromatin dynamics. In contrast to the expression of the C-terminus, expression of the Rpa49 N-Terminus showed drastic differences between *RPA49* and *rpa49*↓ strains (Figure 61 "*RPA49* + *N-Term*" and "*rpa49*↓+ *N-Term*"). While the *RPA49* strain expressing the Rpa49 N-terminus samples showed similar chromatin dynamics as the same strain expressing the full-length Rpa49 or its C-terminal domain, the *rpa49*↓ strain expressing the N-terminus was strongly compromised in the re-establishment of open 35S rRNA gene copies: The increase in the amount of open copies was very weak and the separation of the bands derived from open and closed copies fragments was extremely poor. Interestingly, the defect in chromatin opening was even stronger than observed for the *rpa49*↓ strain with no additional expression of the N-terminus (compare Figure 57 *"rpa49↓"* with Figure 61 *"rpa49↓+ N-Term"*). Thus, the expression of the N-terminus of Rpa49 seems to be insufficient to overcome (and even enforces) the Rpa49 depletion defect in 35S rRNA gene chromatin dynamics.

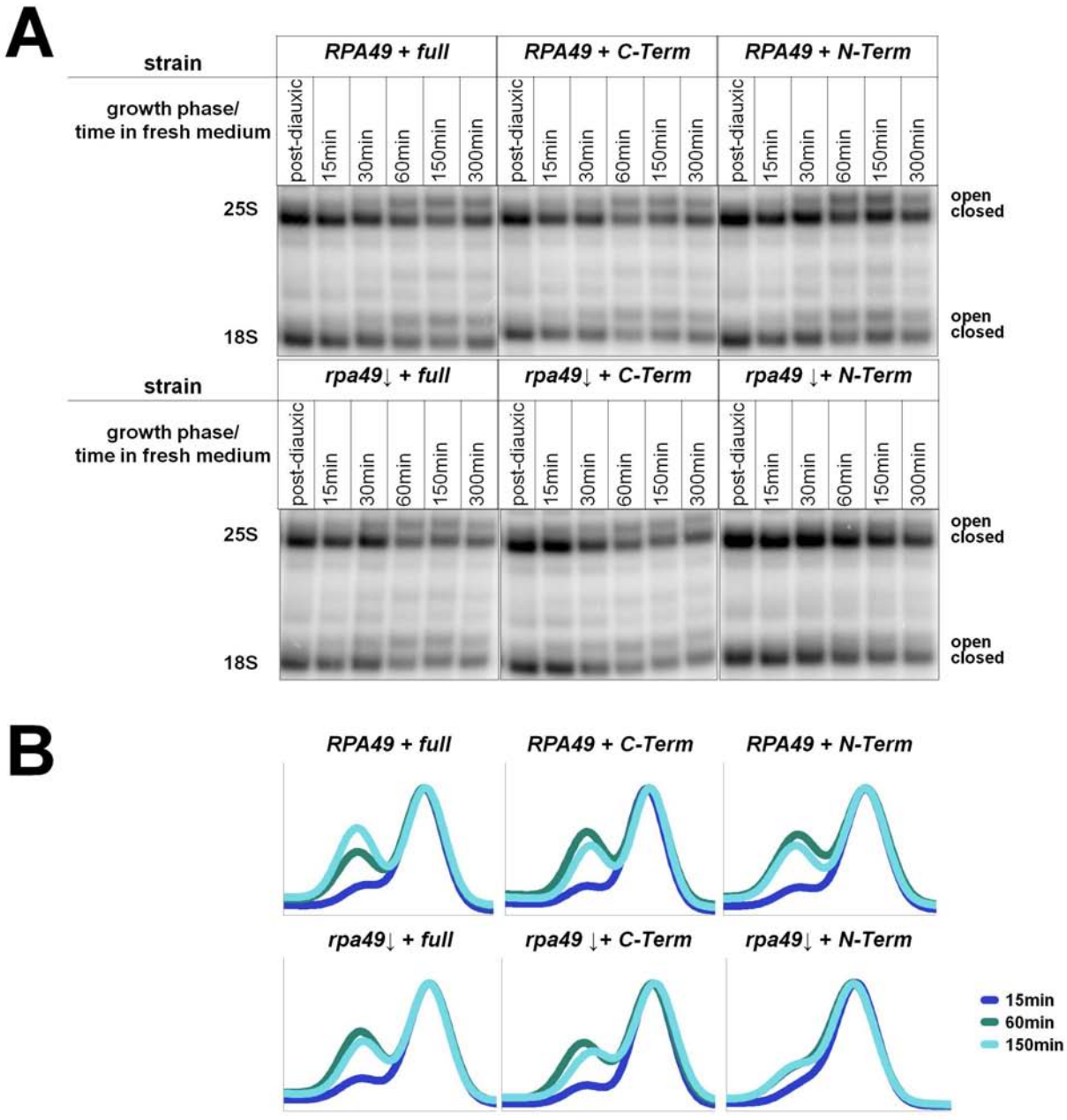
A
strain
RPA49 + full
RPA49 + C-Term
RPA49 + N-Term
growth phase/
time in fresh medium
post-diauxic
15min
30min
60min
150min
300min
25S
18S
open
closed
rpa49↓ + full
rpa49↓ + C-Term
rpa49 ↓+ N-Term
B
RPA49 + full
RPA49 + C-Term
RPA49 + N-Term
rpa49↓ + full
rpa49 ↓+ C-Term
rpa49↓ + N-Term
15min
60min
150min

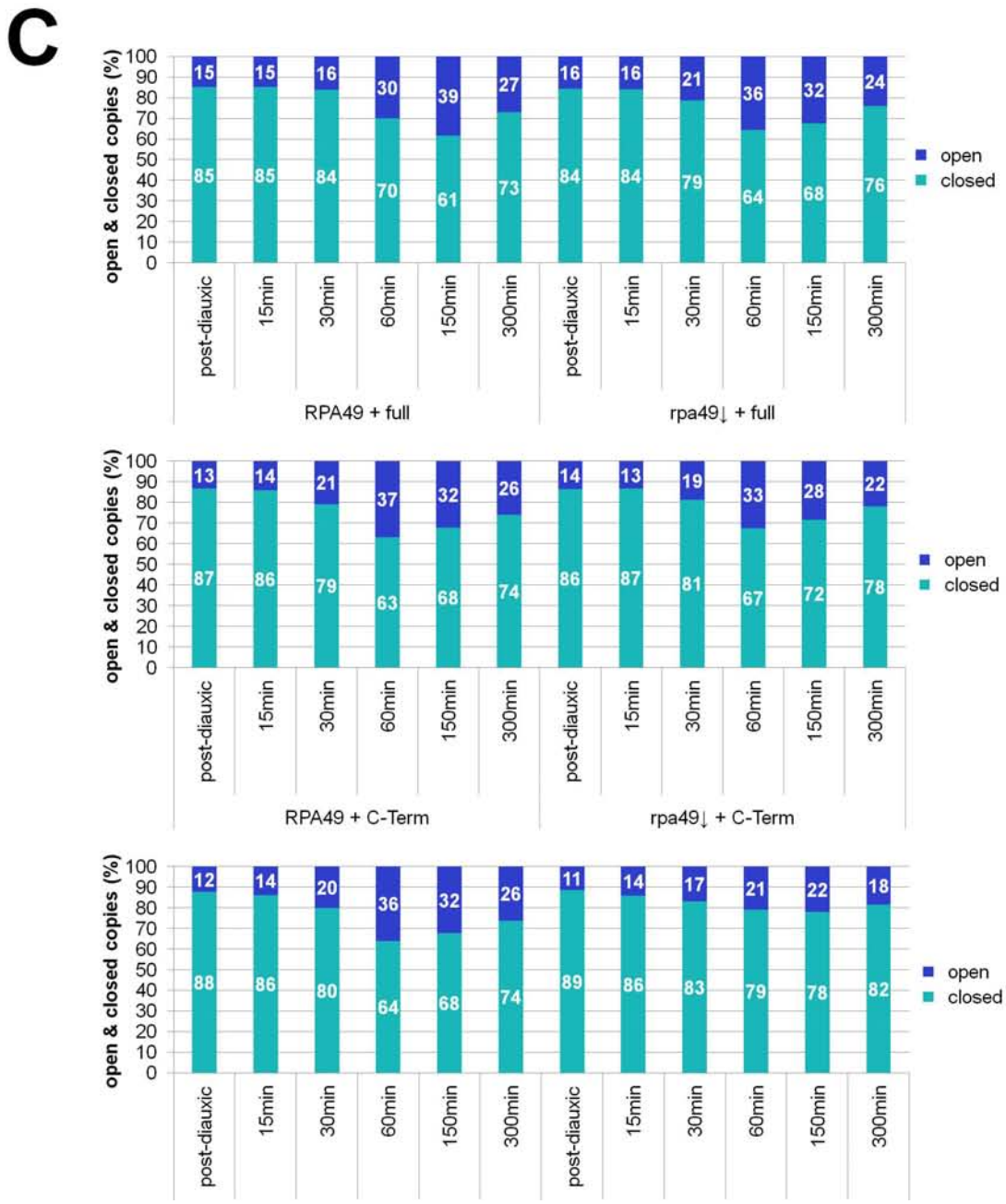

Figure 61: Psoralen accessibility at post diauxic shift phase in the presence and after depletion of *Rpa49* in strains expressing full length, C-terminus, or N-terminus of *Rpa49*

Yeast strains y3536 (*RPA49*, additional expression of *pPGK1: RPA49* (full)), y3544 (*RPA49,* additional expression of the C-terminal domain of Rpa49 (aa 116-426 (C-Term)) controlled by p*PGK1*), y3540 (*RPA49,* additional expression of the N-terminal domain of Rpa49 (aa 1-116 (N-Term)) controlled by p*PGK1*), y3534 *(rpa49*↓, "full"), y3538 (*rpa49*↓, N-Term), and y3542 (*rpa49*↓, C-Term*)* were cultured in YPD medium according to Figure 22 and Figure 57(see OD Figure 29 in the appendix for culture ODs). **(A)** Psoralen analysis. An autoradiograph after hybridization with the 3.5kb rDNA probe is shown. The origin of the sample is indicated at the top. On the left it is indicated from which EcoRI rDNA fragment the signal is derived. On the right the positions of fragments derived from either the open or the closed chromatin state are labeled. **(B)** Profile analysis of the psoralen samples shown in (A) according to Figure 26. **(C)** Ratio of open and closed rDNA copies. The calculation was made according to Figure 26. The exact percent values are indicated as white numbers in the bars.

Additional ChIP experiments with the *rpa49*↓ strains either additionally expressing the full-length Rpa49, or the C-terminus of Rpa49, or the N-terminus of Rpa49 were conducted to analyze the amount of Pol I associated with the rDNA under these conditions (Figure 62).

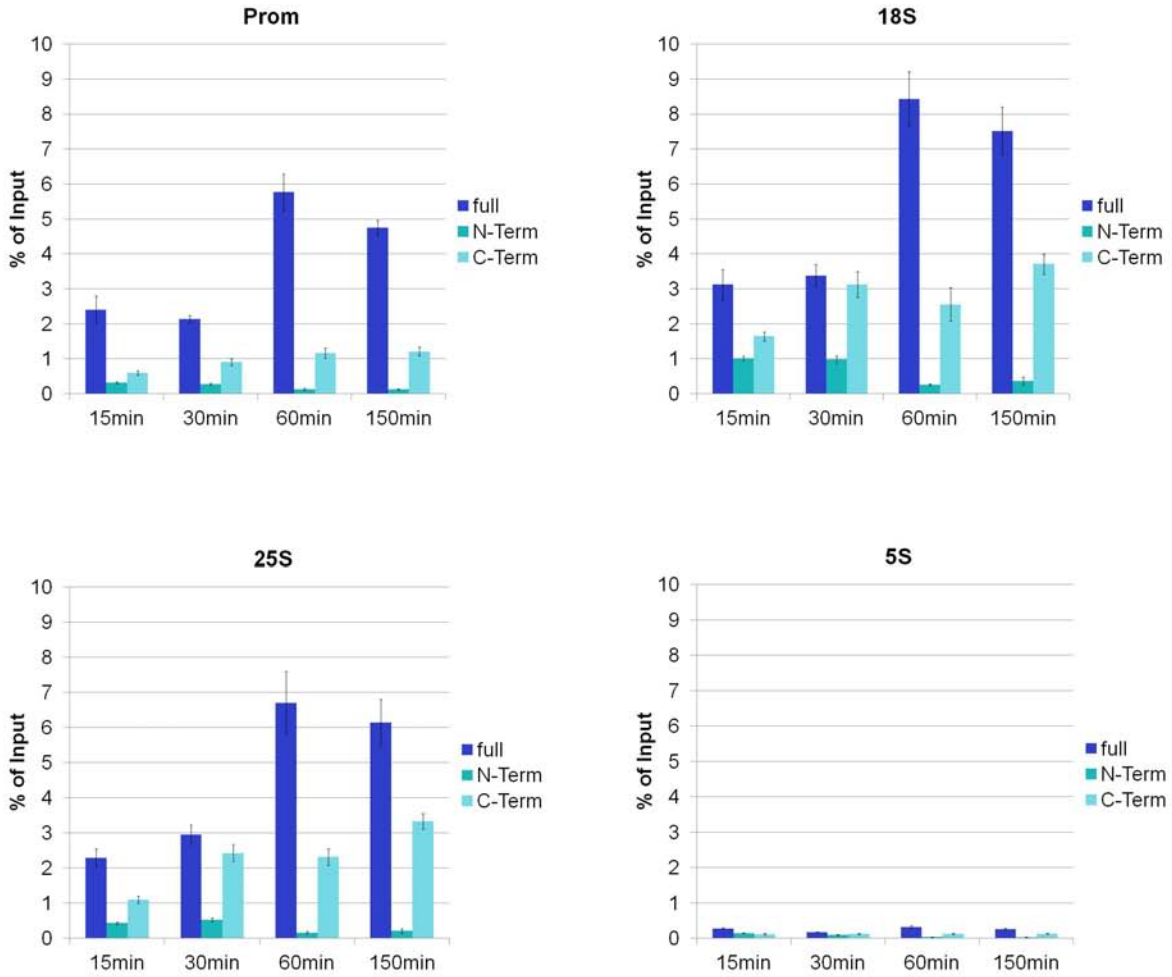

Figure 62: Rpa135-ProtA ChiP experiments upon exit from post diauxic shift phase in the presence and after depletion of Rpa49 in strains expressing full length, C-Terminus, or N-Terminus of Rpa49

Yeast strains y3534 *(rpa49*↓, "full"), y3538 (*rpa49*↓, N-Term), and y3542 (*rpa49*↓, C-Term*)* were cultured in YPD medium according to Figure 22 and Figure 57 (see OD Figure 30 in the appendix for culture ODs). ChIP was performed according to Figure 27 with IgG sepharose. The graphs depict the percentage of the input of the respective DNA fragment (indicated at the top of each diagram) co-precipitating with the ProtA-tagged fusion protein at the indicated growth phases. Error bars indicate standard deviation errors derived from three independent ChIP experiments, each analyzed in triplicate qPCRs. The respective qPCR amplicons are depicted in Figure 28. The 5S qPCR amplicon serves as a background control for Rpa135-ProtA co-precipitated DNA.

The expression of full-length Rpa49 led to a strong increase in the amount of co-precipitated DNA already 60min after the transfer to fresh medium (Figure 62 "full"). Interestingly, the highest amount of co-precipitated DNA was observed for the 18S amplicon and not as shown for the *RPA49* strain for the promoter amplicon (Figure 58). Expression of the C-terminus of Rpa49 led to an increase in the co-precipitated DNA

amount upon exit from post diauxic sift phase (Figure 62 "C-Term"). However, the maximum level of co-precipitated DNA was still significantly lower than upon expression of the full-length protein. In contrast, expression of the N-terminus of Rpa49 even led to a slight reduction of co-precipitated DNA for samples taken at the later time points after exit from post diauxic shift phase. (Figure 62 "N-Term").

Taken together, expressing the C-terminus of Rpa49 upon Rpa49 depletion led to 35S rRNA gene chromatin dynamics upon exit from post diauxic shift phase similar to those observed for *RPA49* strains. However, the C-terminus did not fully rescue the decrease in Pol I association levels observed upon Rpa49 depletion, which is different to results obtained in a previous study (Beckouet et al., 2008). The N-terminus of Rpa49 did not rescue 35S rRNA gene chromatin dynamics or Pol I association levels upon Rpa49 depletion. However, the finding that expression of the Rpa49 C-terminal domain alone did not fully restore Pol I recruitment to 35S rDNA as observed in an *RPA49* strain, could indicate that the N-terminus might play a role in increasing a high polymerase loading rate. This might be due to the fact that the Rpa49 N-terminus is important for the interaction with Rpa34 and that the formation of the Rpa49/34 heterodimer in turn is important for efficient interaction with the Pol I enzyme (Beckouet et al., 2008, Geiger et al 2010). However, it has to be mentioned that western blot analysis of the expression of either the full-length, the C-terminus, or the N-terminus only gave a signal for the full-length and C-terminus expression (Supplemental Figure 8 in the appendix). This could either be due to a loss of the small N-terminus during blotting or due to a insufficient expression. The latter potentially obscured the results. Thus, it has first to be clarified if the N-terminus is really expressed. Therefore the effect of the expression of the N-terminus is not further discussed in this thesis.

III Discussion

In this PhD thesis chromatin dynamics upon transition to and exit from stationary phase were investigated. The aim was to elucidate, which factors are involved in the establishment and maintenance of the observed chromatin states.

III.1 rDNA chromatin composition changes with transition to stationary phase are partly dependent on Rpd3

III.1.1 35S rRNA gene chromatin state transition accompanies a potentially multileveled downregulation of Pol I transcription

Transition to stationary phase led to an almost complete closing of 35S rRNA gene copies in WT cells as observed here, as well as in various other studies (Babl, 2012; Dammann et al., 1993; Fahy et al., 2005; Sandmeier et al., 2002) (in this work see e.g. Figure 19 "WT", Figure 56 "*NET1RPD3*"). The comprehensive analysis revealed that this chromatin state transition was accompanied by several changes in chromatin composition.

Since transition to the closed 35S rDNA chromatin state should correlate with nucleosome deposition, changes in the association of histone H3 with the rDNA were analyzed (Figure 31). As expected, more copies adopted the closed chromatin state, but strikingly H3 association with the closed chromatin state –as measured by efficiency of ChEC- was diminished (Figure 31 B and C). This is contradictory to studies where histone association with the 35S rDNA increased with transition to stationary phase (Johnson et al., 2013), but is probably explainable by the use of different methods. While Johnson et al. (2013) used ChIP with untagged histones, in the present study ChEC was used for detection of changes in association levels of H3. A substantial amount of closed copies resisted Hht1-MNase mediated cleavage in stationary phase (Figure 31 C "stat"). On a nucleosomal array nucleases such as MNase digest mainly the linker DNA between nucleosomes (Hewish and Burgoyne, 1973). The putative linker histone Hho1 was shown to be involved in higher order chromatin compaction and protection against MNase digestion in stationary phase (Schäfer et al., 2008). Thus, the Hht1-MNase resistant fraction of closed copies might potentially be associated with Hho1 and

therefore protected from Hht1-MNase digestion. A deletion of *HHO1* in the Hht1-MNase expressing strain could test this hypothesis. Since Hht1 is additionally tagged with a 3xHA tag, ChIP experiments could be used alternatively to ChEC and could reveal further insights in this hypothesis. In support to this hypothesis is the finding that Hho1 was only slightly associated with open 35S rDNA copies in exponential phase, but significantly associated with closed copies upon transition to stationary phase (Figure 32). This is in accordance with earlier data and supports the suggestion that Hho1 plays a role in the compaction of rDNA chromatin with transition to stationary phase and might stimulate Pol I transcription in exponential phase (Babl, 2012; Freidkin and Katcoff, 2001; Levy et al., 2008; Schäfer et al., 2008). However, Hho1 was not required for the closing of copies upon transition to stationary phase (Babl, 2012; data not shown). Interestingly, Hmo1, the potential partial homolog of UBF in higher eukaryotes, was recently suggested to function as a linker histone together with Hho1 (Panday and Grove, 2016). Nevertheless, in this study the proposed function of Hmo1 as a linker histone was partly based on the similarity of the C-terminal, lysine rich domain of Hmo1 to the C-terminus of Hho1. But this domain is also important for the nuclear import of Hmo1 (Albert et al., 2013) and thus deletion of this domain probably leads to phenotypes similar to complete *HMO1* deletion. However, from the results presented in this thesis Hmo1 and Hho1 behave almost mutually exclusive in their binding to 35S rDNA. Interestingly, for UBF and H1 in higher eukaryotes it was proposed that association of one of both proteins is excluding the association of the other (Kermekchiev et al., 1997; Kuhn and Grummt, 1992; Sanij et al., 2008). This could suggest important roles for Hmo1 and Hho1 in the maintenance of the open or the closed chromatin state respectively. However, in yeast Hho1 was not necessary for the closing of copies upon transition to stationary phase (Babl, 2012; data not shown). Overall, Hho1 seems to be dispensable in yeast, since its deletion does not lead to a specific phenotype or growth defect (Patterton et al., 1998). Hho1 is a repressor of rDNA recombination, thus suggesting a possible role in maintenance of genome integrity, but *hho1*Δ cells exhibit only a slight ageing phenotype and do not show increased levels of ERCs such as *sir2*Δ cells (Downs et al., 2003; Li et al., 2008). Thus the specific function of Hho1 association with the 35S rDNA remains unclear.

In contrast to Hho1, association of Hmo1 – a component of the open chromatin state (Babl, 2012; Merz et al., 2008; Wittner et al., 2011) - with the rDNA decreased upon transition to stationary phase. Unexpectedly, a significant population of rRNA genes was still bound by the protein (Figure 30 A and B). Interestingly, in the Hmo1-MNase expressing strain a substantially higher amount of open copies was found in stationary

phase samples when compared to strains where Hmo1 is expressed without a tag (see e.g. Figure 29 C or Figure 33 C). Thus, the expression of C-terminally tagged Hmo1 might stabilize interaction of Hmo1 with its binding sites and thus the open chromatin state. Accordingly, Hmo1 preferentially interacted with open, nucleosome depleted 35S rRNA gene copies in both, exponentially growing, and in stationary phase cells (Figure 30 C). In good correlation with a decrease in the number of open 35S rDNA copies Hmo1 association dropped upon transition to stationary phase (Figure 30 B). These findings are in accordance to other studies (Babl, 2012; Johnson et al., 2013), but contradict a more recent study in which Hmo1 was highly enriched at the 35S rRNA genes in stationary phase (Wang et al., 2016). However, in the latter study, Hmo1 association with the rDNA during exponential growth, which appears to be fairly established (Berger et al., 2007; Goetze et al., 2010; Hall et al., 2006; Kasahara et al., 2007; Merz et al., 2008; Wittner et al., 2011), was if at all only barely detectable. During the master thesis, which built the basis of the present work, it was already observed that Hmo1-MNase persisted at the rDNA upon exit from exponential phase. This had led to the hypothesis, that Hmo1 might prime rRNA gene copies for transcription when more favorable growth conditions are present (Babl, 2012). However, it was found here, that the deletion of *HMO1* did not significantly affect Pol I transcription re-initiation upon exit from stationary phase (Supplemental Figure 9 in the appendix). Thus, these experiments did not provide evidence that Hmo1-bound 35S rDNA provides an optimized template for Pol I transcription. This is additionally supported by the finding that Hmo1 is not required for Pol I transcription, whereas Pol I transcription is required for Hmo1 deposition on open rDNA copies (Goetze et al., 2010; Kasahara et al., 2007; Wittner et al., 2011). Since association of Hmo1 and association of histones seem to be mutually exclusive at various genomic loci in yeast (Bermejo et al., 2009; Merz et al., 2008), Hmo1 could potentially function in a DNA protective manner on open rDNA copies in stationary phase similar to Hho1 on closed rDNA copies (Panday and Grove, 2016; Schäfer et al., 2008). All aspects considered, Hmo1 association with the rDNA decreases potentially as a consequence to an overall reduction of Pol I transcription concomitant with residual replication events or spontaneous dissociation of Hmo1 and subsequent replication independent nucleosome deposition. However, it cannot be excluded that Hmo1 might have additional functions at the rDNA regulating overall nucleolar morphology even in stationary phase (Wang et al., 2016).

Pol I association with the rDNA drastically decreased upon exit from exponential growth phase and further decreased during the diauxic shift and the post-diauxic growth phase to no detectable association in stationary phase (Babl, 2012; Claypool et al., 2004; Fahy

et al., 2005; Sandmeier et al., 2002) (this work Figure 29, Figure 43 "RPD3", and Supplemental Figure 9 "WT", "log" "stat"). This decrease in Pol I association correlates with a transition from the open to the closed 35S rDNA chromatin state. However, as already discussed in the introduction (see section I.2.4.1.1), the reduction in the amount of open copies might not always correlate with the reduction in Pol I association (Fahy et al., 2005). The observed down-regulation of Pol I transcription has been mainly attributed to impaired Tor signaling upon growth to stationary phase, when nutrients get limiting (Claypool et al., 2004; Milkereit and Tschochner, 1998; Zaragoza et al., 1998). Earlier studies correlated this observation with a decrease in the initiation-competent form of Pol I in complex with Rrn3 in stationary phase or upon inhibition of the Tor pathway by rapamycin (Claypool et al., 2004; Milkereit and Tschochner, 1998; Philippi et al., 2010; Reiter et al., 2011). Accordingly, it was confirmed here that Rrn3 association drastically decreased already at the diauxic shift and was at a near background level in stationary phase (Figure 53 "*RPD3*"). Rrn3 is conserved from yeast to human with TIF-IA as its mammalian homolog (Bodem et al., 2000; Moorefield et al., 2000). Interestingly, TIF-IA was shown to be differentially phosphorylated in response to adaptation to changes in cellular nutrient or energy levels, or general stress signals (Hoppe et al., 2009; Mayer et al., 2004, 2005; Zhao et al., 2003). For yeast Rrn3, however, there was so far no direct evidence for regulatory phosphorylation sites. Nevertheless, it was shown that a phospho-mimetic mutation of a serine patch conserved and phosphorylated in TIF-IA, prevents Rrn3 binding to Pol I *in vitro* and reduces cell growth and Pol I gene occupancy *in vivo* (Blattner et al., 2011).

Besides Rrn3 at least three other factors, UAF, TBP and CF, are involved in the formation of the Pol I pre-initiation complex (see section I.2.4.1.4) and are thus potential targets for regulation upon transition to stationary phase. In the present study, the UAF-component Rrn9 was shown to stay associated with its binding site from exponential to stationary phase (Figure 33 and Figure 48 "*RPD3*"). This is in accordance to data presented by Claypool et al. (2004). UAF shows some functional similarities to mammalian UBF, such as influencing the promoter architecture or initiation of Pol I transcription (Bazett-Jones et al., 1994; Hontz et al., 2008; Leblanc et al., 1993; Merz et al., 2008; Sanij et al., 2008) (discussed in (Hamperl et al. (2013)). UBF is a target of Pol I transcription regulation. It was shown to be regulated by phosphorylation in dependence of growth factors (Stefanovsky et al., 2006a, 2006b) or during the cell cycle (Voit and Grummt, 2001) and its association with the rDNA decreases during differentiation processes (Sanij et al., 2008). Additionally, UBF has been proposed to be acetylated thus stimulating Pol I transcription (Pelletier et al., 2000). In yeast, however, no pathways

have so far been described that regulate UAF association in dependence of the cell cycle state or growth phase. The present results support a model in which UAF association with the 35S rDNA promoter is no target for Pol I transcription shutdown upon transition to stationary phase. Interestingly, in this thesis it was shown that the yeast TBP, Spt15, stays associated with the 35S rDNA promoter in stationary phase similar to UAF (Figure 34 and Figure 50 "*RPD3*"). On the other hand Spt15 association with the 5S promoter and with the promoter of the Pol II transcribed ribosomal protein gene *RPS23A* decreased with transition to stationary phase (Figure 50 "*RPD3*"), thus indicating a differential regulation for Pol I, II, and III PIC formation under these conditions. Our finding that TBP behaves similar to UAF is consistent with an earlier study pointing to a robust interaction between TBP and UAF (Steffan et al., 1996). In contrast to UAF and TBP the association of the CF subunit Rrn7 with the core element drastically decreased upon transition to stationary phase similar to Rrn3 (Figure 35 and Figure 52 "*RPD3*"). This indicates that CF is a possible target for regulation of Pol I initiation or that CF association is dependent on Pol I transcription as suggested by the Reeder lab (Aprikian et al., 2001). However, the latter possibility is unlikely due to the finding that CF is present at the 35S rDNA promoter even in the absence of Pol I transcription (Goetze et al., 2010). The mammalian homolog to CF is selectivity factor 1 (SL1). Interestingly it has been suggested to be an important target for regulation during cell differentiation (Comai et al., 2000) and mitosis (Heix et al., 1998) and its acetylation stimulated Pol I transcription *in vitro* (Muth et al., 2001). Along these lines, we found that Tor pathway inhibition by rapamycin treatment did not lead to a decrease of CF association with the rDNA promoter (Supplemental Figure 1 "*RPD3*") (Philippi et al., 2010). This suggested that CF regulation could be derived by a different pathway and independently of Rrn3 regulation.

Another factor that was investigated and showed a decrease in association with transition to stationary phase was Net1 (Figure 36 and Figure 55 "*RPD3*"). Net1 was suggested to stimulate Pol I transcription (Shou et al., 2001) and recently its C-terminal domain has been linked to this property (Hannig, 2015). Thus, Net1 might play also a role in the downregulation of Pol I transcription upon transition to stationary phase.

The comprehensive analysis of the chromatin composition upon growth to stationary phase thus confirmed that the downregulation of Pol I transcription is to a large extent due to an inactivation of the Tor pathway and regulated via Rrn3 (Claypool et al., 2004; Milkereit and Tschochner, 1998). Additionally, CF and Net1 were identified as potential targets of regulation upon transition to stationary phase. Interestingly, inhibition of the Tor

pathway by rapamycin did not regulate CF interaction with the 35S rDNA promoter and does not lead to a complete shutdown of Pol I transcription (Philippi et al., 2010; Reiter et al., 2011). Thus it is possible that a second regulation step involving CF and Net1 is needed upon transition to stationary phase for complete shutdown of Pol I transcription and closing of copies. A model in which closing of copies and downregulation of Pol I transcription are independently regulated was suggested by the Nomura lab, proposing a role for the deacetylase Rpd3 (Oakes et al., 2006).

III.1.2 The deacetylase Rpd3 might prevent residual Pol I transcription independently of Tor inhibition

In *rpd3Δ* cells 35S rRNA genes are kept in an open chromatin state, despite of the Tor-dependent downregulation of Pol I transcription (Babl, 2012; Johnson et al., 2013; Oakes et al., 2006; Sandmeier et al., 2002). Two main pathways for the action of Rpd3 on the rDNA can be imagined. First, Rpd3 might be directly involved in the closing of copies by acting on histones potentially as a histone chaperone (Chen et al., 2012; Johnson et al., 2013). Second, deletion of *RPD3* might lead to a dysregulation in a process that establishes and maintains open copies. A factor maintaining open 35S rRNA gene copies even in the absence of high Pol I transcription rates -as it is the case in stationary phase- is Hmo1 (Wittner et al., 2011). We could show that Hmo1 is associated with all open copies in exponential and stationary phase in an *rpd3*Δ strain (Figure 44) (Babl, 2012), thus being a likely candidate for the maintenance of open copies in this genetic background. However, Hmo1 became an unlikely candidate for an Rpd3 dependent regulation, since its deletion did not suppress the *rpd3*Δ phenotype (Babl, 2012) (Figure 41). Additionally, we found that the absence of Rpd3 does not only lead to a persistence of open copies in stationary phase, but the fraction of open copies even increased under these conditions (see e.g. Figure 19 "*rpd3Δ"* and Figure 56 "*rpd3*Δ"). Thus, a pathway in which *RPD3* deletion leads to a dysregulation of a factor or process establishing the open copies became more likely. The only known process that establishes open 35S rRNA gene chromatin to date is Pol I transcription (Wittner et al., 2011). Using a strain where Pol I initiation can be conditionally shut down (*rrn3ts*) this hypothesis could be confirmed. The shutdown of Pol I transcription initiation led to a suppression of the *rpd3*Δ phenotype and this effect was even stronger when *HMO1* was additionally deleted (Figure 39 and Figure 41). This suggested additionally a role for Hmo1 in maintenance of open 35S rRNA gene copies in the absence of Pol I transcription as it was already shown during G1 arrest (Wittner et al., 2011). Thus, deletion of *RPD3* seems to lead to a slightly increased amount of Pol I transcription in stationary phase (Figure 42 and Figure

43), which is sufficient to keep the 35S rDNA copies in the open state. It is reasonable to assume that this is supported by the absence of replication in stationary cells, which acts as the main process in closing of 35S rDNA copies (Lucchini and Sogo, 1995; Wittner et al., 2011).

Since the Pol I PIC formation was partly affected by the transition to stationary phase in *RPD3* cells (see previous section), it was hypothesized that Rpd3 might be involved in the regulation of this complex, thus leading to a complete reduction of Pol I transcription in stationary phase. As in *RPD3* cells, UAF and TBP were still associated with their binding sites in *rpd3*Δ cells in stationary phase (Figure 47, Figure 48 "*rpd3*Δ*"*, Figure 49, and Figure 50 "*rpd3*Δ*"*). However, in *rpd3*Δ strains these factors were preferentially associated with open copies (Figure 47 C and Figure 49 C), whereas they associated with closed 35S rRNA genes in *RPD3* cells. Therefore UAF and TBP might prime copies for transcription upon exit from stationary phase.

Different than in *RPD3* strains, CF association persisted in *rpd3*Δ strains also in stationary phase (Figure 51 and Figure 52 "*rpd3*Δ*"*). The association of CF with the core promoter was also independent of the Tor pathway in *rpd3*Δ cells (Supplemental Figure 1 "*rpd3*Δ*"* in the appendix). Additionally, Net1 association only slightly decreased in this genetic background (Figure 54 and Figure 55 "*rpd3*Δ*"*). The truncation of the C-terminal (MDM) domain - which was suggested to be important for the Pol I stimulation by Net1 (Hannig, 2015) - compromised the *rpd3*Δ phenotype (Figure 56). Thus, CF and Net1 are potentially both in one pathway which is regulated by Rpd3. However, so far it is not clear if CF or Net1 is a direct target of Rpd3 or rather which of these factors is the upstream and which the downstream partner. Since Net1 was suggested to stimulate Pol I transcription via Rrn3 (Hannig, 2015; Shou et al., 2001) and the docking of the initiation competent Pol I-Rrn3 complex is downstream of core factor association with the core promoter (see section I.2.4.1.4) it can be hypothesized that CF is upstream to Net1, or alternatively that both factors act cooperatively to recruit Pol I via Rrn3 to the promoter.

So far we were not able to clarify if CF or Net1 are direct targets of Rpd3. Along these lines, to date the only potential modification of CF was a phosphorylation of Rrn11 (Holt et al., 2009). CF is also active in *in vitro* assays when purified from E.coli, suggesting that covalent modifications of CF are not necessary for efficient transcription (Bedwell et al., 2012). However, for the mammalian CF homolog SL1 acetylation stimulating Pol I transcription *in vitro* has been described (Muth et al., 2001). Recently it was suggested that CF is related to the Pol II transcription factor TFIIB (Knutson and Hahn, 2011) and for human TFIIB an autoacetylation function has been shown (Choi et al., 2003). For the

Pol III initiation machinery it has been shown, that TFIIIC together with the acetyltransferase GCN5 and the cofactor TRRAP are recruited to the 5S rRNA genes in dependency of c-Myc and this is accompanied by a rapid TFIIIB recruitment and histone H3 acetylation ultimately leading to Pol III transcription initiation (Kenneth et al., 2007). Net1 has been shown to be phosphorylated at multiple serine residues (Azzam et al., 2004; Holt et al., 2009; Huber et al., 2009; Swaney et al., 2013), some of which are located in the C-terminal domain required for the stimulation of Pol I transcription initiation. Interestingly, if the truncated C-terminal domain of Net1 is expressed and isolated from yeast it migrates with a slower mobility in SDS PAGE than expected from its molecular weight (Hannig, 2015). Since phosphatase treatment still did not result in an electrophoretic mobility expected for this domain (Hannig, 2015), this could point to further modifications. Thus, although experimental evidence is lacking it cannot be excluded that CF and Net1 are modified by acetylation. In the future it should be tested via 2D polyacrylamide gel electrophoresis and western blot or via mass spectrometry if CF and/or Net1 are modified in dependence of Rpd3.

In the course of this thesis it was already tested if interference with the enzymatic activity of Rpd3 could phenocopy the *rpd3*Δ phenotype. First, the common deacetylase inhibitor trichostatin A (TSA) (Grunstein, 1990; Yoshida et al., 1995) was used and the effect on the rDNA chromatin state was monitored by psoralen photocrosslinking (Supplemental Figure 4 in the appendix). Unexpectedly, only a very mild opening of copies was observed upon prolonged times of TSA treatment. However, this could be explained by the finding that TSA shows only 20% inhibition of members of the HDAC class to which Rpd3 belongs (Carmen et al., 1996). Second, the rDNA chromatin state with transition to stationary phase in strains where the putative deacetylase motif of Rpd3 was mutated by single amino acid substitutions was investigated (Kadosh and Struhl, 1998). Also here, the effect of the single mutations monitored with psoralen photocrosslinking was only very mild and not significant (Supplemental Figure 5 in the appendix). One might argue that the single substitutions are not sufficient for inhibition of Rpd3 deacetylase activity, but Chen et al. (2012) showed that already one single substitution leads to increased histone acetylation levels *in vivo*. Thus, apart of its deacetylase activity Rpd3 might potentially also function as nucleosome stabilizer at the rDNA as it was suggested by Johnson et al., (2013). However, deletion of the gene coding for one of the major acetyltransferases in yeast Gcn5 (Brownell et al., 1996; Grant et al., 1997) and thus an antagonist of Rpd3 slightly compromised the *rpd3*Δ phenotype (Supplemental Figure 3 "*gcn5*Δ*rpd3*Δ" in the appendix). The *rpd3*Δ phenotype was so far not found in other

deacetylase mutants, as for example the *SIR2* deacetylase (Sandmeier et al., 2002). Here we could additionally show that deletion of the *HDA1* deacetylase gene (Carmen et al., 1996; Rundlett et al., 1996) has no detectable effect on the rDNA chromatin state upon transition to stationary phase (Supplemental Figure 3 "*hda1*Δ*"* in the appendix). As further evidence for specificity, we found that deletion of the Rpd3S and Rpd3L specific subunit Sin3 led to the *rpd3*Δ phenotype (Supplemental Figure 3 "*sin3*Δ" in the appendix). Therefore, the third Rpd3 complex (Rpd3µ) (Baker et al., 2013) is probably not involved in the establishment of the *rpd3*Δ phenotype. For Pol II genes it was already shown that the Rpd3S complex is recruited by elongating Pol II to sites of Set2 derived H3K36 methylation (Carrozza et al., 2005; Govind et al., 2010; Joshi and Struhl, 2005; Keogh et al., 2005; Li et al., 2007). To test if this Set2-Rpd3S pathway is also involved in the chromatin transitions upon stationary phase at the rDNA, we deleted *SET2.* However, *set2*Δ cells were able to close 35S rRNA gene copies upon transition to stationary phase as long as Rpd3 was present (Supplemental Figure 3 "*set2*Δ" and "*set2*Δ*rpd3*Δ" in the appendix). Thus, the effect of Rpd3 on rDNA chromatin is probably not mediated via Set2 derived methylation, and as a consequence via the Rpd3S complex. Altogether, this is in good agreement with earlier results suggesting that Rpd3L might be the complex targeting the rDNA (Johnson, 2013).

Recently, it was suggested that Rpd3 is required for yeast cells to enter quiescence and stay viable over prolonged times in this state (McKnight et al., 2015). In this study they also showed that Hda1 is not involved in the quiescence entry program and that both Rpd3 complexes (S and L) have non-overlapping functions in transition to quiescence. They suggested that a global promoter specific deacetylation by Rpd3L is required for the entry into quiescence, but Rpd3S is additionally important for quiescence maintenance. However, Sandmeier et al., (2002) did not find a changed acetylation pattern at the rDNA in *rpd3*Δ cells, but the same group later suggested that Rpd3 functions in nucleosome assembly at the rDNA (Johnson et al., 2013). Therefore, it is also possible, that deletion of *RPD3* leads to a changed chromatin environment at the rDNA promoter which alleviates access for CF and Net1. Here the UAF components histone H3 and H4 could act as potential targets, that are deacetylated by Rpd3. Interestingly, McKnight et al., (2015) also suggested that Rpd3 is most important for global chromatin and transcription reprogramming after the diauxic shift. This is in accordance to our finding, that the *rpd3*Δ phenotype is enhanced when cells were grown on non-fermentable carbon sources (Supplemental Figure 2 "non fermentable" in the appendix).

Taken together, we could show that Rpd3 is involved in the closing of copies upon transition to stationary phase in a CF and Net1 influencing manner, but probably independent of the Tor pathway as suggested by Oakes et al. (2006). This mechanism might be especially important after the diauxic shift for the entry into quiescence.

III.2 The Pol I subunit A49 is potentially important for proper re-initiation of Pol I transcription and fast adaptation of the chromatin state upon exit from stationary phase

Yeast is able to exit from stationary phase (Zaman et al., 2008) which is accompanied by a drastic increase in Pol I transcription in correlation with an opening of 35S rRNA gene copies (Fahy et al., 2005). Thus, this situation is ideal to study Pol I transcription through a nucleosomal template *in vivo*. Therefore, it was used to test if Pol I transcription mediated opening of chromatin was dependent on the Rpa49 subunit, which was suggested to be important for transcription of nucleosomal templates *in vitro* (Merkl, 2013).

The chromatin state transition from closed to open was only slightly impaired in the absence of Rpa49 upon exit from post-diauxic shift phase (Figure 57), whereas Pol I occupancy at the rDNA was drastically reduced under these conditions (Figure 58). The latter finding is in full accordance with the suggested role of Rpa49 in high polymerase loading rate (Albert et al., 2011; Beckouet et al., 2008; Liljelund et al., 1992), but did provide only little evidence for a strong function of Rpa49 in 35S rDNA chromatin opening. In the *in vivo* experiments it could, however, not be excluded that Rpa49 depletion was not complete and thus, the observed opening of copies might have been mediated by residual WT Pol I molecules. On the other hand, 35S rRNA gene copies can be opened even in the complete absence of Rpa49 (O. Gadal, personal communication). In any case, these data support the finding that open copies can be established and maintained even with a low Pol I loading rate as it is also observed in stationary phase when *RPD3* is deleted (Babl, 2012; Sandmeier et al., 2002; this study).

It was also tested, if the reduced Pol I loading rate upon Rpa49 depletion is due to a reduced ability of the enzyme to transcribe through nucleosomes. Thus, we additionally deleted *RPD3* and monitored the chromatin state transitions and Pol I loading rate upon exit from post-diauxic phase. The deletion of *RPD3* led to the persistence of open copies after exit from exponential phase, even if Rpa49 was depleted and the open copies were

further maintained upon re-entry to exponential phase (Figure 59). This finding is interesting, since it shows that not every defect in Pol I initiation or loading leads to a prevention of the establishment of the *rpd3*Δ phenotype as it was observed for the *net1trunc* strain (Figure 56). However, the low association of Pol I with the 35S rRNA gene in the absence of Rpa49 was not suppressed by deletion of *RPD3* resulting in an open chromatin state (Figure 60). Although it was shown that *RPD3* and *RPA49* are synthetically lethal (Lin et al., 2008), Rpa49 depleted *rpd3*Δ cells were viable and even started to divide after exit from post-diauxic phase (OD Figure 27 and OD Figure 28 in the appendix). This might confirm the hypothesis that Rpa49 depletion was not complete and the establishment of the *rpd3*Δ phenotype might then be due to residual intact Pol I molecules. In the future it should be tested, if we are able to confirm the described synthetic lethality.

Different functions have been assigned to the C- and the N-terminal domain of Rpa49. The N-terminal domain is important for dimerization of Rpa49 with Rpa34, and for the intrinsic RNA cleavage activity of Pol I. The C-terminal domain is important for a high polymerase occupancy, Pol I initiation, and processivity (Albert et al., 2011; Beckouet et al., 2008; Geiger et al., 2010; Huet et al., 1975). Here we could show, that expression of the C-terminal domain of Rpa49 completely suppresses the delayed 35S rDNA chromatin opening of an Rpa49 depletion strain (Figure 61 "*rpa49*↓*+C-Term*") and in large parts restored Pol I occupancy within 35S rRNA genes (Figure 62). In the future, it could be tested, if the co-expression of the N-terminal and the C-terminal domain leads to complete restoration of WT Pol I association levels with the 35S rDNA.

Taken together, Rpa49 - and especially its C-terminal domain – is likely important for high Pol I loading rates and rapid establishment of the open chromatin state upon exit from post-diauxic or stationary phase.

III.3 Conclusion

Taken together the following model could explain the chromatin state transitions in dependence of Rpd3.

In exponential phase an equilibrium of opening by high rates of Pol I transcription and of closing by replication leads to the observed balanced ratio of open and closed 35S rRNA gene copies (Lucchini and Sogo, 1995; Wittner et al., 2011). Upon transition to stationary phase first, Tor pathway inactivation at the diauxic shift leads to a drastic decrease of initiation competent Pol I-Rrn3 complexes and thus a reduced Pol I transcription rate,

while Hmo1 stays - at least in parts - associated. Second, an Rpd3 dependent downregulation of CF and Net1 association with the promoter region leads to complete shutdown of Pol I initiation and transcription when nutrients become more and more limiting. Hmo1 might be evicted by last replication steps, or might dissociate from the rDNA, allowing replication independent nucleosome deposition (RIND), which then eventually leads to closing of copies. When the cells encounter more favorable growth conditions and exit from stationary phase, Tor pathway becomes again active leading to strong (Rpa49-dependent) Pol I transcription initiation correlating with fast nucleosome eviction, Hmo1 association and the re-establishment of the exponential phase equilibrium of chromatin dynamics.

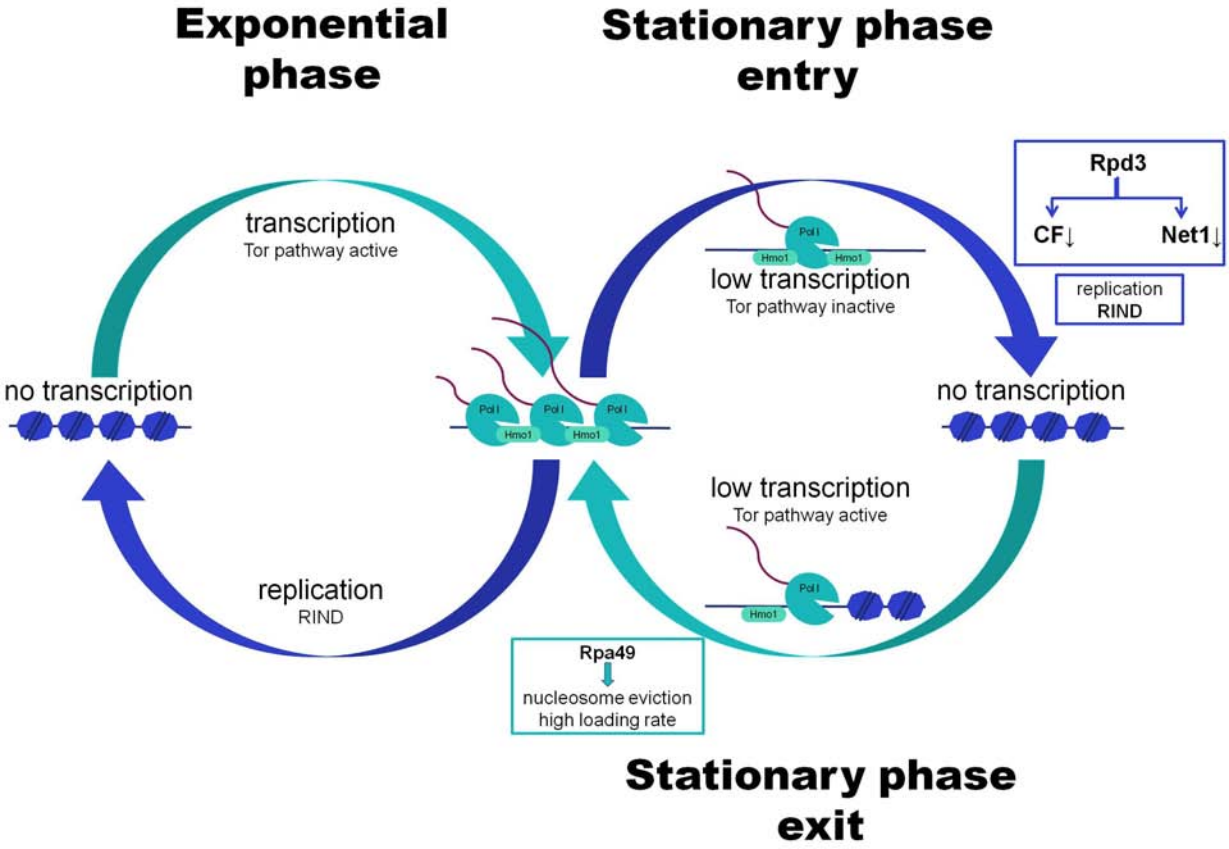

Figure 63: Model for chromatin state transitions in exponential phase and upon entry to and exit from stationary phase

Processes and factors that lead to closing of copies are colored in dark blue, while processes that lead to opening of copies are colored turquoise. During exponential phase an equilibrium between opening by Pol I transcription and closing by replication leads to the observed ratio between open (nucleosome depleted, decorated with Pol I and Hmo1) and closed (nucleosomal, non-transcribed, no association of Hmo1) 35S rDNA copies. Upon transition to stationary phase the Tor pathway is inactivated which results in a low rate of transcription, but still the existence of open copies. In an Rpd3 dependent pathway CF and/or Net1 are then downregulated and transcription is completely shutdown. Last replication steps and replication independent nucleosome deposition (RIND) leads then to closing of copies. Upon exit from stationary phase, nucleosomes are evicted and high Pol I loading rates are only achieved in dependence of Rpa49. (modified and expanded from Wittner et al. (2011))

IV Material and Methods

The material and methods section was adapted according to Babl (2012).

IV.1 Material

IV.1.1 Chemicals

All chemicals and solvents used in this work were purchased at the highest available purity from Sigma-Aldrich, Merck, Fluka, Roth or J.T.Baker, except agarose electrophoresis grade (Invitrogen), Trichostatin A (NEB), bromine phenol blue (Serva), G418/Geneticin (Gibco), milk powder (Sukofin), Nonidet P-40 substitute (NP40) (USB Corporation), Tris ultrapure (USB Corporation) and Tween 20 (Serva). Ingredients for growth media were purchased from BD Biosciences (Bacto Agar, Bacto Peptone, Bacto Tryptone and Bacto Yeast Extract), Sunrise Science Products (Yeast nitrogen base (YNB), amino acids and adenine), Sigma-Aldrich (D(+)-glucose, galactose, amino acids and uracil) and Chemos GmbH (D(+)-raffinose). Water was always purified with an Elga Purelab Ultra device prior to use.

IV.1.2 Media and buffers

Unless stated otherwise, all solutions have been prepared in water that has a resistivity of 18.2 MΩ-cm and total organic content of less than five parts per billion. The pH values were measured at room temperature. Percentage is mass per volume (m/v) and pH was adjusted with HCl or NaOH if not indicated otherwise.

IV.1.2.1 Media

Table 1: Media used during this study

media	ingredients	concentration
LB	tryptone yeast extract NaCl 1M NaOH agar (plates)	1% (w/v) 0.5% (w/v) 0.5% (w/v) 1mM 2% (w/v)
LB + Amp	ampicillin in LB medium	100µg/ml
YPD	yeast extract peptone glucose agar (plates)	1% (w/v) 2% (w/v) 2% (w/v) 2% (w/v)
YPD + Gen	geniticin (G418) in YPD	400 µg/ml

YPAD	adenine in YPD	100mg/l
YPG	yeast extract peptone galactose agar (plates)	1%(w/v) 2%(w/v) 2%(w/v) 2%(w/v)
YPGE (non fermentable carbon source medium)	yeast extract peptone glycerol ethanol (after autoclaving) agar (plates)	1% (w/v) 2% (w/v) 3% (v/v) 3% (v/v) 2% (w/v)
SCD/G	YNB CSM Glucose/galactose L-histidine L-leucine L-tryptophan agar (plates)	0.67% (w/v) See product sheet 2% (w/v) 20 mg/l 100 mg/l 50 mg/l 2%(w/v)
SCD/G-Trp-Ura	YNB CSM -Arg -Leu - Trp -Ura Glucose/galactose L-leucine L-arginine agar (plates)	0.67% (w/v) 0.062% 2%(w/v) 100mg/l 20mg/l 2%(w/v)

IV.1.2.2 Buffers and solutions

Table 2: Buffers and solutions used in this study

buffer	ingredients	concentration
buffer A (ChEC)	Tris-HCl pH 7.4 Spermine Spermidine KCl EDTA EGTA Proteinase inhibitors (freshly added)	15mM 0.2mM 0.5mM 80mM 20mM 2mM 1x
buffer Ag (ChEC)	Buffer A without EDTA EGTA Proteinase inhibitors (freshly added)	 0.1mM 1x
buffer HU	SDS Tris pH6.8 EDTA β-mercaptoethanol urea bromophenolblue	5% 200mM 1mM 2.13mM 8M
ChIP lysis buffer	Hepes pH 7.5 NaCl EDTA Triton X 100 DOC SDS Proteinase inhibitors (freshly added)	50mM 150mM 1mM 1% (v/v) 0.1% (v/v) 0.1% (v/v) 1x
ChIP Wash 1	Hepes NaCL EDTA Triton-X 100 DOC	50mM 500mM 2mM 1% 2%
ChIP Wash 2	Tris pH 8.0 LiCl DOC Nonidet P40	10mM 250mM 0.5% 0.5%

	EDTA	2mM
denature solution	NaOH NaCl	0.5M 1.5M
10 x DNA loading buffer	Bromphenol blue Xylen cyanol Glycerine	0.25% 0.25% 40%
10x electrophoresis buffer (SDS-PAGE)	Tris glycine SDS	0.25 M 1.92 M 1% (w/v)
hybridization buffer	sodium phosphate buffer pH 7.2 SDS	0.5M 7%
IR buffer	Tris-HCl pH 8 EDTA	50mM 20mM
IRN buffer	NaCl In IR buffer	0.5M
LitPEG	LiOAc Tris-HCl pH 8 EDTA pH 8 Polyethylene glycol PEG3350 (Sigma)	100mM 10mM 1mM 40%
LitSORB	LiOAc Tris-HCl pH 8 EDTA pH 8 Sorbitol pH 8 with HOAc	100mM 10mM 1mM 1M
10xPBS	NaCl KCl $Na_2HPO_4 \cdot 2H_2O$ KH_2PO_4 pH 7.4 with HCl or NaOH	1.37M 27mM 10mM 20mM
PBST	PBS Tween20	1x 0.05%
Ponceau S	Ponceau in 1% acetic acid	0.5%
pretreatment solution	β-mercaptoethanol NaOH	1M 1.85M
100xProtease inhibitors	benzamidine PMSF solvent: ethanol store at -20°C	0.2 M 0.1 M
Proteinase K buffer	Tris pH 7.4 $CaCl_2$	20mM 1mM
Psoralen solution	4,5′,8-Trimethylpsoralen (Trioxsalen) solvent: ethanol	0.2 mg/mL
Rapamycin stock solution	rapamycin solvent: DMSO store at -20°C	1 mg/ml
Rinse buffer	SSC SDS	3x 0.1%
4x SDS sample buffer	Tris pH 6.8 glycerol SDS β-mercaptoethanol bromophenol blue	0.25 M 40% (v/v) 8.4% (w/v) 0.57 M

Sodium phosphate buffer	$Na_2HPO_4 \cdot H_2O$ (1 M) $NaH_2PO_4 \cdot 2 H_2O$ (1 M)	for 1 l 774 ml 226 ml
Southern blot transfer buffer	NH_4OAc	1M
20 x SSC	NaCl Tri-sodium citrate dehydrate pH7 with HCl	3M 0.3M
20xSSPE	NaCl Na_2HPO_4 EDTA	3M 200mM 20mM
stripping solution	SSPE SDS	0.1x 0.5%
TBE buffer	Tris Boric acid EDTA	90mM 90mM 1mM
TE	Tris-HCl pH 8 EDTA	10mM 1mM
transfer buffer (Western blot)	Tris glycine methanol pH8.3	25mM 190mM 20%
TELit	Tris pH 8.0 LiOAc EDTA pH 8.0	10 mM 100 mM 1 mM
Tris (Lower)	Tris SDS pH 8.8 with HCl	1.5 M 0.4% (w/v)
Tris (Upper)	Tris SDS bromophenol blue pH6.8 with HCl	0.5 M 0.4% (w/v)
Trichostatin A stock solution	TSA solvent: EtOH store at -20°C	4mM
wash1	SSC SDS	0.3x 0.1%
wash2	SSC SDS	0.1x 0.1%
wash3	SSC SDS	0.1x 1.5%
Zymolyase solution for yeast DNA preparation	TrisCl pH8 glucose zymolyase 20T	10mM 5% 2%

IV.1.3 Nucleic acids

IV.1.3.1 Nucleotides

For synthesis of DNA molecules the “desoxynucleotide solution mix” by New England Biolabs which contains each of the four desoxynucleotides in 10mM concentration or the dNTP mix by Agilent Technologies which contains each of the four desoxycnucleotides in 25mM concentration were used.

IV.1.3.2 Oligonucleotides

Table 3: Oligonucleotides used in this study. The numbers refer to the oligonucleotides database of the department Biochemistry III, University of Regensburg.

DB#	name	sequence	purpose	gene or locus
153	M13/pUC forward	GTAAAACGACGGCCAGT	colony PCR	
243	Rrn3-pYM-rev.	TAGTTTGTGACGGGCATGTCTCGAAG ATACCTATGAAAAAAGACCATCGATGA ATTCGAGCTCG	integration, PCR cloning	*RRN3*
593	qPCR_4-for	GGGCACCTGTCACTTTGGA	qPCR	*rDNA (UE)*
594	qPCR_4-rev	TTTGCCCTCTCTGTCGCTCT	qPCR	*rDNA (UE)*
678	URA	CACGGTGCAACACTCACTTC	colony PCR	*URA3_KL*
710	M1	TGGAGCAAAGAAATCACCGC	qPCR	*rDNA (25S)*
711	M2	CCGCTGGATTATGGCTGAAC	qPCR	*rDNA (25S)*
712	M3	GAGTCCTTGTGGCTCTTGGC	qPCR	*rDNA (18S)*
713	M4	AATACTGATGCCCCCGACC	qPCR	*rDNA (18S)*
817	rDNA-709_for	GAGGGACGGTTGAAAGTG	probe template PCR	*rDNA (promoter)*
818	rDNA-461_rev	ATACGCTTCAGAGACCCTAA	probe template PCR	*rDNA (promoter)*
920	5S ChIP-F1	GCCATATCTACCAGAAAGCACC	qPCR	*rDNA (5S)*
921	5S ChIP-R1	GATTGCAGCACCTGAGTTTCG	qPCR	*rDNA (5S)*
955	Hmo1_down	TACACTATGGGCAAAGCAAG	amplification of *HMO1* gene - control deletion	*HMO1*
969	Prom ChIP-F2	TCATGGAGTACAAGTGTGAGGA	qPCR	*rDNA (CE)*
970	Prom ChIP-R1	TAACGAACGACAAGCCTACTC	qPCR	*rDNA (CE)*
1156	S3-Rrn3-MNase	GATGGTACCTGGAGTGAAGCAAGCG GGGAATATGAAAGTGATGGGTCGGAT GACTCGTACGCTGCAGGTCGAC	integration, PCR cloning	*RRN3*
1157	S3-Rrn7-MNase	GATGGTACCGACTGCATTTCAAGGAT CAAAAATGCCTGTCTGCATAGGATGA ATTCGTACGCTGCAGGTCGAC	integration, PCR cloning	*RRN7*
1158	S2-Rrn7-MNase	CTACCGCGGAGTATGCATAGAAATAG CAATCCAGCGAGAATAATTTAAAAGG AGATCGATGAATTCGAGCTCG	integration, PCR cloning	*RRN7*
1163	Gal1+138-for	TGTTGCTAGATCGCCTGGTA	probe template PCR	*GAL1*
1164	Gal1+433-rev	TTTCCGGTGCAAGTTTCTTT	probe template PCR	*GAL1*
1167	Nup57+759-for	TGGATCTAATTTACAGCAGCA	probe template PCR	*NUP57*
1168	Nup57+1012-rev	CCTGATCCCACTCTTCTTGA	probe template PCR	*NUP57*
1354	HMO1_KO_f	GATGGTACCCTTATACTCTAGGATGTA CATCCTACCACACACAACAAGCCTGT CACACCTACGACTCACTATAGGG	PCR cloning (amplicon from pBS1539)	*HMO1*
1355	HMO1_KO_r	CTACCGCGGTATTTATTTTAGAAAGAC AGTAGAGTAATAGTAACGAGTTTGTC CGTCCATCCATGGAAAAGAGAAG	PCR cloning (amplicon from pBS1539)	*HMO1*
1362	hmo1_A	TATTACCCGACTCGATTATCTACCA	amplification of *HMO1* gene - control deletion	*HMO1*
1498	RRN9_F	GATGGTACCACGAGTTGGACGACTGC CTCATAGAACTGCCTAATGGGAACAT ATCGTACGCTGCAGGTCGAC	integration, PCR cloning (amplicon from pKM9_TAP)	*RRN9*
1499	RRN9_R	CTACCGCGGATGAATATTTCTTAATGG AAAAAGGTAAAAAAAAGATTTTCTCAT ATCGATGAATTCGAGCTCG	integration, PCR cloning (amplicon from pKM9_TAP)	*RRN9*

1510	RPS23A_cds_f	TCTCCATTCGGTGGTTCTTC	qPCR	*RPS23A*
1511	RPS23A_cds_r	ATCGTTTGGAACGAAAGCAG	qPCR	*RPS23A*
2433	URA3_KL_rev	TTTGTGGACATGGTGCAACT	colony PCR	*URA3_KL*
2682	RPD3_KO_fwd	GATGGTACCCATAAAACAATTGCGCC ATACAAAACATTCGTGGCTACAACTC GATATCCCGTACGCTGCAGGTCGAC	PCR cloning (amplicon from pAG36/37)	*RPD3*
2683	RPD3_rev	CTACCGCGGTTCTTTTGTTTCACATTA TTTATATTCGTATATACTTCCAACTCTT TTTTATCGATGAATTCGAGCTCG	PCR cloning (amplicon from pAG36/37)	*RPD3*
2685	Rpd3_D	TGAACGGAACGCATCAATTA	amplification of *RPD3* gene - control deletion	*RPD3*
3070	Rpd3_up	TGTCCCATATTTTGCCTTGA	amplification of *RPD3* gene - control deletion	*RPD3*
3474	3.5kb 18S fwd	AAACGGCTACCACATCCAAG	PCR amplification of probe template for 3.5kb probe from pNOY373	*rDNA*
3475	3.5kb 25S rev	GTGGTGTCTGATGAGCGTGT	PCR amplification of probe template for 3.5kb probe from pNOY373	*rDNA*
3731	Set2_ko_fwd	GTCGTGCTGTCAAACCTTTCTCCTTTC CTGGTTGTTGTTTTACGTGATCCGTAC GCTGCAGGTCGAC	PCR cloning (amplicon from pAG36/37 for deletion of *SET2*)	*SET2*
3732	Set2_ko_rev	CTTTGGGACAGAAAACGTGAAACAAG CCCCAAATATGCATGTCTGGTTAAATC GATGAATTCGAGCTC	PCR cloning (amplicon from pAG36/37 for deletion of *SET2*)	*SET2*
3733	Set2_A	TGCCGTTGCTTCCTCTATTT	amplification of *SET2* gene - control deletion	*SET2*
3734	Set2_D	TTCCTTTGGGACAGAAAACG	amplification of SET2 gene - control deletion	*SET2*
3879	SacI_RPD3_3'IGS_rev	ATTGGAGCTCTGAATAGTGGTTTTTTA TGC	cloning	*RPD3*
3880	ApaI_pRPD3_fwd	TACCGGGCCCAAGCACAAGAGCAGC TCACC	cloning	*RPD3*
3881	EcoRI_URA3_kl_fwd	CAATGAATTCTATTGAAGACAATCATA TGGGAGAAG	cloning	URA3_KL
3882	EcoRI_URA3_kl_rev	CAATGAATTCTATTGAGAGCGGCCGC TTGTTGTTCC	cloning	URA3_KL
3903	SacII_Prom_fwd	GGTTCATTCAAATTTCTGCC	probe template PCR	rDNA (promoter)
3904	SacII_Prom_rev	CTGCTGGCACCAGACTTGCC	probe template PCR	rDNA (promoter)
4036	SIN3_KO_fwd	ATTTGGAAAAGGACAAAATATCTAAGA AACAAGTTATACATTGTACAAAACGTA CGCTGCAGGTCGAC	PCR cloning (amplicon from pAG36/37 for deletion of *SIN3*)	*SIN3*
4037	SIN3_KO_rev	AAAGACCCTGTCGTACTAAAGATTTTT GTTCTAAATCTAGTTAAAACTACATCG ATGAATTCGAGCTC	PCR cloning (amplicon from pAG36/37 for deletion of *SIN3*)	*SIN3*
4038	GCN5_ko_fwd	GTGAGCCGCCCAAAAGTCTTCAGTTA ACTCAGGTTCGTATTCTACATTAGCGT ACGCTGCAGGTCGAC	PCR cloning (amplicon from pAG36/37 for deletion of *GCN5*)	*GCN5*
4039	GCN5_ko_rev	ATTTATTTCTTCTTCGAAAGGAATAGT AGCGGAAAAGCTTCTTCTACGCAATC GATGAATTCGAGCTC	PCR cloning (amplicon from pAG36/37 for deletion of *GCN5*)	*GCN5*
4040	HDA1_ko_fwd	ATATTGAGAAAGGGAAAGTTGAGCAC TGTAATACGCCGAACAGATTAAGCCG TACGCTGCAGGTCGAC	PCR cloning (amplicon from pAG36/37 for deletion of *HDA1*)	*HDA1*
4041	HDA1_ko_rev	CATAAGGCATGAAGGTTGCCGAAAAA AAATTATTAATGGCCAGTTTTTCCATC	PCR cloning (amplicon from pAG36/37 for	*HDA1*

		GATGAATTCGAGCTC	deletion of *HDA1*)	
4042	SIN3_A	CCCTTTTGTTGTGTTCGTTTG	amplification of *SIN3* gene - control deletion	*SIN3*
4043	SIN3_D	TCAGAAGAAAGACCCTGTCG	amplification of *SIN3* gene - control deletion	*SIN3*
4044	GCN5_A	TGGTAAGGGAAGACCGTGAG	amplification of *GCN5* gene - control deletion	*GCN5*
4045	GCN5_D	TCGTCTCGCCGTACTAAACA	amplification of *GCN5* gene - control deletion	*GCN5*
4046	HDA1_A	GCACTGTAATACGCCGAACA	amplification of *HDA1* gene - control deletion	*HDA1*
4047	HDA1_D	TTCATAAGGCATGAAGGTTGC	amplification of *HDA1* gene - control deletion	*HDA1*

IV.1.3.3 DNA size markers

2-log ladder (NEB): size of fragments (bp): 10000, 8000, 6000, 5000, 4000, 3000, 2000, 1500, 1200, 1000, 900, 800, 700, 600, 500/517, 400, 300, 200, 100

1kB ladder (NEB): size of fragments (bp): 10002, 8001, 6001, 5001, 4001, 3001, 2000, 1500, 1000, 517, 500

100bp ladder (NEB): size of fragments (bp): 1517, 1200, 1000, 900, 800, 700, 600, 500, 517, 400, 300. 200, 100

IV.1.3.4 DNA probes for Southern blot detection

Table 4: Probes

name	synthesis	locus	restriction enzyme	fragment size
3.5kb rDNA	digest of pNOY373 with *Nco*I and purification of 3.5kb fragment or PCR from pNOY373 using primers 3474, 3475	rDNA	EcoRI	2.6, 1.9, 0.7kb
18S	PCR from genomic DNA using primers 3903, 3904	rDNA	XcmI/SacII	2kb
rDNp	PCR from genomic DNA using primers 817, 818	rDNA	XcmI	4.9kb
NUP57	PCR from genomic DNA using primers 1167, 1168	RPS23A	XcmI	4.2kb
GAL1	PCR from genomic DNA using primers 1163, 1164	GAL1-10	XcmI	6.8kb

IV.1.3.5 Plasmids

Table 5: Plasmids used during this study. The numbers refer to the plasmid database of the department Biochemistry III, University of Regensburg

DB#	name	cloning	function	reference
1	pBluescript KS		LacZ T3 and T7 promoter M13 - 20 T7 and SK primer Col E 1 - Origin f1ori (+or -)	Stratagene
97	pBS1539	integration cassette C-terminal: TAP-tag URA3_KL	Vector for PCR mediated URA cassette KO	
190	pNOY373		PCR template for the probe template for 3.5kb probe	Wai et al. (2000)
936	pAG36	TRP1_KL	Vector for PCR mediated TRP cassette KO using S2 and S3 adapter primer	Griesenbeck, Joachim

937	pAG37	URA_KL	Vector for PCR mediated URA cassette KO using S2 and S3 adapter primer	Griesenbeck, Joachim
2293	pKM9-TAP	TAP	Vector for PCR mediated amplification of the TAP tag	Griesenbeck, Joachim
2338	yEPlac112_RPD3_WT	RPD3-Flag WT	Vector for WT RPD3 and subsequent cloning	Kadosh and Struhl (1998)
2339	yEPlac112_RPD3_H150A	RPD3-Flag with point mutation leading to H150 to A	Vector for rpd3 H150A and subsequent cloning	Kadosh and Struhl (1998)
2340	yEPlac112-RPD3-H151A	RPD3-Flag with point mutation leading to H151 to A	Vector for rpd3 H151A and subsequentcloning	(Kadosh and Struhl (1998)
2341	pVB15	pBluescript digested with ApaI and SacI and ligated with ApaI/SacI digested PCR amplicon from genomic Rpd3 using primers 3879 and 3880	HDAC mutant cloning	this study
2342	pVB16	pVB15 digested with EcoRI and ligated with EcoRI cut PCR amplicon from pBS1539 using primers 3881 and 3882	HDAC mutant cloning	this study
2343	pVB17	pVB16 digested with MluI/BamHI and ligated with insert from MluI/BamHI derived yEPlac112_RPD3_WT	HDAC mutant cloning	this study
2345	pVB19	pVB16 digested with MluI/BamHI and ligated with insert from MluI/BamHI derived yEPlac112_RPD3_H150A	HDAC mutant cloning	this study
2347	pVB21	pVB16 digested with MluI/BamHI and ligated with insert from MluI/BamHI derived yEPlac112_RPD3_H151A	HDAC mutant cloning	this study
2382	pBS_ura3_O_IGS_pPGK1_3xHA_RPA49	SphI/SbfI restricted amplicon from yeast gDNA with primer pair 4096/4097 into SphI/SbfI restricted pBS_ura3_0_IGS_pPGK1_URA3KL.	integration	Griesenbeck, Joachim
2383	pBS_ura3-0_pPGK1-rpa49(1-115)_URA3_KL	SphI/SbfI restricted amplicon fromyeast gDNA with primer pair 4098/4096 into SphI/SbfI restricted pBS_ura3_0_IGS_pPGK1_URA3KL.	integration	Griesenbeck, Joachim
2384	pBS_ura3-0_pPGK1_rpa49(116-426)_URA3_KL	SphI/SbfI restricted amplicon fromyeast gDNA with primer pair 4097/4099 into SphI/SbfI restricted pBS_ura3_0_IGS_pPGK1_URA3KL.	integration	Griesenbeck, Joachim

IV.1.4 Enzymes and polypeptides

Table 6: Enzymes and polypeptides used during this study. All enzymes were used with the provided buffers.

enzyme/polypeptide	manufacturer
Antarctic phosphatase	New England Biolabs (NEB)
ColorPlus Prestained Protein Marker, Broad Range (7-175 kDa)	New England Biolabs
GoTaq™ polymerase	Promega
Herculase II Fusion polymerase	Agilent technologies
HotStarTaq-polymerase	Quiagen
Prestained protein-marker broad range	New England Biolabs
Proteinase K	Sigma Aldrich

Restriction endonucleases	New England Biolabs (NEB)
RNAseA	Invitrogen
T4 DNA ligase	New England Biolabs (NEB)
Zymolyase 20T	Seikagaku Corporation

IV.1.5 Antibodies

Table 7: Antibodies used during this study.

anitbody	origin	dilution	manufacturer
Anti-PAP	rabbit	1:3000	Roche
3F10 anti-HA	monoclonal rat	1:5000	Roche
Anti-rat (peroxidase-conjugated)	goat	1:2500	Dianova

IV.1.6 Organisms

IV.1.6.1 Host bacteria

The electro-competent *E. coli* strain "XL1BlueMRF" (Stratagene) was used for cloning. Genotype: Δ(mcrA)183, Δ(mcrCB-hsdSMR-mrr)173, endA1, supE44, thi-1, recA1, gyrA96, relA1, lac, λ-, *F´, proAB, lacIqZΔM15, tn10(tetr)+.

IV.1.6.2 Yeast strains

Table 8 Yeast strains used during this study. The numbers refer to the yeast strain database (DB#) of the department Biochemistry III, University of Regensburg.

DB#	name	genotype	reference or source
207	BY4742	*MATα his31 leu20 lys20 ura30*	Euroscarf
348	NOY505	*MATa ade2-1 ura3-1 his3-11 trp1-1 leu2-3,112 can1-100*	Nogi et al. (1991b)
354	NOY1075	*MATa ade2-1 ura3-1 trp1-1 leu2-3,112 his3-11,15 can1-100 rrn3 (S213P)*	Claypool et al. (2004)
880	yKM26	*MATa ade2-1 ura3-1 trp1-1 leu2-3,112 his3-11 can1-100 RRN3_MNase_3xHA_KAN_MX6*	Merz, Katharina
881	yKM27	*MATta ade2-1 ura3-1 trp1-1 leu2-3,112 his3-11 can1-100 RRN7_MNase_3xHA_KAN_MX6*	Merz, Katharina
1145	yMH22	*MATa ade2-1 ura3-1 trp1-1 leu2-3,112 his3-11 can1-100 HHO1_MNase_3xHA_Kan MX6*	Hondele, Maria
1151	yMH28	*MATa ade2-1 ura3-1 trp1-1 leu2-3,112 his3-11 can1-100 RRN9_MNase_3xHA_Kan MX6*	Hondele, Maria
1185	yR59	*MATa ade2-1 ura3-1 trp1-1 leu2-3,112 his3-11 can1-102 SPT15_MNase_3xHA_Kan MX6*	Stöckl, Ulrike
1453	yMW36	*MATa ade2-1 ura3-1 trp1-1 leu2-3,112 his3-11 can1-100 NET1_MNase_3xHA_KAN_MX6*	Wittner, Manuel
1717	yMW75	*MATa ade2-1 ura3-1 trp1-1 leu2-3,112 his3-11 can1-100 bar1::HIS3 RPA190_MNase_3xHA_KAN_MX6*	Wittner, Manuel
1761	yMW95	*MATa ade2-1 ura3-1 trp1-1 leu2-3,112 his3-11 can1-100 bar1::HIS3 HMO1_MNase_3xHA_KAN_MX6*	Wittner, Manuel
1995	yMW137	*MATa ade2-1 ura3-1 trp1-1 leu2-3,112 his3-11 can1-100 bar1::HIS3 HHT1_MNase_3xHA_KAN_MX6*	Wittner, Manuel
2017	ySH37	*MATa ade2-1 ura3-1 trp1-1 leu2-3,112 his3-11 can1-100 NET1_TAP_KanMX6*	Hamperl, Stephan

2256	yMW158	*MATa ade2-1 ura3-1 trp1-1 leu2-3,112 his3-11 can1-100 rpd3::TRP1_KL bar1::HIS3 RPA190_MNase_3xHA_KAN_MX6*	Wittner, Manuel
2257	yMW159	*MATa ade2-1 ura3-1 trp1-1 leu2-3,112 his3-11 can1-100 rpd3::TRP1_KL bar1::HIS3 HMO1_MNase_3xHA_KAN_MX6*	Wittner, Manuel
2344	yMW163	*MATa ade2-1 ura3-1 trp1-1 leu2-3,112 his3-11 can1-100 rpd3::TRP1_KL bar1::HIS3 HHT1_MNase_3xHA_KAN_MX6*	Wittner, Manuel
2534	yJPF159_1a	*MATα his31 leu20 lys2- ura30 RPA135-TEV-ProtA::kanMX6*	Perez-Fernandez, Jorge
2616	yVB5	*MATa ade2-1 ura3-1 trp1-1 leu2-3,112 his3-11 can1-100 , rpd3::TRP1_KL HHO1_MNase_3xHA_Kan MX6*	Babl (2012)
2670	yJPF162_1a	*MATα his31 leu20 lys2- ura30 RPA135-TEV-ProtA::kanMX6 HIS3MX::GAL::HA-RPA49*	Perez-Fernandez, Jorge
2919	yVB25	*MATa ade2-1 ura3-1 trp1-1 leu2-3,112 his3-11; can1-100 rpd3::k.l.TRP1*	this study
2920	yVB26	*MATa ade2-1 ura3-1 trp1-1 leu2-3,112 his3-11 can1-100 set2::URA3_KL*	this study
2921	yVB27	*MATa ade2-1 ura3-1 trp1-1 leu2-3,112 his3-11,15 can1-100 rrn3 (S213P) rpd3::TRP1_KL*	this study
2945	yVB28	*MATa ade2-1 ura3-1 trp1-1 leu2-3,112 his3-11,15 can1-100 rrn3 (S213P) hmo1::URA3_KL*	this study
2946	yVB29	*MATa ade2-1 ura3-1 trp1-1 leu2-3,112 his3-11 can1-100 rpd3::TRP1_KL set2::URA3_KL*	this study
2947	yVB30	*MATa ade2-1 ura3-1 trp1-1 leu2-3,112 his3-11,15 can1-100 rrn3 (S213P) rpd3::TRP1_KL; hmo1::URA3_KL*	this study
3023	yVB43	*MATa ade2-1 ura3-1 trp1-1 leu2-3,112 his3-11 can1-100 rpd3::TRP1_KL RRN3_MNase_3xHA_KAN_MX6*	this study
3024	yVB44	*MATa ade2-1 ura3-1 trp1-1 leu2-3,112 his3-11 can1-100 rpd3::TRP1_KL RRN7_MNase_3xHA_KAN_MX6*	this study
3028	yVB48	*MATa ade2-1 ura3-1 trp1-1 leu2-3,112 his3-11 can1-100 rpd3::TRP1_KL RRN9_MNase_3xHA_Kan MX6*	this study
3030	yVB50	*MATa ade2-1 ura3-1 trp1-1 leu2-3,112 his3-11 can1-100 rpd3::TRP1_KL SPT15_MNase_3xHA_Kan MX6*	this study
3033	ySE2-1	*MATa ade2-1 ura3-1 trp1-1 leu2-3,112 his3-11 can1-100 rpd3::TRP1_KL NET1_MNase_3xHA_KAN_MX6*	this study
3078	yR_Rpa135-TAP_1	*MATa ade2-1 ura3-1 trp1-1 leu2-3,112 his3-11 can1-100 RPA135_TAP_KanMX6*	Griesenbeck, Joachim
3116	yVB51_1_Susi	*MATa ade2-1 ura3-1 trp1-1 leu2-3,112 his3-11 can1-100 RRN7_TAP_KanMX6*	this study
3118	yVB52_1_Schöne	*MATa ade2-1 ura3-1 trp1-1 leu2-3,112 his3-11 can1-100 RRN9_TAP_KanMX6*	this study
3120	yVB53_1_Tarzan	*MATa ade2-1 ura3-1 trp1-1 leu2-3,112 his3-11 can1-100 RRN3_TAP_KanMX6*	this study
3122	yVB54_1_Aladin	*MATa ade2-1 ura3-1 trp1-1 leu2-3,112 his3-11 can1-100 rpd3::TRP1_KL RRN7_TAP_KanMX6*	this study
3124	yVB55_1_Bernhard	*MATa ade2-1 ura3-1 trp1-1 leu2-3,112 his3-11 can1-100 rpd3::TRP1_KL RRN9_TAP_KanMX6*	this study
3126	yVB56_1_Micky	*MATa ade2-1 ura3-1 trp1-1 leu2-3,112 his3-11 can1-100 rpd3::TRP1_KL RRN3_TAP_KanMX6*	this study
3131	yVB58_2_Schwefel	*MATa ade2-1 ura3-1 trp1-1 leu2-3,112 his3-11 can1-100 rpd3::TRP1_KL NET1_TAP_KanMX6*	this study

3136	yVB61_1_Chip	*MATa ade2-1 ura3-1 trp1-1 leu2-3,112 his3-11 can1-100 rpd3::TRP1_KL RPA135_TAP_KanMX6*	this study
3226	yVB62_1_Adam	*MATa ade2-1 ura3-1 trp1-1 leu2-3,112 his3-11 can1-100 hmo1::URA3_KL RPA135_TAP_KanMX6*	this study
3228	yVB63_1_Bambi	*MATa ade2-1 ura3-1 trp1-1 leu2-3,112 his3-11 can1-100 rpd3::TRP1_KL inserted WT RPD3 with URA KL*	this study
3230	yVB64_1_Batman	*MATa ade2-1 ura3-1 trp1-1 leu2-3,112 his3-11 can1-100 rpd3::TRP1_KL inserted H150A RPD3 with URA KL*	this study
3232	yVB65_1_Luke	*MATa ade2-1 ura3-1 trp1-1 leu2-3,112 his3-11 can1-100 rpd3::TRP1_KL inserted H151A RPD3 with URA KL*	this study
3315	yVB66_1	*MATa ade2-1 ura3-1 trp1-1 leu2-3,112 his3-11 can1-100 sin3::TRP1_KL*	this study
3317	yVB67_1	*MATa ade2-1 ura3-1 trp1-1 leu2-3,112 his3-11 can1-100 hda1::TRP1_KL*	this study
3319	yVB68_1	*MATa ade2-1 ura3-1 trp1-1 leu2-3,112 his3-11 can1-100 gcn5::URA3_KL*	this study
3321	yVB69_1	*MATa ade2-1 ura3-1 trp1-1 leu2-3,112 his3-11 can1-100 rpd3::TRP1_KL gcn5::URA3_KL*	this study
3323	yVB70_1_Tim	*MATα his31 leu20 lys2- ura30 RPA135-TEV-ProtA::kanMX6 rpd3::URA3_KL*	this study
3325	yVB71_1_Itchy	*MATα his31 leu20 lys2- ura30 RPA135-TEV-ProtA::kanMX6 HIS3MX::GAL::HA-RPA49 rpd3::URA3_KL*	this study
3327	yVB72_1_Balu	*MATa ade2-1 ura3-1 trp1-1 leu2-3,112 his3-11 can1-100 Spt15-TAP_KAN_MX6*	this study
3329	yVB73_1_Maja	*MATa ade2-1 ura3-1 trp1-1 leu2-3,112 his3-11 can1-100 rpd3::TRP1_KL Spt15-TAP_KAN_MX6*	this study
3534	yVB76_1_Ernie	*MATα his31 leu20 lys2- ura30 RPA135-TEV-ProtA::kanMX6 HIS3MX::GAL::HA-RPA49; ura3-0::pPGK1:3xHA-Rpa49-URA3 KL*	this study
3536	yVB77_1_Pinky	*MATα his31 leu20 lys2- ura30 RPA135-TEV-ProtA::kanMX6 ura3-0::pPGK1:3xHA-Rpa49-URA3 KL*	this study
3538	yVB78_1_Barbie	*MATα his31 leu20 lys2- ura30 RPA135-TEV-ProtA::kanMX6 HIS3MX::GAL::HA-RPA49 ura3-0::pPGK1:3xHA-rpa49 (1-115)-URA3 KL*	this study
3540	yVB79_1_Frodo	*MATα his31 leu20 lys2- ura30 RPA135-TEV-ProtA::kanMX6 ura3-0::pPGK1:3xHA-rpa49 (1-115)-URA3 KL*	this study
3542	yVB80_1_Hänsel	*MATα his31 leu20 lys2- ura30 RPA135-TEV-ProtA::kanMX6 HIS3MX::GAL::HA-RPA49 ura3-0::pPGK1:3xHA-rpa49 (116-426)-URA3 KL*	this study
3544	yVB81_1_Max	*MATα his31 leu20 lys2- ura30 RPA135-TEV-ProtA::kanMX6 ura3-0::pPGK1:3xHA-rpa49 (116-426)-URA3 KL*	this study
3671	3649_ rpd3_ net1_1051_B2	*MATa ade2-1 trp1-1 can1-100 leu2-3,112 his3-11,15 ura3-1 GAL psi+ ssd1- d2 net1(1-1051):12xFLAG_HIS3MX rpd3::TRP1_KL*	this study (Katharina Hannig)
3672	3649_ rpd3 _A2	*MATα ade2-1 trp1-1 can1-100 leu2-3,112 his3-11,15 ura3 GAL psi+ ssd1- d2 rpd3::TRP1_KL*	this study (Katharina Hannig)
3673	3649_net1_1051_C 2	*MATa ade2-1 trp1-1 can1-100 leu2-3,112 his3-11,15 ura3 GAL psi+ ssd1- d2 net1(1-1051):12xFLAG_HIS3MX*	this study (Katharina Hannig)
3725	3649_ wt_1	*MATa ade2-1 trp1-1 can1-100 leu2-3,112 his3-11,15 ura3 GAL psi+ ssd1- d2*	this study (Katharina Hannig)

IV.1.7 Equipment

Table 9: Equipment used during this study.

device	manufacturer
-80°C freezer (Ultra Low)	Sanyo
Balances	Sartorius/Kern
BAS cassette 2040	Fuji
BAS-III imaging plate	Fuji
Biofuge Fresco refrigerated tabletop centrifuge	Hereaus
Biofuge Pico tabletop centrifuge	Hereaus
Bioruptor sonicator	Diagenode
Blacklight blue lamps 15 W	Sankyo-Denki
C4i centrifuge	Jouan
CR4i refrigerated centrifuge	Jouan
C412 centrfuge	Jouan
Digital pH-meter	Knick
DNA cross-linking system Fluo-Link tFL20.M	Vilber Loumat
Electrophoresis system model 45-2010-i	Peqlab Biotechnologie GmBH
Electroporation device Micropulser	Biorad
Eraser	Raytest
Erlenmeyer flasks	Schott/VWR
FLA-3000	Fuji
Gel Max UV transilluminator	INTAS
Glass bottles	Schott
Hybridization tubes	Bachofer, Rettberg
Hybridization oven	Peqlab Biotechnologie GmBH
Hybridization oven	Grant Boekel
Ice machine	Ziegra
IKA-Vibrax VXR	IKA
Incubators	Memmert
Lyophilisator	Eppendorf
Magnetic stirrer	Heidolph
Megafuge 16R	Thermo Scientific
Millipore water system (ELGA)	Purelab
Multipette	Brand
PCR Sprint thermocycler	Hybaid
peqSTAR 96 Univerasl Gradient	Peqlab Biotechnologie GmBH
Pipetboy	IBS Integra
Pipettes	Gilson
Power Pac 3000 power supplies	Biorad
Rotor Gene RG-3000	Corbett Research
Safe imager	Invitrogen
Shake incubators Multitron / Minitron	Infors
Special accuracy weighing machine	Sartorius
Sub-cell Gt Agarose Gel Electrophoresis System	Biorad
Thermomixer® Dry Block Heating Shaker	Eppendorf
Trans-Blot SD Semi-dry transfer cell	Biorad
Ultrospec 3100pro spectrophotometer	Amersham

IV.1.8 Kits

Table 10: Kits used during this study

kit	manufacturer
peqGOLD Plasmid Miniprep Kit I	PeqLab
peqGOLD Cycle Pure Kit	PeqLab
Quiaex II Gel extraction Kit	Quiagen
Quiaquick PCR purification kit	Quiagen
RadPrime Labeling Kit	Invitrogen

IV.1.9 Consumables

Table 11: Material consumed during this study.

consumable	manufacturer
24-well-plates	Sarstedt
[α-32P]dATP (10 mCi/mL)	Hartmann analytics
BM Chemiluminescence Blotting Substrate (POD)	Roche
ColorPlus Prestained Protein Marker, Broad Range (7-175 kDa)	New England Biolabs
Falcon tubes (15ml/50ml)	Sarstedt
Filter paper 3MM	Whatman
Gene pulser cuvettes	BioRad
Glass beads (0.75-1 mm)	Roth
Glow Writer™ Autoradiography Marking Pen	Diversified Biotech
IgG sepharose TM 6 Fast Flow	GE Healthcare
Immobilon-P transfer membrane	Millipore
Inoculation loops	Sarstedt
Multiwell plates (24 wells)	Sarstedt
Pipette tips (10-1000µl)	Sarstedt
Pipettes (2-50ml)	Sarstedt
Positive TM membrane	MP Biomedicals
ProbeQuant™ G-50 Micro Columns	GE Healthcare
Protein Assay Dye Reagent Concentrate	Biorad
Psoralen (Trimethylpsoralen)	Sigma Aldrich
Rapamycin	Sigma Aldrich
reaction tubes (1.5ml, 2ml)	Sarstedt
Roti®-P/C/I	Roth
Salmon Sperm DNA (10 mg/ml)	Invitrogen
SYBR Green	Roche
SYBR Safe DNA Gel Stain	Invitrogen
Trichostatin A	New England Biolabs
Whatman®blotting paper 3MM	Whatman

IV.1.10 Software

Table 12: Software used during and for this study

software	producer
Acrobat Reader X	Adobe
Image Reader LAS-3000 v.2.2	Fujifilm
Microsoft Office 2007	Microsoft
ND-1000 v.3.5.2	Peqlab Biotechnologie GmbH
MultiGauge v.3.0	Fujifilm
PeakFit v.4.0.5.0	AISN software
Rotor-Gene 6000	Corbett Research
Image Reader FLA-3000 v.1.8	Fujifilm

IV.2 Methods

IV.2.1 Enzymatic manipulation of DNA and RNA

IV.2.1.1 Polymerase chain reaction (PCR)

Two different PCRs were used during this work. Depending on the importance of the amplicon bearing any mutation, the GoTaq™ Polymerase (Promega) was used for analytical PCR and the Herculase II Fusion Polymerase (Agilent Technologies) was used for production of proof-read amplicons, which were designed for cloning.

IV.2.1.1.1 GoTaq™ polymerase

All reactions were made in a total volume of 30µl in either a 0.2 or a 0.5ml tube. Each reaction contained the DNA to be amplified and was applied according Table 13.

Table 13: Reaction mixture for GoTaq polymerase PCR.

Ingredient	µl/30µl	Final concentration
5x green GoTaq™ buffer	6	1x (1.5mM $MgCl_2$)
10mM each dNTP	0.6	200µM
Forward primer (10µM)	0.6	0.2µM
Reverse primer (10µM)	0.6	0.2µM
GoTaq™Polymerase (5U/µl)	0.15	0.75U/30µl
Distilled H_2O	22.05	

Program used for the GoTaq™ PCR (Table 14):

Table 14: Program for GoTaq polymerase PCR

step	time	temperature	cycles	comment
Initial denaturation	3 min	95°C	1x	For genomic DNA time extended
denaturation	15sec	95°C	35x	Extended time for genomic DNA
annealing	30sec	54°C		Extended time for genomic DNA, temperature according to primer T_M
extension	1min/kb	72°C		
final extension	5min	72°C	1	
storage	forever	4°C		

IV.2.1.1.2 Herculase II fusion polymerase

All reactions were made in a volume of 50µl in 0.2 or 0.5ml tubes. The reactions were applied according to the Table 15.

Table 15: Reaction mixture for Herculase II PCR

Ingredient	µl/50µl	Final concentration
5x Herc II reaction buffer	10	1x (2mM $MgCl_2$)
25mM each dNTP	0.5	250µM each
Forward primer (10µM)	1.25	0.25µM
Reverse primer (10µM)	1.25	0.25µM
Herculase II (5U/µl)	1	5U//50µl
Distilled H_2O	35	

Program used for PCRs with the Herculase II fusion polymerase (Table 16).

Table 16: Herculase II fusion polymerase PCR program.

step	time	temperature	cycles	comment
Inital denaturation	2 min	95°C	1x	For genomic DNA time extended
denaturation	10sec	95°C	2x	Extended time for genomic DNA
annealing	20sec	40°C		Extended time for genomic DNA,
extension	30sec/kb	72°C		
denaturation	10sec	95°C	33x	Extended time for genomic DNA
annealing	20sec	54°C		Extended time for genomic DNA, temperature according to the primer T_M
extension	30sec/kb	72°C		
Final extension	3min	72°C	1x	
Storage	Forever	4°C		

Since the Herculase II fusion polymerase is a Pfu-based polymerase and therefore exhibits 3' to 5' exonuclease proofreading activity it was important to inactivate the

enzyme immediately after the final extension step by purification of the reaction or by storage at -20°C.

IV.2.1.2 Restriction enzyme digestion

Digestion with sequence specific restriction endonucleases was performed in buffer and temperature as indicated by the manufacturer (NEB). Analytical digestions were made in a volume of 20µl with 1µl enzyme per 1µg of DNA. Preparative digestions were made in volumes of up to 50µl. The total glycerol concentration (present in the enzyme storage buffer) did never exceed 5%.

IV.2.1.3 Dephosphorylation of vector DNA after restriction enzyme digestion

To prevent religation of vector DNA in the ligation reaction the vector was dephosphorylated with Antarctic phosphatase (NEB). To a 20µl digestion reaction 2.3µl of Antarctic phosphatase buffer (10x) and 0.7µl of Antarctic phosphatase were added. The dephosphorylation was done overnight or for at least one hour at 37°C. Afterwards the phosphatase was heat inactivated for 20min at 65°C, DNA was purified and used for the ligation reaction.

IV.2.1.4 Ligation

For cloning of DNA sequences into vectors, first the amount of purified, restriction enzyme digested DNA was measured by UV spectrometry. Second the amount of insert that has to be used for the ligation was calculated with the following formula:

ng insert = ratio insert/vector x ((ng vector/kb insert)/kb vector)

10-20ng of vector DNA were used for 10µl ligation reaction with 1x T4 DNA ligase buffer, 500U T4 DNA ligase, the respective amount of purified insert and vector DNA and then filled up with distilled water. The ligation reaction was performed for one hour at room temperature or overnight at 16°C. For transformation of electrocompetent *Escherichia coli* 1-2µl of the ligation reaction were used.

IV.2.2 Purification of nucleic acids

IV.2.2.1 Plasmid isolation

Plasmid DNA was isolated from *E. coli* cells using kits. For minipreps (up to 5ml of culture) the PeqGOLD DNA miniprep kit (PeqLab) was used. The preparations were done as indicated by the kit manufacturer. In principle the pelleted cells were lysed with

NaOH and SDS containing buffers and the alkaline lysate was then neutralized with KOAc containing buffers. Thereby proteins and genomic DNA were precipitated. After pelleting the plasmid containing supernatant was transferred to a silikamembrane column (PeqGOLD DNA miniprep kit) where the DNA was bound under low salt conditions. After some washing steps to remove RNA and remaining proteins the DNA was eluted with a high salt buffer and precipitated with isopropanol and resuspended in TE or water or in the case of the PeqGOLD miniprep kit directly eluted with TE or water.

IV.2.2.2 Isolation of genomic DNA from yeast

A yeast culture was grown overnight in 5ml YP(A)D, pelleted and afterwards resuspended in 500µl H_2O. After spinning down for a second time the cells were resuspended in 500µl 1M sorbitol, 0.1M EDTA and 3µl of 2% zymolyase (10mM TrisCl pH8, 5% glucose, 2% zymolyase) were added. The cell wall digestion was done at 37°C for 60 minutes. Hereafter the spheroblasts were spun down (5000 x g, 5min, RT in a table-top centrifuge), the supernatant was discarded and 500µl buffer IR, and 50µl of 10% SDS were added. After vortexing until the lysis was complete the mixture was incubated for 30 minutes at 65°C. Then 200µl of 5M KOAc were added and the precipitation of proteins was done by incubation for 20 minutes on ice and subsequent centrifugation (10,000 x g, 20min, 4°C). The supernatant was then transferred to a new microtube and 4µl of RNAseA (20mg/ml) were added. RNA digestion was done overnight at room temperature. Genomic DNA was precipitated with 750µl isopropanol at -20°C for at least one hour. After pelleting the DNA (10,000 x g, 20min, 4°C) a washing step with 250µl 70% ethanol was performed and afterwards the pellet was air-dried. Genomic DNA was then resuspended in 50µl TE.

IV.2.2.3 Phenol extraction

DNA was extracted using a 25:24:1 mixture of phenol-chloroform-isoamyl alcohol. Approximately the same volume of the mixture was added to the sample and then vortexed thoroughly. To separate the phases the samples were centrifuged at room temperature for at least two minutes. Thereafter about one third of the total volume of the sample was taken slowly from the upper aqueous phase and were transferred to a new microtube. It was important to transfer nothing of the thin layer between the two phases and to take the aliquot while not disturbing the phase separation to avoid contamination with phenol.

IV.2.2.4 Ethanol precipitation

By addition of 1/10 volume of NaOAc or 1 volume of IRN buffer the salt concentration was raised to at least 0.25M if the samples did not yet contain an adequate amount. The precipitation was then done by addition of 2.5 volumes 100% ice cold ethanol. The samples were then stored at -20°C for at least 20min. After centrifugation (20min, full speed, -4°C) and discarding of the supernatant the DNA was washed with 70% (v/v) ice cold ethanol, air dried and resuspended in TE or water.

IV.2.2.5 Purification of PCR products

PCR products were purfied using kits. During this work the QUIAquick PCR purification kit (Quiagen) and the PeqGOLD Cycle Pure Kit (Peqlab) were used. In prinicple DNA was bound to a silicate gel column, washed and then eluted with 10mM Tris pH 8 or water.

IV.2.2.6 Purification of nucleic acids from agarose gels

To purify DNA from agarose gels the QUIAEX II Gel extraction kit (Quiagen) was used. To get an appropriate yield of purified DNA at least one µg of DNA was applied to agarose gel electrophoresis. The gel piece with the respective DNA was cut out and treated according to the manufacturer's instructions. In principle the gel piece was solubilized and afterwards the DNA was bound to silica particles in the presence of chaotropic salts, washed and then eluted in H_2O or 10mM Tris buffer.

IV.2.3 Quantitative and qualitative analysis of nucleic acids

IV.2.3.1 UV spectrometry

The concentration of purified DNA samples was measured using the Nanodrop 2000 UV-spectrophotometer (Thermo Scientific). The nanodrop UV-spectrophotometer technology detects the absorbance of small volumes of DNA samples at 260nm wavelength and measures at the same time the purity by detecting the absorbance at 280nm (protein absorbance wavelength). Pure DNA has an absorbance ratio (260nm/280nm) of about 1.8 to 2.0.

IV.2.3.2 Agarose gel electrophoresis

During this work for gel electrophoresis 1% (w/v) agarose was used for 1x TBE gels with SYBR SAFE (added in a dilution of 1:10.000, except psoralen gels). The separation of the DNA fragments of different lengths was done with 3 to 5 V per cm in 1x TBE buffer.

In addition to the samples 2-log ladder (500µg/ml in 1x DNA loading buffer) was loaded to the gel for determination of the fragment sizes.

IV.2.3.3 Southern blot, hybridization and detection of radioactively labeled probes

IV.2.3.3.1 Southern blot

For transfer of DNA from agarose gels to positively charged nylon membranes (Positive^{TM} Membrane, MP Biomedicals) Southern blot was used. Before blotting the DNA in the gels was denatured by two incubations for 15min in denature solution (0.5M NaOH, 1.5M NaCl) on a shaker. Afterwards the gels were transferred to blotting solution (1M NH_4OAc) and also twice shook for 15min. The DNA was transferred to the membrane by capillary flow through a blotting piling. The assembling of the southern blot was as following: Over a basin filled with blotting solution a bridge was deposited consisting of a plastic plane with two thin Whatman papers (Whatman 3MM, 16.5x35cm) of which the ends were in the basin. On the sides of these papers two straps of parafilm were laid to prevent bypass of capillary flow. The gel was then put onto this bridge upside down. The membrane and a second layer consisting of three Whatman papers (16.5x20cm) was applied to the piling. To be sure no air bubbles hamper the capillary flow a plastic pipette was rolled over the whole pile. Afterwards paper towels (about 10cm) were laid on the top of the blot and it was covered with a sleigh of a gel pouring apparatus and a weight to prevent interruption of capillary flow. All layers except the paper towels were soaked in blotting solution before usage. The blotting was performed over night and afterwards the membrane was dried. The DNA was crosslinked to the membrane via UV light (0.3J/cm^2) which leads to thymine bases binding covalently to the amino groups of the membrane.

IV.2.3.3.2 Production of radioactively labeled probes and hybridization

All probes were prepared using the RadPrime DNA labeling system (Invitrogen). The radioactive base used for southern blots was α-[^{32}P]-dATP. About 25ng of the probe template was first denatured for 5min in a boiling water bath and afterwards cooled on ice. 3µl of a 500µM each dNTP (except dATP) and 20µl of a random primer solution were added. Afterwards 5µl of α-[^{32}P]-dATP (approximately 50µCi) and 1µl Klenow fragment were added. The reaction was incubated for 10min at 37°C and then 5µl of Stop buffer were added. The sample was cleaned up by size exclusion spin chromatography using illustra ProbeQuant™ G-50 Micro Columns (GE-Healthcare).

150µl of prewarmed salmon sperm DNA were added and the probe was heated at 95-100°C for 5min and then immediately chilled on ice before use.

For the hybridization up to two membranes separated by meshes were stacked into one hybridization tube. The membranes were prehybridized for 1h at hybridization temperature (65°C) in 50ml hybridization buffer (0.5M sodium phosphate buffer pH 7.2, 7% SDS). Afterwards the 50ml hybridization buffer were discarded and new prewarmed 15ml and the probe were added to the hybridization tube. Hybridization was performed over night at 65°C on a rotating wheel in a hybridization oven. Thereafter the buffer was discarded and the membranes were once rinsed with 3x SSC, 0.1% SDS. Then three washing steps, each two times for 15 minutes were made: First with buffer wash1 (0.3x SSC, 0.1% SDS), second with buffer wash2 (0.1x SSC, 0.1% SDS) and third with buffer wash3 (0.1x SSC, 1.5% SDS). The blots were dried and put into a transparent foil.

If one blot had to be hybridized with a second probe, it was treated with stripping solution (0.1x SSPE, 0.5%SDS) for 15min at 80°C three times or until no radioactivity was detectable any longer and afterwards hybridized as described above with a new probe.

IV.2.3.3.3 Detection of radioactively labeled probes

Radioactively labeled blots in foil were put into a BAS cassette 2040. An erased BAS-III imaging plate (IP) was put on the blots. According to the intensity of the radioactive signal the exposure took place for a few hours or up to several days. Afterwards the IPs were scanned with 100µM resolution in a phosphor imager (FLA3000 by Fujifilm).

IV.2.3.3.4 Quantification of Southern blots

The *MultiGauge* 3.0 (Fujifilm) software offers the opportunity to quantify radioactive signals.

For ChEC data the "Quant" module in the "Measure" mode of *MultiGauge* was used. All single measurement areas were of the same size. The obtained date were then further processed and calculated with Microsoft *Excel*. Two different ways of quantification were made according to the analyzed proteins. These are described in the results section II.1.2.

For psoralen blots the "profile" in the "Measure" mode of *MultiGauge* was used to detect signal intensities for each lane and then transferred to *Microsoft Excel* and there refined and normalized to the respective peak values. The normalized profiles were then plotted against the migration distance in the gel. The obtained raw data were processed with the

PeakFit software (Systat Software Inc.) using a Gaussian basis function (r^2 values fit >0.95). The quantification is explained in more detail in the results section II.1.2.

IV.2.4 Formaldehyde crosslink

For cells in exponential growth phase (~OD 0.5) 50ml of liquid culture were taken and added to 1.35ml of formaldehyde (37% v/v) to a final concentration of about 1%. The cells were shaken for 15min at growth temperature and thereafter the crosslink was quenched with 2.5ml of 2.5M glycine (final concentration 125mM) at room temperature for 5min. The cells were then spun down (4500rpm, 5min, 4°C), resuspended in 1ml cold IRN buffer, transferred to a microtube and spun down a second time. After discarding the supernatant the cell pellet was frozen in liquid nitrogen and stored at -80°C. For cells of higher ODs (for example in stationary growth phase) the volumes were adapted to get about the same size of cell pellet. Two yield similar formaldehyde per cell concentrations, the aliquots after exponential phase (diauxic shift, post-diauxic phase, stationary phase) were added to 1.35ml formaldehyde and prewarmed medium (50ml - volume of the aliquot) and then treated as exponential phase samples.

IV.2.5 Nuclei preparation

For the preparation of nuclei all steps were performed on ice to prevent quality loss. The cells were washed three times in total with 900µl buffer A and 1x Protease inhibitors (benzamidin and PMSF) and spun down after each step in a microcentrifuge (16,000 x g for 2min at 4°C). The supernatant was always discarded and after the last washing step cells were resuspended in 350µl of buffer A and 1x Protease inhibitors. About 450µl of glass beads (Ø 0.75-1.00mm) were added so that there was always a liquid coverage of the beads. For cell disruption the mixture was then shaken for 10min at full speed in a Vibrax shaker at 4°C. To separate the cell lysate from the glass beads the microtubes were pierced at bottom and top with a red-hot cannula and put in 15ml falcon tubes. The collection of the crude lysate was done by centrifugation in a microcentrifuge (130 x g for 2min at 4°C). After transfer to new 1.5ml microtubes the lysate was washed two times with 900µl buffer A. The supernatant after centrifugation in a microcentrifuge (16,000 x g for 2min at 4°C) was discarded and the pellets were then either immediately used for further analysis or frozen in liquid nitrogen and stored at -80°C.

IV.2.6 Chromatin Endogenous Cleavage (ChEC)

With the Chromatin Endogenous Cleavage (ChEC) method the association of a protein with chromatin can be analyzed. The protein of interest has to be fused to MNase (Micrococcus Nuclease), an unspecific restriction endonuclease that needs Ca^{2+} ions for activity. The cells expressing the MNase-fusionprotein were first formaldehyde crosslinked and after that the preparation of nuclei took place. The nuclei were resuspended in 450 µl buffer Ag after the last washing step. Thereafter an incubation step at 30°C for two minutes was performed. The samples were incubated for the whole time course at 30°C and 750rpm in a Thermomixer and two-times 80 µl zero-control were taken. After that the MNase digestion was started through addition of 0.1M $CaCl_2$ to a final concentration of 2mM. 80µl time point aliquots were taken after three, ten and 60 minutes of digestion (or adapted to the amount of the protein associated with DNA) and the MNase activity was stopped by pipetting the aliquot into 100µl IRN buffer. Before an aliquot was taken the samples were vortexed to counteract nuclei sedimentation. Subsequent to the time course the zero-controls were filled up with 100µl IRN-buffer Thereafter 10µl of 10% SDS (final concentration 0.5 %) and 2µl of proteinase K (20 mg/ml) were added and the samples were incubated at least one hour at 56°C. To invert the formaldehyde-crosslink an overnight incubation at 65°C took place. Afterwards the DNA was extracted with phenol-chloroform-isoamyl alcohol, precipitated with ethanol and then resuspended in TE buffer containing 0.50ng/µl RNaseA. RNA was digested at 37°C for at least one hour.

IV.2.7 Psoralen photocrosslinking

IV.2.7.1 Psoralen photocrosslinking

Psoralen crosslinking followed either directly after the nuclei preparation or after ChEC (see IV.2.7.2 for this case). All steps were performed on ice. The nuclei were prepared similar to ChEC, but resuspended in 500µl of buffer A and 1x Protease inhibitors after the last washing step. 100µl of this suspension were used for psoralen-crosslinking and were therefore transferred to a 24-well plate. The remaining nuclei suspension was frozen in liquid nitrogen and stored at -80°C. To the 100µl used for the experiment the same volume of IRN buffer was added (total volume of 200µl). Thereafter 10µl of TMP (trimethylpsoralen 0.2mg/ml in ethanol) were added to all samples except one control, where instead 10µl of ethanol were used. The plate was then incubated for 5min in the dark and after this step the photocrosslinking was done by irradiating the plate (without lid) with UV A light (315-400nm) for at least 5min in a distance of 2-3cm. After each

irradiation new 10µl of either psoralen or ethanol were added and the suspension was again irradiated for further 6min, 7min, and 8min respectively. In total four times 10µl (40µl) were added and the complete irradiation time was at least 26min. Afterwards the samples were transferred to new microtubes and Proteinase K treatment and reversion of the formaldehyde crosslink took place.

IV.2.7.2 ChEC/ psoralen photocrosslinking combination

For subsequent psoralen crosslinking after ChEC the nuclei-aliquots were splitted after the MNase digestion time course: 60µl out of the 180µl were used for psoralen treatment and the other 120µl were used for ChEC-analysis and worked up as described above. For psoralen photocrosslinking the 60µl were transferred in a 24-well plate and 140 µl of IRN buffer were added (total volume 200µl). The crosslinking was performed as described above (see IV.2.7.1).

IV.2.8 DNA workup, RED and AGE of ChEC and psoralen samples

IV.2.8.1 DNA workup

After activation of MNase fusion proteins (ChEC) and/or psoralen the nuclei were incubated 10µl of 10% SDS and 2µl of Proteinase K (20mg/ml) and samples were incubated for one hour at 56°C. For reversion of the formaldehyde crosslink the cells were then incubated at 65°C over night or at least 8 hours. The extraction of DNA was done using phenol-chloroform-isoamyl alcohol. One volume of phenol-chloroform-isoamyl alcohol was added to one volume of sample and mixed thoroughly. After centrifugation for at least 3min the upper phase was transferred to a new microtube. For psoralen treated samples an additional extraction step took place. One volume of chloroform was added and again the upper phase was transferred to a new microtube after mixing and centrifugation. Afterwards one sample volume of IRN buffer was added. The samples were mixed and then precipitation of DNA took place by addition of 2.5 volumes (sample and IRN buffer) of 100% ethanol and incubation for at least 20min at -20°C followed by at least 20min of centrifugation. After air-drying the DNA pellet was resuspended in 30µl (ChEC and ChEC-psoralen samples) or 50µl (psoralen samples) TE buffer containing 50ng/µl RNaseA. RNA digest took place at 37°C for at least one hour.

IV.2.8.2 Restriction enzyme digestion

For psoralen samples first for each sample the amount of DNA was measured by loading an aliquot to an agarose gel containing SYBR® Safe and subsequent quantification using

the FLA 3000 and *MultiGauge*. With Microsoft Excel the amount of sample needed to use approximately the same amount of DNA in all samples was calculated. For the mock ethanol control (without psoralen) only 2µl of sample were used. 12.5µl of each sample (for psoralen samples maximally 15µl sample and the amount was adapted with H_2O according to the calculation described above) were used for the restriction enzyme digest. In this work all psoralen and ChEC-psoralen samples were digested either with EcoRI or XcmI/SacII and all ChEC samples were digested with XcmI. To each sample 0.6µl of restriction enzyme, 2µl of the respective 10x NEB buffer and the respective amount of H_2O to reach a final reaction volume of 20µl were added. The digestion reaction was then incubated at the optimal digestion temperature over night. The reaction was stopped by addition of 10x loading buffer.

IV.2.8.3 Agarose gel electrophoresis

Psoralen samples were loaded to 1% agarose gels containing no SYBR® Safe (since this DNA intercalator impairs the shift of psoralen crosslinked DNA). 300ml gels with narrow slots (since separation of psoralen-crosslinked and non-crosslinked DNA becomes clearer with narrow slots) were used. For ChEC samples 250ml 1% agarose gels containing SYBR® Safe with normal slots were used. Electrophoresis was done with 6V/cm for approximately 6h for ChEC samples or 8h respectively until the bromophenolblue band just had migrated out of the gel for psoralen-crosslinked samples. Psoralen gels were afterwards irradiated with 254nm UV light for 3min at each side to reverse the psoralen crosslink (crucial step, since denaturation of DNA and hybridization is only successful if the psoralen crosslink is removed).

IV.2.9 ChIP

For ChIP cell sample collection was performed as described already for ChEC (see section IV.2.4 for details). The cell pellets were washed with 500µl cold ChIP lysis buffer (1min, 13000rpm, 4°C in a tabletop centrifuge).The pellet was resuspended in 300µl cold lysis buffer and cold glass beads (0.75-1mm) were added, so that a thin liquid layer still covered the beads. The samples were shaken at full speed three times 15min in a Vibrax shaker with 10min on ice between each step. The cell lysate was disrupted as described for ChEC by piercing bottom and lid of the microtube with a red-hot cannula, putting the microtube in a 15ml falcon tube, and centrifugation for 2min at 130 x g at 4°C. The volume of the cell suspension was adapted to approximately 500µl in the falcon tube with cold lysis buffer. Sonication took place for four times 7min in a Bioruptor (Diagenode) with the following settings: 30s pulse, 30s pause, energy level high. Between each round

fresh ice was added to the water bath to prevent overheating of the samples. Afterwards the sonicated cell suspension was transferred to a fresh microtube and volume was adapted to 1ml. Cell debris was removed by centrifugation (20min, 13000rpm, 4°C). The supernatant was split in six aliquots. Three times 40µl were added to 250µl IRN buffer (=input samples) and three times 200µl were used for immunoprecipitation (=IP samples). The input samples were incubated at 4°C during the immunoprecipitation.

During cell disruption three times 80µl of IgG sepharose were prepared for immunoprecipitation. Therefore the IgG sepharose aliquots were washed two times with 1ml cold lysis buffer (centrifugation 1min, 2000rpm, 4°C with 3min on a rotating wheel at 4°C in between the washing steps).

The three 200µl disrupted and sonicated cell aliquots were then added to the prepared IgG sepharose aliquots. Immunoprecipitation took place for at least 3h or over night at 4°C on a rotating wheel.

After immunoprecipitation sepharose was washed three times with lysis buffer, twice with wash buffer 1, twice with wash buffer 2, and one time with TE buffer. All washing steps were performed by 1min centrifugation with 2000rpm at 4°C and 3min on a rotating wheel at 4°C in between each washing step. Afterwards 250µl IRN buffer were added. RNA was digested by the addition of 4µl RNase A (20mg/ml) for 1h at 37°C shaking in a thermomixer (1000rpm). Proteinase K treatment subsequently was performed by addition of 15µl 10%SDS and 4µl proteinase K (20mg/ml) for 1h at 56°C in a thermomixer (1000rpm). Reversion of the formaldehyde crosslink was done over night at 65°C without shaking.

For DNA extraction 300µl phenol/chloroform/isoamyl alcohol solution were added and samples (input and IP) were mixed thoroughly for at least 20s on a vortexing device. Phase separation took place during five to ten minutes centrifugation (13000rpm, RT). 200µl of the upper phase were transferred to a fresh microtube and 600µl ice cold 100% EtOH and 2µl glycogen (20µg/µl) were added. After mixing the samples DNA was precipitated for at least 1h at -20°C and subsequent centrifugation for 45min (13000rpm, 4°C). The supernatant was carefully removed and DNA was dried at RT for at least one hour. DNA pellets were resuspended in 50µl TE buffer (30min, RT, 14000rpm in a thermomixer).

For subsequent qPCR analysis input samples were diluted 1:500 and IP samples 1:100 in H_2O.

IV.2.10 Quantitative real-time PCR (qPCR)

qPCR was used to measure the amount of a specific DNA fragment with high accuracy. The amount of DNA present at the end of each single PCR cycle was detected by measuring the fluorescence of SYBR-Green (Roche). SYBR-Green is a dye that shows fluorescence when bound to DNA double helices, but not in solution (excitation at 509nm, emission at 526nm). Therefore, the intensity of the fluorescence signal allows direct measurement of the amount of DNA present in a sample. qPCR reactions were performed in 0.1ml tubes, the reaction volume was 20µl. The reaction contained 4µl of DNA sample and 16µl of master mix. The master mix contained 4pmol of the forward and the reverse primer, 0.25µl of a 1:400000 SYBR-Green stock solution in DMSO, 0.4U HotStarTaq-polymerase (Qiagen) and premix. Premix consisted of $MgCl_2$ (to adjust a final concentration of 2.5mM in the qPCR reaction), dNTPs (final concentration 0.2mM in the qPCR reaction) and 10 x PCR buffer (Qiagen; 1 x final concentration in the qPCR reaction). SYBR-Green was thawed in the dark. qPCR was performed in a Rotor-Gene RG3000 system (Corbett Research). SYBR-Green was excited at 480nm; fluorescence was recorded at 510nm. Data were evaluated by analyzing the data with the comparative quantitation module of the RotorGene analysis software. The obtained data were then further processed with *Microsoft Excel* with respect to the 25fold dilution of the input samples compared to the IP samples (5fold less lysate and 5fold higher dilution of the DNA for the input samples).

IV.2.11 Manipulation and culture of Escherichia coli

IV.2.11.1 Preparation of electrocompetent bacteria

Only electrocompetent cells were used in this work, since the plasmid uptake is increased in comparison to chemical competent cells. For the preparation of electrocompetent bacteria the *E. coli* XL1-blue strain was cultured overnight in SOB medium to an OD_{600} ~ 3. Afterwards the culture was diluted 1:100 in prewarmed (37°C) SOB and grown while vigorous aeration was given through shaking (300rpm). When the culture reached an OD_{600} between 0.4 and 0.6 it was chilled on ice for 15min. Afterwards the cells were centrifuged and resuspended in 400ml ice-cold sterile water. After a second centrifugation step the cells were resuspended in 200ml ice-cold sterile water and centrifuged again. After resuspension in 10ml cold and sterile 10% (v/v) glycerol the cell suspension was transferred to a Falcon tube and centrifuged for a last time. The pellet was then resuspended in 1.5ml cold, sterile 10% (v/v) glycerol and aliquots of 50 to 100µl were stored at -80°C.

IV.2.11.2 Transformation by electroporation

Through electroporation transient membrane pores form in *E. coli* (Neumann and Rosenheck, 1972). To transform electrocompetent *E. coli* about 1ng of plasmid DNA or up to 2µl of a ligation reaction were added to cells thawed on ice. For a background control a ligation reaction where no insert was added was used. The cells were then given in a precooled 0.2cm electroporation cuvette. The cuvettes were toweled on the outside to prevent a short-curcuit and the exposure to electric charge was performed in a micropulser with the program EC2. Immediately after the pulse 800µl of LB medium was added, the cells were transferred to a microtube and incubated at 37°C for 30-60min to allow the antibiotics resistance to develop (enzyme β-lactamase for ampicillin resistance). Thereafter 90µl of the culture were taken and plated on LB_{Amp} for a 1:10 dilution. The remaining cells were spun down (4000rpm, 3min, RT in a microcentrifuge), the supernatant was dumped and the pellet was resuspended in the residual supernatant and also plated on LB_{Amp}. The plates were incubated at 37°C overnight. To check for positive clones single colonies were picked on the next day with a pipette tip, streaked out on a LB_{Amp} plate and of each of those clones a few cells, which remained in the tip were diluted in an appropriate colony PCR mix.

IV.2.11.3 Liquid culture

Single clones were picked and cultured in 5-50ml LB_{Amp} (50µg/ml ampicillin) at 37°C in sterile tubes or Erlenmeyer flasks.

IV.2.12 Manipulation and culture of *S. cerevisiae*

IV.2.12.1 Preparation of competent yeast cells

If yeast cells are treated with alkali cations (e.g. Li^+, Cs^+, K^+) their ability of uptaking linear or circular DNA is induced (Ito et al., 1983). To obtain competent yeast cells 50ml cultures of the respective strain were grown overnight to an OD_{600} of 0.5 to 0.7. The cells were spun down (2000rpm, 5min, RT) and resuspended in 0.5 volume (25ml) sterile H_2O. After a second centrifugation step the cell pellet was washed in 0.1 volume (5ml) LitSORB. The pellet was then resuspended in 360µl LitSORB per 50ml culture and 40µl of boiled Carrier-DNA (salmon sperm DNA, Invitrogen) were added. After mixture 50µl aliquots were taken and stored at -80°C.

IV.2.12.2 Transformation of yeast cells

Competent yeast cells were thawed on ice and 5-10µg of DNA (for plasmid DNA 100-500ng) diluted in a preferably small volume of TE or water were added. Thereafter 330µl of LitPEG (40% w/v PEG 3350 in TELit) were added and the cells were kept for 30 minutes at RT in a rotating shaker. Afterwards 43µl of pure, sterile DMSO were added and the transformation-mixture was incubated for 15min at 42°C. The cells were then spun down (3min, 2000rpm, RT), the supernatant was removed and the cell pellet was resuspended in 100µl sterile H_2O and plated on the respective selective medium. If the marker was antibiotics resistance the cells were incubated in full medium for 1-2 generation times before plating on the respective antibiotic plate. These plates were replica-plated using sterile velvet scarves to reduce the number of false-positive clones.

IV.2.12.3 Liquid culture

Liquid yeast cultures were inoculated from plates with single colonies in the appropriate medium. Small volume cultures (precultures, cultures for DNA-preparation) were incubated in sterile plastic tubes (10ml tubes, culture volume did not exceed 5ml). Higher volume cultures were grown in sterile glass flasks. The flasks were not filled higher than 1/3 of the total volume.

IV.2.12.4 Permanent yeast culture

A stationary growing 2ml yeast culture was mixed with 1ml 50% (w/v) sterile glycerol and separated to two aliquots. The aliquots were then stored at -80°C.

IV.2.13 Protein biochemical methods

IV.2.13.1 Denaturing protein extraction of yeast cells

0.5 to 3 OD of cells were suspended in 1ml cold water. 150µl fresh pretreatment solution (1M β-mercaptoethanol, 1.85M NaOH) were added. The cells were incubated for 15min on ice and afterwards 150µl 55% trichloroacetic acid (TCA) were added and the samples were mixed. After a second incubation step for 10min on ice the cells were spun down for 10min with 13,000rpm at 4°C. After discarding the supernatant completely the pellet was resuspended in 100µl buffer HU (5% SDS, 200mM Tris pH6.8, 1mM EDTA, 2.13mM β-mercaptoethanol, 8M urea, bromophenolblue; store at -20°C) per OD_{600} unit and neutralized with ammonia if the color turned to yellow. Hereafter the samples were incubated for 10min at 65°C mixing to denature the proteins and then spun down for

1min with 13,000rpm at RT to pellet insoluble cell particles. An adequate volume of the supernatant was analyzed in SDS-PAGE.

IV.2.13.2 SDS polyacrylamide gel electrophoresis

To separate proteins according to their molecular weight SDS polyacrylamide gel electrophoresis was used mainly as described by Laemmli (1970). The gel system consisted of a lower separating gel and a upper stacking gel. The higher the molecular weight of the protein of interest, the lower was the percentage of the separating gel.

separating gel	**6%**	**8%**	**10%**	**12.5%**	**14.5%**
H2O	5.5ml	4.82ml	4.2ml	3.3ml	2.68ml
4x Lower Tris	2.5ml	2.5ml	2.5ml	2.5ml	2.5ml
30% Acrylamide (AA) + 0.8% Bis-AA	2.0ml	2.68ml	3.3ml	4.2ml	4.82ml
10% SDS	100µl				
TEMED	5µl				
25% APS	50µl				

stacking gel	**6%**	**4%**
H2O	2.75ml	3.05ml
4x Upper Tris	1.25ml	1.25ml
30% AA + 0.8% bAA	1.00ml	0.65ml
10% SDS	100µl	
TEMED	5µl	
25% APS	50µl	

Gels were run at 140V for 1.5h or until the bromophenolblue band just ran out the gel in 1x electrophoresis buffer. Pre-stained or ColorPlus pre-stained marker (NEB) were used as molecular weight markers.

IV.2.13.3 Western Blot

Gels containing separated proteins were blotted to a PVDF membrane using a Trans-Blot SD Semi-Dry Transfer Cell. The blotting pile consisted of from bottom to top: Two thin 3MM Whatman papers soaked in transfer buffer (25mM Tris, 190mM glycine, 20% methanol, pH8.3), the membrane (Immobilon PSQ 0.2µm, Millipore) (activated first in methanol and then soaked in transfer buffer), the gel and a second time two thin 3MM

Whatman papers soaked in transfer buffer. All Whatman papers were soaked to be only slightly wet and not drippy. To remove air bubbles, which impede the blotting, it was rolled over the whole pile with a Falcon tube and enclosed air was thus pressed out. Blotting was performed at 24V for at least 1h. To monitor the success of blotting the membrane was afterwards stained with Ponceau S.

IV.2.13.4 Ponceau staining

Western blot membranes can be stained with Ponceau S (0.5% Ponceau in 1% acetic acid). The membrane was incubated for 2min in Ponceau staining solution and afterwards destained in H_2O until the protein bands were visible.

IV.2.13.5 Detection of proteins by chemiluminescence

To reduce unspecific signals the membrane was first blocked with blocking solution (5% milk powder in 1x PBST) for 1h at RT or overnight at 4°C while shaking. The membrane was wrapped into a 50ml Falcon tube containing the primary antibody solution (5ml 1% milk powder in 1x PBST, primary antibody in an appropriate dilution). The incubation took place rotating for 1h at RT. Afterwards the membrane was washed two times for 10min in 1xPBST at RT. The incubation with the second antibody, which is fused to horseradish peroxidase (POD), took again place in a Falcon tube in an appropriate dilution in 5ml 1% milk in 1x PBST and was done for 30-45min at RT while rotating. Hereafter the membrane was washed two times for 10min at RT in 1x PBST. POD catalyzes the oxidation of diacylhydrazides via an activated intermediate that decays to the ground state by emission of light in the visible range. After washing the membrane it was put between two sheets of a thin, transparent plastic bag and covered with a liquid film of reaction substrates (BM chemiluminescence blotting substrate (POD), Roche). The PSM bands were marked with a fluorescent pen and the detection followed immediately after addition of the substrate in a LAS-3000 fluorescent reader (Fuji).

References

Abe, T., Sugimura, K., Hosono, Y., Takami, Y., Akita, M., Yoshimura, A., Tada, S., Nakayama, T., Murofushi, H., Okumura, K., et al. (2011). The Histone Chaperone Facilitates Chromatin Transcription (FACT) Protein Maintains Normal Replication Fork Rates. J. Biol. Chem. *286*, 30504–30512.

Adams, C.R., and Kamakaka, R.T. (1999). Chromatin assembly: biochemical identities and genetic redundancy. Curr. Opin. Genet. Dev. *9*, 185–190.

Ahmad, K., and Henikoff, S. (2002). Histone H3 variants specify modes of chromatin assembly. Proc. Natl. Acad. Sci. U. S. A. *99 Suppl 4*, 16477–16484.

Alabert, C., and Groth, A. (2012). Chromatin replication and epigenome maintenance. Nat. Rev. Mol. Cell Biol. *13*, 153–167.

Albert, B., Léger-Silvestre, I., Normand, C., Ostermaier, M.K., Pérez-Fernández, J., Panov, K.I., Zomerdijk, J.C.B.M., Schultz, P., and Gadal, O. (2011). RNA polymerase I-specific subunits promote polymerase clustering to enhance the rRNA gene transcription cycle. J. Cell Biol. *192*, 277–293.

Albert, B., Perez-Fernandez, J., Léger-Silvestre, I., and Gadal, O. (2012). Regulation of ribosomal RNA production by RNA polymerase I: does elongation come first? Genet. Res. Int. *2012*, 276948.

Albert, B., Colleran, C., Léger-Silvestre, I., Berger, A.B., Dez, C., Normand, C., Perez-Fernandez, J., McStay, B., and Gadal, O. (2013). Structure-function analysis of Hmo1 unveils an ancestral organization of HMG-Box factors involved in ribosomal DNA transcription from yeast to human. Nucleic Acids Res. *41*, 10135–10149.

Alberts, B., Bray, D., Lewis, J., Ralf, M., Roberts, K., and Watson, J. (2002). Molecular Biology of the Cell (Garland).

Allan, J., Mitchell, T., Harborne, N., Bohm, L., and Crane-Robinson, C. (1986). Roles of H1 domains in determining higher order chromatin structure and H1 location. J. Mol. Biol. *187*, 591–601.

Allen, C., Büttner, S., Aragon, A.D., Thomas, J.A., Meirelles, O., Jaetao, J.E., Benn, D., Ruby, S.W., Veenhuis, M., Madeo, F., et al. (2006). Isolation of quiescent and nonquiescent cells from yeast stationary-phase cultures. J. Cell Biol. *174*, 89–100.

ALLFREY, V.G., FAULKNER, R., and MIRSKY, A.E. (1964). ACETYLATION AND METHYLATION OF HISTONES AND THEIR POSSIBLE ROLE IN THE REGULATION OF RNA SYNTHESIS. Proc. Natl. Acad. Sci. U. S. A. *51*, 786–794.

Allis, C.D., Berger, S.L., Cote, J., Dent, S., Jenuwien, T., Kouzarides, T., Pillus, L., Reinberg, D., Shi, Y., Shiekhattar, R., et al. (2007). New nomenclature for chromatin-modifying enzymes. Cell *131*, 633–636.

Andersen, J.S., Lam, Y.W., Leung, A.K.L., Ong, S.-E., Lyon, C.E., Lamond, A.I., and Mann, M. (2005). Nucleolar proteome dynamics. Nature *433*, 77–83.

Annunziato, A.T. (2005). Split Decision: What Happens to Nucleosomes during DNA Replication? J. Biol. Chem. *280*, 12065–12068.

Aprikian, P., Moorefield, B., and Reeder, R.H. (2000). TATA binding protein can stimulate core-directed transcription by yeast RNA polymerase I. Mol. Cell. Biol. *20*, 5269–5275.

Aprikian, P., Moorefield, B., and Reeder, R.H. (2001). New model for the yeast RNA polymerase I transcription cycle. Mol. Cell. Biol. *21*, 4847–4855.

Aragon, A.D., Rodriguez, A.L., Meirelles, O., Roy, S., Davidson, G.S., Tapia, P.H., Allen, C., Joe, R., Benn, D., and Werner-Washburne, M. (2008). Characterization of differentiated quiescent and nonquiescent cells in yeast stationary-phase cultures. Mol. Biol. Cell *19*, 1271–1280.

Arents, G., and Moudrianakis, E.N. (1993). Topography of the histone octamer surface: repeating structural motifs utilized in the docking of nucleosomal DNA. Proc. Natl. Acad. Sci. U. S. A. *90*, 10489–10493.

Arents, G., and Moudrianakis, E.N. (1995). The histone fold: a ubiquitous architectural motif utilized in DNA compaction and protein dimerization. Proc. Natl. Acad. Sci. U. S. A. *92*, 11170–11174.

Arents, G., Burlingame, R.W., Wang, B.C., Love, W.E., and Moudrianakis, E.N. (1991). The nucleosomal core histone octamer at 3.1 A resolution: a tripartite protein assembly and a left-handed superhelix. Proc. Natl. Acad. Sci. U. S. A. *88*, 10148–10152.

Azzam, R., Chen, S.L., Shou, W., Mah, A.S., Alexandru, G., Nasmyth, K., Annan, R.S., Carr, S.A., and Deshaies, R.J. (2004). Phosphorylation by cyclin B-Cdk underlies release of mitotic exit activator Cdc14 from the nucleolus. Science *305*, 516–519.

Babl, V. (2012). Chromatin dynamics at the ribosomal DNA locus of the budding yeast Saccharomyces cerevisiae (Regensburg).

Babl, V., Stöckl, U., Tschochner, H., Milkereit, P., and Griesenbeck, J. (2015). Chromatin Endogenous Cleavage (ChEC) as a Method to Quantify Protein Interaction with Genomic DNA in Saccharomyces cerevisiae. Methods Mol. Biol. Clifton NJ *1334*, 219–232.

Baker, L.A., Ueberheide, B.M., Dewell, S., Chait, B.T., Zheng, D., and Allis, C.D. (2013). The Yeast Snt2 Protein Coordinates the Transcriptional Response to Hydrogen Peroxide-Mediated Oxidative Stress. Mol. Cell. Biol. *33*, 3735–3748.

Bannister, A.J., and Kouzarides, T. (2011). Regulation of chromatin by histone modifications. Cell Res. *21*, 381–395.

Bao, Y., and Shen, X. (2007). INO80 subfamily of chromatin remodeling complexes. Mutat. Res. *618*, 18–29.

Bates, D.L., and Thomas, J.O. (1981). Histones H1 and H5: one or two molecules per nucleosome? Nucleic Acids Res. *9*, 5883–5894.

Baxevanis, A.D., and Landsman, D. (1998). Histone Sequence Database: new histone fold family members. Nucleic Acids Res. *26*, 372–375.

Bazett-Jones, D.P., Leblanc, B., Herfort, M., and Moss, T. (1994). Short-range DNA looping by the Xenopus HMG-box transcription factor, xUBF. Science *264*, 1134–1137.

Beckouet, F., Labarre-Mariotte, S., Albert, B., Imazawa, Y., Werner, M., Gadal, O., Nogi, Y., and Thuriaux, P. (2008). Two RNA polymerase I subunits control the binding and release of Rrn3 during transcription. Mol. Cell. Biol. *28*, 1596–1605.

Bedwell, G.J., Appling, F.D., Anderson, S.J., and Schneider, D.A. (2012). Efficient transcription by RNA polymerase I using recombinant core factor. Gene *492*, 94–99.

Belotserkovskaya, R., Oh, S., Bondarenko, V.A., Orphanides, G., Studitsky, V.M., and Reinberg, D. (2003). FACT facilitates transcription-dependent nucleosome alteration. Science *301*, 1090–1093.

Berger, A.B., Decourty, L., Badis, G., Nehrbass, U., Jacquier, A., and Gadal, O. (2007). Hmo1 is required for TOR-dependent regulation of ribosomal protein gene transcription. Mol. Cell. Biol. *27*, 8015–8026.

Bermejo, R., Capra, T., Gonzalez-Huici, V., Fachinetti, D., Cocito, A., Natoli, G., Katou, Y., Mori, H., Kurokawa, K., Shirahige, K., et al. (2009). Genome-organizing factors Top2 and Hmo1 prevent chromosome fragility at sites of S phase transcription. Cell *138*, 870–884.

Beullens, M., Mbonyi, K., Geerts, L., Gladines, D., Detremerie, K., Jans, A.W., and Thevelein, J.M. (1988). Studies on the mechanism of the glucose-induced cAMP signal in glycolysis and glucose repression mutants of the yeast Saccharomyces cerevisiae. Eur. J. Biochem. FEBS *172*, 227–231.

Bier, M., Fath, S., and Tschochner, H. (2004). The composition of the RNA polymerase I transcription machinery switches from initiation to elongation mode. FEBS Lett. *564*, 41–46.

Blank, T.A., and Becker, P.B. (1995). Electrostatic Mechanism of Nucleosome Spacing. J. Mol. Biol. *252*, 305–313.

Blattner, C., Jennebach, S., Herzog, F., Mayer, A., Cheung, A.C.M., Witte, G., Lorenzen, K., Hopfner, K.-P., Heck, A.J.R., Aebersold, R., et al. (2011). Molecular basis of Rrn3-regulated RNA polymerase I initiation and cell growth. Genes Dev. *25*, 2093–2105.

Bodem, J., Dobreva, G., Hoffmann-Rohrer, U., Iben, S., Zentgraf, H., Delius, H., Vingron, M., and Grummt, I. (2000). TIF-IA, the factor mediating growth-dependent control of ribosomal RNA synthesis, is the mammalian homolog of yeast Rrn3p. EMBO Rep. *1*, 171–175.

Boeckmann, L., Takahashi, Y., Au, W.-C., Mishra, P.K., Choy, J.S., Dawson, A.R., Szeto, M.Y., Waybright, T.J., Heger, C., McAndrew, C., et al. (2013). Phosphorylation of centromeric histone H3 variant regulates chromosome segregation in Saccharomyces cerevisiae. Mol. Biol. Cell *24*, 2034–2044.

Bolzer, A., Kreth, G., Solovei, I., Koehler, D., Saracoglu, K., Fauth, C., Müller, S., Eils, R., Cremer, C., Speicher, M.R., et al. (2005). Three-dimensional maps of all chromosomes in human male fibroblast nuclei and prometaphase rosettes. PLoS Biol. *3*, e157.

Bönisch, C., and Hake, S.B. (2012). Histone H2A variants in nucleosomes and chromatin: more or less stable? Nucleic Acids Res. *40*, 10719–10741.

Bordi, L., Cioci, F., and Camilloni, G. (2001). In Vivo Binding and Hierarchy of Assembly of the Yeast RNA Polymerase I Transcription Factors. Mol. Biol. Cell *12*, 753–760.

Borkhardt, B., and Nielsen, O.F. (1981). An electron microscopic analysis of transcription of nucleolar chromatin isolated from Tetrahymena pyriformis. Chromosoma *84*, 131–143.

Boucherie, H. (1985). Protein synthesis during transition and stationary phases under glucose limitation in Saccharomyces cerevisiae. J. Bacteriol. *161*, 385–392.

Brewer, B.J., and Fangman, W.L. (1988). A replication fork barrier at the 3' end of yeast ribosomal RNA genes. Cell *55*, 637–643.

Brewer, B.J., Lockshon, D., and Fangman, W.L. (1992). The arrest of replication forks in the rDNA of yeast occurs independently of transcription. Cell *71*, 267–276.

Brownell, J.E., Zhou, J., Ranalli, T., Kobayashi, R., Edmondson, D.G., Roth, S.Y., and Allis, C.D. (1996). Tetrahymena histone acetyltransferase A: a homolog to yeast Gcn5p linking histone acetylation to gene activation. Cell *84*, 843–851.

Bryant, J.M., Govin, J., Zhang, L., Donahue, G., Pugh, B.F., and Berger, S.L. (2012). The linker histone plays a dual role during gametogenesis in Saccharomyces cerevisiae. Mol. Cell. Biol. *32*, 2771–2783.

Bryk, M., Banerjee, M., Murphy, M., Knudsen, K.E., Garfinkel, D.J., and Curcio, M.J. (1997). Transcriptional silencing of Ty1 elements in the RDN1 locus of yeast. Genes Dev. *11*, 255–269.

Buck, S.W., Gallo, C.M., and Smith, J.S. (2004). Diversity in the Sir2 family of protein deacetylases. J. Leukoc. Biol. *75*, 939–950.

Busti, S., Coccetti, P., Alberghina, L., and Vanoni, M. (2010). Glucose Signaling-Mediated Coordination of Cell Growth and Cell Cycle in Saccharomyces Cerevisiae. Sensors *10*, 6195–6240.

Cameroni, E., Hulo, N., Roosen, J., Winderickx, J., and De Virgilio, C. (2004). The novel yeast PAS kinase Rim 15 orchestrates G0-associated antioxidant defense mechanisms. Cell Cycle Georget. Tex *3*, 462–468.

Canzio, D., Chang, E.Y., Shankar, S., Kuchenbecker, K.M., Simon, M.D., Madhani, H.D., Narlikar, G.J., and Al-Sady, B. (2011). Chromodomain-Mediated Oligomerization of HP1 Suggests a Nucleosome-Bridging Mechanism for Heterochromatin Assembly. Mol. Cell *41*, 67–81.

Carmen, A.A., Rundlett, S.E., and Grunstein, M. (1996). HDA1 and HDA3 are components of a yeast histone deacetylase (HDA) complex. J. Biol. Chem. *271*, 15837–15844.

Carroll, A.S., and O'Shea, E.K. (2002). Pho85 and signaling environmental conditions. Trends Biochem. Sci. *27*, 87–93.

Carrozza, M.J., Li, B., Florens, L., Suganuma, T., Swanson, S.K., Lee, K.K., Shia, W.-J., Anderson, S., Yates, J., Washburn, M.P., et al. (2005). Histone H3 methylation by Set2 directs deacetylation of coding regions by Rpd3S to suppress spurious intragenic transcription. Cell *123*, 581–592.

Casperson, G.F., Walker, N., Brasier, A.R., and Bourne, H.R. (1983). A guanine nucleotide-sensitive adenylate cyclase in the yeast Saccharomyces cerevisiae. J. Biol. Chem. *258*, 7911–7914.

Casperson, G.F., Walker, N., and Bourne, H.R. (1985). Isolation of the gene encoding adenylate cyclase in Saccharomyces cerevisiae. Proc. Natl. Acad. Sci. U. S. A. *82*, 5060–5063.

Chang, Y.-Y., Juhász, G., Goraksha-Hicks, P., Arsham, A.M., Mallin, D.R., Muller, L.K., and Neufeld, T.P. (2009). Nutrient-dependent regulation of autophagy through the target of rapamycin pathway. Biochem. Soc. Trans. *37*, 232–236.

Chen, X.-F., Kuryan, B., Kitada, T., Tran, N., Li, J.-Y., Kurdistani, S., Grunstein, M., Li, B., and Carey, M. (2012). The rpd3 core complex is a chromatin stabilization module. Curr. Biol. CB *22*, 56–63.

Choder, M. (1991). A general topoisomerase I-dependent transcriptional repression in the stationary phase in yeast. Genes Dev. *5*, 2315–2326.

Choder, M. (1993). A growth rate-limiting process in the last growth phase of the yeast life cycle involves RPB4, a subunit of RNA polymerase II. J. Bacteriol. *175*, 6358–6363.

Choi, J.K., and Howe, L.J. (2009). Histone acetylation: truth of consequences? Biochem. Cell Biol. Biochim. Biol. Cell. *87*, 139–150.

Choi, C.H., Hiromura, M., and Usheva, A. (2003). Transcription factor IIB acetylates itself to regulate transcription. Nature *424*, 965–969.

Choudhary, C., Kumar, C., Gnad, F., Nielsen, M.L., Rehman, M., Walther, T.C., Olsen, J.V., and Mann, M. (2009). Lysine acetylation targets protein complexes and co-regulates major cellular functions. Science *325*, 834–840.

Clapier, C.R., and Cairns, B.R. (2009). The biology of chromatin remodeling complexes. Annu. Rev. Biochem. *78*, 273–304.

Claypool, J.A., French, S.L., Johzuka, K., Eliason, K., Vu, L., Dodd, J.A., Beyer, A.L., and Nomura, M. (2004). Tor Pathway Regulates Rrn3p-Dependent Recruitment of Yeast RNA Polymerase I to the Promoter but Does Not Participate in Alteration of the Number of Active Genes. Mol. Biol. Cell *15*, 946–956.

Collas, P. (2010). The current state of chromatin immunoprecipitation. Mol. Biotechnol. *45*, 87–100.

Comai, L., Song, Y., Tan, C., and Bui, T. (2000). Inhibition of RNA polymerase I transcription in differentiated myeloid leukemia cells by inactivation of selectivity factor 1. Cell Growth Differ. Mol. Biol. J. Am. Assoc. Cancer Res. *11*, 63–70.

Conconi, A. (1987). Correlation between gene activity and chromatin structure in mouse erythroleukemia cells. Swiss Federal Institute of Technology of Zurich.

Conconi, A. (2005). The yeast rDNA locus: a model system to study DNA repair in chromatin. DNA Repair *4*, 897–908.

Conconi, A., Widmer, R.M., Koller, T., and Sogo, J.M. (1989). Two different chromatin structures coexist in ribosomal RNA genes throughout the cell cycle. Cell *57*, 753–761.

Conconi, A., Bespalov, V.A., and Smerdon, M.J. (2002). Transcription-coupled repair in RNA polymerase I-transcribed genes of yeast. Proc. Natl. Acad. Sci. U. S. A. *99*, 649–654.

Crabtree, H.G. (1929). Observations on the carbohydrate metabolism of tumours. Biochem. J. *23*, 536–545.

Cramer, P., Armache, K.-J., Baumli, S., Benkert, S., Brueckner, F., Buchen, C., Damsma, G.E., Dengl, S., Geiger, S.R., Jasiak, A.J., et al. (2008). Structure of eukaryotic RNA polymerases. Annu. Rev. Biophys. *37*, 337–352.

Crespo, J.L., Powers, T., Fowler, B., and Hall, M.N. (2002). The TOR-controlled transcription activators GLN3, RTG1, and RTG3 are regulated in response to intracellular levels of glutamine. Proc. Natl. Acad. Sci. U. S. A. *99*, 6784–6789.

Culotta, V., and Sollner-Webb, B. (1988). Sites of topoisomerase I action on X. laevis ribosomal chromatin: transcriptionally active rDNA has an approximately 200 bp repeating structure. Cell *52*, 585–597.

Cutter, A.R., and Hayes, J.J. (2015). A brief review of nucleosome structure. FEBS Lett. *589*, 2914–2922.

Cyrne, L., Martins, L., Fernandes, L., and Marinho, H.S. (2003). Regulation of antioxidant enzymes gene expression in the yeast Saccharomyces cerevisiae during stationary phase. Free Radic. Biol. Med. *34*, 385–393.

Daban, J.-R. (2011). Electron microscopy and atomic force microscopy studies of chromatin and metaphase chromosome structure. Micron Oxf. Engl. 1993 *42*, 733–750.

Dame, R.T. (2005). The role of nucleoid-associated proteins in the organization and compaction of bacterial chromatin. Mol. Microbiol. *56*, 858–870.

Dammann, R., Lucchini, R., Koller, T., and Sogo, J.M. (1993). Chromatin structures and transcription of rDNA in yeast Saccharomyces cerevisiae. Nucleic Acids Res. *21*, 2331–2338.

Dammann, R., Lucchini, R., Koller, T., and Sogo, J.M. (1995). Transcription in the yeast rRNA gene locus: distribution of the active gene copies and chromatin structure of their flanking regulatory sequences. Mol. Cell. Biol. *15*, 5294–5303.

Davey, C.A., Sargent, D.F., Luger, K., Maeder, A.W., and Richmond, T.J. (2002). Solvent mediated interactions in the structure of the nucleosome core particle at 1.9 a resolution. J. Mol. Biol. *319*, 1097–1113.

Davidson, G.S., Joe, R.M., Roy, S., Meirelles, O., Allen, C.P., Wilson, M.R., Tapia, P.H., Manzanilla, E.E., Dodson, A.E., Chakraborty, S., et al. (2011). The proteomics of quiescent and nonquiescent cell differentiation in yeast stationary-phase cultures. Mol. Biol. Cell *22*, 988–998.

Davies, H.G. (1967). Fine structure of heterochromatin in certain cell nuclei. Nature *214*, 208–210.

Davis, A.H., Reudelhuber, T.L., and Garrard, W.T. (1983). Varigated chromatin structures of mouse ribosomal RNA genes. J. Mol. Biol. *167*, 133–155.

De Nobel, J.G., Klis, F.M., Munnik, T., Priem, J., and van den Ende, H. (1990). An assay of relative cell wall porosity in Saccharomyces cerevisiae, Kluyveromyces lactis and Schizosaccharomyces pombe. Yeast Chichester Engl. *6*, 483–490.

De Virgilio, C. (2012). The essence of yeast quiescence. FEMS Microbiol. Rev. *36*, 306–339.

De Virgilio, C., and Loewith, R. (2006a). Cell growth control: little eukaryotes make big contributions. Oncogene *25*, 6392–6415.

De Virgilio, C., and Loewith, R. (2006b). The TOR signalling network from yeast to man. Int. J. Biochem. Cell Biol. *38*, 1476–1481.

Dekker, J., Rippe, K., Dekker, M., and Kleckner, N. (2002). Capturing chromosome conformation. Science *295*, 1306–1311.

DeLange, R.J., Fambrough, D.M., Smith, E.L., and Bonner, J. (1969). Calf and pea histone IV. 3. Complete amino acid sequence of pea seedling histone IV; comparison with the homologous calf thymus histone. J. Biol. Chem. *244*, 5669–5679.

DeRisi, J.L., Iyer, V.R., and Brown, P.O. (1997). Exploring the metabolic and genetic control of gene expression on a genomic scale. Science *278*, 680–686.

Dion, M.F., Altschuler, S.J., Wu, L.F., and Rando, O.J. (2005). Genomic characterization reveals a simple histone H4 acetylation code. Proc. Natl. Acad. Sci. U. S. A. *102*, 5501–5506.

Dorigo, B., Schalch, T., Bystricky, K., and Richmond, T.J. (2003). Chromatin fiber folding: requirement for the histone H4 N-terminal tail. J. Mol. Biol. *327*, 85–96.

Dorigo, B., Schalch, T., Kulangara, A., Duda, S., Schroeder, R.R., and Richmond, T.J. (2004). Nucleosome arrays reveal the two-start organization of the chromatin fiber. Science *306*, 1571–1573.

Downs, J.A., Kosmidou, E., Morgan, A., and Jackson, S.P. (2003). Suppression of Homologous Recombination by the Saccharomyces cerevisiae Linker Histone. Mol. Cell *11*, 1685–1692.

Drazic, A., Myklebust, L.M., Ree, R., and Arnesen, T. (2016). The world of protein acetylation. Biochim. Biophys. Acta BBA - Proteins Proteomics *1864*, 1372–1401.

Drew, H.R., and Travers, A.A. (1985). DNA bending and its relation to nucleosome positioning. J. Mol. Biol. *186*, 773–790.

Ehrenhofer-Murray, A.E. (2004). Chromatin dynamics at DNA replication, transcription and repair. Eur. J. Biochem. FEBS *271*, 2335–2349.

Eisenmann, D.M., Dollard, C., and Winston, F. (1989). SPT15, the gene encoding the yeast TATA binding factor TFIID, is required for normal transcription initiation in vivo. Cell *58*, 1183–1191.

Elion, E.A., and Warner, J.R. (1984). The major promoter element of rRNA transcription in yeast lies 2 kb upstream. Cell *39*, 663–673.

Elion, E.A., and Warner, J.R. (1986). An RNA polymerase I enhancer in Saccharomyces cerevisiae. Mol. Cell. Biol. *6*, 2089–2097.

Elsaesser, S.J., and Allis, C.D. (2010). HIRA and Daxx constitute two independent histone H3.3-containing predeposition complexes. Cold Spring Harb. Symp. Quant. Biol. *75*, 27–34.

Engel, C., Sainsbury, S., Cheung, A.C., Kostrewa, D., and Cramer, P. (2013). RNA polymerase I structure and transcription regulation. Nature *502*, 650–655.

Engel, C., Plitzko, J., and Cramer, P. (2016). RNA polymerase I-Rrn3 complex at 4.8 Å resolution. Nat. Commun. *7*, 12129.

Fahy, D., Conconi, A., and Smerdon, M.J. (2005). Rapid changes in transcription and chromatin structure of ribosomal genes in yeast during growth phase transitions. Exp. Cell Res. *305*, 365–373.

Fan, Y., Nikitina, T., Morin-Kensicki, E.M., Zhao, J., Magnuson, T.R., Woodcock, C.L., and Skoultchi, A.I. (2003). H1 linker histones are essential for mouse development and affect nucleosome spacing in vivo. Mol. Cell. Biol. *23*, 4559–4572.

Fan, Y., Nikitina, T., Zhao, J., Fleury, T.J., Bhattacharyya, R., Bouhassira, E.E., Stein, A., Woodcock, C.L., and Skoultchi, A.I. (2005). Histone H1 depletion in mammals alters global chromatin structure but causes specific changes in gene regulation. Cell *123*, 1199–1212.

Fangman, W.L., and Brewer, B.J. (1991). Activation of replication origins within yeast chromosomes. Annu. Rev. Cell Biol. *7*, 375–402.

Fatica, A., and Tollervey, D. (2002). Making ribosomes. Curr. Opin. Cell Biol. *14*, 313–318.

Fernández-Tornero, C., Moreno-Morcillo, M., Rashid, U.J., Taylor, N.M.I., Ruiz, F.M., Gruene, T., Legrand, P., Steuerwald, U., and Müller, C.W. (2013). Crystal structure of the 14-subunit RNA polymerase I. Nature *502*, 644–649.

Field, J., Nikawa, J., Broek, D., MacDonald, B., Rodgers, L., Wilson, I.A., Lerner, R.A., and Wigler, M. (1988). Purification of a RAS-responsive adenylyl cyclase complex from Saccharomyces cerevisiae by use of an epitope addition method. Mol. Cell. Biol. *8*, 2159–2165.

Finch, J.T., and Klug, A. (1976). Solenoidal model for superstructure in chromatin. Proc. Natl. Acad. Sci. U. S. A. *73*, 1897–1901.

Foe, V.E., Wilkinson, L.E., and Laird, C.D. (1976). Comparative organization of active transcription units in Oncopeltus fasciatus. Cell *9*, 131–146.

Foltz, D.R., Jansen, L.E.T., Bailey, A.O., Yates, J.R., Bassett, E.A., Wood, S., Black, B.E., and Cleveland, D.W. (2009). Centromere-specific assembly of CENP-a nucleosomes is mediated by HJURP. Cell *137*, 472–484.

François, J., and Parrou, J.L. (2001). Reserve carbohydrates metabolism in the yeast Saccharomyces cerevisiae. FEMS Microbiol. Rev. *25*, 125–145.

Fraser, J., Williamson, I., Bickmore, W.A., and Dostie, J. (2015). An Overview of Genome Organization and How We Got There: from FISH to Hi-C. Microbiol. Mol. Biol. Rev. MMBR *79*, 347–372.

Freidkin, I., and Katcoff, D.J. (2001). Specific distribution of the Saccharomyces cerevisiae linker histone homolog HHO1p in the chromatin. Nucleic Acids Res. *29*, 4043–4051.

French, S.L., Osheim, Y.N., Cioci, F., Nomura, M., and Beyer, A.L. (2003). In exponentially growing Saccharomyces cerevisiae cells, rRNA synthesis is determined by the summed RNA polymerase I loading rate rather than by the number of active genes. Mol. Cell. Biol. *23*, 1558–1568.

Fromont-Racine, M., Senger, B., Saveanu, C., and Fasiolo, F. (2003). Ribosome assembly in eukaryotes. Gene *313*, 17–42.

Fuge, E.K., Braun, E.L., and Werner-Washburne, M. (1994). Protein synthesis in long-term stationary-phase cultures of Saccharomyces cerevisiae. J. Bacteriol. *176*, 5802–5813.

Fussner, E., Ching, R.W., and Bazett-Jones, D.P. (2011). Living without 30nm chromatin fibers. Trends Biochem. Sci. *36*, 1–6.

Gadal, O., Labarre, S., Boschiero, C., and Thuriaux, P. (2002). Hmo1, an HMG-box protein, belongs to the yeast ribosomal DNA transcription system. EMBO J. *21*, 5498–5507.

Galdieri, L., Mehrotra, S., Yu, S., and Vancura, A. (2010). Transcriptional regulation in yeast during diauxic shift and stationary phase. Omics J. Integr. Biol. *14*, 629–638.

Gancedo, J.M. (1998). Yeast carbon catabolite repression. Microbiol. Mol. Biol. Rev. MMBR *62*, 334–361.

Gancedo, J.M. (2008). The early steps of glucose signalling in yeast. FEMS Microbiol. Rev. *32*, 673–704.

Ganguli, D., Chereji, R.V., Iben, J.R., Cole, H.A., and Clark, D.J. (2014). RSC-dependent constructive and destructive interference between opposing arrays of phased nucleosomes in yeast. Genome Res. *24*, 1637–1649.

Ganley, A.R.D., Hayashi, K., Horiuchi, T., and Kobayashi, T. (2005). Identifying gene-independent noncoding functional elements in the yeast ribosomal DNA by phylogenetic footprinting. Proc. Natl. Acad. Sci. U. S. A. *102*, 11787–11792.

Gasch, A.P., Spellman, P.T., Kao, C.M., Carmel-Harel, O., Eisen, M.B., Storz, G., Botstein, D., and Brown, P.O. (2000). Genomic expression programs in the response of yeast cells to environmental changes. Mol. Biol. Cell *11*, 4241–4257.

Gasser, S.M., and Laemmli, U.K. (1987). A glimpse at chromosomal order. Trends Genet. *3*, 16–22.

Geiger, S.R., Lorenzen, K., Schreieck, A., Hanecker, P., Kostrewa, D., Heck, A.J.R., and Cramer, P. (2010). RNA polymerase I contains a TFIIF-related DNA-binding subcomplex. Mol. Cell *39*, 583–594.

Georgieva, M., Roguev, A., Balashev, K., Zlatanova, J., and Miloshev, G. (2012). Hho1p, the linker histone of Saccharomyces cerevisiae, is important for the proper chromatin organization in vivo. Biochim. Biophys. Acta *1819*, 366–374.

Gilmour, D.S., and Lis, J.T. (1985). In vivo interactions of RNA polymerase II with genes of Drosophila melanogaster. Mol. Cell. Biol. *5*, 2009–2018.

Glozak, M.A., Sengupta, N., Zhang, X., and Seto, E. (2005). Acetylation and deacetylation of non-histone proteins. Gene *363*, 15–23.

Goetze, H., Wittner, M., Hamperl, S., Hondele, M., Merz, K., Stoeckl, U., and Griesenbeck, J. (2010). Alternative chromatin structures of the 35S rRNA genes in Saccharomyces cerevisiae provide a molecular basis for the selective recruitment of RNA polymerases I and II. Mol. Cell. Biol. *30*, 2028–2045.

Govind, C.K., Qiu, H., Ginsburg, D.S., Ruan, C., Hofmeyer, K., Hu, C., Swaminathan, V., Workman, J.L., Li, B., and Hinnebusch, A.G. (2010). Phosphorylated Pol II CTD Recruits Multiple HDACs, Including Rpd3C(S), for Methylation-Dependent Deacetylation of ORF Nucleosomes. Mol. Cell *39*, 234–246.

Granot, D., and Snyder, M. (1991). Glucose induces cAMP-independent growth-related changes in stationary-phase cells of Saccharomyces cerevisiae. Proc. Natl. Acad. Sci. U. S. A. *88*, 5724–5728.

Granot, D., and Snyder, M. (1993). Carbon source induces growth of stationary phase yeast cells, independent of carbon source metabolism. Yeast Chichester Engl. *9*, 465–479.

Grant, P.A., Duggan, L., Côté, J., Roberts, S.M., Brownell, J.E., Candau, R., Ohba, R., Owen-Hughes, T., Allis, C.D., Winston, F., et al. (1997). Yeast Gcn5 functions in two multisubunit complexes to acetylate nucleosomal histones: characterization of an Ada complex and the SAGA (Spt/Ada) complex. Genes Dev. *11*, 1640–1650.

Gray, J.V., Petsko, G.A., Johnston, G.C., Ringe, D., Singer, R.A., and Werner-Washburne, M. (2004). "Sleeping beauty": quiescence in Saccharomyces cerevisiae. Microbiol. Mol. Biol. Rev. MMBR *68*, 187–206.

Gresham, D., Boer, V.M., Caudy, A., Ziv, N., Brandt, N.J., Storey, J.D., and Botstein, D. (2011). System-level analysis of genes and functions affecting survival during nutrient starvation in Saccharomyces cerevisiae. Genetics *187*, 299–317.

Griesenbeck, J., Wittner, M., Charton, R., and Conconi, A. (2012). Chromatin endogenous cleavage and psoralen crosslinking assays to analyze rRNA gene chromatin in vivo. Methods Mol. Biol. Clifton NJ *809*, 291–301.

Grigoryev, S.A., Arya, G., Correll, S., Woodcock, C.L., and Schlick, T. (2009). Evidence for heteromorphic chromatin fibers from analysis of nucleosome interactions. Proc. Natl. Acad. Sci. U. S. A. *106*, 13317–13322.

Groth, A., Rocha, W., Verreault, A., and Almouzni, G. (2007a). Chromatin Challenges during DNA Replication and Repair. Cell *128*, 721–733.

Groth, A., Corpet, A., Cook, A.J.L., Roche, D., Bartek, J., Lukas, J., and Almouzni, G. (2007b). Regulation of Replication Fork Progression Through Histone Supply and Demand. Science *318*, 1928–1931.

Grummt, I. (2003). Life on a planet of its own: regulation of RNA polymerase I transcription in the nucleolus. Genes Dev. *17*, 1691–1702.

Grunstein, M. (1990). Histone function in transcription. Annu. Rev. Cell Biol. *6*, 643–678.

Grunstein, M. (1997). Histone acetylation in chromatin structure and transcription. Nature *389*, 349–352.

Gruss, C., Wu, J., Koller, T., and Sogo, J.M. (1993). Disruption of the nucleosomes at the replication fork. EMBO J. *12*, 4533–4545.

Haeusler, R.A., and Engelke, D.R. (2006). Spatial organization of transcription by RNA polymerase III. Nucleic Acids Res. *34*, 4826–4836.

Hall, D.B., Wade, J.T., and Struhl, K. (2006). An HMG protein, Hmo1, associates with promoters of many ribosomal protein genes and throughout the rRNA gene locus in Saccharomyces cerevisiae. Mol. Cell. Biol. *26*, 3672–3679.

Hamperl, S., Wittner, M., Babl, V., Perez-Fernandez, J., Tschochner, H., and Griesenbeck, J. (2013). Chromatin states at ribosomal DNA loci. Biochim. Biophys. Acta *1829*, 405–417.

Hamperl, S., Brown, C.R., Garea, A.V., Perez-Fernandez, J., Bruckmann, A., Huber, K., Wittner, M., Babl, V., Stoeckl, U., Deutzmann, R., et al. (2014). Compositional and structural analysis of selected chromosomal domains from Saccharomyces cerevisiae. Nucleic Acids Res. *42*, e2.

Han, M., and Grunstein, M. (1988). Nucleosome loss activates yeast downstream promoters in vivo. Cell *55*, 1137–1145.

Hanada, K., Song, C.Z., Yamamoto, K., Yano, K., Maeda, Y., Yamaguchi, K., and Muramatsu, M. (1996). RNA polymerase I associated factor 53 binds to the nucleolar transcription factor UBF and functions in specific rDNA transcription. EMBO J. *15*, 2217–2226.

Hannig, K. (2015). Net1 - ein modular aufgebautes und multifunktionales Protein im Nukleolus der Hefe Saccharomyces cerevisiae. Universität Regensburg.

Hansen, J.C. (2002). Conformational Dynamics of the Chromatin Fiber in Solution: Determinants, Mechanisms, and Functions. Annu. Rev. Biophys. Biomol. Struct. *31*, 361–392.

Hanson, C.V., Shen, C.K., and Hearst, J.E. (1976). Cross-linking of DNA in situ as a probe for chromatin structure. Science *193*, 62–64.

Hardie, D.G. (2007). AMP-activated/SNF1 protein kinases: conserved guardians of cellular energy. Nat. Rev. Mol. Cell Biol. *8*, 774–785.

Hartley, P.D., and Madhani, H.D. (2009). Mechanisms that specify promoter nucleosome location and identity. Cell *137*, 445–458.

Hassan, A.H., Neely, K.E., and Workman, J.L. (2001). Histone acetyltransferase complexes stabilize swi/snf binding to promoter nucleosomes. Cell *104*, 817–827.

Hassan, A.H., Prochasson, P., Neely, K.E., Galasinski, S.C., Chandy, M., Carrozza, M.J., and Workman, J.L. (2002). Function and selectivity of bromodomains in anchoring chromatin-modifying complexes to promoter nucleosomes. Cell *111*, 369–379.

Hayes, J.J., and Wolffe, A.P. (1993). Preferential and asymmetric interaction of linker histones with 5S DNA in the nucleosome. Proc. Natl. Acad. Sci. U. S. A. *90*, 6415–6419.

He, C., and Klionsky, D.J. (2009). Regulation mechanisms and signaling pathways of autophagy. Annu. Rev. Genet. *43*, 67–93.

Hedbacker, K., and Carlson, M. (2008). SNF1/AMPK pathways in yeast. Front. Biosci. J. Virtual Libr. *13*, 2408–2420.

Heitman, J., Movva, N.R., and Hall, M.N. (1991). Targets for cell cycle arrest by the immunosuppressant rapamycin in yeast. Science *253*, 905–909.

Heix, J., Vente, A., Voit, R., Budde, A., Michaelidis, T.M., and Grummt, I. (1998). Mitotic silencing of human rRNA synthesis: inactivation of the promoter selectivity factor SL1 by cdc2/cyclin B-mediated phosphorylation. EMBO J. *17*, 7373–7381.

Henikoff, S., and Ahmad, K. (2005). Assembly of Variant Histones into Chromatin. Annu. Rev. Cell Dev. Biol. *21*, 133–153.

Hereford, L., Fahrner, K., Woolford, J., Rosbash, M., and Kaback, D.B. (1979). Isolation of yeast histone genes H2A and H2B. Cell *18*, 1261–1271.

Herman, P.K. (2002). Stationary phase in yeast. Curr. Opin. Microbiol. *5*, 602–607.

Hernandez-Verdun, D. (2006). Nucleolus: from structure to dynamics. Histochem. Cell Biol. *125*, 127–137.

Hewish, D.R., and Burgoyne, L.A. (1973). Chromatin sub-structure. The digestion of chromatin DNA at regularly spaced sites by a nuclear deoxyribonuclease. Biochem. Biophys. Res. Commun. *52*, 504–510.

Hilt, W., and Wolf, D.H. (1992). Stress-induced proteolysis in yeast. Mol. Microbiol. *6*, 2437–2442.

Hiltunen, J.K., Mursula, A.M., Rottensteiner, H., Wierenga, R.K., Kastaniotis, A.J., and Gurvitz, A. (2003). The biochemistry of peroxisomal beta-oxidation in the yeast Saccharomyces cerevisiae. FEMS Microbiol. Rev. *27*, 35–64.

van Holde, K.E. (1989). Chromatin (New York, NY: Springer New York).

Holt, L.J., Tuch, B.B., Villén, J., Johnson, A.D., Gygi, S.P., and Morgan, D.O. (2009). Global analysis of Cdk1 substrate phosphorylation sites provides insights into evolution. Science *325*, 1682–1686.

Hontz, R.D., French, S.L., Oakes, M.L., Tongaonkar, P., Nomura, M., Beyer, A.L., and Smith, J.S. (2008). Transcription of multiple yeast ribosomal DNA genes requires targeting of UAF to the promoter by Uaf30. Mol. Cell. Biol. *28*, 6709–6719.

Hoppe, S., Bierhoff, H., Cado, I., Weber, A., Tiebe, M., Grummt, I., and Voit, R. (2009). AMP-activated protein kinase adapts rRNA synthesis to cellular energy supply. Proc. Natl. Acad. Sci. *106*, 17781–17786.

Horn, P.J., and Peterson, C.L. (2002). Molecular biology. Chromatin higher order folding--wrapping up transcription. Science *297*, 1824–1827.

Hsieh, F.-K., Kulaeva, O.I., Patel, S.S., Dyer, P.N., Luger, K., Reinberg, D., and Studitsky, V.M. (2013). Histone chaperone FACT action during transcription through chromatin by RNA polymerase II. Proc. Natl. Acad. Sci. U. S. A. *110*, 7654–7659.

Huang, J., and Moazed, D. (2003). Association of the RENT complex with nontranscribed and coding regions of rDNA and a regional requirement for the replication fork block protein Fob1 in rDNA silencing. Genes Dev. *17*, 2162–2176.

Huber, A., Bodenmiller, B., Uotila, A., Stahl, M., Wanka, S., Gerrits, B., Aebersold, R., and Loewith, R. (2009). Characterization of the rapamycin-sensitive phosphoproteome reveals that Sch9 is a central coordinator of protein synthesis. Genes Dev. *23*, 1929–1943.

Huber, A., French, S.L., Tekotte, H., Yerlikaya, S., Stahl, M., Perepelkina, M.P., Tyers, M., Rougemont, J., Beyer, A.L., and Loewith, R. (2011). Sch9 regulates ribosome biogenesis via Stb3, Dot6 and Tod6 and the histone deacetylase complex RPD3L. EMBO J. *30*, 3052–3064.

Huberts, D.H.E.W., Niebel, B., and Heinemann, M. (2012). A flux-sensing mechanism could regulate the switch between respiration and fermentation. FEMS Yeast Res. *12*, 118–128.

Huet, J., Buhler, J.M., Sentenac, A., and Fromageot, P. (1975). Dissociation of two polypeptide chains from yeast RNA polymerase A. Proc. Natl. Acad. Sci. U. S. A. *72*, 3034–3038.

Ide, S., Miyazaki, T., Maki, H., and Kobayashi, T. (2010). Abundance of ribosomal RNA gene copies maintains genome integrity. Science *327*, 693–696.

Ito, H., Fukuda, Y., Murata, K., and Kimura, A. (1983). Transformation of intact yeast cells treated with alkali cations. J. Bacteriol. *153*, 163–168.

Jackson, V. (1978). Studies on histone organization in the nucleosome using formaldehyde as a reversible cross-linking agent. Cell *15*, 945–954.

Jackson, V. (1988). Deposition of newly synthesized histones: hybrid nucleosomes are not tandemly arranged on daughter DNA strands. Biochemistry (Mosc.) *27*, 2109–2120.

Jackson, V., Shires, A., Tanphaichitr, N., and Chalkley, R. (1976). Modifications to histones immediately after synthesis. J. Mol. Biol. *104*, 471–483.

Jenuwein, T., and Allis, C.D. (2001). Translating the histone code. Science *293*, 1074–1080.

Jiang, R., and Carlson, M. (1997). The Snf1 protein kinase and its activating subunit, Snf4, interact with distinct domains of the Sip1/Sip2/Gal83 component in the kinase complex. Mol. Cell. Biol. *17*, 2099–2106.

Johnson, E.M., Matthews, H.R., Littau, V.C., Lothstein, L., Bradbury, E.M., and Allfrey, V.G. (1978). The structure of chromatin containing DNA complementary to 19 S and 26 S ribosomal RNA in active and inactive stages of Physarum polycephalum. Arch. Biochem. Biophys. *191*, 537–560.

Johnson, E.M., Campbell, G.R., and Allfrey, V.G. (1979). Different nucleosome structures on transcribing and nontranscribing ribosomal gene sequences. Science *206*, 1192–1194.

Johnson, J.M., French, S.L., Osheim, Y.N., Li, M., Hall, L., Beyer, A.L., and Smith, J.S. (2013). Rpd3- and Spt16-Mediated Nucleosome Assembly and Transcriptional Regulation on Yeast Ribosomal DNA Genes. Mol. Cell. Biol. *33*, 2748–2759.

Jones, H.S., Kawauchi, J., Braglia, P., Alen, C.M., Kent, N.A., and Proudfoot, N.J. (2007). RNA polymerase I in yeast transcribes dynamic nucleosomal rDNA. Nat. Struct. Mol. Biol. *14*, 123–130.

Jonkers, I., and Lis, J.T. (2015). Getting up to speed with transcription elongation by RNA polymerase II. Nat. Rev. Mol. Cell Biol. *16*, 167–177.

Jorgensen, P., Rupes, I., Sharom, J.R., Schneper, L., Broach, J.R., and Tyers, M. (2004). A dynamic transcriptional network communicates growth potential to ribosome synthesis and critical cell size. Genes Dev. *18*, 2491–2505.

Joshi, A.A., and Struhl, K. (2005). Eaf3 Chromodomain Interaction with Methylated H3-K36 Links Histone Deacetylation to Pol II Elongation. Mol. Cell *20*, 971–978.

Ju, Q., and Warner, J.R. (1994). Ribosome synthesis during the growth cycle of Saccharomyces cerevisiae. Yeast Chichester Engl. *10*, 151–157.

Kadosh, D., and Struhl, K. (1997). Repression by Ume6 involves recruitment of a complex containing Sin3 corepressor and Rpd3 histone deacetylase to target promoters. Cell *89*, 365–371.

Kadosh, D., and Struhl, K. (1998). Histone deacetylase activity of Rpd3 is important for transcriptional repression in vivo. Genes Dev. *12*, 797–805.

Kaeberlein, M. (2010). Lessons on longevity from budding yeast. Nature *464*, 513–519.

Kamakaka, R.T., and Biggins, S. (2005). Histone variants: deviants? Genes Dev. *19*, 295–310.

Kan, P.-Y., Lu, X., Hansen, J.C., and Hayes, J.J. (2007). The H3 tail domain participates in multiple interactions during folding and self-association of nucleosome arrays. Mol. Cell. Biol. *27*, 2084–2091.

Kasahara, K., Ohtsuki, K., Ki, S., Aoyama, K., Takahashi, H., Kobayashi, T., Shirahige, K., and Kokubo, T. (2007). Assembly of regulatory factors on rRNA and ribosomal protein genes in Saccharomyces cerevisiae. Mol. Cell. Biol. *27*, 6686–6705.

Kasahara, K., Ohyama, Y., and Kokubo, T. (2011). Hmo1 directs pre-initiation complex assembly to an appropriate site on its target gene promoters by masking a nucleosome-free region. Nucleic Acids Res. *39*, 4136–4150.

Kaufman, P.D., Kobayashi, R., Kessler, N., and Stillman, B. (1995). The p150 and p60 subunits of chromatin assemblyfactor I: A molecular link between newly synthesized histories and DNA replication. Cell *81*, 1105–1114.

Kayne, P.S., Kim, U.J., Han, M., Mullen, J.R., Yoshizaki, F., and Grunstein, M. (1988). Extremely conserved histone H4 N terminus is dispensable for growth but essential for repressing the silent mating loci in yeast. Cell *55*, 27–39.

Keener, J., Dodd, J.A., Lalo, D., and Nomura, M. (1997). Histones H3 and H4 are components of upstream activation factor required for the high-level transcription of yeast rDNA by RNA polymerase I. Proc. Natl. Acad. Sci. U. S. A. *94*, 13458–13462.

Keener, J., Josaitis, C.A., Dodd, J.A., and Nomura, M. (1998). Reconstitution of yeast RNA polymerase I transcription in vitro from purified components. TATA-binding protein is not required for basal transcription. J. Biol. Chem. *273*, 33795–33802.

Kempers-Veenstra, A.E., Musters, W., Dekker, A.F., Klootwijk, J., and Planta, R.J. (1985). Deletion mapping of the yeast Pol I promoter. Curr. Genet. *10*, 253–260.

Kenneth, N.S., Ramsbottom, B.A., Gomez-Roman, N., Marshall, L., Cole, P.A., and White, R.J. (2007). TRRAP and GCN5 are used by c-Myc to activate RNA polymerase III transcription. Proc. Natl. Acad. Sci. U. S. A. *104*, 14917–14922.

Keogh, M.-C., Kurdistani, S.K., Morris, S.A., Ahn, S.H., Podolny, V., Collins, S.R., Schuldiner, M., Chin, K., Punna, T., Thompson, N.J., et al. (2005). Cotranscriptional set2 methylation of histone H3 lysine 36 recruits a repressive Rpd3 complex. Cell *123*, 593–605.

Kermekchiev, M., Workman, J.L., and Pikaard, C.S. (1997). Nucleosome binding by the polymerase I transactivator upstream binding factor displaces linker histone H1. Mol. Cell. Biol. *17*, 5833–5842.

Keys, D.A., Vu, L., Steffan, J.S., Dodd, J.A., Yamamoto, R.T., Nogi, Y., and Nomura, M. (1994). RRN6 and RRN7 encode subunits of a multiprotein complex essential for the initiation of rDNA transcription by RNA polymerase I in Saccharomyces cerevisiae. Genes Dev. *8*, 2349–2362.

Keys, D.A., Lee, B.S., Dodd, J.A., Nguyen, T.T., Vu, L., Fantino, E., Burson, L.M., Nogi, Y., and Nomura, M. (1996). Multiprotein transcription factor UAF interacts with the upstream element of the yeast RNA polymerase I promoter and forms a stable preinitiation complex. Genes Dev. *10*, 887–903.

Kimura, H., and Cook, P.R. (2001). Kinetics of core histones in living human cells: little exchange of H3 and H4 and some rapid exchange of H2B. J. Cell Biol. *153*, 1341–1353.

Kireeva, M.L., Walter, W., Tchernajenko, V., Bondarenko, V., Kashlev, M., and Studitsky, V.M. (2002). Nucleosome remodeling induced by RNA polymerase II: loss of the H2A/H2B dimer during transcription. Mol. Cell *9*, 541–552.

Klein, C., and Struhl, K. (1994). Protein kinase A mediates growth-regulated expression of yeast ribosomal protein genes by modulating RAP1 transcriptional activity. Mol. Cell. Biol. *14*, 1920–1928.

Knezetic, J.A., and Luse, D.S. (1986). The presence of nucleosomes on a DNA template prevents initiation by RNA polymerase II in vitro. Cell *45*, 95–104.

Knutson, B.A., and Hahn, S. (2011). Yeast Rrn7 and human TAF1B are TFIIB-related RNA polymerase I general transcription factors. Science *333*, 1637–1640.

Kobayashi, T. (2003). The Replication Fork Barrier Site Forms a Unique Structure with Fob1p and Inhibits the Replication Fork. Mol. Cell. Biol. *23*, 9178–9188.

Kobayashi, T. (2006). Strategies to maintain the stability of the ribosomal RNA gene repeats. Genes Genet. Syst. *81*, 155–161.

Kobayashi, T. (2011). Regulation of ribosomal RNA gene copy number and its role in modulating genome integrity and evolutionary adaptability in yeast. Cell. Mol. Life Sci. CMLS *68*, 1395–1403.

Kobayashi, T., and Horiuchi, T. (1996). A yeast gene product, Fob1 protein, required for both replication fork blocking and recombinational hotspot activities. Genes Cells Devoted Mol. Cell. Mech. *1*, 465–474.

Kobayashi, T., Hidaka, M., Nishizawa, M., and Horiuchi, T. (1992). Identification of a site required for DNA replication fork blocking activity in the rRNA gene cluster in Saccharomyces cerevisiae. Mol. Gen. Genet. MGG *233*, 355–362.

Kobayashi, T., Heck, D.J., Nomura, M., and Horiuchi, T. (1998). Expansion and contraction of ribosomal DNA repeats in Saccharomyces cerevisiae: requirement of replication fork blocking (Fob1) protein and the role of RNA polymerase I. Genes Dev. *12*, 3821–3830.

Kolter, R., Siegele, D.A., and Tormo, A. (1993). The stationary phase of the bacterial life cycle. Annu. Rev. Microbiol. *47*, 855–874.

Korber, P., and Barbaric, S. (2014). The yeast PHO5 promoter: from single locus to systems biology of a paradigm for gene regulation through chromatin. Nucleic Acids Res. *42*, 10888–10902.

Kornberg, R.D. (1974). Chromatin structure: a repeating unit of histones and DNA. Science *184*, 868–871.

Kornberg, R.D., and Lorch, Y. (1995). Interplay between chromatin structure and transcription. Curr. Opin. Cell Biol. *7*, 371–375.

Kornberg, R.D., and Thomas, J.O. (1974). Chromatin structure; oligomers of the histones. Science *184*, 865–868.

Kornberg, A., Rao, N.N., and Ault-Riché, D. (1999). Inorganic polyphosphate: a molecule of many functions. Annu. Rev. Biochem. *68*, 89–125.

Kouzarides, T. (2007). Chromatin modifications and their function. Cell *128*, 693–705.

Krogan, N.J., Cagney, G., Yu, H., Zhong, G., Guo, X., Ignatchenko, A., Li, J., Pu, S., Datta, N., Tikuisis, A.P., et al. (2006). Global landscape of protein complexes in the yeast Saccharomyces cerevisiae. Nature *440*, 637–643.

Kruithof, M., Chien, F.-T., Routh, A., Logie, C., Rhodes, D., and van Noort, J. (2009). Single-molecule force spectroscopy reveals a highly compliant helical folding for the 30-nm chromatin fiber. Nat. Struct. Mol. Biol. *16*, 534–540.

Kuhn, A., and Grummt, I. (1992). Dual role of the nucleolar transcription factor UBF: trans-activator and antirepressor. Proc. Natl. Acad. Sci. U. S. A. *89*, 7340–7344.

Kuhn, C.-D., Geiger, S.R., Baumli, S., Gartmann, M., Gerber, J., Jennebach, S., Mielke, T., Tschochner, H., Beckmann, R., and Cramer, P. (2007). Functional architecture of RNA polymerase I. Cell *131*, 1260–1272.

Kulaeva, O.I., Gaykalova, D.A., Pestov, N.A., Golovastov, V.V., Vassylyev, D.G., Artsimovitch, I., and Studitsky, V.M. (2009). Mechanism of chromatin remodeling and recovery during passage of RNA polymerase II. Nat. Struct. Mol. Biol. *16*, 1272–1278.

Kulkens, T., van Heerikhuizen, H., Klootwijk, J., Oliemans, J., and Planta, R.J. (1989). A yeast ribosomal DNA-binding protein that binds to the rDNA enhancer and also close to the site of Pol I transcription initiation is not important for enhancer functioning. Curr. Genet. *16*, 351–359.

Kulkens, T., Riggs, D.L., Heck, J.D., Planta, R.J., and Nomura, M. (1991). The yeast RNA polymerase I promoter: ribosomal DNA sequences involved in transcription initiation and complex formation in vitro. Nucleic Acids Res. *19*, 5363–5370.

Kulkens, T., van der Sande, C.A., Dekker, A.F., van Heerikhuizen, H., and Planta, R.J. (1992). A system to study transcription by yeast RNA polymerase I within the chromosomal context: functional analysis of the ribosomal DNA enhancer and the RBP1/REB1 binding sites. EMBO J. *11*, 4665–4674.

Kurat, C.F., Natter, K., Petschnigg, J., Wolinski, H., Scheuringer, K., Scholz, H., Zimmermann, R., Leber, R., Zechner, R., and Kohlwein, S.D. (2006). Obese yeast: triglyceride lipolysis is functionally conserved from mammals to yeast. J. Biol. Chem. *281*, 491–500.

Kurat, C.F., Wolinski, H., Petschnigg, J., Kaluarachchi, S., Andrews, B., Natter, K., and Kohlwein, S.D. (2009). Cdk1/Cdc28-dependent activation of the major triacylglycerol lipase Tgl4 in yeast links lipolysis to cell-cycle progression. Mol. Cell *33*, 53–63.

Kuret, J., Johnson, K.E., Nicolette, C., and Zoller, M.J. (1988). Mutagenesis of the regulatory subunit of yeast cAMP-dependent protein kinase. Isolation of site-directed mutants with altered binding affinity for catalytic subunit. J. Biol. Chem. *263*, 9149–9154.

Laemmli, U.K. (1970). Cleavage of structural proteins during the assembly of the head of bacteriophage T4. Nature *227*, 680–685.

Lalo, D., Steffan, J.S., Dodd, J.A., and Nomura, M. (1996). RRN11 encodes the third subunit of the complex containing Rrn6p and Rrn7p that is essential for the initiation of rDNA transcription by yeast RNA polymerase I. J. Biol. Chem. *271*, 21062–21067.

Landsman, D. (1996). Histone H1 in Saccharomyces cerevisiae: a double mystery solved? Trends Biochem. Sci. *21*, 287–288.

Lang, W.H., Morrow, B.E., Ju, Q., Warner, J.R., and Reeder, R.H. (1994). A model for transcription termination by RNA polymerase I. Cell *79*, 527–534.

Lavelle, C., and Foray, N. (2014). Chromatin structure and radiation-induced DNA damage: from structural biology to radiobiology. Int. J. Biochem. Cell Biol. *49*, 84–97.

Leblanc, B., Read, C., and Moss, T. (1993). Recognition of the Xenopus ribosomal core promoter by the transcription factor xUBF involves multiple HMG box domains and leads to an xUBF interdomain interaction. EMBO J. *12*, 513–525.

Léger-Silvestre, I., Trumtel, S., Noaillac-Depeyre, J., and Gas, N. (1999). Functional compartmentalization of the nucleus in the budding yeast Saccharomyces cerevisiae. Chromosoma *108*, 103–113.

Lempiäinen, H., and Shore, D. (2009). Growth control and ribosome biogenesis. Curr. Opin. Cell Biol. *21*, 855–863.

Lesage, G., and Bussey, H. (2006). Cell wall assembly in Saccharomyces cerevisiae. Microbiol. Mol. Biol. Rev. MMBR *70*, 317–343.

Lesage, P., Yang, X., and Carlson, M. (1996). Yeast SNF1 protein kinase interacts with SIP4, a C6 zinc cluster transcriptional activator: a new role for SNF1 in the glucose response. Mol. Cell. Biol. *16*, 1921–1928.

Levy, A., Eyal, M., Hershkovits, G., Salmon-Divon, M., Klutstein, M., and Katcoff, D.J. (2008). Yeast linker histone Hho1p is required for efficient RNA polymerase I processivity and transcriptional silencing at the ribosomal DNA. Proc. Natl. Acad. Sci. U. S. A. *105*, 11703–11708.

Li, B., Carey, M., and Workman, J.L. (2007). The role of chromatin during transcription. Cell *128*, 707–719.

Li, C., Mueller, J.E., Elfline, M., and Bryk, M. (2008). Linker histone H1 represses recombination at the ribosomal DNA locus in the budding yeast Saccharomyces cerevisiae. Mol. Microbiol. *67*, 906–919.

Li, H., Tsang, C.K., Watkins, M., Bertram, P.G., and Zheng, X.F.S. (2006). Nutrient regulates Tor1 nuclear localization and association with rDNA promoter. Nature *442*, 1058–1061.

Lifton, R.P., Goldberg, M.L., Karp, R.W., and Hogness, D.S. (1978). The organization of the histone genes in Drosophila melanogaster: functional and evolutionary implications. Cold Spring Harb. Symp. Quant. Biol. *42 Pt 2*, 1047–1051.

Liljelund, P., Mariotte, S., Buhler, J.M., and Sentenac, A. (1992). Characterization and mutagenesis of the gene encoding the A49 subunit of RNA polymerase A in Saccharomyces cerevisiae. Proc. Natl. Acad. Sci. U. S. A. *89*, 9302–9305.

Lillie, S.H., and Pringle, J.R. (1980). Reserve carbohydrate metabolism in Saccharomyces cerevisiae: responses to nutrient limitation. J. Bacteriol. *143*, 1384–1394.

Lin, C.W., Moorefield, B., Payne, J., Aprikian, P., Mitomo, K., and Reeder, R.H. (1996). A novel 66-kilodalton protein complexes with Rrn6, Rrn7, and TATA-binding protein to promote polymerase I transcription initiation in Saccharomyces cerevisiae. Mol. Cell. Biol. *16*, 6436–6443.

Lin, S.S., Manchester, J.K., and Gordon, J.I. (2003). Sip2, an N-myristoylated beta subunit of Snf1 kinase, regulates aging in Saccharomyces cerevisiae by affecting cellular histone kinase activity, recombination at rDNA loci, and silencing. J. Biol. Chem. *278*, 13390–13397.

Lin, Y., Qi, Y., Lu, J., Pan, X., Yuan, D.S., Zhao, Y., Bader, J.S., and Boeke, J.D. (2008). A comprehensive synthetic genetic interaction network governing yeast histone acetylation and deacetylation. Genes Dev. *22*, 2062–2074.

Liu, Z., Sekito, T., Spírek, M., Thornton, J., and Butow, R.A. (2003). Retrograde signaling is regulated by the dynamic interaction between Rtg2p and Mks1p. Mol. Cell *12*, 401–411.

Lohr, D. (1983). Chromatin structure differs between coding and upstream flanking sequences of the yeast 35S ribosomal genes. Biochemistry (Mosc.) *22*, 927–934.

Lorch, Y., LaPointe, J.W., and Kornberg, R.D. (1987). Nucleosomes inhibit the initiation of transcription but allow chain elongation with the displacement of histones. Cell *49*, 203–210.

Lu, J.-Y., Lin, Y.-Y., Sheu, J.-C., Wu, J.-T., Lee, F.-J., Chen, Y., Lin, M.-I., Chiang, F.-T., Tai, T.-Y., Berger, S.L., et al. (2011). Acetylation of yeast AMPK controls intrinsic aging independently of caloric restriction. Cell *146*, 969–979.

Lu, X., Wontakal, S.N., Kavi, H., Kim, B.J., Guzzardo, P.M., Emelyanov, A.V., Xu, N., Hannon, G.J., Zavadil, J., Fyodorov, D.V., et al. (2013). Drosophila H1 Regulates the Genetic Activity of Heterochromatin by Recruitment of Su(var)3-9. Science *340*, 78–81.

Lucchini, R., and Sogo, J.M. (1992). Different chromatin structures along the spacers flanking active and inactive Xenopus rRNA genes. Mol. Cell. Biol. *12*, 4288–4296.

Lucchini, R., and Sogo, J.M. (1995). Replication of transcriptionally active chromatin. Nature *374*, 276–280.

Lucchini, R., and Sogo, J.M. (1998). The Dynamic Structure of Ribosomal RNA Gene Chromatin. In Ranscription of Ribosomal RNA Genes by Eukaryotic RNA Polymerase I, 1st Edition, (Springer), p.

Lucchini, R., Wellinger, R.E., and Sogo, J.M. (2001). Nucleosome positioning at the replication fork. EMBO J. *20*, 7294–7302.

Luger, K., Mäder, A.W., Richmond, R.K., Sargent, D.F., and Richmond, T.J. (1997). Crystal structure of the nucleosome core particle at 2.8 A resolution. Nature *389*, 251–260.

Luger, K., Dechassa, M.L., and Tremethick, D.J. (2012). New insights into nucleosome and chromatin structure: an ordered state or a disordered affair? Nat. Rev. Mol. Cell Biol. *13*, 436–447.

Luk, E., Ranjan, A., Fitzgerald, P.C., Mizuguchi, G., Huang, Y., Wei, D., and Wu, C. (2010). Stepwise histone replacement by SWR1 requires dual activation with histone H2A.Z and canonical nucleosome. Cell *143*, 725–736.

MacAlpine, D.M., and Almouzni, G. (2013). Chromatin and DNA Replication. Cold Spring Harb. Perspect. Biol. *5*, a010207–a010207.

Maeshima, K., Hihara, S., and Eltsov, M. (2010). Chromatin structure: does the 30-nm fibre exist in vivo? Curr. Opin. Cell Biol. *22*, 291–297.

Mais, C., Wright, J.E., Prieto, J.-L., Raggett, S.L., and McStay, B. (2005). UBF-binding site arrays form pseudo-NORs and sequester the RNA polymerase I transcription machinery. Genes Dev. *19*, 50–64.

Maresca, T.J., and Heald, R. (2006). The long and the short of it: linker histone H1 is required for metaphase chromosome compaction. Cell Cycle Georget. Tex *5*, 589–591.

Marfella, C.G.A., and Imbalzano, A.N. (2007). The Chd family of chromatin remodelers. Mutat. Res. *618*, 30–40.

Marion, R.M., Regev, A., Segal, E., Barash, Y., Koller, D., Friedman, N., and O'Shea, E.K. (2004). Sfp1 is a stress- and nutrient-sensitive regulator of ribosomal protein gene expression. Proc. Natl. Acad. Sci. U. S. A. *101*, 14315–14322.

Marmorstein, R., and Zhou, M.-M. (2014). Writers and Readers of Histone Acetylation: Structure, Mechanism, and Inhibition. Cold Spring Harb. Perspect. Biol. *6*, a018762.

Martin, D.E., Soulard, A., and Hall, M.N. (2004). TOR regulates ribosomal protein gene expression via PKA and the Forkhead transcription factor FHL1. Cell *119*, 969–979.

Martinez, M.J., Roy, S., Archuletta, A.B., Wentzell, P.D., Anna-Arriola, S.S., Rodriguez, A.L., Aragon, A.D., Quiñones, G.A., Allen, C., and Werner-Washburne, M. (2004). Genomic analysis of stationary-phase and exit in Saccharomyces cerevisiae: gene expression and identification of novel essential genes. Mol. Biol. Cell *15*, 5295–5305.

Marzluff, W.F., Gongidi, P., Woods, K.R., Jin, J., and Maltais, L.J. (2002). The human and mouse replication-dependent histone genes. Genomics *80*, 487–498.

Matsumoto, K., Uno, I., and Ishikawa, T. (1984). Identification of the structural gene and nonsense alleles for adenylate cyclase in Saccharomyces cerevisiae. J. Bacteriol. *157*, 277–282.

Mayer, C., Zhao, J., Yuan, X., and Grummt, I. (2004). mTOR-dependent activation of the transcription factor TIF-IA links rRNA synthesis to nutrient availability. Genes Dev. *18*, 423–434.

Mayer, C., Bierhoff, H., and Grummt, I. (2005). The nucleolus as a stress sensor: JNK2 inactivates the transcription factor TIF-IA and down-regulates rRNA synthesis. Genes Dev. *19*, 933–941.

McCartney, R.R., and Schmidt, M.C. (2001). Regulation of Snf1 kinase. Activation requires phosphorylation of threonine 210 by an upstream kinase as well as a distinct step mediated by the Snf4 subunit. J. Biol. Chem. *276*, 36460–36466.

McCartney, R.R., Rubenstein, E.M., and Schmidt, M.C. (2005). Snf1 kinase complexes with different beta subunits display stress-dependent preferences for the three Snf1-activating kinases. Curr. Genet. *47*, 335–344.

McDaniel, S.L., and Strahl, B.D. (2013). Stress-Free with Rpd3: a Unique Chromatin Complex Mediates the Response to Oxidative Stress. Mol. Cell. Biol. *33*, 3726–3727.

McKnight, J.N., Boerma, J.W., Breeden, L.L., and Tsukiyama, T. (2015). Global Promoter Targeting of a Conserved Lysine Deacetylase for Transcriptional Shutoff during Quiescence Entry. Mol. Cell *59*, 732–743.

McMahon, M.E., Stamenkovich, D., and Petes, T.D. (1984). Tandemly arranged variant 5S ribosomal RNA genes in the yeast Saccharomyces cerevisiae. Nucleic Acids Res. *12*, 8001–8016.

Mélèse, T., and Xue, Z. (1995). The nucleolus: an organelle formed by the act of building a ribosome. Curr. Opin. Cell Biol. *7*, 319–324.

Mello, J.A., Silljé, H.H.W., Roche, D.M.J., Kirschner, D.B., Nigg, E.A., and Almouzni, G. (2002). Human Asf1 and CAF-1 interact and synergize in a repair-coupled nucleosome assembly pathway. EMBO Rep. *3*, 329–334.

Meluh, P.B., Yang, P., Glowczewski, L., Koshland, D., and Smith, M.M. (1998). Cse4p is a component of the core centromere of Saccharomyces cerevisiae. Cell *94*, 607–613.

Merkl, P. (2013). Comparative studies on elongation and termination of the three RNA polymerases from S.cerevisiae in vitro. Universität Regensburg.

Merkl, P., Perez-Fernandez, J., Pilsl, M., Reiter, A., Williams, L., Gerber, J., Bohm, M., Deutzmann, R., Griesenbeck, J., Milkereit, P., et al. (2014). Binding of the Termination Factor Nsi1 to Its Cognate DNA Site Is Sufficient To Terminate RNA Polymerase I Transcription In Vitro and To Induce Termination In Vivo. Mol. Cell. Biol. *34*, 3817–3827.

Merz, K., Hondele, M., Goetze, H., Gmelch, K., Stoeckl, U., and Griesenbeck, J. (2008). Actively transcribed rRNA genes in S. cerevisiae are organized in a specialized chromatin associated with the high-mobility group protein Hmo1 and are largely devoid of histone molecules. Genes Dev. *22*, 1190–1204.

Meyerink, J.H., Klootwijk, J., Planta, R.J., van der Ende, A., and van Bruggen, E.F. (1979). Extrachromosomal circular ribosomal DNA in the yeast Saccharomyces carlsbergensis. Nucleic Acids Res. *7*, 69–76.

Milkereit, P., and Tschochner, H. (1998). A specialized form of RNA polymerase I, essential for initiation and growth-dependent regulation of rRNA synthesis, is disrupted during transcription. EMBO J. *17*, 3692–3703.

Milkereit, P., Schultz, P., and Tschochner, H. (1997). Resolution of RNA polymerase I into dimers and monomers and their function in transcription. Biol. Chem. *378*, 1433–1443.

Miller, O.L., Jr, and Beatty, B.R. (1969). Visualization of nucleolar genes. Science *164*, 955–957.

Mohrmann, L., and Verrijzer, C.P. (2005). Composition and functional specificity of SWI2/SNF2 class chromatin remodeling complexes. Biochim. Biophys. Acta *1681*, 59–73.

Moir, R.D., Lee, J., Haeusler, R.A., Desai, N., Engelke, D.R., and Willis, I.M. (2006). Protein kinase A regulates RNA polymerase III transcription through the nuclear localization of Maf1. Proc. Natl. Acad. Sci. U. S. A. *103*, 15044–15049.

Moorefield, B., Greene, E.A., and Reeder, R.H. (2000). RNA polymerase I transcription factor Rrn3 is functionally conserved between yeast and human. Proc. Natl. Acad. Sci. U. S. A. *97*, 4724–4729.

Morales, V., Giamarchi, C., Chailleux, C., Moro, F., Marsaud, V., Le Ricousse, S., and Richard-Foy, H. (2001). Chromatin structure and dynamics: Functional implications. Biochimie *83*, 1029–1039.

Moss, T. (2004). At the crossroads of growth control; making ribosomal RNA. Curr. Opin. Genet. Dev. *14*, 210–217.

Moss, T., and Stefanovsky, V.Y. (2002). At the Center of Eukaryotic Life. Cell *109*, 545–548.

Mousson, F., Ochsenbein, F., and Mann, C. (2007). The histone chaperone Asf1 at the crossroads of chromatin and DNA checkpoint pathways. Chromosoma *116*, 79–93.

Muller, M., Lucchini, R., and Sogo, J.M. (2000). Replication of Yeast rDNA Initiates Downstream of Transcriptionally Active Genes. Mol. Cell *5*, 767–777.

Münkel, C., Eils, R., Dietzel, S., Zink, D., Mehring, C., Wedemann, G., Cremer, T., and Langowski, J. (1999). Compartmentalization of interphase chromosomes observed in simulation and experiment. J. Mol. Biol. *285*, 1053–1065.

Muscarella, D.E., Vogt, V.M., and Bloom, S.E. (1987). Characterization of ribosomal RNA synthesis in a gene dosage mutant: the relationship of topoisomerase I and chromatin structure to transcriptional activity. J. Cell Biol. *105*, 1501–1513.

Musters, W., Knol, J., Maas, P., Dekker, A.F., van Heerikhuizen, H., and Planta, R.J. (1989). Linker scanning of the yeast RNA polymerase I promoter. Nucleic Acids Res. *17*, 9661–9678.

Muth, V., Nadaud, S., Grummt, I., and Voit, R. (2001). Acetylation of TAF(I)68, a subunit of TIF-IB/SL1, activates RNA polymerase I transcription. EMBO J. *20*, 1353–1362.

Natarajan, K., Meyer, M.R., Jackson, B.M., Slade, D., Roberts, C., Hinnebusch, A.G., and Marton, M.J. (2001). Transcriptional profiling shows that Gcn4p is a master regulator of gene expression during amino acid starvation in yeast. Mol. Cell. Biol. *21*, 4347–4368.

Neuhaus (2010). World's "oldest beer" found in shipwreck - CNN.com.

Neumann, E., and Rosenheck, K. (1972). Permeability changes induced by electric impulses in vesicular membranes. J. Membr. Biol. *10*, 279–290.

Neuman-Silberberg, F.S., Bhattacharya, S., and Broach, J.R. (1995). Nutrient availability and the RAS/cyclic AMP pathway both induce expression of ribosomal protein genes in Saccharomyces cerevisiae but by different mechanisms. Mol. Cell. Biol. *15*, 3187–3196.

Neuwald, A.F., and Landsman, D. (1997). GCN5-related histone N-acetyltransferases belong to a diverse superfamily that includes the yeast SPT10 protein. Trends Biochem. Sci. *22*, 154–155.

Nightingale, K.P., O'Neill, L.P., and Turner, B.M. (2006). Histone modifications: signalling receptors and potential elements of a heritable epigenetic code. Curr. Opin. Genet. Dev. *16*, 125–136.

Nishino, Y., Eltsov, M., Joti, Y., Ito, K., Takata, H., Takahashi, Y., Hihara, S., Frangakis, A.S., Imamoto, N., Ishikawa, T., et al. (2012). Human mitotic chromosomes consist predominantly of irregularly folded nucleosome fibres without a 30-nm chromatin structure. EMBO J. *31*, 1644–1653.

de Nobel, H., Ruiz, C., Martin, H., Morris, W., Brul, S., Molina, M., and Klis, F.M. (2000). Cell wall perturbation in yeast results in dual phosphorylation of the Slt2/Mpk1 MAP kinase and in an Slt2-mediated increase in FKS2-lacZ expression, glucanase resistance and thermotolerance. Microbiol. Read. Engl. *146 (Pt 9)*, 2121–2132.

de Nobel, J.G., Klis, F.M., Priem, J., Munnik, T., and van den Ende, H. (1990). The glucanase-soluble mannoproteins limit cell wall porosity in Saccharomyces cerevisiae. Yeast Chichester Engl. *6*, 491–499.

Nogi, Y., Yano, R., and Nomura, M. (1991a). Synthesis of large rRNAs by RNA polymerase II in mutants of Saccharomyces cerevisiae defective in RNA polymerase I. Proc. Natl. Acad. Sci. U. S. A. *88*, 3962–3966.

Nogi, Y., Vu, L., and Nomura, M. (1991b). An approach for isolation of mutants defective in 35S ribosomal RNA synthesis in Saccharomyces cerevisiae. Proc. Natl. Acad. Sci. U. S. A. *88*, 7026–7030.

Noll, M. (1974). Subunit structure of chromatin. Nature *251*, 249–251.

Oakes, M., Nogi, Y., Clark, M.W., and Nomura, M. (1993). Structural alterations of the nucleolus in mutants of Saccharomyces cerevisiae defective in RNA polymerase I. Mol. Cell. Biol. *13*, 2441–2455.

Oakes, M.L., Siddiqi, I., French, S.L., Vu, L., Sato, M., Aris, J.P., Beyer, A.L., and Nomura, M. (2006). Role of histone deacetylase Rpd3 in regulating rRNA gene transcription and nucleolar structure in yeast. Mol. Cell. Biol. *26*, 3889–3901.

van Oevelen, C.J.C., van Teeffelen, H.A.A.M., van Werven, F.J., and Timmers, H.T.M. (2006). Snf1p-dependent Spt-Ada-Gcn5-acetyltransferase (SAGA) recruitment and chromatin remodeling activities on the HXT2 and HXT4 promoters. J. Biol. Chem. *281*, 4523–4531.

Olins, A.L., and Olins, D.E. (1974). Spheroid chromatin units (v bodies). Science *183*, 330–332.

Orlando, V. (2000). Mapping chromosomal proteins in vivo by formaldehyde-crosslinked-chromatin immunoprecipitation. Trends Biochem. Sci. *25*, 99–104.

Osley, M.A. (1991). The regulation of histone synthesis in the cell cycle. Annu. Rev. Biochem. *60*, 827–861.

Oudet, P., Gross-Bellard, M., and Chambon, P. (1975). Electron microscopic and biochemical evidence that chromatin structure is a repeating unit. Cell *4*, 281–300.

Panday, A., and Grove, A. (2016). The high mobility group protein HMO1 functions as a linker histone in yeast. Epigenetics Chromatin *9*.

Papamichos-Chronakis, M., Gligoris, T., and Tzamarias, D. (2004). The Snf1 kinase controls glucose repression in yeast by modulating interactions between the Mig1 repressor and the Cyc8-Tup1 co-repressor. EMBO Rep. *5*, 368–372.

Patterton, H.G., Landel, C.C., Landsman, D., Peterson, C.L., and Simpson, R.T. (1998). The biochemical and phenotypic characterization of Hho1p, the putative linker histone H1 of Saccharomyces cerevisiae. J. Biol. Chem. *273*, 7268–7276.

Paul, A.L., and Ferl, R.J. (1999). Higher-order chromatin structure: looping long molecules. Plant Mol. Biol. *41*, 713–720.

Pederson, T. (1998). The plurifunctional nucleolus. Nucleic Acids Res. *26*, 3871–3876.

Peeters, T., Louwet, W., Geladé, R., Nauwelaers, D., Thevelein, J.M., and Versele, M. (2006). Kelch-repeat proteins interacting with the Galpha protein Gpa2 bypass adenylate cyclase for direct regulation of protein kinase A in yeast. Proc. Natl. Acad. Sci. U. S. A. *103*, 13034–13039.

Pelletier, G., Stefanovsky, V.Y., Faubladier, M., Hirschler-Laszkiewicz, I., Savard, J., Rothblum, L.I., Côté, J., and Moss, T. (2000). Competitive recruitment of CBP and Rb-HDAC regulates UBF acetylation and ribosomal transcription. Mol. Cell *6*, 1059–1066.

Pepenella, S., Murphy, K.J., and Hayes, J.J. (2014). Intra- and inter-nucleosome interactions of the core histone tail domains in higher-order chromatin structure. Chromosoma *123*, 3–13.

Pereira, S.L., and Reeve, J.N. (1998). Histones and nucleosomes in Archaea and Eukarya: a comparative analysis. Extrem. Life Extreme Cond. *2*, 141–148.

Perry, C.A., Allis, C.D., and Annunziato, A.T. (1993). Parental nucleosomes segregated to newly replicated chromatin are underacetylated relative to those assembled de novo. Biochemistry (Mosc.) *32*, 13615–13623.

Peterson, C.L., and Laniel, M.-A. (2004). Histones and histone modifications. Curr. Biol. *14*, R546–R551.

Petes, T.D. (1979). Yeast ribosomal DNA genes are located on chromosome XII. Proc. Natl. Acad. Sci. U. S. A. *76*, 410–414.

Petes, T.D., and Botstein, D. (1977). Simple Mendelian inheritance of the reiterated ribosomal DNA of yeast. Proc. Natl. Acad. Sci. U. S. A. *74*, 5091–5095.

Peyroche, G., Milkereit, P., Bischler, N., Tschochner, H., Schultz, P., Sentenac, A., Carles, C., and Riva, M. (2000). The recruitment of RNA polymerase I on rDNA is mediated by the interaction of the A43 subunit with Rrn3. EMBO J. *19*, 5473–5482.

Pfeiffer, T., and Morley, A. (2014). An evolutionary perspective on the Crabtree effect. Front. Mol. Biosci. *1*.

Pfeiffer, T., Schuster, S., and Bonhoeffer, S. (2001). Cooperation and competition in the evolution of ATP-producing pathways. Science *292*, 504–507.

Philippi, A., Steinbauer, R., Reiter, A., Fath, S., Leger-Silvestre, I., Milkereit, P., Griesenbeck, J., and Tschochner, H. (2010). TOR-dependent reduction in the expression level of Rrn3p lowers the activity of the yeast RNA Pol I machinery, but does not account for the strong inhibition of rRNA production. Nucleic Acids Res. *38*, 5315–5326.

Philippsen, P., Thomas, M., Kramer, R.A., and Davis, R.W. (1978). Unique arrangement of coding sequences for 5 S, 5.8 S, 18 S and 25 S ribosomal RNA in Saccharomyces cerevisiae as determined by R-loop and hybridization analysis. J. Mol. Biol. *123*, 387–404.

Phillips, D.M., and Johns, E.W. (1965). A FRACTIONATION OF THE HISTONES OF GROUP F2A FROM CALF THYMUS. Biochem. J. *94*, 127–130.

Pilsl, M., Crucifix, C., Papai, G., Krupp, F., Steinbauer, R., Griesenbeck, J., Milkereit, P., Tschochner, H., and Schultz, P. (2016). Structure of the initiation-competent RNA polymerase I and its implication for transcription. Nat. Commun. *7*, 12126.

Piñon, R. (1978). Folded chromosomes in non-cycling yeast cells: evidence for a characteristic g0 form. Chromosoma *67*, 263–274.

Piskur, J., Rozpedowska, E., Polakova, S., Merico, A., and Compagno, C. (2006). How did Saccharomyces evolve to become a good brewer? Trends Genet. TIG *22*, 183–186.

Planta, R.J. (1997). Regulation of ribosome synthesis in yeast. Yeast Chichester Engl. *13*, 1505–1518.

Plesset, J., Ludwig, J.R., Cox, B.S., and McLaughlin, C.S. (1987). Effect of cell cycle position on thermotolerance in Saccharomyces cerevisiae. J. Bacteriol. *169*, 779–784.

Pokholok, D.K., Harbison, C.T., Levine, S., Cole, M., Hannett, N.M., Lee, T.I., Bell, G.W., Walker, K., Rolfe, P.A., Herbolsheimer, E., et al. (2005). Genome-wide Map of Nucleosome Acetylation and Methylation in Yeast. Cell *122*, 517–527.

Politz, J.C., Lewandowski, L.B., and Pederson, T. (2002). Signal recognition particle RNA localization within the nucleolus differs from the classical sites of ribosome synthesis. J. Cell Biol. *159*, 411–418.

Porrua, O., and Libri, D. (2015). Transcription termination and the control of the transcriptome: why, where and how to stop. Nat. Rev. Mol. Cell Biol. *16*, 190–202.

Powers, T., and Walter, P. (1999). Regulation of ribosome biogenesis by the rapamycin-sensitive TOR-signaling pathway in Saccharomyces cerevisiae. Mol. Biol. Cell *10*, 987–1000.

Prior, C.P., Cantor, C.R., Johnson, E.M., Littau, V.C., and Allfrey, V.G. (1983). Reversible changes in nucleosome structure and histone H3 accessibility in transcriptionally active and inactive states of rDNA chromatin. Cell *34*, 1033–1042.

Probst, A.V., Dunleavy, E., and Almouzni, G. (2009). Epigenetic inheritance during the cell cycle. Nat. Rev. Mol. Cell Biol. *10*, 192–206.

Prokesch, S. (1991). Small British Brewers Make a Dent. N. Y. Times.

Puig, S., Matallana, E., and Pérez-Ortín, J.E. (1999). Stochastic nucleosome positioning in a yeast chromatin region is not dependent on histone H1. Curr. Microbiol. *39*, 168–172.

Radman-Livaja, M., Verzijlbergen, K.F., Weiner, A., van Welsem, T., Friedman, N., Rando, O.J., and van Leeuwen, F. (2011). Patterns and Mechanisms of Ancestral Histone Protein Inheritance in Budding Yeast. PLoS Biol. *9*, e1001075.

Radonjic, M., Andrau, J.-C., Lijnzaad, P., Kemmeren, P., Kockelkorn, T.T.J.P., van Leenen, D., van Berkum, N.L., and Holstege, F.C.P. (2005). Genome-wide analyses reveal RNA polymerase II located upstream of genes poised for rapid response upon S. cerevisiae stationary phase exit. Mol. Cell *18*, 171–183.

Randez-Gil, F., Bojunga, N., Proft, M., and Entian, K.D. (1997). Glucose derepression of gluconeogenic enzymes in Saccharomyces cerevisiae correlates with phosphorylation of the gene activator Cat8p. Mol. Cell. Biol. *17*, 2502–2510.

Ranjan, A., Mizuguchi, G., FitzGerald, P.C., Wei, D., Wang, F., Huang, Y., Luk, E., Woodcock, C.L., and Wu, C. (2013). Nucleosome-free region dominates histone acetylation in targeting SWR1 to promoters for H2A.Z replacement. Cell *154*, 1232–1245.

Raška, I., Dundr, M., Koberna, K., Melčák, I., Risueño, M.-C., and Török, I. (1995). Does the Synthesis of Ribosomal RNA Take Place within Nucleolar Fibrillar Centers or Dense Fibrillar Components? A Critical Appraisal. J. Struct. Biol. *114*, 1–22.

Raska, I., Shaw, P.J., and Cmarko, D. (2006). Structure and function of the nucleolus in the spotlight. Curr. Opin. Cell Biol. *18*, 325–334.

Raška, I., Shaw, P.J., and Cmarko, D. (2006). New Insights into Nucleolar Architecture and Activity. In International Review of Cytology, (Elsevier), pp. 177–235.

Reeder, R.H. (1989). Regulatory elements of the generic ribosomal gene. Curr. Opin. Cell Biol. *1*, 466–474.

Reeder, R.H., and Lang, W.H. (1997). Terminating transcription in eukaryotes: lessons learned from RNA polymerase I. Trends Biochem. Sci. *22*, 473–477.

Reeder, R.H., Guevara, P., and Roan, J.G. (1999). Saccharomyces cerevisiae RNA polymerase I terminates transcription at the Reb1 terminator in vivo. Mol. Cell. Biol. *19*, 7369–7376.

Reeve, J.N. (2003). Archaeal chromatin and transcription. Mol. Microbiol. *48*, 587–598.

Reiter, A., Steinbauer, R., Philippi, A., Gerber, J., Tschochner, H., Milkereit, P., and Griesenbeck, J. (2011). Reduction in ribosomal protein synthesis is sufficient to explain major effects on ribosome production after short-term TOR inactivation in Saccharomyces cerevisiae. Mol. Cell. Biol. *31*, 803–817.

Reiter, A., Hamperl, S., Seitz, H., Merkl, P., Perez-Fernandez, J., Williams, L., Gerber, J., Németh, A., Léger, I., Gadal, O., et al. (2012). The Reb1-homologue Ydr026c/Nsi1 is required for efficient RNA polymerase I termination in yeast: RNA polymerase I-transcription termination *in vivo*. EMBO J. *31*, 3480–3493.

Richmond, T.J., and Davey, C.A. (2003). The structure of DNA in the nucleosome core. Nature *423*, 145–150.

Robinson, P.J.J., and Rhodes, D. (2006). Structure of the “30 nm” chromatin fibre: a key role for the linker histone. Curr. Opin. Struct. Biol. *16*, 336–343.

Rochman, M., Malicet, C., and Bustin, M. (2010). HMGN5/NSBP1: a new member of the HMGN protein family that affects chromatin structure and function. Biochim. Biophys. Acta *1799*, 86–92.

Rohde, J.R., Bastidas, R., Puria, R., and Cardenas, M.E. (2008). Nutritional control via Tor signaling in Saccharomyces cerevisiae. Curr. Opin. Microbiol. *11*, 153–160.

Ronne, H. (1995). Glucose repression in fungi. Trends Genet. TIG *11*, 12–17.

Roosen, J., Engelen, K., Marchal, K., Mathys, J., Griffioen, G., Cameroni, E., Thevelein, J.M., De Virgilio, C., De Moor, B., and Winderickx, J. (2005). PKA and Sch9 control a molecular switch important for the proper adaptation to nutrient availability. Mol. Microbiol. *55*, 862–880.

Roth, S.Y., and Allis, C.D. (1996). Histone Acetylation and Chromatin Assembly: A Single Escort, Multiple Dances? Cell *87*, 5–8.

Rozpędowska, E., Hellborg, L., Ishchuk, O.P., Orhan, F., Galafassi, S., Merico, A., Woolfit, M., Compagno, C., and Piškur, J. (2011). Parallel evolution of the make–accumulate–consume strategy in Saccharomyces and Dekkera yeasts. Nat. Commun. *2*, 302.

Ruan, W., Lehmann, E., Thomm, M., Kostrewa, D., and Cramer, P. (2011). Evolution of Two Modes of Intrinsic RNA Polymerase Transcript Cleavage. J. Biol. Chem. *286*, 18701–18707.

Rubenstein, E.M., McCartney, R.R., Zhang, C., Shokat, K.M., Shirra, M.K., Arndt, K.M., and Schmidt, M.C. (2008). Access denied: Snf1 activation loop phosphorylation is controlled by availability of the phosphorylated threonine 210 to the PP1 phosphatase. J. Biol. Chem. *283*, 222–230.

de Ruijter, A.J.M., van Gennip, A.H., Caron, H.N., Kemp, S., and van Kuilenburg, A.B.P. (2003). Histone deacetylases (HDACs): characterization of the classical HDAC family. Biochem. J. *370*, 737–749.

Ruiz-Carrillo, A., Wangh, L., and Allfrey, V. (1975). Processing of newly synthesized histone molecules. Science *190*, 117–128.

Ruiz-Roig, C., Viéitez, C., Posas, F., and De Nadal, E. (2010). The Rpd3L HDAC complex is essential for the heat stress response in yeast: Rpd3 is essential for heat stress cellular adaptation. Mol. Microbiol. *76*, 1049–1062.

Rundlett, S.E., Carmen, A.A., Kobayashi, R., Bavykin, S., Turner, B.M., and Grunstein, M. (1996). HDA1 and RPD3 are members of distinct yeast histone deacetylase complexes that regulate silencing and transcription. Proc. Natl. Acad. Sci. U. S. A. *93*, 14503–14508.

S M Paranjape, R T Kamakaka, and Kadonaga, and J.T. (1994). Role of Chromatin Structure in the Regulation of Transcription by RNA Polymerase II. Annu. Rev. Biochem. *63*, 265–297.

Saffer, L.D., and Miller, O.L. (1986). Electron microscopic study of Saccharomyces cerevisiae rDNA chromatin replication. Mol. Cell. Biol. *6*, 1148–1157.

Sainsbury, S., Bernecky, C., and Cramer, P. (2015). Structural basis of transcription initiation by RNA polymerase II. Nat. Rev. Mol. Cell Biol. *16*, 129–143.

Saka, K., Ide, S., Ganley, A.R.D., and Kobayashi, T. (2013). Cellular Senescence in Yeast Is Regulated by rDNA Noncoding Transcription. Curr. Biol. *23*, 1794–1798.

v**an der Sande, C.A.F.M., Kulkens, T., Kramer, A.B., de Wijs, I.J., van Heerikhuizen, H., Klootwijk, J., and Planta, R.J. (1989).** Termination of transcription by yeast RNA polymerase I. Nucleic Acids Res. *17*, 9127–9146.

Sandman, K., Soares, D., and Reeve, J.N. (2001). Molecular components of the archaeal nucleosome. Biochimie *83*, 277–281.

Sandmeier, J.J., French, S., Osheim, Y., Cheung, W.L., Gallo, C.M., Beyer, A.L., and Smith, J.S. (2002). RPD3 is required for the inactivation of yeast ribosomal DNA genes in stationary phase. EMBO J. *21*, 4959–4968.

Sanij, E., Poortinga, G., Sharkey, K., Hung, S., Holloway, T.P., Quin, J., Robb, E., Wong, L.H., Thomas, W.G., Stefanovsky, V., et al. (2008). UBF levels determine the number of active ribosomal RNA genes in mammals. J. Cell Biol. *183*, 1259–1274.

Santangelo, G.M. (2006). Glucose signaling in Saccharomyces cerevisiae. Microbiol. Mol. Biol. Rev. MMBR *70*, 253–282.

Santangelo, G.M., Tornow, J., McLaughlin, C.S., and Moldave, K. (1988). Properties of promoters cloned randomly from the Saccharomyces cerevisiae genome. Mol. Cell. Biol. *8*, 4217–4224.

Santhanam, A., Hartley, A., Düvel, K., Broach, J.R., and Garrett, S. (2004). PP2A phosphatase activity is required for stress and Tor kinase regulation of yeast stress response factor Msn2p. Eukaryot. Cell *3*, 1261–1271.

Schäfer, G., McEvoy, C.R.E., and Patterton, H.-G. (2008). The Saccharomyces cerevisiae linker histone Hho1p is essential for chromatin compaction in stationary phase and is displaced by transcription. Proc. Natl. Acad. Sci. U. S. A. *105*, 14838–14843.

Scheer, U., and Benavente, R. (1990). Functional and dynamic aspects of the mammalian nucleolus. BioEssays News Rev. Mol. Cell. Dev. Biol. *12*, 14–21.

Scheer, U., and Hock, R. (1999). Structure and function of the nucleolus. Curr. Opin. Cell Biol. *11*, 385–390.

Scheer, U., Trendelenburg, M.F., Krohne, G., and Franke, W.W. (1977). Lengths and patterns of transcriptional units in the amplified nucleoli of oocytes of Xenopus laevis. Chromosoma *60*, 147–167.

Schmid, M., Durussel, T., and Laemmli, U.K. (2004). ChIC and ChEC; genomic mapping of chromatin proteins. Mol. Cell *16*, 147–157.

Schneider, D.A. (2012). RNA polymerase I activity is regulated at multiple steps in the transcription cycle: Recent insights into factors that influence transcription elongation. Gene *493*, 176–184.

Schultz, M.C., Brill, S.J., Ju, Q., Sternglanz, R., and Reeder, R.H. (1992). Topoisomerases and yeast rRNA transcription: negative supercoiling stimulates initiation and topoisomerase activity is required for elongation. Genes Dev. *6*, 1332–1341.

Segal, E., Fondufe-Mittendorf, Y., Chen, L., Thåström, A., Field, Y., Moore, I.K., Wang, J.-P.Z., and Widom, J. (2006). A genomic code for nucleosome positioning. Nature *442*, 772–778.

Seto, E., and Yoshida, M. (2014). Erasers of Histone Acetylation: The Histone Deacetylase Enzymes. Cold Spring Harb. Perspect. Biol. *6*, a018713–a018713.

Shamji, A.F., Kuruvilla, F.G., and Schreiber, S.L. (2000). Partitioning the transcriptional program induced by rapamycin among the effectors of the Tor proteins. Curr. Biol. CB *10*, 1574–1581.

Shematorova, E.K., and Shpakovskiĭ, G.V. (2002). [Structure and function of eukaryotic nuclear DNA-dependent RNA polymerase I]. Mol. Biol. (Mosk.) *36*, 3–26.

Shen, X., and Gorovsky, M.A. (1996). Linker Histone H1 Regulates Specific Gene Expression but Not Global Transcription In Vivo. Cell *86*, 475–483.

Shibahara, K., and Stillman, B. (1999). Replication-dependent marking of DNA by PCNA facilitates CAF-1-coupled inheritance of chromatin. Cell *96*, 575–585.

Shogren-Knaak, M., Ishii, H., Sun, J.-M., Pazin, M.J., Davie, J.R., and Peterson, C.L. (2006). Histone H4-K16 acetylation controls chromatin structure and protein interactions. Science *311*, 844–847.

Shou, W., Sakamoto, K.M., Keener, J., Morimoto, K.W., Traverso, E.E., Azzam, R., Hoppe, G.J., Feldman, R.M., DeModena, J., Moazed, D., et al. (2001). Net1 stimulates RNA polymerase I transcription and regulates nucleolar structure independently of controlling mitotic exit. Mol. Cell *8*, 45–55.

Siddiqi, I.N., Dodd, J.A., Vu, L., Eliason, K., Oakes, M.L., Keener, J., Moore, R., Young, M.K., and Nomura, M. (2001). Transcription of chromosomal rRNA genes by both RNA polymerase I and II in yeast uaf30 mutants lacking the 30 kDa subunit of transcription factor UAF. EMBO J. *20*, 4512–4521.

Sinclair, D.A., and Guarente, L. (1997). Extrachromosomal rDNA circles--a cause of aging in yeast. Cell *91*, 1033–1042.

Smets, B., Ghillebert, R., De Snijder, P., Binda, M., Swinnen, E., De Virgilio, C., and Winderickx, J. (2010). Life in the midst of scarcity: adaptations to nutrient availability in Saccharomyces cerevisiae. Curr. Genet. *56*, 1–32.

Smith, J.S., and Boeke, J.D. (1997). An unusual form of transcriptional silencing in yeast ribosomal DNA. Genes Dev. *11*, 241–254.

Smith, M.M., and Andrésson, O.S. (1983). DNA sequences of yeast H3 and H4 histone genes from two non-allelic gene sets encode identical H3 and H4 proteins. J. Mol. Biol. *169*, 663–690.

Smith, S., and Stillman, B. (1989). Purification and characterization of CAF-I, a human cell factor required for chromatin assembly during DNA replication in vitro. Cell *58*, 15–25.

Sobel, R.E., Cook, R.G., Perry, C.A., Annunziato, A.T., and Allis, C.D. (1995). Conservation of deposition-related acetylation sites in newly synthesized histones H3 and H4. Proc. Natl. Acad. Sci. U. S. A. *92*, 1237–1241.

Sogo, J.M., Ness, P.J., Widmer, R.M., Parish, R.W., and Koller, T. (1984). Psoralen-crosslinking of DNA as a probe for the structure of active nucleolar chromatin. J. Mol. Biol. *178*, 897–919.

Sogo, J.M., Stahl, H., Koller, T., and Knippers, R. (1986). Structure of replicating simian virus 40 minichromosomes. The replication fork, core histone segregation and terminal structures. J. Mol. Biol. *189*, 189–204.

Song, F., Chen, P., Sun, D., Wang, M., Dong, L., Liang, D., Xu, R.-M., Zhu, P., and Li, G. (2014). Cryo-EM study of the chromatin fiber reveals a double helix twisted by tetranucleosomal units. Science *344*, 376–380.

Srivastava, A.K., and Schlessinger, D. (1991). Structure and organization of ribosomal DNA. Biochimie *73*, 631–638.

Stefanovsky, V., Langlois, F., Gagnon-Kugler, T., Rothblum, L.I., and Moss, T. (2006a). Growth factor signaling regulates elongation of RNA polymerase I transcription in mammals via UBF phosphorylation and r-chromatin remodeling. Mol. Cell *21*, 629–639.

Stefanovsky, V.Y., Langlois, F., Bazett-Jones, D., Pelletier, G., and Moss, T. (2006b). ERK modulates DNA bending and enhancesome structure by phosphorylating HMG1-boxes 1 and 2 of the RNA polymerase I transcription factor UBF. Biochemistry (Mosc.) *45*, 3626–3634.

Steffan, J.S., Keys, D.A., Dodd, J.A., and Nomura, M. (1996). The role of TBP in rDNA transcription by RNA polymerase I in Saccharomyces cerevisiae: TBP is required for upstream activation factor-dependent recruitment of core factor. Genes Dev. *10*, 2551–2563.

Steffan, J.S., Keys, D.A., Vu, L., and Nomura, M. (1998). Interaction of TATA-binding protein with upstream activation factor is required for activated transcription of ribosomal DNA by RNA polymerase I in Saccharomyces cerevisiae in vivo. Mol. Cell. Biol. *18*, 3752–3761.

Stepanchick, A., Zhi, H., Cavanaugh, A.H., Rothblum, K., Schneider, D.A., and Rothblum, L.I. (2013). DNA binding by the ribosomal DNA transcription factor rrn3 is essential for ribosomal DNA transcription. J. Biol. Chem. *288*, 9135–9144.

Stevens, B. (1981). Mitochondrial Structure. Cold Spring Harb. Monogr. Arch. *11A*, 471–504.

Stoler, S., Keith, K.C., Curnick, K.E., and Fitzgerald-Hayes, M. (1995). A mutation in CSE4, an essential gene encoding a novel chromatin-associated protein in yeast, causes chromosome nondisjunction and cell cycle arrest at mitosis. Genes Dev. *9*, 573–586.

Strahl, B.D., and Allis, C.D. (2000). The language of covalent histone modifications. Nature *403*, 41–45.

Strahl-Bolsinger, S., Hecht, A., Luo, K., and Grunstein, M. (1997). SIR2 and SIR4 interactions differ in core and extended telomeric heterochromatin in yeast. Genes Dev. *11*, 83–93.

Straight, A.F., Shou, W., Dowd, G.J., Turck, C.W., Deshaies, R.J., Johnson, A.D., and Moazed, D. (1999). Net1, a Sir2-associated nucleolar protein required for rDNA silencing and nucleolar integrity. Cell *97*, 245–256.

Sullivan, S., Sink, D.W., Trout, K.L., Makalowska, I., Taylor, P.M., Baxevanis, A.D., and Landsman, D. (2002). The Histone Database. Nucleic Acids Res. *30*, 341–342.

Sutherland, C.M., Hawley, S.A., McCartney, R.R., Leech, A., Stark, M.J.R., Schmidt, M.C., and Hardie, D.G. (2003). Elm1p is one of three upstream kinases for the Saccharomyces cerevisiae SNF1 complex. Curr. Biol. CB *13*, 1299–1305.

Swaney, D.L., Beltrao, P., Starita, L., Guo, A., Rush, J., Fields, S., Krogan, N.J., and Villén, J. (2013). Global analysis of phosphorylation and ubiquitylation cross-talk in protein degradation. Nat. Methods *10*, 676–682.

Syed, S.H., Goutte-Gattat, D., Becker, N., Meyer, S., Shukla, M.S., Hayes, J.J., Everaers, R., Angelov, D., Bednar, J., and Dimitrov, S. (2010). Single-base resolution mapping of H1-nucleosome interactions and 3D organization of the nucleosome. Proc. Natl. Acad. Sci. U. S. A. *107*, 9620–9625.

Tagami, H., Ray-Gallet, D., Almouzni, G., and Nakatani, Y. (2004). Histone H3.1 and H3.3 complexes mediate nucleosome assembly pathways dependent or independent of DNA synthesis. Cell *116*, 51–61.

Takata, H., Hanafusa, T., Mori, T., Shimura, M., Iida, Y., Ishikawa, K., Yoshikawa, K., Yoshikawa, Y., and Maeshima, K. (2013). Chromatin Compaction Protects Genomic DNA from Radiation Damage. PLoS ONE *8*, e75622.

Takeshige, K., Baba, M., Tsuboi, S., Noda, T., and Ohsumi, Y. (1992). Autophagy in yeast demonstrated with proteinase-deficient mutants and conditions for its induction. J. Cell Biol. *119*, 301–311.

Tamaki, H. (2007). Glucose-stimulated cAMP-protein kinase A pathway in yeast Saccharomyces cerevisiae. J. Biosci. Bioeng. *104*, 245–250.

Tanabe, H., Müller, S., Neusser, M., von Hase, J., Calcagno, E., Cremer, M., Solovei, I., Cremer, C., and Cremer, T. (2002). Evolutionary conservation of chromosome territory arrangements in cell nuclei from higher primates. Proc. Natl. Acad. Sci. U. S. A. *99*, 4424–4429.

Thanbichler, M., Wang, S.C., and Shapiro, L. (2005). The bacterial nucleoid: A highly organized and dynamic structure. J. Cell. Biochem. *96*, 506–521.

Thatcher, T.H., and Gorovsky, M.A. (1994). Phylogenetic analysis of the core histones H2A, H2B, H3, and H4. Nucleic Acids Res. *22*, 174–179.

Thevelein, null, Cauwenberg, null, Colombo, null, De Winde JH, null, Donation, null, Dumortier, null, Kraakman, null, Lemaire, null, Ma, null, Nauwelaers, null, et al. (2000). Nutrient-induced signal transduction through the protein kinase A pathway and its role in the control of metabolism, stress resistance, and growth in yeast. Enzyme Microb. Technol. *26*, 819–825.

Thiry, M., and Lafontaine, D.L.J. (2005). Birth of a nucleolus: the evolution of nucleolar compartments. Trends Cell Biol. *15*, 194–199.

Thoma, F., Koller, T., and Klug, A. (1979). Involvement of histone H1 in the organization of the nucleosome and of the salt-dependent superstructures of chromatin. J. Cell Biol. *83*, 403–427.

Thomas, M.R., and O'Shea, E.K. (2005). An intracellular phosphate buffer filters transient fluctuations in extracellular phosphate levels. Proc. Natl. Acad. Sci. U. S. A. *102*, 9565–9570.

Thomson, J.M., Gaucher, E.A., Burgan, M.F., De Kee, D.W., Li, T., Aris, J.P., and Benner, S.A. (2005). Resurrecting ancestral alcohol dehydrogenases from yeast. Nat. Genet. *37*, 630–635.

Toda, T., Cameron, S., Sass, P., Zoller, M., Scott, J.D., McMullen, B., Hurwitz, M., Krebs, E.G., and Wigler, M. (1987a). Cloning and characterization of BCY1, a locus encoding a regulatory subunit of the cyclic AMP-dependent protein kinase in Saccharomyces cerevisiae. Mol. Cell. Biol. *7*, 1371–1377.

Toda, T., Cameron, S., Sass, P., Zoller, M., and Wigler, M. (1987b). Three different genes in S. cerevisiae encode the catalytic subunits of the cAMP-dependent protein kinase. Cell *50*, 277–287.

Toussaint, M., Levasseur, G., Tremblay, M., Paquette, M., and Conconi, A. (2005). Psoralen photocrosslinking, a tool to study the chromatin structure of RNA polymerase I--transcribed ribosomal genes. Biochem. Cell Biol. Biochim. Biol. Cell. *83*, 449–459.

Treitel, M.A., and Carlson, M. (1995). Repression by SSN6-TUP1 is directed by MIG1, a repressor/activator protein. Proc. Natl. Acad. Sci. U. S. A. *92*, 3132–3136.

Tremblay, M., Charton, R., Wittner, M., Levasseur, G., Griesenbeck, J., and Conconi, A. (2014). UV light-induced DNA lesions cause dissociation of yeast RNA polymerases-I and establishment of a specialized chromatin structure at rRNA genes. Nucleic Acids Res. *42*, 380–395.

Tremethick, D.J. (2007). Higher-order structures of chromatin: the elusive 30 nm fiber. Cell *128*, 651–654.

Trendelenburg, M.F., Scheer, U., and Franke, W.W. (1973). Structural organization of the transcription of ribosomal DNA in oocytes of the house cricket. Nature. New Biol. *245*, 167–170.

Tsang, C.K., Bertram, P.G., Ai, W., Drenan, R., and Zheng, X.F.S. (2003). Chromatin-mediated regulation of nucleolar structure and RNA Pol I localization by TOR. EMBO J. *22*, 6045–6056.

Tsukada, M., and Ohsumi, Y. (1993). Isolation and characterization of autophagy-defective mutants of Saccharomyces cerevisiae. FEBS Lett. *333*, 169–174.

Tyler, J.K., Adams, C.R., Chen, S.R., Kobayashi, R., Kamakaka, R.T., and Kadonaga, J.T. (1999). The RCAF complex mediates chromatin assembly during DNA replication and repair. Nature *402*, 555–560.

Ushinsky, S.C., Bussey, H., Ahmed, A.A., Wang, Y., Friesen, J., Williams, B.A., and Storms, R.K. (1997). Histone H1 in Saccharomyces cerevisiae. Yeast Chichester Engl. *13*, 151–161.

Vander Heiden, M.G., Cantley, L.C., and Thompson, C.B. (2009). Understanding the Warburg effect: the metabolic requirements of cell proliferation. Science *324*, 1029–1033.

Vannini, A., and Cramer, P. (2012). Conservation between the RNA polymerase I, II, and III transcription initiation machineries. Mol. Cell *45*, 439–446.

Venema, J., and Tollervey, D. (1999). Ribosome Synthesis in Saccharomyces cerevisiae. Annu. Rev. Genet. *33*, 261–311.

Verreault, A., Kaufman, P.D., Kobayashi, R., and Stillman, B. (1996). Nucleosome Assembly by a Complex of CAF-1 and Acetylated Histones H3/H4. Cell *87*, 95–104.

Viktorovskaya, O.V., and Schneider, D.A. (2015). Functional divergence of eukaryotic RNA polymerases: unique properties of RNA polymerase I suit its cellular role. Gene *556*, 19–26.

Visintin, R., and Amon, A. (2000). The nucleolus: the magician's hat for cell cycle tricks. Curr. Opin. Cell Biol. *12*, 372–377.

Voit, R., and Grummt, I. (2001). Phosphorylation of UBF at serine 388 is required for interaction with RNA polymerase I and activation of rDNA transcription. Proc. Natl. Acad. Sci. U. S. A. *98*, 13631–13636.

Vu, L., Siddiqi, I., Lee, B.S., Josaitis, C.A., and Nomura, M. (1999). RNA polymerase switch in transcription of yeast rDNA: role of transcription factor UAF (upstream activation factor) in silencing rDNA transcription by RNA polymerase II. Proc. Natl. Acad. Sci. U. S. A. *96*, 4390–4395.

Wagner, E.J., and Carpenter, P.B. (2012). Understanding the language of Lys36 methylation at histone H3. Nat. Rev. Mol. Cell Biol. *13*, 115–126.

Wai, H., Johzuka, K., Vu, L., Eliason, K., Kobayashi, T., Horiuchi, T., and Nomura, M. (2001). Yeast RNA polymerase I enhancer is dispensable for transcription of the chromosomal rRNA gene and cell growth, and its apparent transcription enhancement from ectopic promoters requires Fob1 protein. Mol. Cell. Biol. *21*, 5541–5553.

Wai, H.H., Vu, L., Oakes, M., and Nomura, M. (2000). Complete deletion of yeast chromosomal rDNA repeats and integration of a new rDNA repeat: use of rDNA deletion strains for functional analysis of rDNA promoter elements in vivo. Nucleic Acids Res. *28*, 3524–3534.

Waldron, C. (1977). Synthesis of ribosomal and transfer ribonucleic acids in yeast during a nutritional shift-up. J. Gen. Microbiol. *98*, 215–221.

Wang, X., and Hayes, J.J. (2008). Acetylation mimics within individual core histone tail domains indicate distinct roles in regulating the stability of higher-order chromatin structure. Mol. Cell. Biol. *28*, 227–236.

Wang, D., Mansisidor, A., Prabhakar, G., and Hochwagen, A. (2016). Condensin and Hmo1 Mediate a Starvation-Induced Transcriptional Position Effect within the Ribosomal DNA Array. Cell Rep. *14*, 1010–1017.

Wang, Y., Pierce, M., Schneper, L., Güldal, C.G., Zhang, X., Tavazoie, S., and Broach, J.R. (2004). Ras and Gpa2 mediate one branch of a redundant glucose signaling pathway in yeast. PLoS Biol. *2*, E128.

Warner, J.R. (1989). Synthesis of ribosomes in Saccharomyces cerevisiae. Microbiol. Rev. *53*, 256–271.

Warner, J.R. (1999). The economics of ribosome biosynthesis in yeast. Trends Biochem. Sci. *24*, 437–440.

Wei, Y., Tsang, C.K., and Zheng, X.F.S. (2009). Mechanisms of regulation of RNA polymerase III-dependent transcription by TORC1. EMBO J. *28*, 2220–2230.

Werner-Washburne, M., Braun, E., Johnston, G.C., and Singer, R.A. (1993). Stationary phase in the yeast Saccharomyces cerevisiae. Microbiol. Rev. *57*, 383–401.

Werner-Washburne, M., Braun, E.L., Crawford, M.E., and Peck, V.M. (1996). Stationary phase in Saccharomyces cerevisiae. Mol. Microbiol. *19*, 1159–1166.

White, C.L., Suto, R.K., and Luger, K. (2001). Structure of the yeast nucleosome core particle reveals fundamental changes in internucleosome interactions. EMBO J. *20*, 5207–5218.

Whitehouse, I., and Smith, D.J. (2013). Chromatin dynamics at the replication fork: there's more to life than histones. Curr. Opin. Genet. Dev. *23*, 140–146.

Widom, J. (1998). Structure, dynamics, and function of chromatin in vitro. Annu. Rev. Biophys. Biomol. Struct. *27*, 285–327.

Williams, S.P., Athey, B.D., Muglia, L.J., Schappe, R.S., Gough, A.H., and Langmore, J.P. (1986). Chromatin fibers are left-handed double helices with diameter and mass per unit length that depend on linker length. Biophys. J. *49*, 233–248.

Winderickx, J., Holsbeeks, I., Lagatie, O., Giots, F., Thevelein, J., and de Winde, H. (2003). From feast to famine; adaptation to nutrient availability in yeast. In Yeast Stress Responses, S. Hohmann, and W.H. Mager, eds. (Berlin, Heidelberg: Springer Berlin Heidelberg), pp. 305–386.

Wittmeyer, J., and Formosa, T. (1997). The Saccharomyces cerevisiae DNA polymerase alpha catalytic subunit interacts with Cdc68/Spt16 and with Pob3, a protein similar to an HMG1-like protein. Mol. Cell. Biol. *17*, 4178–4190.

Wittmeyer, J., Joss, L., and Formosa, T. (1999). Spt16 and Pob3 of *Saccharomyces cerevisiae* Form an Essential, Abundant Heterodimer That Is Nuclear, Chromatin-Associated, and Copurifies with DNA Polymerase α. Biochemistry (Mosc.) *38*, 8961–8971.

Wittner, M. (2012). Establishment and maintenance of 35S rRNA gene chromatin states in Saccharomyces cerevisiae. University, Regensburg, Germany.

Wittner, M., Hamperl, S., Stöckl, U., Seufert, W., Tschochner, H., Milkereit, P., and Griesenbeck, J. (2011). Establishment and maintenance of alternative chromatin states at a multicopy gene locus. Cell *145*, 543–554.

Wojtczak, L. (1996). The Crabtree effect: a new look at the old problem. Acta Biochim. Pol. *43*, 361–368.

Woodcock, C.L., and Dimitrov, S. (2001). Higher-order structure of chromatin and chromosomes. Curr. Opin. Genet. Dev. *11*, 130–135.

Workman, J.L., and Kingston, R.E. (1998). Alteration of Nucleosome Structure as a Mechanism of Transcriptional Regulation. Annu. Rev. Biochem. *67*, 545–579.

Wu, C., Bingham, P.M., Livak, K.J., Holmgren, R., and Elgin, S.C. (1979). The chromatin structure of specific genes: I. Evidence for higher order domains of defined DNA sequence. Cell *16*, 797–806.

Yamamoto, K., Yamamoto, M., Hanada, K. -i., Nogi, Y., Matsuyama, T., and Muramatsu, M. (2004). Multiple Protein-Protein Interactions by RNA Polymerase I-Associated Factor PAF49 and Role of PAF49 in rRNA Transcription. Mol. Cell. Biol. *24*, 6338–6349.

Yamamoto, R.T., Nogi, Y., Dodd, J.A., and Nomura, M. (1996). RRN3 gene of Saccharomyces cerevisiae encodes an essential RNA polymerase I transcription factor which interacts with the polymerase independently of DNA template. EMBO J. *15*, 3964–3973.

Yan, G., Shen, X., and Jiang, Y. (2006). Rapamycin activates Tap42-associated phosphatases by abrogating their association with Tor complex 1. EMBO J. *25*, 3546–3555.

Yang, X.-J., and Seto, E. (2008). The Rpd3/Hda1 family of lysine deacetylases: from bacteria and yeast to mice and men. Nat. Rev. Mol. Cell Biol. *9*, 206–218.

Yang, C.H., Lambie, E.J., Hardin, J., Craft, J., and Snyder, M. (1989). Higher order structure is present in the yeast nucleus: autoantibody probes demonstrate that the nucleolus lies opposite the spindle pole body. Chromosoma *98*, 123–128.

Yang, Z., Huang, J., Geng, J., Nair, U., and Klionsky, D.J. (2006). Atg22 recycles amino acids to link the degradative and recycling functions of autophagy. Mol. Biol. Cell *17*, 5094–5104.

Yoshida, M., Horinouchi, S., and Beppu, T. (1995). Trichostatin A and trapoxin: Novel chemical probes for the role of histone acetylation in chromatin structure and function. BioEssays *17*, 423–430.

Yoshikawa, Y., Mori, T., Magome, N., Hibino, K., and Yoshikawa, K. (2008). DNA compaction plays a key role in radioprotection against double-strand breaks as revealed by single-molecule observation. Chem. Phys. Lett. *456*, 80–83.

Zaman, S., Lippman, S.I., Zhao, X., and Broach, J.R. (2008). How Saccharomyces responds to nutrients. Annu. Rev. Genet. *42*, 27–81.

Zaragoza, D., Ghavidel, A., Heitman, J., and Schultz, M.C. (1998). Rapamycin induces the G0 program of transcriptional repression in yeast by interfering with the TOR signaling pathway. Mol. Cell. Biol. *18*, 4463–4470.

Zhang, H., Roberts, D.N., and Cairns, B.R. (2005). Genome-wide dynamics of Htz1, a histone H2A variant that poises repressed/basal promoters for activation through histone loss. Cell *123*, 219–231.

Zhang, N., Wu, J., and Oliver, S.G. (2009). Gis1 is required for transcriptional reprogramming of carbon metabolism and the stress response during transition into stationary phase in yeast. Microbiol. Read. Engl. *155*, 1690–1698.

Zhao, J., Yuan, X., Frödin, M., and Grummt, I. (2003). ERK-Dependent Phosphorylation of the Transcription Initiation Factor TIF-IA Is Required for RNA Polymerase I Transcription and Cell Growth. Mol. Cell *11*, 405–413.

Zlatanova, J., and Thakar, A. (2008). H2A.Z: View from the Top. Structure *16*, 166–179.

Zlatanova, J., Caiafa, P., and Van Holde, K. (2000). Linker histone binding and displacement: versatile mechanism for transcriptional regulation. FASEB J. Off. Publ. Fed. Am. Soc. Exp. Biol. *14*, 1697–1704.

Zlatanova, J., Seebart, C., and Tomschik, M. (2007). Nap1: taking a closer look at a juggler protein of extraordinary skills. FASEB J. Off. Publ. Fed. Am. Soc. Exp. Biol. *21*, 1294–1310.

Zlotnik, H., Fernandez, M.P., Bowers, B., and Cabib, E. (1984). Saccharomyces cerevisiae mannoproteins form an external cell wall layer that determines wall porosity. J. Bacteriol. *159*, 1018–1026.

Appendix

Supplemental figures

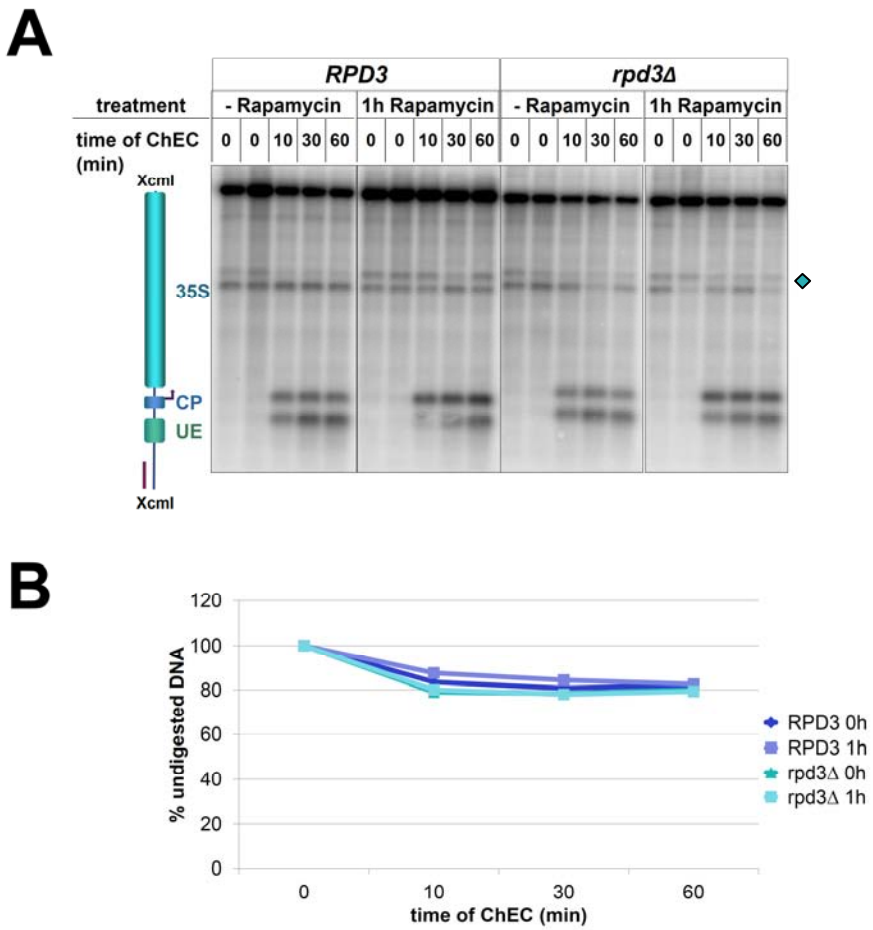

Supplemental Figure 1: Rrn7-MNase mediated cleavage at the rDNA upon rapamycin treatment in *RPD3* and *rpd3*Δ

Yeast strains y881 (Rrn7 with C-terminal MNase expressed from the endogenous locus, *RPD3*) and y3024 (Rrn7 with C-terminal MNase expressed from the endogenous locus, *rpd3*Δ) were cultured to mid exponential phase and samples were collected before and 1h after the addition of 200ng/ml rapamycin to the medium (see OD Figure 31 for the culture ODs). The cell samples were treated and ChEC analysis was carried out as described in the legend of Figure 29. **(A)** Analysis of ChEC samples. An autoradiograph of a Southern blot after hybridization with the rDNp probe is shown. Samples without the addition of rapamycin (-Rapamycin) and samples after 1h rapamycin treatment (1h Rapamycin) are shown. A rhomb on the right indicates unspecific cleavage events. **(B)** Quantification of Rrn7-MNase mediated degradation shown in (A): The analysis was conducted according to Figure 25B.

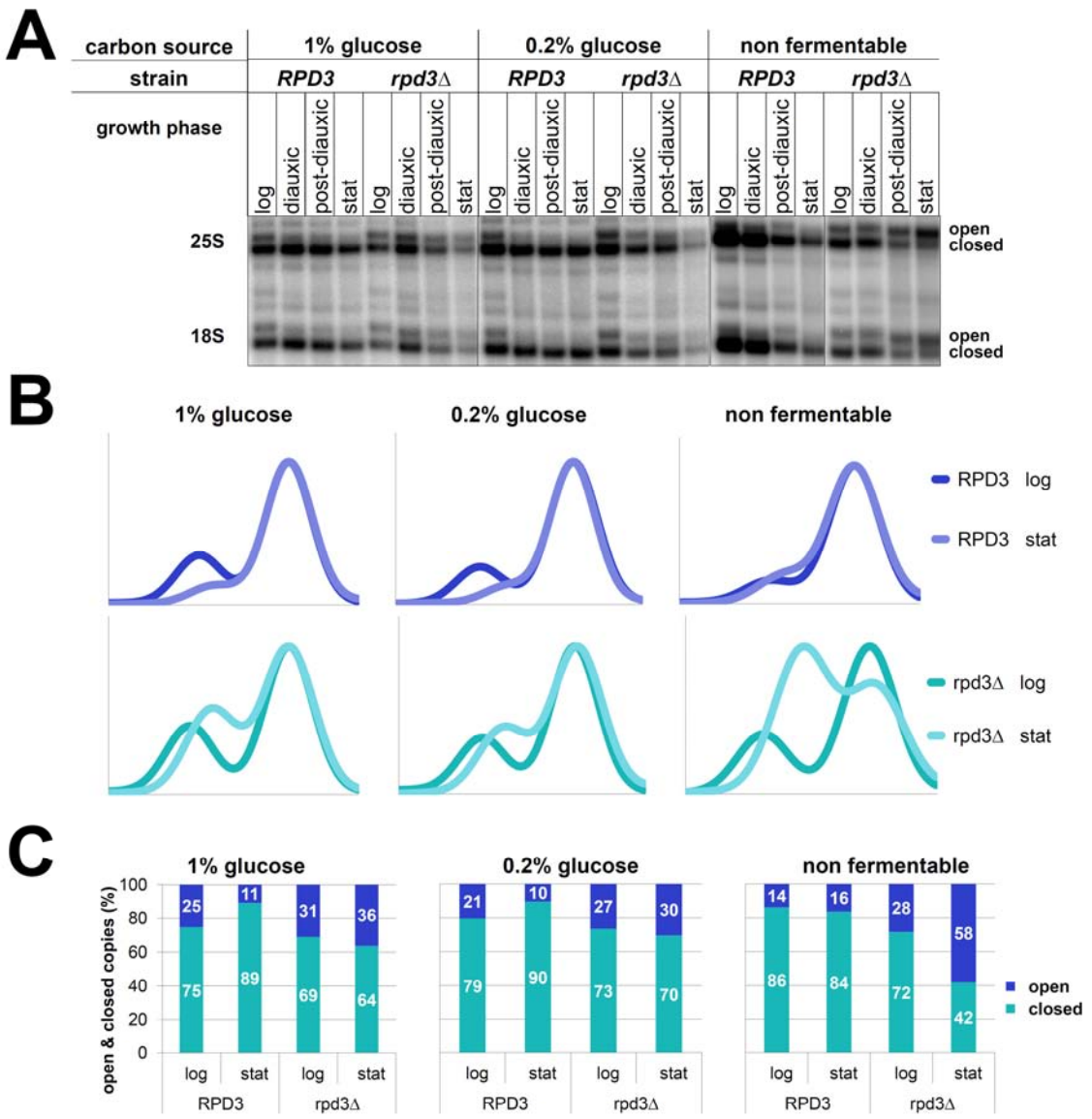

Supplemental Figure 2: Psoralen accessibility of the rDNA in *RPD3* and *rpd3*Δ cells upon growth in low glucose and non fermentable carbon source medium

Strains y348 (*RPD3*) and y2919 (*rpd3*Δ) were cultured in YP medium containing either half (1% glucose), or a tenth (0.2% glucose) of the normal glucose amount, or 3% glycerol and 3% ethanol (non fermentable) according to Figure 21 (see OD Figure 32 for the culture ODs). Psoralen analysis was conducted according to Figure 10 and Figure 23 without preceding ChEC analysis. **(A)** Psoralen analysis. An autoradiograph after hybridization with the 3.5kb rDNA probe is shown. The origin of the sample is indicated at the top (for the non fermentable carbon source medium the samples are labeled in the same way as for the others even if there is no log phase and post-diauxic growth phase). On the left it is indicated from which EcoRI rDNA fragment the signal is derived. On the right the positions of fragments derived from either the open or the closed chromatin state are labeled. **(B)** Profile analysis of the log and stat Psoralen signals shown in (A) according to Figure 26. **(C)** Ratio of open and closed rDNA copies for log and stat samples. The calculation was made according to Figure 26. The exact percent value is indicated as white numbers in the bars.

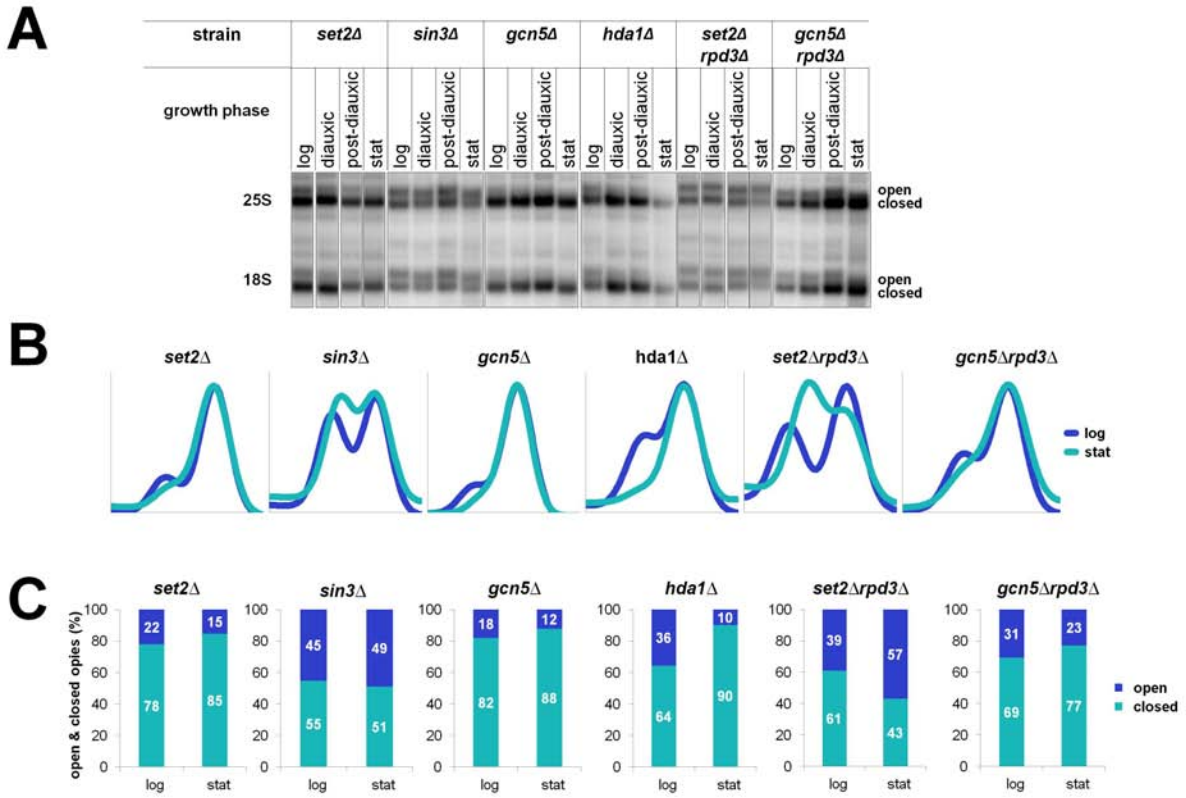

Supplemental Figure 3: Psoralen accessibility of the rDNA in different deletion strains upon growth to stationary phase

Strains y2920 (*set2*Δ), y3315 (*sin3*Δ), y3319 (*gcn5*Δ), y3317 (*hda1*Δ), y2946 (*rpd3*Δ*set2*Δ), and y3321 (*rpd3*Δ*gcn5*Δ) were cultured in YPAD according to Figure 21 (see OD Figure 33 for the culture ODs). Psoralen analysis was conducted according to Figure 10 and Figure 23 without preceding ChEC analysis. **(A)** Psoralen analysis. An autoradiograph after hybridization with the 3.5kb rDNA probe is shown. The origin of the sample is indicated at the top. On the left it is indicated from which EcoRI rDNA fragment the signal is derived. On the right the positions of fragments derived from either the open or the closed chromatin state are labeled. **(B)** Profile analysis of the Psoralen signals of log and stat samples shown in (A) according to Figure 26. **(C)** Ratio of open and closed rDNA copies for log and stat samples. The calculation was made according to Figure 26. The exact percent value is indicated as white numbers in the bars.

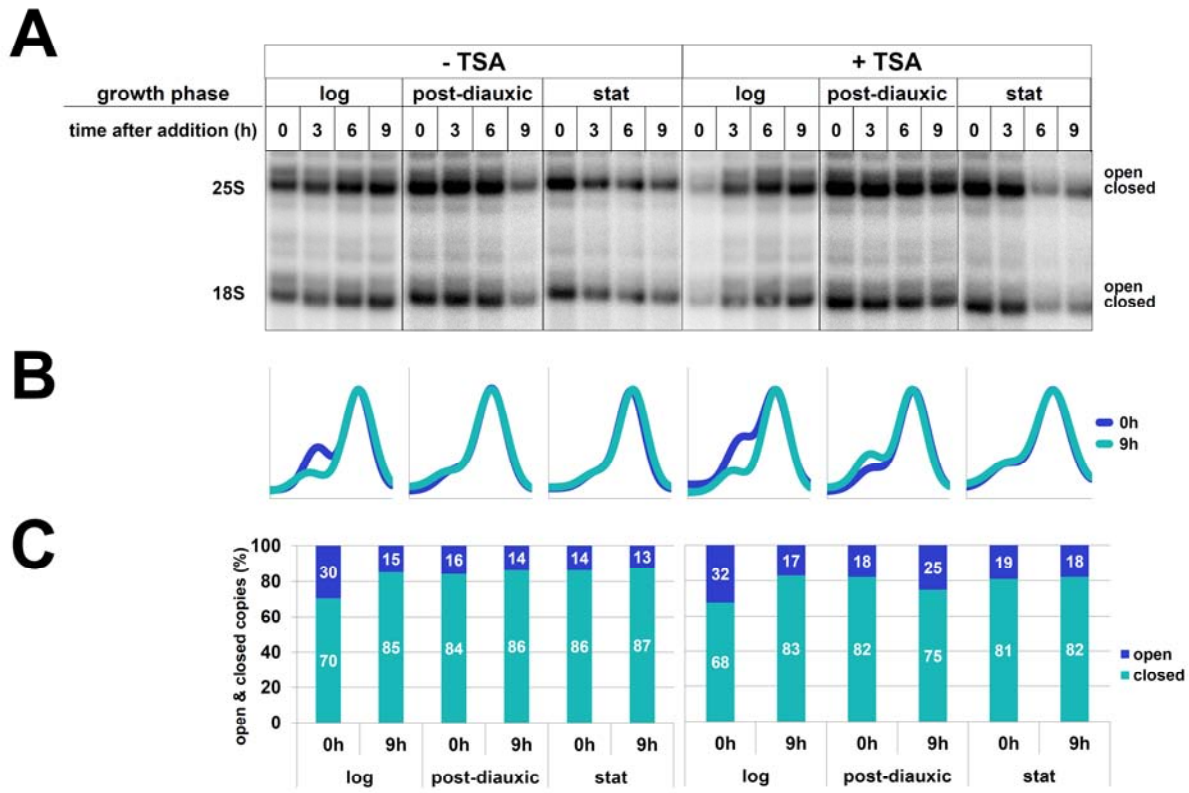

Supplemental Figure 4: Psoralen accessibility of the rDNA upon treatment with TSA in different growth phases

Strain y348 was cultured in YPAD and samples except the diauxic shift sample were collected according to Figure 21 (see OD Figure 34 for the culture ODs). At each growth phase either TSA dissolved in ethanol (+ TSA) was added to a final concentration of 50µM. As control the same volume of ethanol was added (-TSA). Psoralen analysis was conducted according to Figure 10 and Figure 23 without preceding ChEC analysis. **(A)** Psoralen analysis. An autoradiograph after hybridization with the 3.5kb rDNA probe is shown. The origin of the sample is indicated at the top. On the left it is indicated from which EcoRI rDNA fragment the signal is derived. On the right the positions of fragments derived from either the open or the closed chromatin state are labeled. **(B)** Profile analysis of the samples after 0h and 9h of TSA treatment shown in (A) according to Figure 26. The respective profile analyses are arranged according to the autoradiographs shown in (A). **(C)** Ratio of open and closed rDNA copies after 0h and 9h of TSA treatment. The calculation was made according to Figure 26. The exact percent value is indicated as white numbers in the bars.

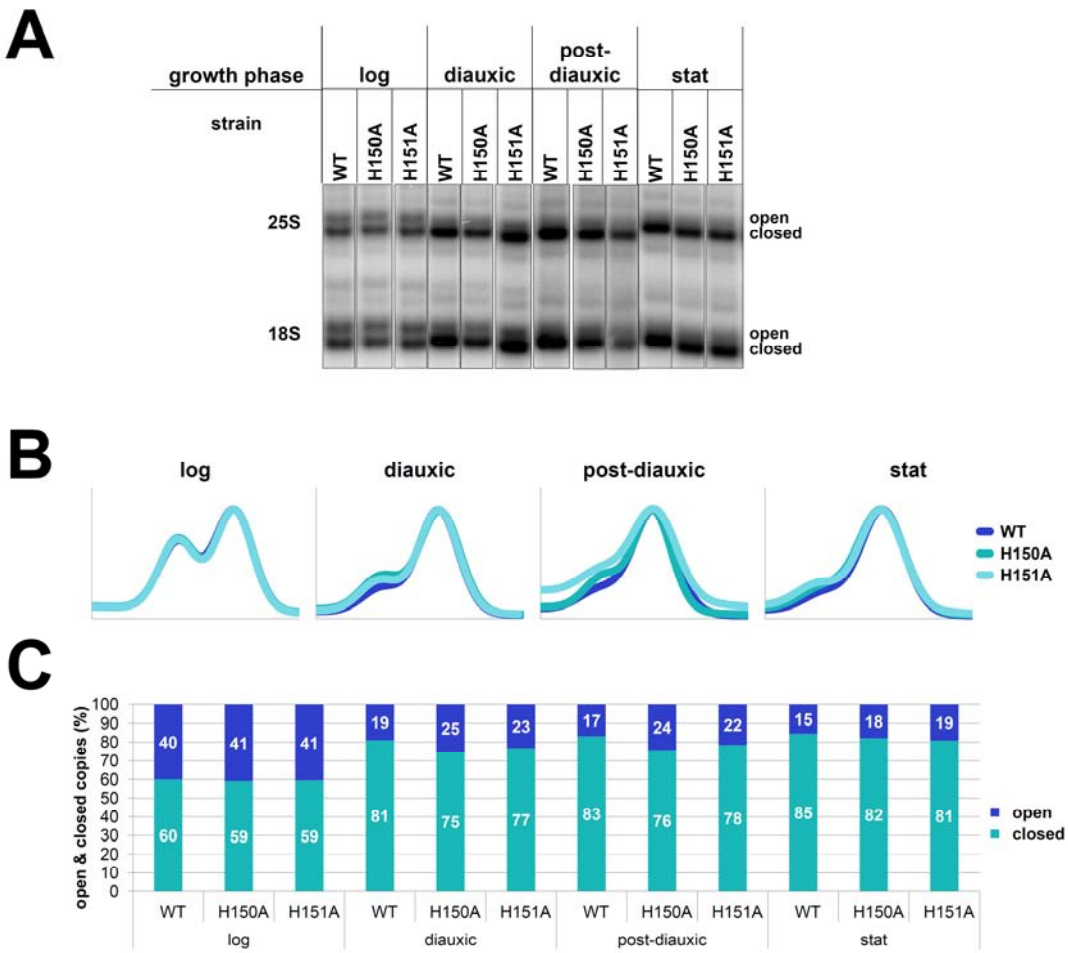

Supplemental Figure 5: Psoralen accessibility of the rDNA upon mutation of the putative deacetylase motif of Rpd3

Strains y3228 (*RPD3*), y3230 (*rpd3H150A*), and y3232 (*rpd3H151A*) were cultured in YPAD according to Figure 21 (see OD Figure 35 for the culture ODs). Psoralen analysis was conducted according to Figure 10 and Figure 23 without preceding ChEC analysis. **(A)** Psoralen analysis. An autoradiograph after hybridization with the 3.5kb rDNA probe is shown. The origin of the sample is indicated at the top. On the left it is indicated from which EcoRI rDNA fragment the signal is derived. On the right the positions of fragments derived from either the open or the closed chromatin state are labeled. **(B)** Profile analysis of the psoralen samples shown in (A) according to Figure 26. **(C)** Ratio of open and closed rDNA copies. The calculation was made according to Figure 26. The exact percent value is indicated as white numbers in the bars.

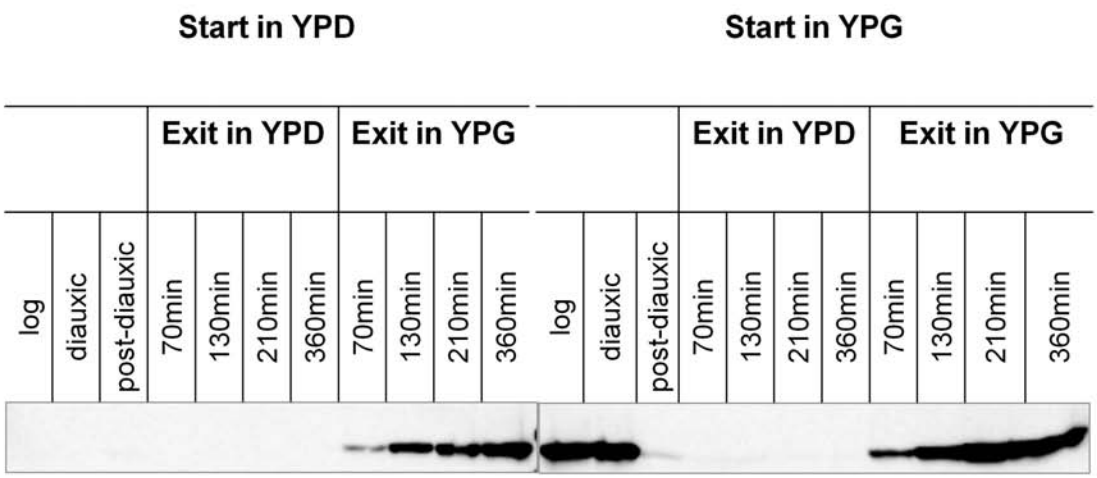

Supplemental Figure 6: Rpa49 depletion in YPD and expression in YPG

Indicated samples from strain y2670 (*rpa49↓)* were subjected to Western Blot analysis with an antibody detecting the HA-tag (α-HA 3F10). 2% of the samples taken at the indicated timepoints were loaded to the gel.

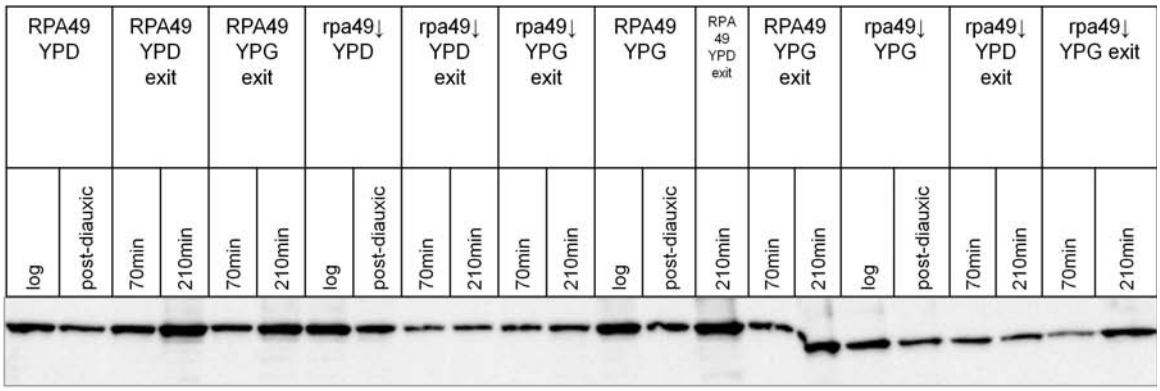

Supplemental Figure 7: Rpa135-ProtA levels in dependence of Rpa49 depletion or expression

Indicated samples from strains y2534 (*RPA49*) and y2670 (*rpa49↓)* were subjected to Western Blot analysis with an antibody detecting the HA-tag (α-HA 3F10). 2% of the samples taken at the indicated timepoints were loaded to the gel.

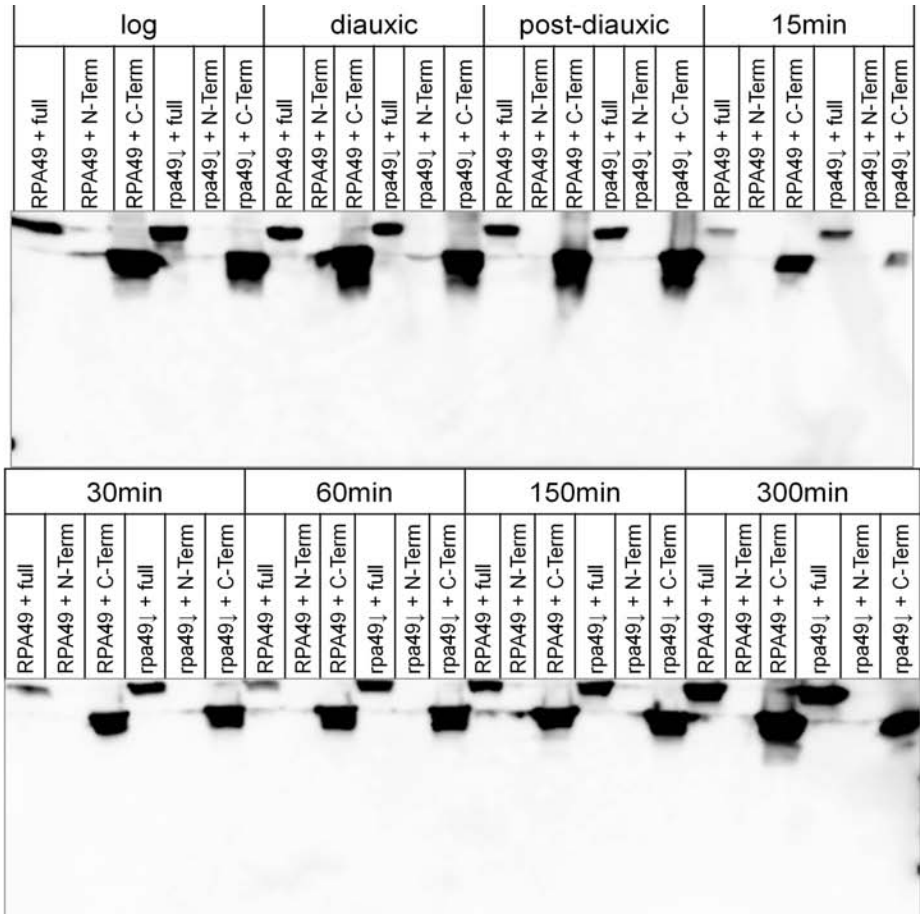

Supplemental Figure 8: Expression of full length Rpa49, Rpa49-N-Terminus, and Rpa49-C-Terminus

The indicated samples from strains y3536 (*RPA49*, additional expression of *pPGK1: RPA49-3xHA* (full)), y3544 (*RPA49,* additional expression of the C-terminal domain of Rpa49-3xHA (aa 116-426 (C-Term)) controlled by p*PGK1*), y3540 (*RPA49,* additional expression of the N-terminal domain of Rpa49-3xHA (aa 1-116 (N-Term)) controlled by p*PGK1*), y3534 *(rpa49*↓, "full"), y3538 (*rpa49*↓, N-Term)*,* and y3542 (*rpa49*↓, C-Term*)* were subjected to western blot analysis with an antibody detecting the HA-tag (α-HA 3F10). No signal was detected for the N-terminus. 2% of the samples taken at the indicated time points were loaded to the gel.

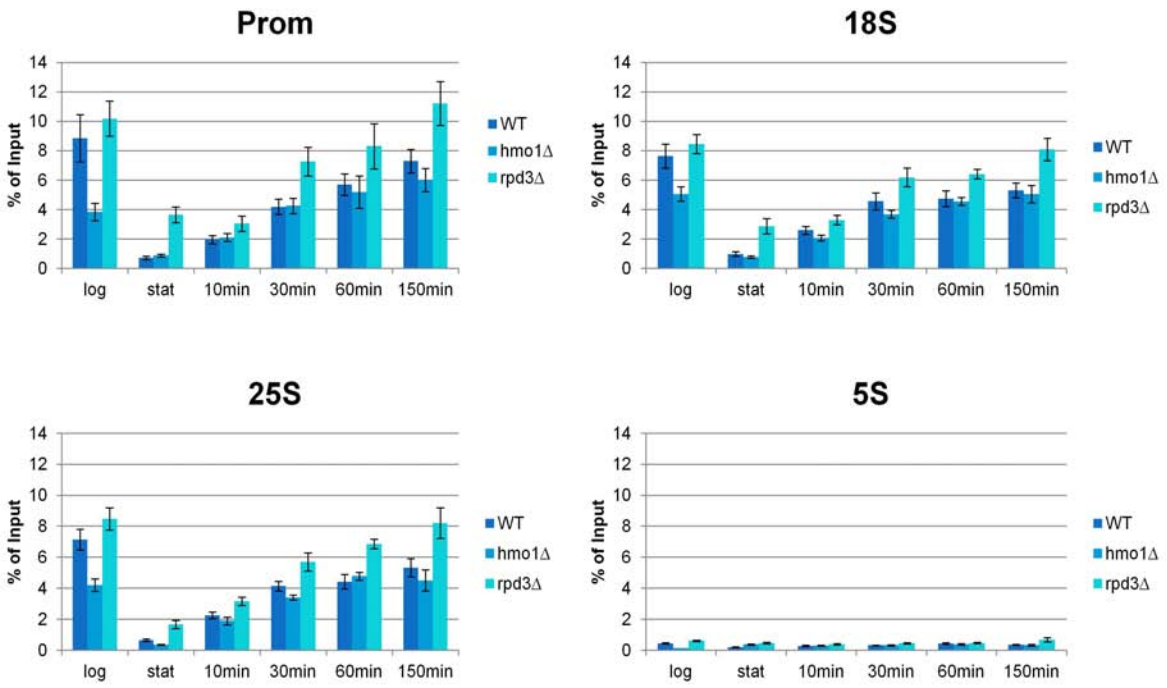

Supplemental Figure 9: Rpa135-TAP specifically co-precipitated 35S rDNA fragments upon transition to and exit from stationary phase in *WT, hmo1Δ,* and *rpd3Δ* strains

Yeast strains y3078 (Rpa135 with a C-terminal TAP-tag expressed from the endogenous locus, *WT*), y3226 (Rpa135 with a C-terminal TAP-tag expressed from the endogenous locus, *hmo1Δ*), and y3136 (Rpa135 with a C-terminal TAP-tag expressed from the endogenous locus, *rpd3*Δ) were cultured and samples were collected according to Figure 22. ChIP was performed according to Figure 27 with IgG sepharose beads. The graphs depict the percentage of the input of the respective DNA fragment (indicated at the top of each diagram) co-precipitating with the TAP-tagged fusion protein at the indicated growth phases. Error bars indicate standard deviation errors derived from three independent ChIP experiments, each analyzed in triplicate qPCRs. The positions of the respective qPCR amplicons within the rDNA locus are depicted in Figure 28. The 5S qPCR amplicon serves as a background control for DNA co-precipitating with Rpa135-TAP.

Culture ODs

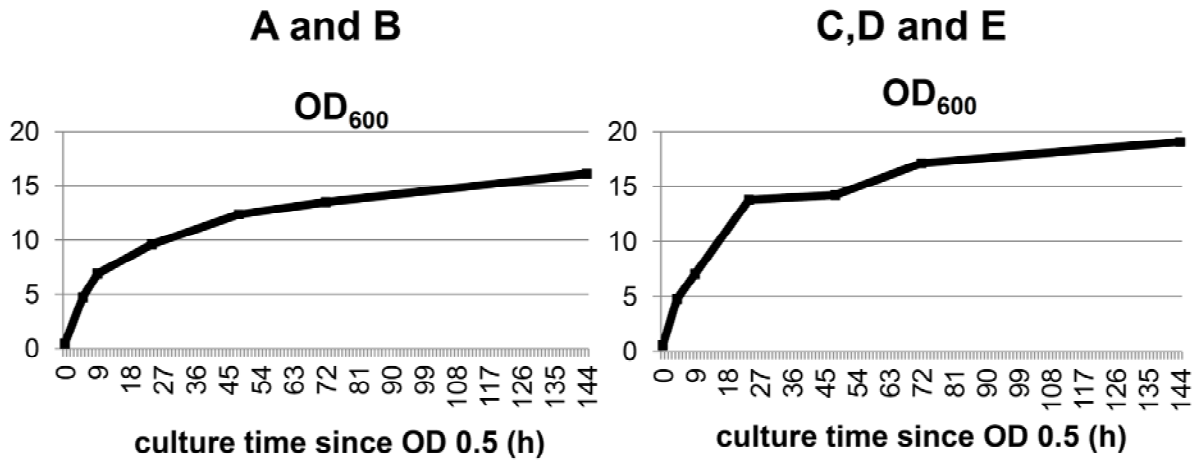

OD Figure 1: y1717 (*RPA190-MN*) culture ODs

Two cultures were made: One was used in this thesis for ChEC analysis (A and B) and one was used for ChEC-Psoralen analysis (C, D and E).

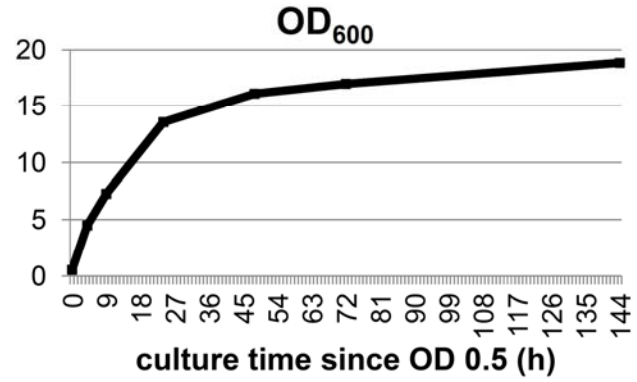

OD Figure 2: y1761 (*HMO1-MN*) culture ODs

The culture was used for ChEC and ChEC-Psoralen analysis.

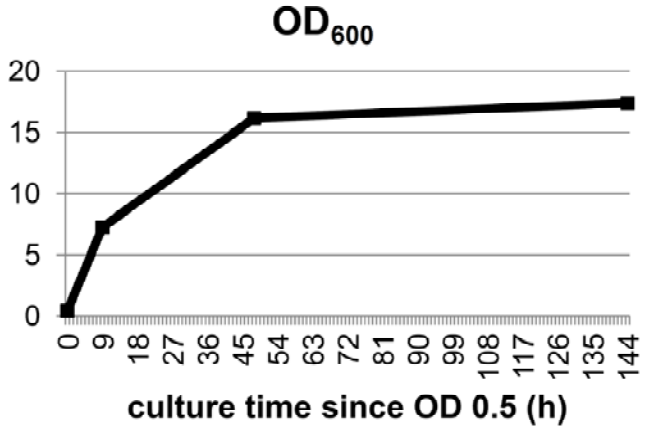

OD Figure 3: y1995 (*HHT1-MN*) culture ODs

The culture was used for ChEC and ChEC-Psoralen analysis.

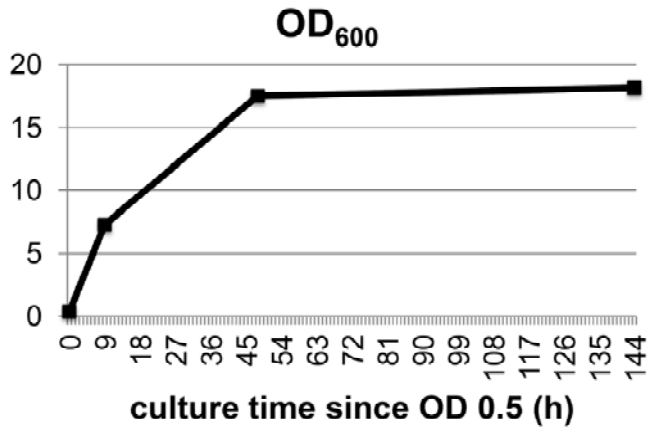

OD Figure 4: y1145 (*HHO1-MN*) culture ODs

The culture was used for ChEC and ChEC-Psoralen analysis.

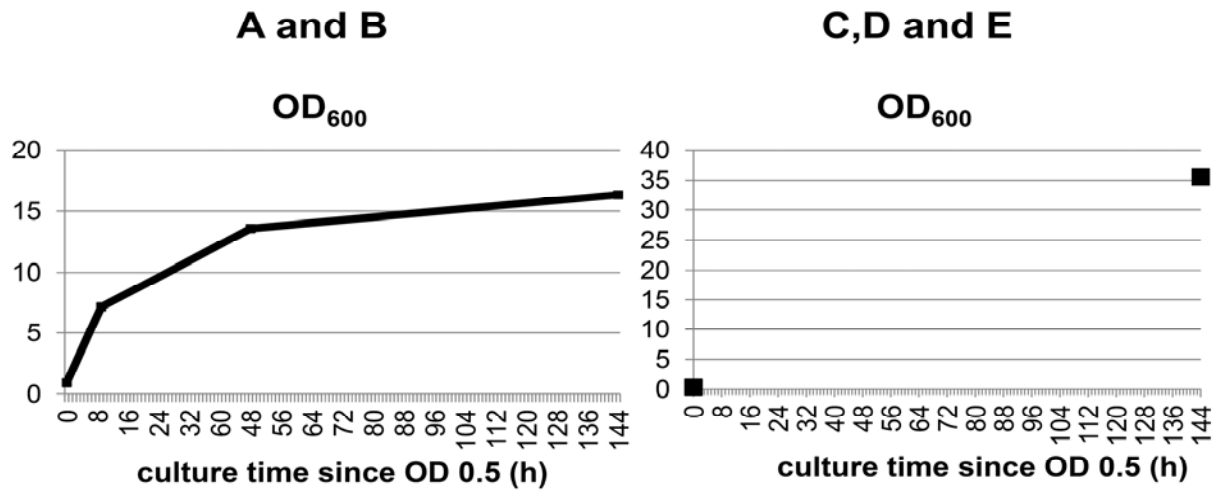

OD Figure 5: y1151 (*RRN9-MN*) culture ODs

Two cultures were made: One was used in this thesis for ChEC analysis (A and B) and one was used for ChEC-Psoralen analysis (C, D and E).

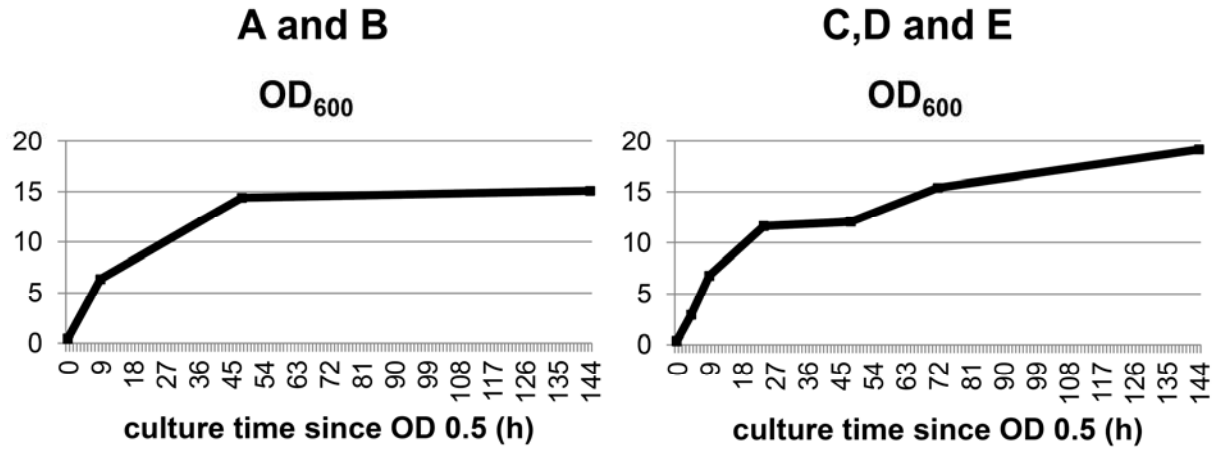

OD Figure 6: y1185 (*SPT15-MN*) culture ODs

Two cultures were made: One was used in this thesis for ChEC analysis (A and B) and one was used for ChEC-Psoralen analysis (C, D and E).

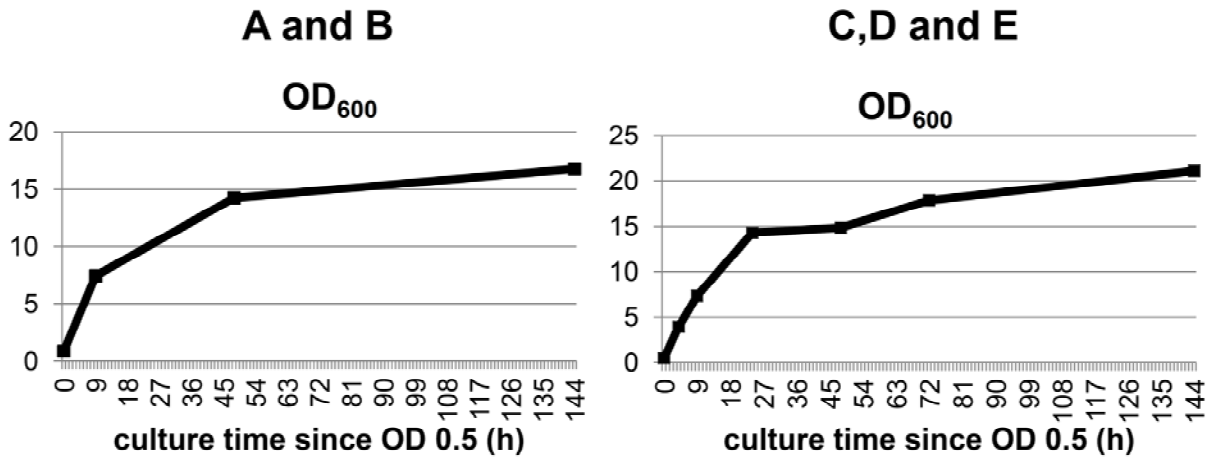

OD Figure 7: y881 (*RRN7-MN*) culture ODs

Two cultures were made: One was used in this thesis for ChEC analysis (A and B) and one was used for ChEC-Psoralen analysis (C, D and E).

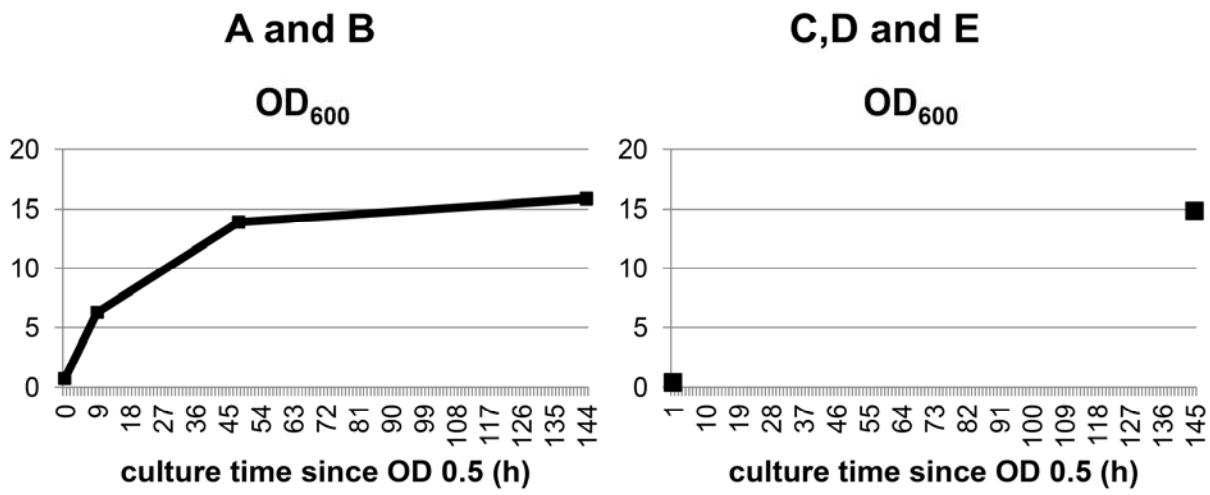

OD Figure 8: y1453 (*NET1-MN*) culture ODs

Two cultures were made: One was used in this thesis for ChEC analysis (A and B) and one was used for ChEC-Psoralen analysis (C, D and E).

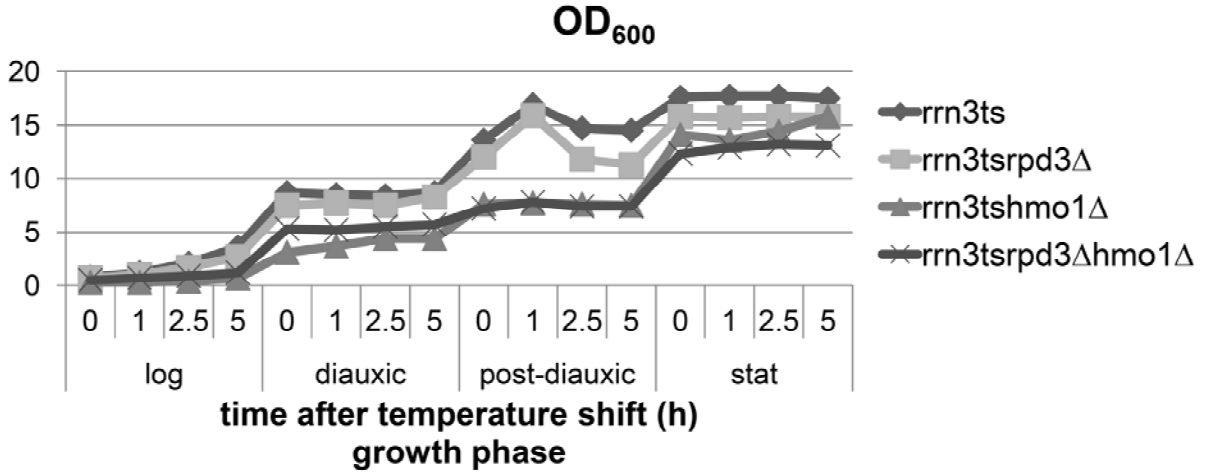

OD Figure 9: Culture ODs for strains y354 (*rrn3ts*), y2921 (*rrn3tsrpd3*Δ), y2945 (*rrn3tshmo1*Δ) and y2947 (*rrn3tsrpd3*Δ*hmo1*Δ)

The time at the restrictive temperature at the respective growth phase is indicated on the x-axis.

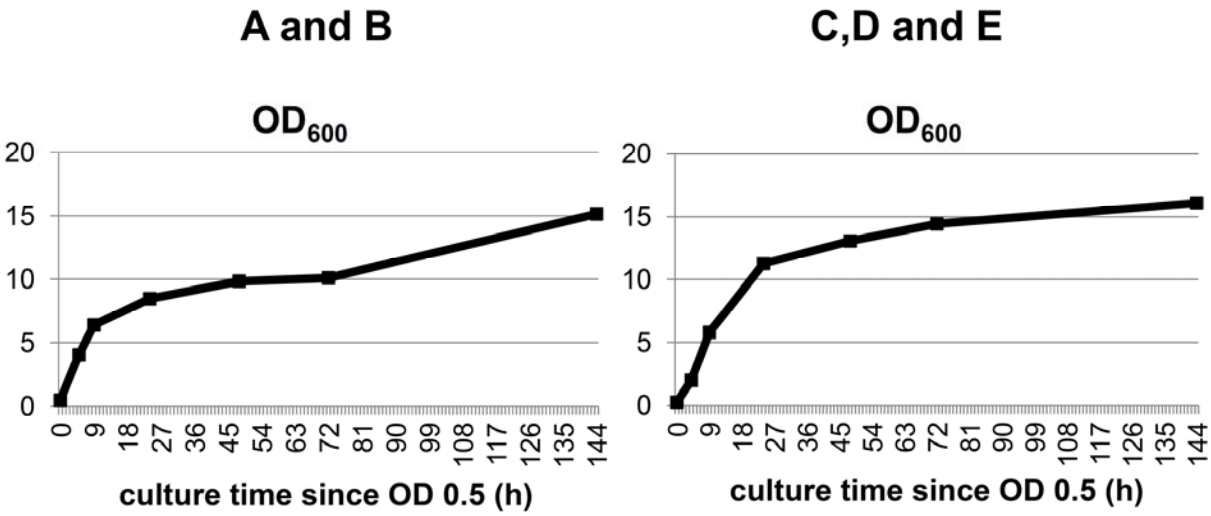

OD Figure 10: y2256 (*RPA190-MN rpd3*Δ) culture ODs

Two cultures were made: One was used in this thesis for ChEC analysis (A and B) and one was used for ChEC-Psoralen analysis (C, D and E).

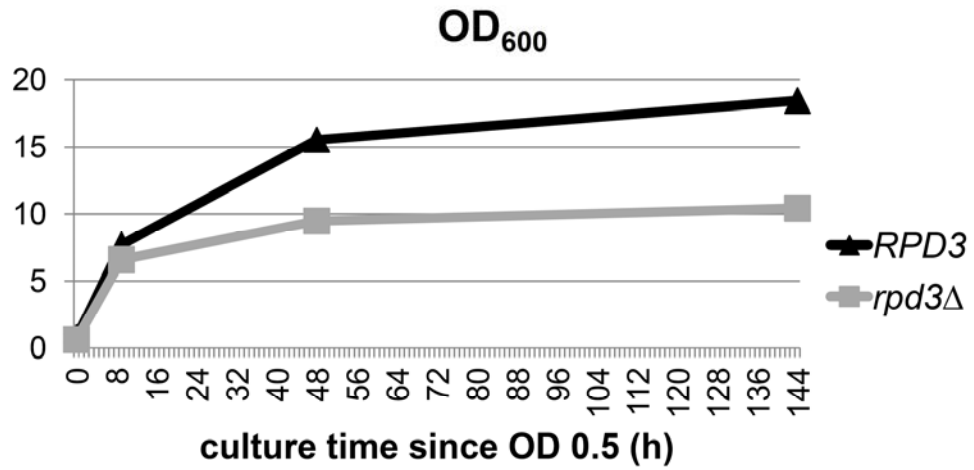

OD Figure 11: Culture ODs for y3078 (*RPA135-TAP RPD3*) and y3136 (*RPA135-TAP rpd3*Δ)

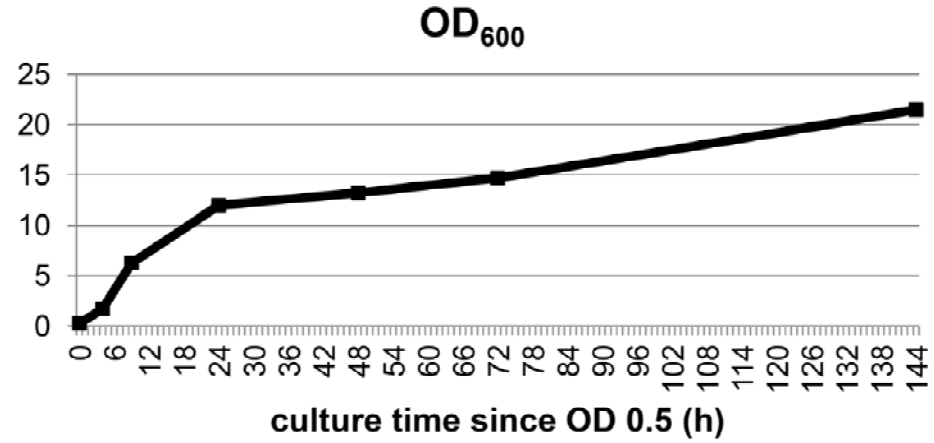

OD Figure 12: y2257 (*HMO1-MN rpd3*Δ*)* culture ODs

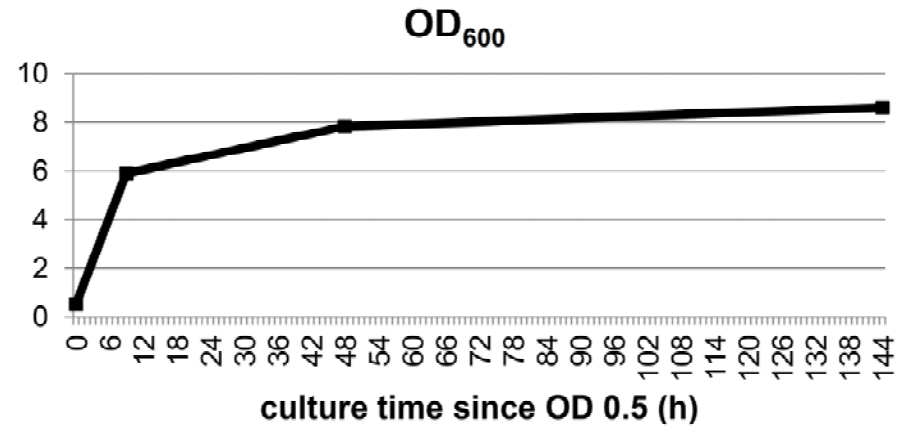

OD Figure 13: y2334 (*HHT1-MN rpd3*Δ) culture ODs

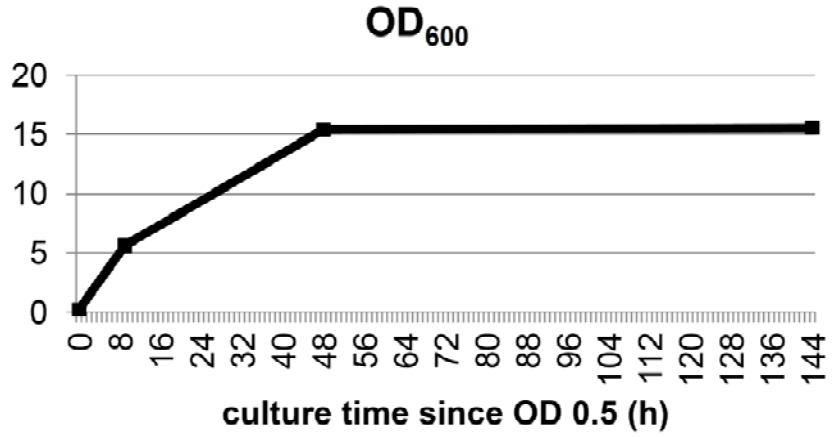

OD Figure 14: y2616 (*HHO1-MN rpd3*Δ) culture ODs

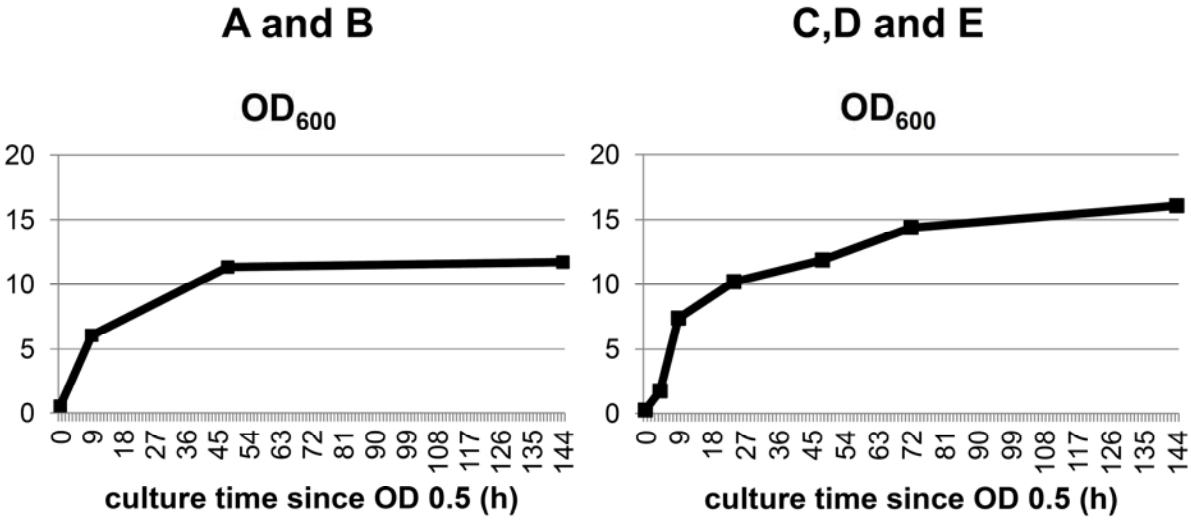

OD Figure 15: y3028 (*RRN9-MN rpd3*Δ) culture ODs

Two cultures were made: One was used in this thesis for ChEC analysis (A and B) and one was used for ChEC-Psoralen analysis (C, D and E).

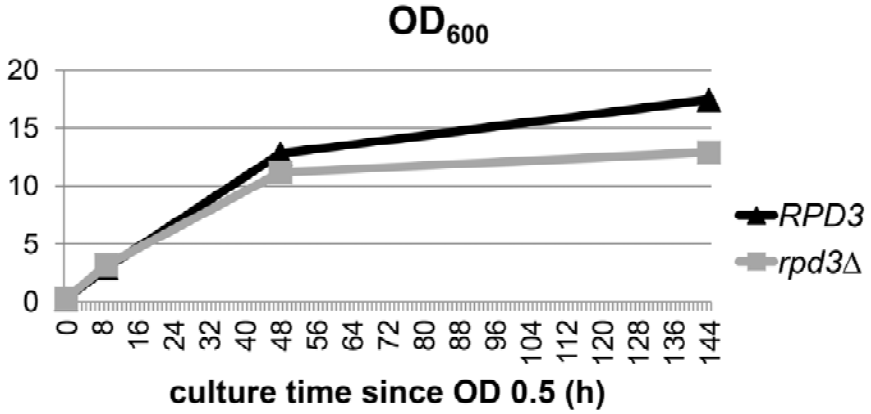

OD Figure 16: Culture ODs for y3118 (*RRN9-TAP RPD3*) and y3124 (*RRN9-TAP rpd3*Δ)

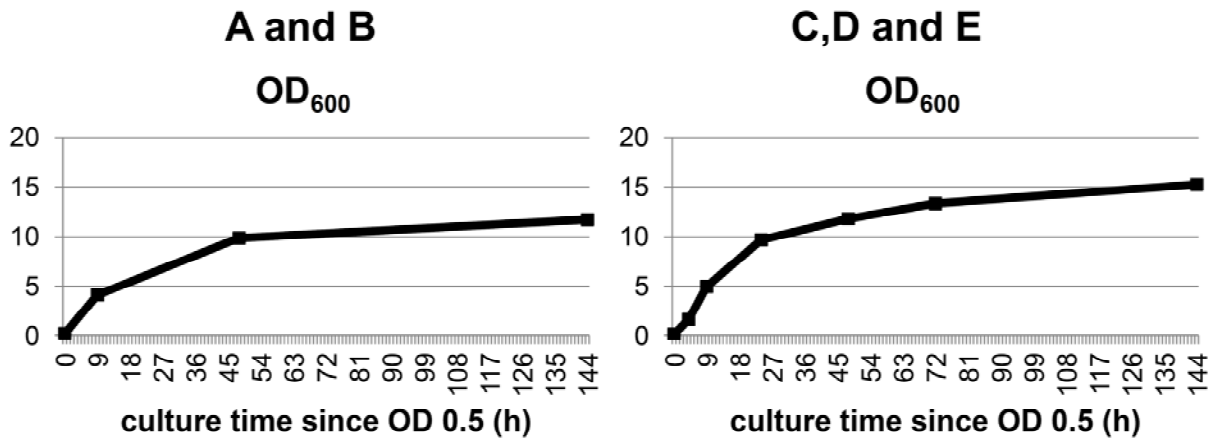

OD Figure 17: y3030 (*SPT15-MN rpd3*Δ) culture ODs

Two cultures were made: One was used in this thesis for ChEC analysis (A and B) and one was used for ChEC-Psoralen analysis (C, D and E).

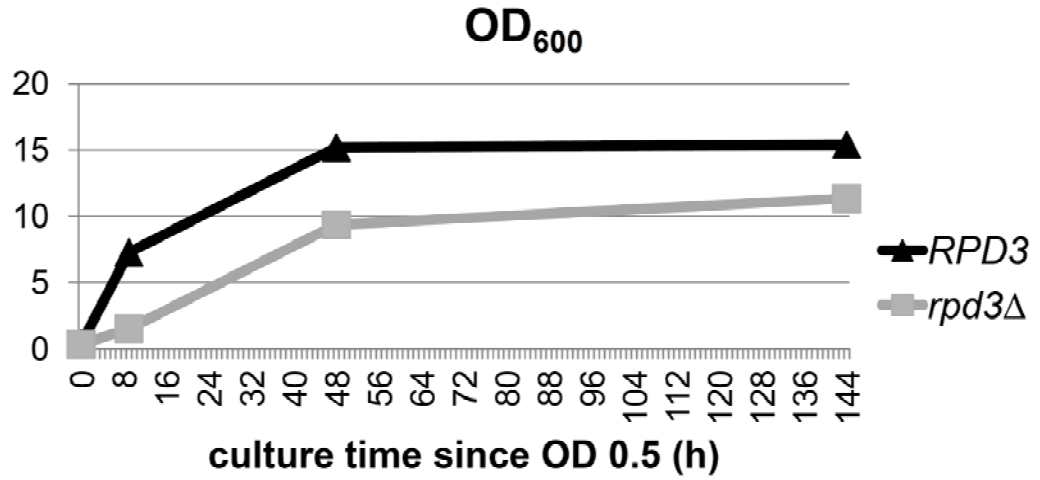

OD Figure 18: Culture ODs for y3327 (*SPT15-TAP RPD3*) and y3329 (*SPT15-TAP rpd3*Δ)

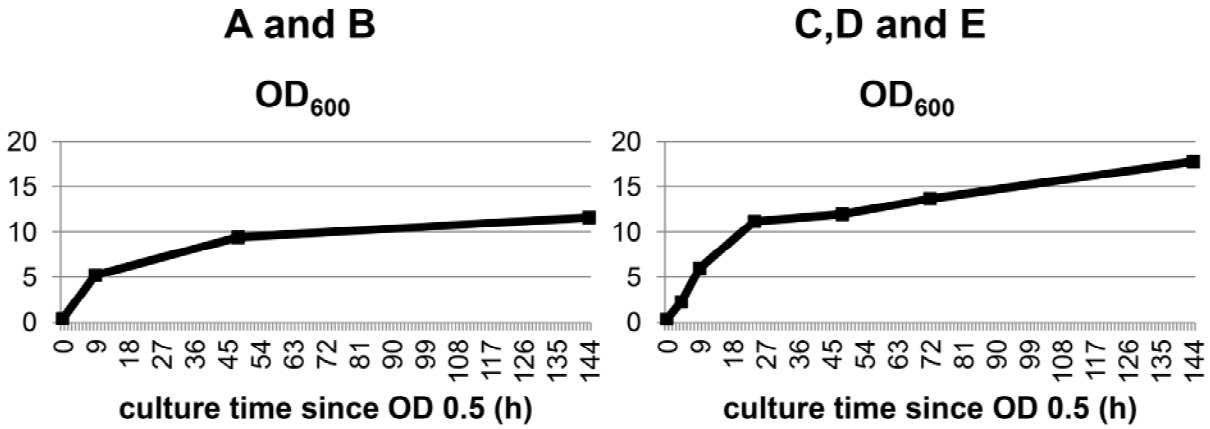

OD Figure 19: y3024 (*RRN7-MN rpd3*Δ) culture ODs

Two cultures were made: One was used in this thesis for ChEC analysis (A and B) and one was used for ChEC-Psoralen analysis (C, D and E).

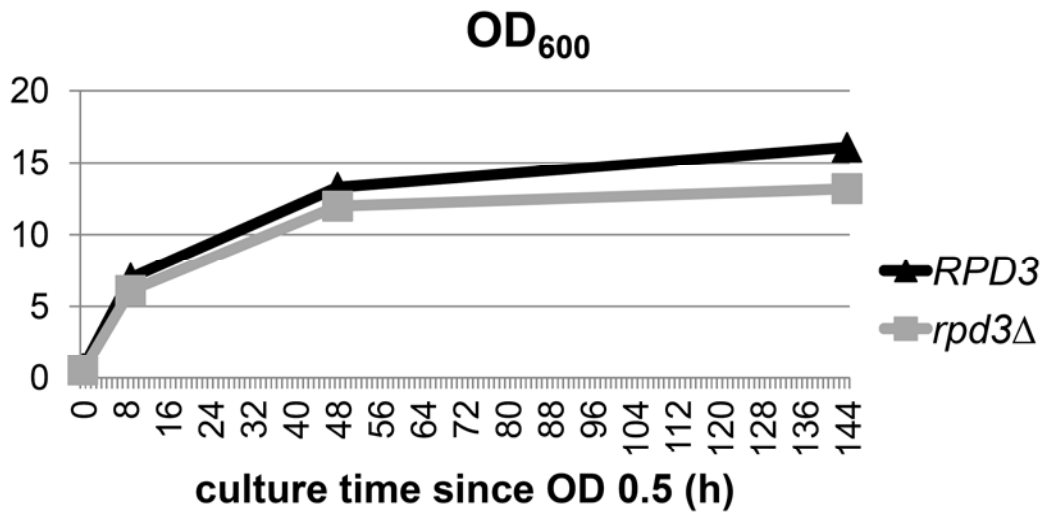

OD Figure 20: Culture ODs for y3116 (*RRN7-TAP RPD3*) and y3122 (*RRN7-TAP rpd3*Δ)

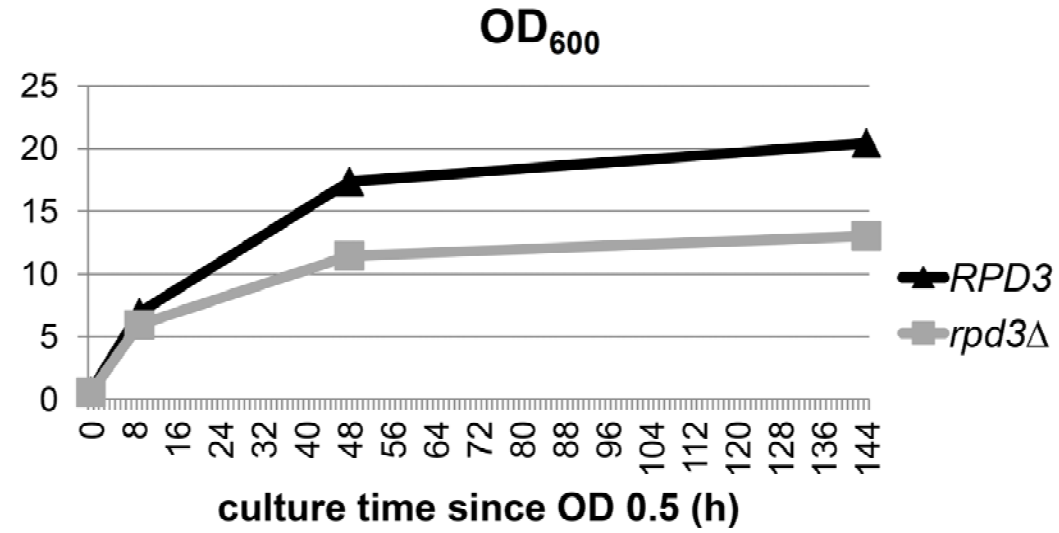

OD Figure 21: Culture ODs for y3120 (*RRN3-TAP RPD3*) and y3126(*RRN3-TAP rpd3*Δ)

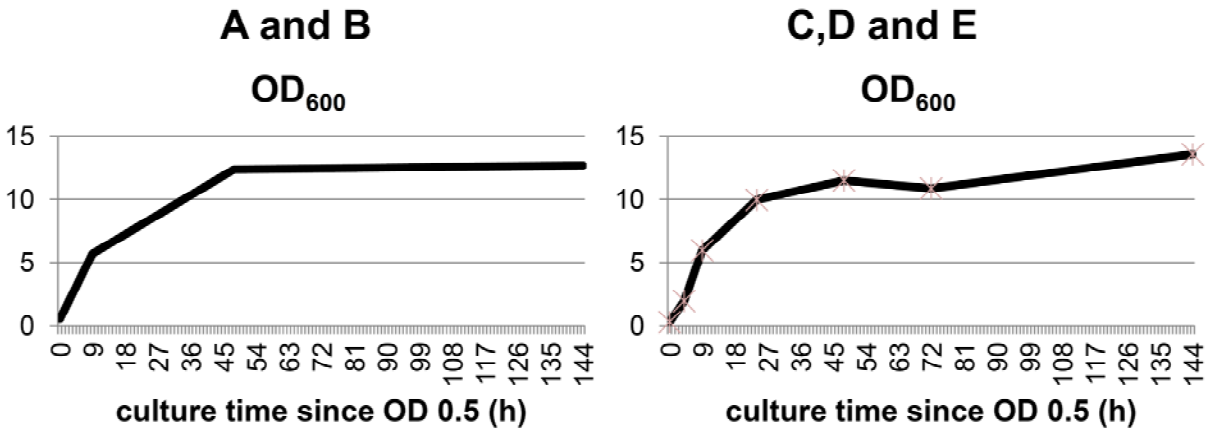

OD Figure 22: y3033 (*NET1-MN rpd3*Δ) culture ODs

Two cultures were made: One was used in this thesis for ChEC analysis (A and B) and one was used for ChEC-Psoralen analysis (C, D and E).

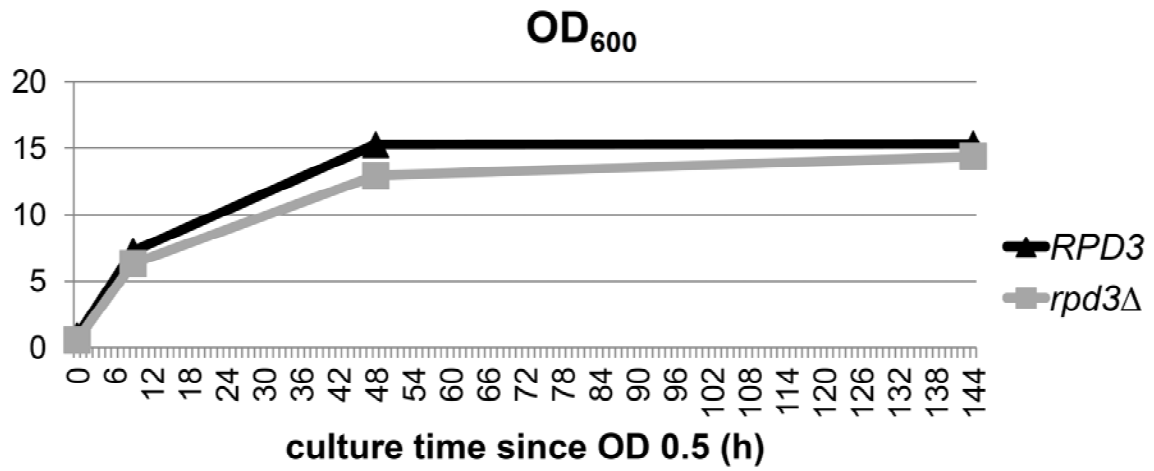

OD Figure 23: Culture ODs for y2017 (*NET1-TAP RPD3*) and y3131 (*NET1-TAP rpd3*Δ)

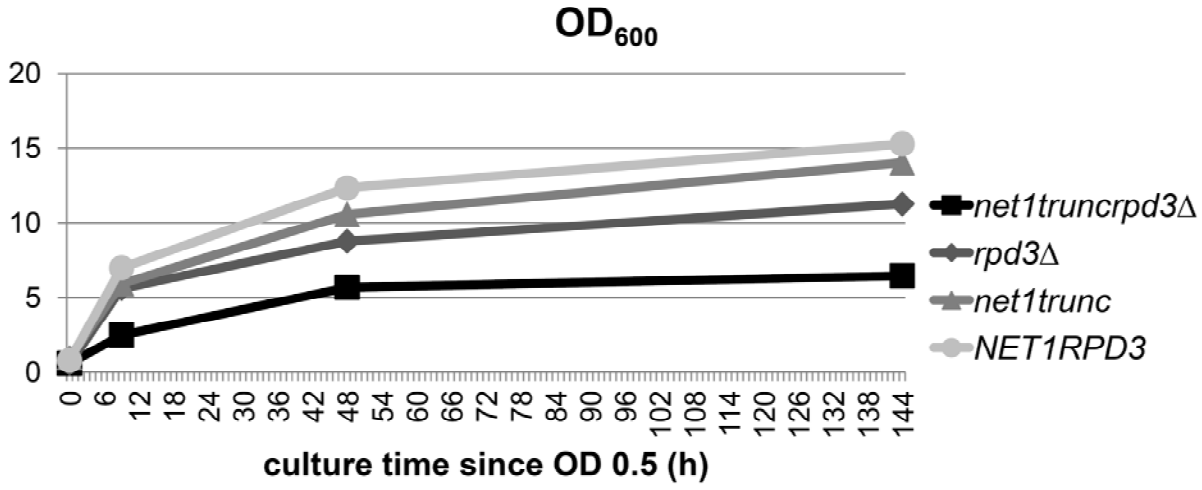

OD Figure 24: Culture ODs for y3725 (*NET1 RPD3*) y3672 (*NET1 rpd3*Δ) y3673 (*net1trunc RPD3*) and y3671 (*net1trunc rpd3*Δ)

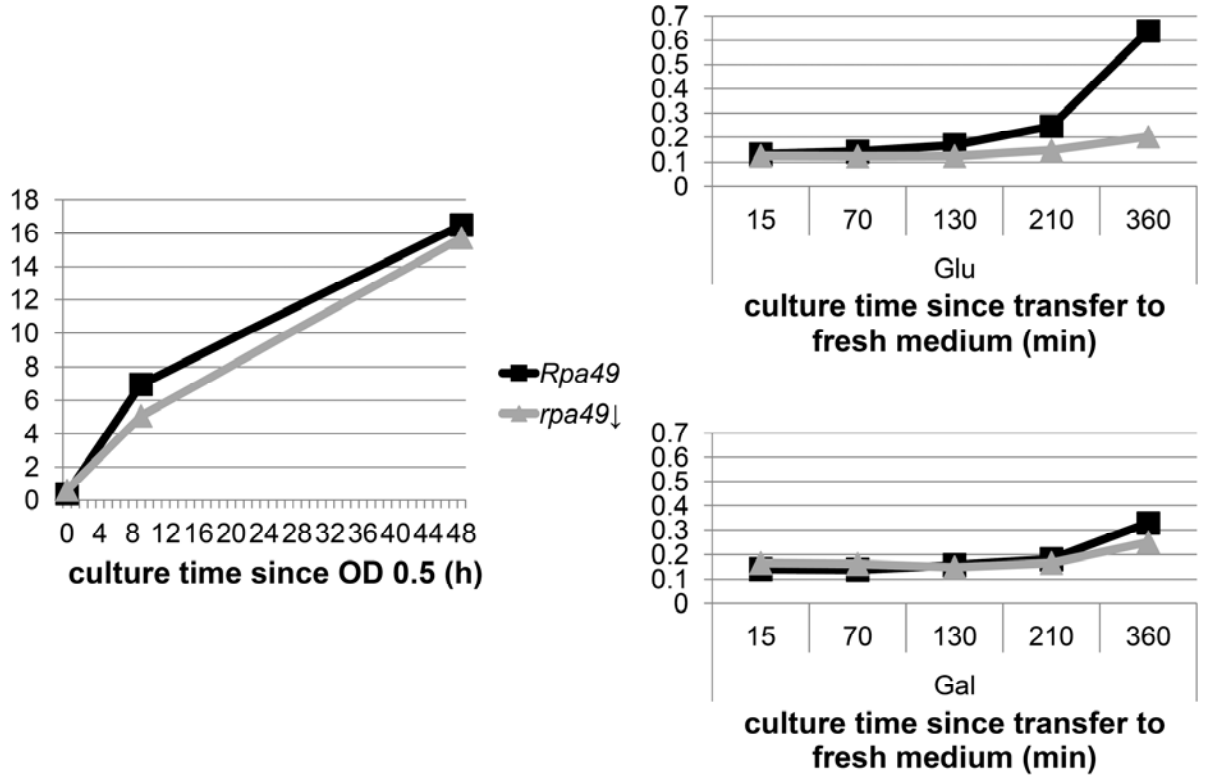

OD Figure 25: Culture ODs for y207 (*RPA49*) and y2670 (*rpa49↓*)

The strains were cultured in YPD for 48h (left diagram) and then transferred to fresh YPD (right upper diagram) and to fresh YPG (right lower diagram).

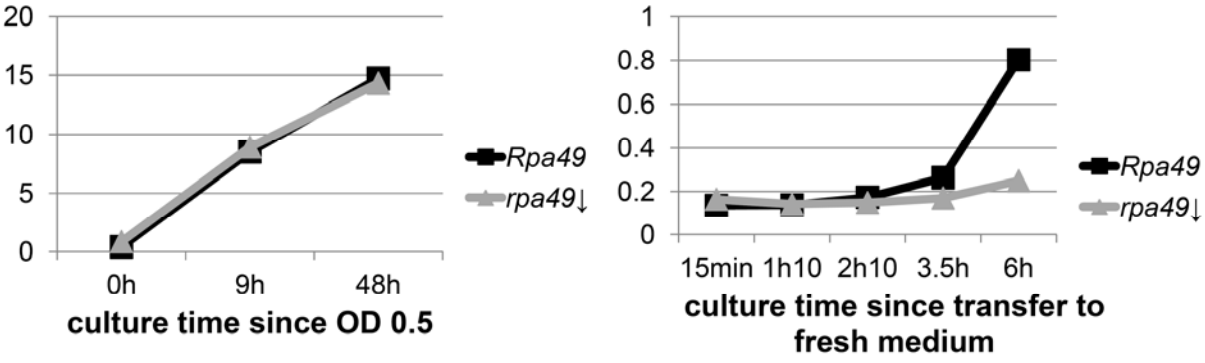

OD Figure 26: Culture ODs for y2534 (*RPA49*) and y2670 (*rpa49↓*)

The strains were cultured in YPD for 48h (left diagram) and then transferred to fresh YPD (right diagram).

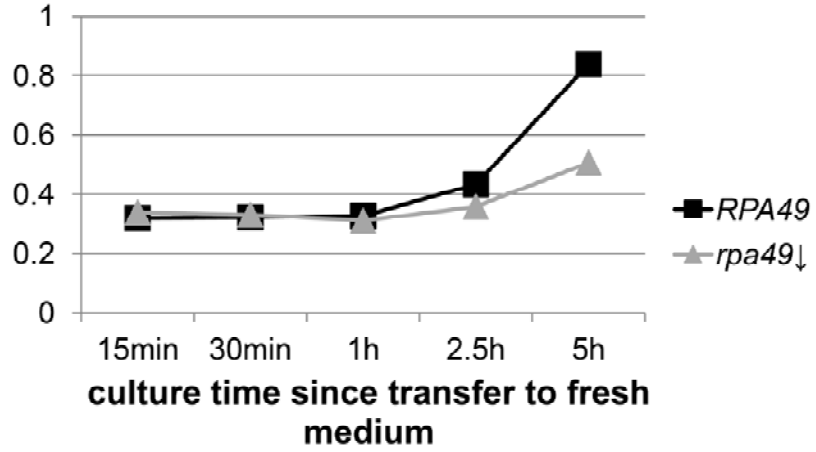

OD Figure 27: Culture ODs since transfer from stationary phase to fresh medium of strains y3323 (*RPA49 rpd3*Δ) and y3325 (*rpa49*↓ *rpd3*Δ)

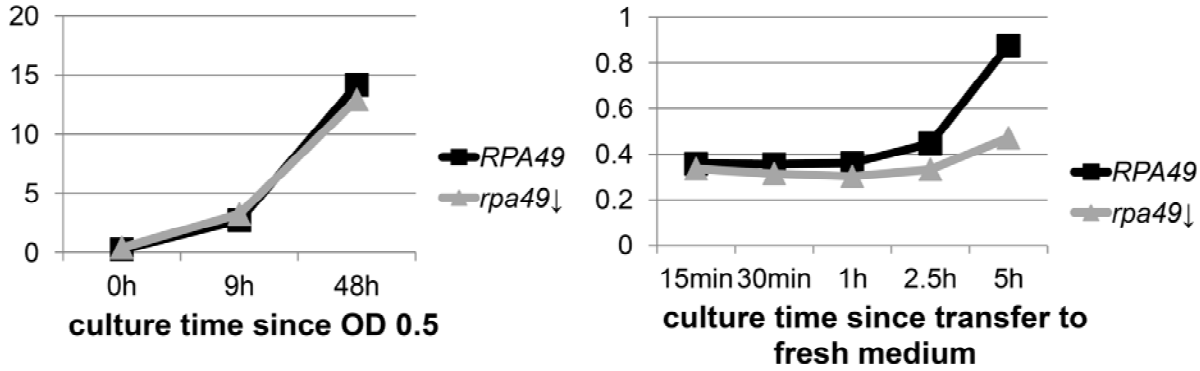

OD Figure 28: Culture ODs for strains y3323 (*RPA49 rpd3*Δ) and y 3325 (*rpa49*↓ *rpd3*Δ)

The strains were cultured in YPD for 48h (left diagram) and then transferred to fresh YPD (right diagram).

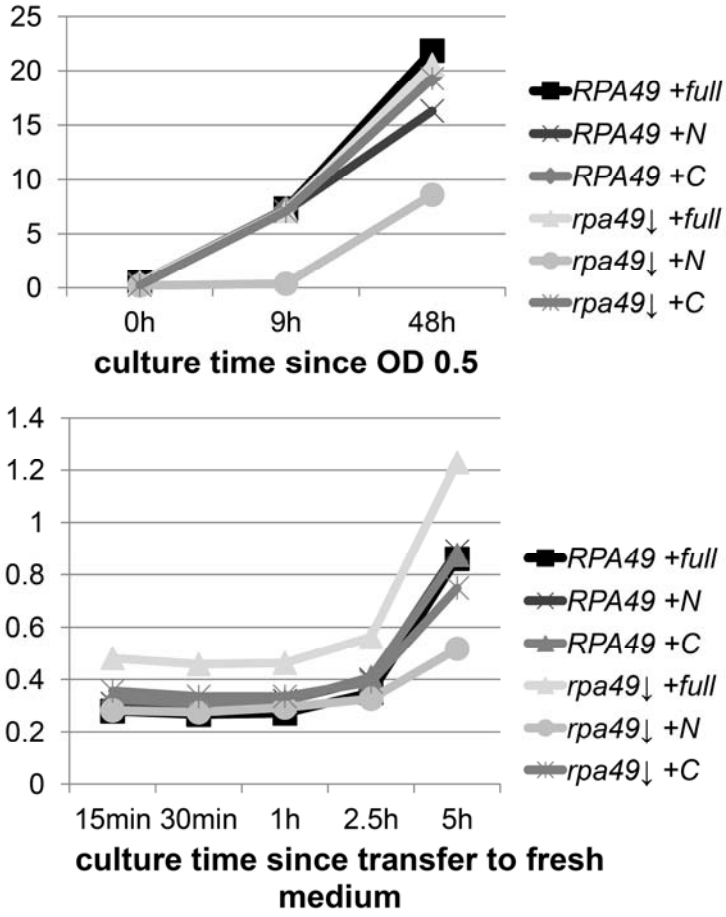

OD Figure 29: Culture ODs for strains y3536 (*RPA49 + full*), y3540 (*RPA49 + N-Term*), y3544 (*RPA49 + C-Term*), y 3534 (*rpa49↓ + full*), y3538 (*rpa49↓ + N-Term*) and y3542 (*rpa49↓ + C-Term*)

The strains were cultured in YPD for 48h (upper diagram) and then transferred to fresh YPD (lower diagram).

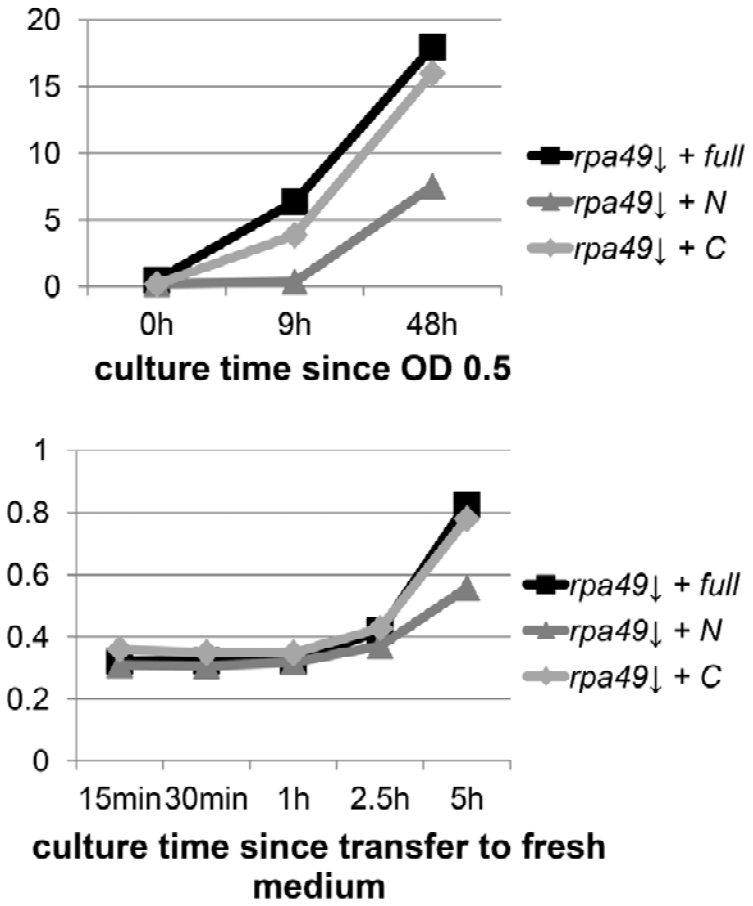

OD Figure 30: Culture ODs for strains y 3534 (*rpa49*↓ *+ full*), y3538 (*rpa49*↓ *+ N-Term*) and y3542 (*rpa49*↓ *+ C-Term*)

The strains were cultured in YPD for 48h (upper diagram) and then transferred to fresh YPD (lower diagram).

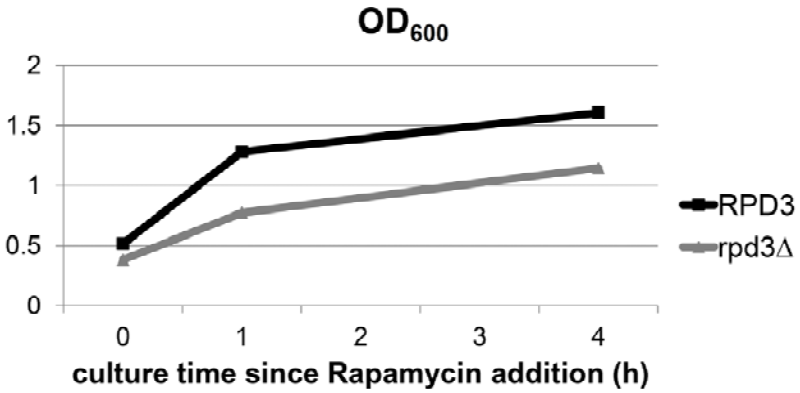

OD Figure 31: y881 (*RRN7-MN RPD3*) and y3024 (*RRN7-MN rpd3*Δ) Rapamycin treatment ODs

The cells were grown ON to OD 0.5 and then Rapamycin was added. The culture was incubated for 4h after Rapamycin addition.

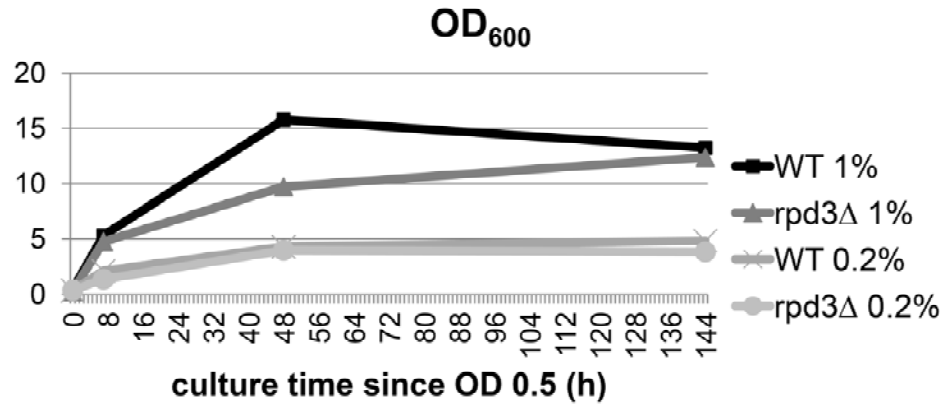

OD Figure 32:Culture ODs for strains y348 (*RPD3*) and y2919 (*rpd3Δ*) for different glucose concentrations

The ODs for the non-fermentable carbon source are not available.

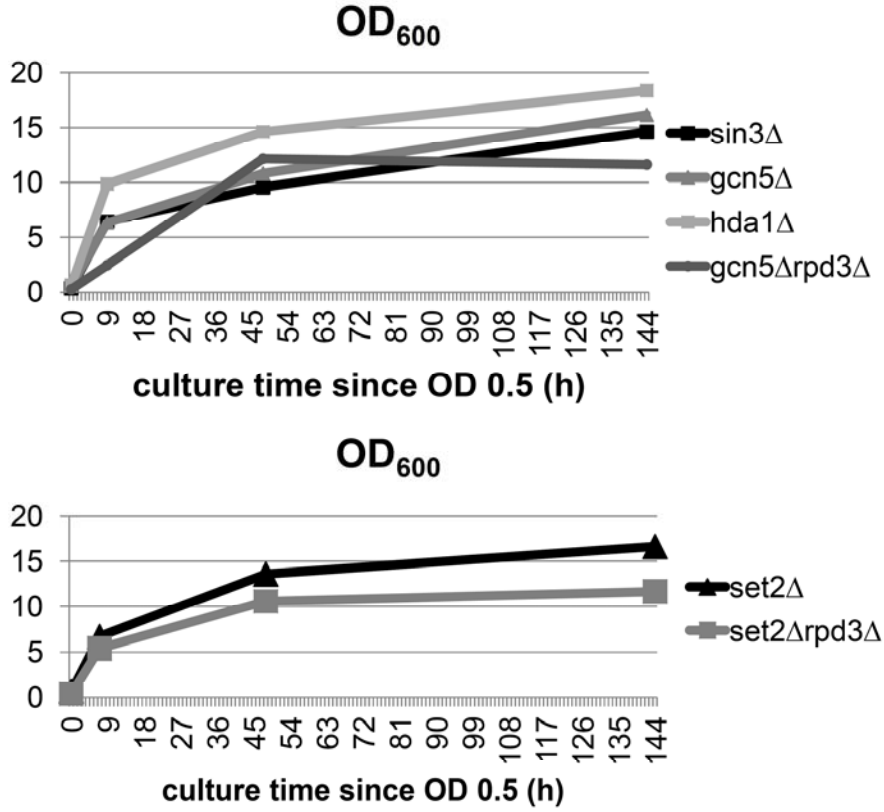

OD Figure 33: Culture ODs for strains y3315(*sin3*Δ), y3319 (*gcn5*Δ), y3317 (*hda1*Δ), y3321 (*rpd3*Δ*gcn5*Δ) and y2920 (*set2*Δ), y2946 (*rpd3*Δ*set2*Δ)

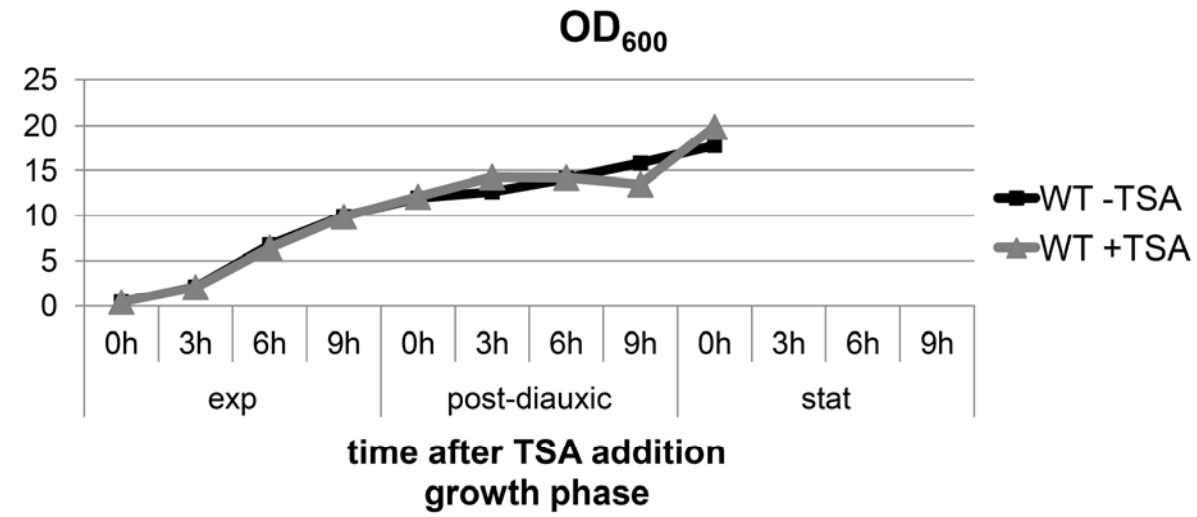

OD Figure 34: Culture ODs without and after TSA addition for strain y348

The time after TSA addition in the respective growth phase is shown on the x-axis.

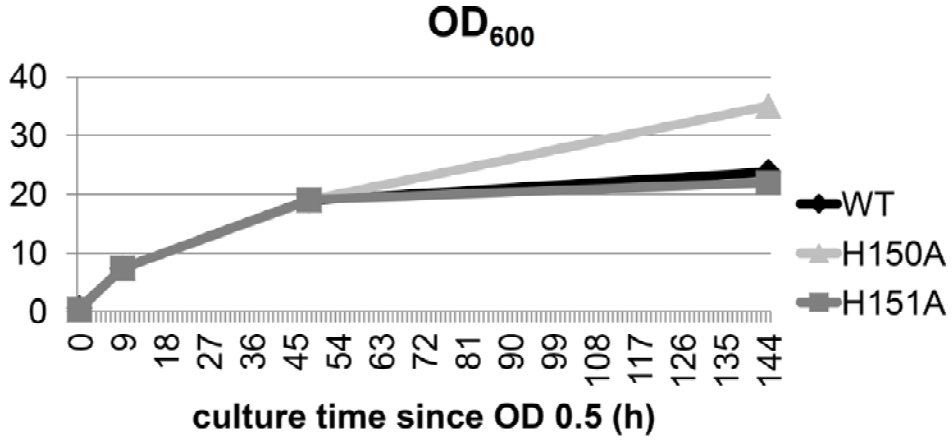

OD Figure 35: Culture ODs for y3228 (WT), y3230 (rpd3 H150A), y3232 (rpd3 H151A)

Abbreviations

5S	5S rDNA
18S	18S region of the 35S rDNA
25S	25S region of the 35S rDNA
AGE	agarose gel electrophoresis
ARS	autonomously replicating sequence
app./~	approximately
CE	Core element
CEN	centromere
cf.	confer to
CF	Core factor
ChEC	Chromatin Endogenous Cleavage
ChIP	Chromatin Immunoprecipitation
C-terminal	carboxy terminal
diauxic	diauxic shift
DNA	desoxyribonucleic acid
dNTP	desoxyribonucleoside-5'-triphosphate
EDTA	ethylen diamine tetraacetic acid
e.g.	for example
EGTA	ethylene glycol tetraacetic acid
ENH	enhancer
E-pro	bidirectional Pol II promoter in the rDNA
FA-X	formaldehyde crosslink
g	gram(s)
h	hour(s)
HDAC	histone deacetylase
k	kilo

kb	kilobase
l	liter
log	logarithmic/exponential growth phase
M	molar (mol/l)
m	milli/meter
min	minute(s)
MNase	micrococcal nuclease
n	nano
NEB	New England Biolabs
N-terminal	amino terminal
OD(600)	optical density at 600nm
ON	overnight
P/Prom	Promoter region of the 35S rDNA
PCR	polymerase chain reaction
pH	negative decadic logarithm [H^+]
Pol I	RNA polymerase I
Pol II	RNA polymerase II
Pol III	RNA polymerase III
post-diauxic	post-diauxic growth phase
ProtA	Protein A
PTM	posttranslational modification
qPCR	quantitative real-time PCR
RAPA	Rapamycin
rDNA	ribosomal DNA
RED	restriction enzyme digest
RNA	ribonucleic acid
RP	ribosomal protein
rpm	rotations per minute

rRNA	ribosomal RNA
RT	room temperature
S	sedimentation coefficient
S. cerevisiae	*Saccharomyces cerevisiae*
SDS	Sodium dodecyl sulfate
stat	stationary phase
TAP	tandem affinity purification
Taq	*Thermus aquaticus*
TBP	TATA-box binding protein
TE	Tris EDTA
TEL	telomere
Tris	tris (hydoxymethyl) amino methane
ts	temperature sensitive
TSA	Trichostatin A
U	units
UAF	Upstream activating factor
UE	Upstream element
µ	micro
UV	ultraviolet (light)
WT	wildtype
YNB	Yeast nitrogen base
YP(A)D	Yeast extract, Peptone, (Adenine), Dextrose medium
YPG	Yeast extract, Peptone, Galactose medium

Acknowledgments

Ich möchte mich bei allen bedanken, die während der langen Zeit für mich da waren und zum Gelingen dieser Arbeit beigetragen haben.

Als erstes möchte ich mich bei meinem Doktorvater **PD Dr. Joachim Griesenbeck** bedanken. Ich hätte mir keinen besseren Betreuer wünschen können. Und weil ich ja weiß, dass du das bisher immer ganz nett fandest, gibt es jetzt auch hier am Ende meiner Arbeit (und damit leider auch am Ende meiner Zeit am Institut) noch ein kleines Dankeschön-Gedicht.

Kaum war die Masterarbeit abgegeben,

da ging es schon los, das Doktorandenleben.

Die Frage war noch nicht geklärt,

was in der stationären Phase zu offenen Kopien führt.

Drum hieß es Weiterforschen mit Rpd3.

Wessen Acetylgruppe setzt die HDAC denn nun frei?

Ganz sicher ist es auch jetzt am Ende nicht,

der Leser ist bestimmt auf weitere Ergebnisse erpicht.

Diese Arbeit konnte zu keinem 100%igen Ergebnis führen,

aber eins kann ich ganz sicher beschwören:

Ohne deine Hilfe, Unterstützung und Motivation,

ohne so manches "du schaffst das schon",

ohne die supidupi- spitzenmäßige Supervision,

hätte ich das Doktoranden-Karriereband wohl abgerissen,

ohne all das wäre mir diese Arbeit nie geglückt.

Ich muss schon sagen, Achim, das ist echt verrückt,

wie viel Zeit und Mühe du hier investiert hast,

so dass am Ende hoffentlich alles passt.

Ob früh, ob spät, ob Wochenende oder Feiertag,

du hattest wirklich immer für mich Zeit und Rat.

Jetzt kann ich dafür nur noch ein ganz herzliches und riesengroßes "Danke" sagen

und eine fertige Arbeit ans Prüfungsamt tragen.

Natürlich möchte ich mich auch bei **Prof. Dr. Herbert Tschochner** bedanken, dass er mir die Möglichkeit gegeben hat, diese Arbeit in seinem Labor durchzuführen. Ich möchte mich bedanken, weil du immer ein großartiger Chef warst, mir die Möglichkeit gegeben hast das OddPols und das EMBO Chromatin and Epigenetics Meeting zu besuchen, immer zu wissenschaftlichen Diskussionen bereit warst, mir das Rpa49-Projekt als neues Thema anvertraut hast und mich als "das blonde Ribosom" "berühmt" gemacht hast.

Dr. Philipp Milkereit möchte ich für die vielen Diskussionen danken. Dadurch wurden viele neue Ideen geschmiedet und ich bin mir sicher, dass diese Diskussionen maßgeblich zum Gelingen dieser Arbeit beigetragen haben. Außerdem möchte ich mich für die vielen Erheiterungen durch deinen unvergleichlichen trockenen Humor bei verschiedenen Gesprächen und Erzählungen bedanken.

Prof. Dr. Wolfgang Seufert möchte ich dafür danken, dass er sich als Mentor um mein Thema bemüht hat und sich nun bereit erklärt hat, diese Arbeit zu begutachten und mich zu prüfen. Seiner Mitarbeiterin **Dr. Katharina Hannig** möchte ich dafür danken, dass sie die Net1-Trunkationsstämme hergestellt hat.

Prof. Dr. Klaus Grasser möchte ich schon jetzt dafür danken, dass er sich bereit erklärt hat mich in meinem Kolloquium zu prüfen.

Prof. Dr. Antonio Conconi möchte ich für sein Mentorat danken.

Bei der **DFG** und der **bayerischen Forschungsallianz** möchte ich mich für das Funding bedanken. Ohne diese finanzielle Unterstützung wäre diese Arbeit nicht möglich gewesen.

Dr. Jorge Pérez-Fernández und **Dr. Sébastien Ferreira-Cerca** möchte ich für die vielen Diskussionen und Ideen rund um mein Thema und für die vielen - auch nicht wissenschaftlichen - Gespräche in unserem Büro danken. Es war wirklich eine gute Zeit bei euch. Und Jorge: Nein es ist nicht Pol II !!!

Ich möchte mich außerdem bei allen aktuellen und ehemaligen Mitgliedern der **Chromatin Crew** bedanken. Lieber **Achim**, lieber **Christopher**, liebe **Kristin** und liebe **Uli**, ihr seid wirklich spitzenmäßige Kollegen und Freunde. Ich kann es nur vom letzten Weihnachtsgedicht wiederholen: Ihr seid eine klasse Truppe! Und könnt ihr alles schaffen? JA ihr schafft das! Kristin möchte ich hier nochmal extra danken, dass sie mir gerade während meiner Schreibphase auch so viel Mut zugesprochen hat und sich über die Zeit zu einer echten Freundin entwickelt hat und Christopher möchte ich danken,

dass er sich als mein "Kratzbaum" bereit gestellt hat, wenn ich mal so richtig mies gelaunt war und meinem Unmut ein wenig Luft machen musste.

Auch wenn sie nicht in der Chromatin-Subgruppe ist, möchte ich mich hier noch ganz herzlich bei **Gisela** bedanken. Du bist wirklich der Lab-Manager und dennoch die gute Seele des Labors. Vielen Dank für die vielen, vielen Gespräche und deine so oft benötigten aufmunternden Worte.

Außerdem möchte ich mich bei meinen Praktikanten und Praktikantinnen **Stewart McEwen, Tobias Strunz, Katharina Kossmann, Dennis Nagl** und **Lena Cook** bedanken. Insbesondere Tobi, Dennis und Lena haben mich bei meiner Doktorarbeit wirklich toll unterstützt.

Ich möchte mich bei **allen Mitgliedern des Lehrstuhls** für ihre Hilfsbereitschaft und Freundlichkeit und dafür, dass sie dafür gesorgt haben, dass ich mich wirklich unglaublich wohl gefühlt habe und deshalb motiviert arbeiten konnte, bedanken. Viele von euch sind für mich längst nicht mehr nur Kollegen, sondern Freunde geworden und auch wenn sich meine aktive Zeit am Institut jetzt langsam dem Ende zuneigt, werdet ihr mich mit Sicherheit nicht komplett los. Dafür habe ich euch einfach zu sehr ins Herz geschlossen. Eine "Feierabend-Halbe" ist bestimmt irgendwann mal wieder drin.

Bei meinen beiden Schwestern **Verena** und **Aja** möchte ich mich für die moralische Unterstützung und dafür, dass sie immer an mich geglaubt haben und mich motiviert haben bedanken. Bei Aja möchte ich mich auch für das Korrekturlesen in letzter Minute bedanken und dafür, dass sie die Optik meines Werkes gelobt hat. Wenigstens einer, der mein stimmiges Farbkonzept bemerkt hat...

Meinen **Eltern** möchte ich danken, dass sie mich während meines Studiums unterstützt haben und es so überhaupt erst möglich wurde, dass ich bis zur Doktorarbeit kommen konnte. Ich weiß: Ihr habt an sich keine Ahnung, was ich da die letzten Jahre so getrieben habe, aber ich weiß auch, dass ihr trotzdem stolz auf mich seid.

Last but not least möchte ich mich bei dir, lieber **Alex**, bedanken. Für unsere gemeinsame Zeit außerhalb des Labors, in der du mir die nötige Auszeit vom stressigen Doktorandenleben geben konntest und mich so oft aufgefangen hast, wenn ich dachte es kann nicht mehr weitergehen. Auch wenn ich mich hier wiederhole, aber der Satz aus der Danksagung meiner Masterarbeit gilt einfach immer noch: Danke, dass du mir den Rücken gestärkt und freigehalten hast. Und du weißt ja: ily!